

Alma Mater Studiorum – Università di Bologna

Dottorato di Ricerca in

Biologia Cellulare e Molecolare

Ciclo XXXI

Settore Concorsuale di afferenza: 05/A2 – Fisiologia Vegetale

Settore Scientifico disciplinare: BIO/04 – Fisiologia Vegetale

**Study of carbon metabolism in plants:
from enzymes to the organism, from physiology to stress.**

Candidato

Dr. Libero Gurrieri

Supervisore

Chiar.ma Prof.ssa Francesca Sparla

Coordinatore Dottorato

Chiar.mo Prof. Giovanni Capranico

Esame finale anno 2019

Abstract

The study of primary carbon metabolism in plants concerns different aspects of plant physiology and plant-environment interactions. Since carbon metabolism starts with CO₂ fixation, it involves one of the biggest process regarding living beings on Earth. Photosynthesis produce carbohydrates that are, directly or indirectly, consumed by the autotrophic organisms and release the oxygen necessary for aerobic production of energy. Thus plants as primary producers are responsible for two fundamental processes for life.

In my 3-year PhD several aspects of plant carbon metabolism have been studied. *In vitro* characterization of recombinant enzymes highlighted biochemical and regulatory features, while *in vivo* analysis on *Arabidopsis thaliana* pinpointed new functions for enzymes through the development and in response to stress.

The phosphoribulokinase from the plant *Arabidopsis thaliana* and the green algae *Chlamydomonas reinhardtii* has been characterized from a structural and biochemical point of view. The crystallographic structure of both enzymes has been solved, providing the first structural information on redox-sensitive phosphoribulokinase from plants. Both enzymes share a conserved homodimeric structure with 18 strands forming a β -sheet and the two catalytic sites positioned at the edges of the dimer. New hypothesis on the structural base of redox regulation have been inferred. Further characterization has been carried out analyzing enzymes structure in solution by size exclusion chromatography coupled with small angle X-ray scattering and redox properties, like midpoint redox potential and thioredoxin reactivation.

A second *in vitro* study has been performed on the α -amylase 3 (*AtAMY3*) from *Arabidopsis thaliana*. This enzyme is not necessary for normal starch degradation in mesophyll cells but is important for starch degradation under osmotic stress (Thalman et al., 2016) and guard cell functionality (Horrer et al., 2016). *AtAMY3* has been found target of glutathionylation *in vitro* by western blotting and the three glutathionylation sites have been identified by mass spectrometry. Assaying enzymatic activity after incubation with oxidized glutathione showed an inhibitory effect, afterwards the recovery of *AtAMY3* functionality upon incubation with reduced glutathione, glutaredoxins and thioredoxin have been investigated. The analysis highlighted different reactivity with these three agents and the possibility of concomitant redox modification, *i.e.* glutathionylation and disulfide bond, occurring after the exposure to glutathione.

In the last two chapters the focus moved to the *in vivo* function of carbon metabolism enzymes. In particular in Chapter 4 *Arabidopsis thaliana* T-DNA lines have been identified and studied to understand which metabolic pathways are involved in carbon mobilization and osmotic stress adaptation. After a preliminary screening, T-DNA lines for *SPSA2* (Sucrose-phosphate Synthase

A2), *SUS1* (Sucrose synthase 1), *GWD2* (Glucan, Water Dikinase 2) emerged as interesting. On these lines carbohydrate and amino acids content, especially proline, has been monitored during stress treatment highlighting severe impairments in the accumulation of several sugars and proline. This reduction could affect the recover of osmotic balance and metabolic processes leading to incomplete or weaker stress response. Thus *SPSA2*, *SUS1* and *GWD2* resulted important for metabolic adaptation to stress, even if further analysis are needed to understand their specific role. In Chapter 5 the role of the three dikinases from *Arabidopsis thaliana* have been investigated in plant development, focusing on seed formation. Among these three, *GWD1* is the most known and studied, despite its role out of mesophyll cells and tubers is not known. The other dikinases, *PWD* and *GWD2*, have been poorly studied and the *in vivo* function of *GWD2* is still unknown. The analysis of T-DNA lines carrying insertions in the corresponding dikinase genes showed same developmental defects and a new role in seed development can be suggested for *GWD2* and *PWD*. On the whole, several sides and features of carbon metabolism in plants still remain to be understood, even for a 70-year topic like the Calvin-Benson cycle, making stimulating the study of a process of primary importance for the life on our planet.

Table of contents

Thesis summary	1
1. Introduction	3
1.1 Carbon and life	3
1.2 Photosynthesis and carbon	3
1.2.1 Photosynthetic electron transport	4
1.2.2 The Calvin-Benson cycle	6
1.2.3 Adaptations to improve CO ₂ fixation	8
1.2.4 Other pathways for carbon fixation	9
1.3 The metabolism of starch in leaves	11
1.3.1 Diurnal starch biosynthesis	12
1.3.2 Starch degradation at night	14
1.3.3 The cytosolic metabolism of starch-released sugars	17
1.4 Sucrose metabolism	18
1.4.1 Sucrose biosynthesis in photosynthetic tissues	18
1.4.2 Phloem loading and sucrose transport	18
1.4.3 Phloem unloading and sucrose degradation	20
1.5 Carbon fluxes under abiotic stress	21
1.6 Regulation of carbon metabolism	23
1.6.1 The redox regulation	24
1.6.1.1 The thioredoxin system and NADPH-thioredoxin reductase in chloroplast	25
1.6.1.2 Redox modification by glutathione and oxygen and nitrogen reactive species	26
1.6.2 The circadian clock	27
1.6.3 Carbon metabolism controls growth by sugar sensing	29
1.7 Regulation of Calvin-Benson cycle	32
1.8 Regulation of leaf starch metabolism	34
1.8.1 Regulation at protein level	34
1.8.2 Time-dependent regulation of starch metabolism	35
1.9 Regulation of sucrose metabolism and phloem transport	36
1.9.1 Sucrose-phosphate synthases are regulated at different levels	37
1.9.2 Control of sucrose transporters	37
1.9.3 Regulation of sucrose degradation	38

2. Photosynthetic CO₂ assimilation:

the last gap in the structural proteome is closed	41
2.1 Abstract	41
2.2 Results and discussion	42
2.3 Materials and methods	51
2.3.1 Protein expression and purification	51
2.3.2 Activity assay and determination of pH- and temperature-dependence	51
2.3.4 Thioredoxin specificity and redox titration	52
2.3.4 Determination of the pK _a values of the catalytic cysteines	52
2.3.5 Crystallization and data collection	52
2.3.6 Structure solution and refinement	53
2.3.7 Small angle X-ray scattering data collection	54
2.3.8 Small angle X-ray scattering data analysis	54
2.3.9 Modelling from SAXS data	54
2.3.10 Data availability	55
Addendum	56

3. Glutathionylation of *Arabidopsis thaliana* AMY3 and regulation by glutaredoxins and thioredoxins *in vitro*

3.1 Brief introduction	73
3.2 Materials and methods	76
3.2.1 Expression and purification of recombinant AMY3 from <i>Arabidopsis thaliana</i>	76
3.2.2 Biotinylated GSSG assay	77
3.2.3 MALDI-ToF Mass Spectrometry	77
3.2.4 AtAMY3 activity assay and oxidative treatments	78
3.2.5 Determination of cysteines pK _a	78
3.2.6 Reactivation of glutathionylated AtAMY3 by GSH, GRX and TRX	78
3.3 Results	80
3.3.1 AtAMY3 is target of glutathionylation <i>in vitro</i>	80
3.3.2 Determination of catalytic cysteine pK _a	81
3.3.3 Glutathione protects AtAMY3 from irreversible oxidation and inhibition	82
3.3.4 GSH reactivates glutathionylated AtAMY3 and redoxins speed up the process	84
3.3.5 Both GRX and TRX are required for complete recovery of AtAMY3 activity	85

3.4 Discussion and concluding remarks	87
4. Enzymatic components involved in sugar and proline accumulation under osmotic stress in <i>Arabidopsis thaliana</i>	90
4.1 Brief introduction	90
4.2 Materials and methods	93
4.2.1 Plant material and growth conditions	93
4.2.2 Selection of homozygous lines	93
4.2.3 Water content measures	94
4.2.4 Lipid peroxidation measurements	94
4.2.5 Leaf starch quantification	95
4.2.6 Proline and amino acids quantifications	96
4.2.7 Soluble sugar quantification	96
4.2.8 Reducing sugar quantification	97
4.2.9 Glucose and fructose assay	97
4.2.10 Quantification of carbohydrates in the cell wall	98
4.2.11 Quantitative Real Time PCR analysis	99
4.3 Results	101
4.3.1 Water content under osmotic stress	101
4.3.2 Generation of oxidative stress under osmotic stress	101
4.3.3 Proline accumulation under stress and amino acids levels	103
4.3.4 Transitory starch at the end of the day	104
4.3.5 Changing in soluble sugar levels	105
4.3.6 Carbohydrate content in the cell wall	106
4.3.7 Gene expression profile of <i>GWD2</i> , <i>SUS1</i> , <i>SPSA2</i> and <i>P5CS1</i>	107
4.4 Discussion and concluding remarks	110
4.5 Addendum	113
4.5.2 Selection of homozygous T-DNA lines	113
4.5.3 Oxidative stress levels in T-DNA lines	113
5. The analysis of the different functions of starch-phosphorylating enzymes during the development of <i>Arabidopsis thaliana</i> plants discloses an unexpected role for the cytosolic isoform GWD2	115
5.1 Abstract	115

5.2 Introduction	116
5.3 Materials and methods	118
5.3.1 Genotype analysis	118
5.3.2 Plant growth conditions	119
5.3.3 Phenotypic characterization	119
5.3.4 Scanning electron microscopy	120
5.3.5 Quantification of starch, protein and lipids in seeds	120
5.4 Results	121
5.4.1 Isolation of homozygous T-DNA lines and leaf starch quantification	121
5.4.2 Seeds shape and composition	121
5.4.3 Seed morphology and permeability	123
5.4.4 Seed viability and primary root growth	125
5.4.5 Transition from vegetative to reproductive growth and plant fitness	125
5.4.6 Rescue by light	126
5.5 Discussion	127
6. Ringraziamenti	131
7. References	133

Thesis summary

During the years of my PhD, plant carbon metabolism has been approached with two different focuses: study the biochemistry of enzymes *in vitro* and understanding the physiological role of enzymes *in vivo*. In both cases physiological and stress conditions were considered.

The Chapter 1 is a comprehensive introduction on primary carbon metabolism, passing from the collection of light energy and carbon fixation to starch and sucrose metabolism. In addition, two insights are provided on carbon metabolism under abiotic stress and regulation of carbon metabolism, *i.e.* Calvin-Benson cycle, starch metabolism, sucrose metabolism.

Starting with the entry of carbon in the living world, an enzyme of Calvin-Benson cycle has been characterized. In Chapter 2, the crystallographic structures and regulatory properties of phosphoribulokinase from the green algae *Chlamydomonas reinhardtii* and the plant *Arabidopsis thaliana* have been studied. The structure have been solved in collaboration with the Dr. Simona Fermani of Department of Chemistry "G. Ciamician" (University of Bologna) and Dr. Stephane D. Lemaire (CNRS - Paris).

Then in Chapter 3 the regulation of the α -amylase 3 (*AtAMY3*) of *Arabidopsis thaliana* by glutathione has been characterized. *AtAMY3* is involved in starch mobilization for guard cells movement and in response to osmotic stress. The chapter focuses on glutathionylation, a post-translational redox modifications which can occur when oxidative stress raises inside cellular compartments.

The last two chapters illustrate two studies on *Arabidopsis thaliana* plants. In Chapter 5 the adaptation of carbon metabolism to osmotic stress has been investigated using T-DNA lines for enzymes involved in carbon metabolism which are not essential for normal plant physiology.

In the last chapter, Chapter 6, the focus went back to physiological conditions and three T-DNA lines for the three *Arabidopsis* dikinases have been studied. One of these enzymes, GWD1, has been examined several times and in different species starting from the '90s. However, the other two, PWD and GWD2, remained poorly studied. In this analysis, the development of plants carrying T-DNA insertions has been monitored and different parameters on seeds and plants have been evaluated to understand the function of GWD1, PWD and GWD2 along the plant life cycle.

1. Introduction

1.1 Carbon and life

Life is based on organic molecules, made of carbon backbones bound to different functional groups. Forming different bonds carbon can produce a wide range of molecules with distinct size and features, like nucleic acids, proteins and carbohydrates. Furthermore, the possibility to react with different elements (hydrogen, oxygen, nitrogen, phosphorus and sulphur) and these reactions can occur in water, making carbon-based molecules suitable for the Earth.

Different strategies evolved among living beings to satisfy the carbon demand. In autotrophy, the organic compounds are produced using inorganic sources from the environment. Reducing power to fix carbon is obtained from the energy of light (photoautotrophs) or oxidation of inorganic compounds (chemoautotrophs). In heterotrophy, carbon is directly obtained from organic sources. For these reasons, the first organisms are called producers and the latter consumers. The photosynthesis fix 1/6 of the atmospheric carbon (Ciais et al., 1997), allowing a massive entry of carbon in the living world. Among the photosynthetic producers land plants, together with algae and cyanobacteria, are the main participants in the entry of carbon into the biosphere.

1.2 Photosynthesis and carbon

The oxygenic photosynthesis evolved on the Earth 2.4 billion years ago (Hohmann-Marriott and Blankenship, 2011), introducing a novel pathway to obtain reducing power and energy and completely modifying the atmosphere of the planet. These great changing allowed the evolution of the life as we know it (Payne et al., 2009). Nowadays, the oxygenic photosynthetic organisms are the most abundant producers and as such extremely important for human beings. Oxygenic photosynthesis takes advantage of the light energy to split water in oxygen, protons and electrons, leading to the production of NADPH and ATP (Figure 1.1). Thus, the chemical energy (ATP) and the reducing power (NADPH) are consumed by the Calvin-Benson cycle in order to produce sugars from CO₂ (Figure 1.2).

Depending on the organism, the photosynthetic process has different localization. In cyanobacteria, the carbon fixation is localized in specialized structures called carboxysomes and the photosynthetic

electron transport (PET) occurs in specialized portions of membranes called thylakoids. In algae and land plants, photosynthesis is conducted in chloroplasts, specialized organelle originated by cyanobacteria through endosymbiosis. Chloroplasts are characterized by two membranes that delimit an intermembrane space. Inside the inner membrane, the stroma contains the enzymes for the Calvin-Benson cycle and the thylakoids.

1.2.1 Photosynthetic electron transport

The PET makes available the energy of light as chemical energy for the biochemical reactions that are necessary for carbon fixation. The electrons released by the photo-oxidation of water go through a series of protein complexes generating a proton gradient and ending up with the NADP⁺ reduction (Figure 1.1). Two different types of protein complexes are responsible for the harvest of light, both need pigments for their functioning. The smaller complexes are the Light-Harvesting Complexes (LHCs) containing chlorophylls and carotenoids. Whereas, the photosystem I and II (PSI and PSII) are the larger complexes. Both LHCs and PSs interact each other and localize in the thylakoid membranes. The pigments in LHCs collect the electromagnetic radiation of light, resulting in excited electrons. The excitation could be transferred between the nearest pigments by dipole-dipole interaction until it is caught by the PSs. If the energy of the excitation move from a pigment to another, it is called Förster resonance energy transfer, otherwise according to the Redfield theory, initially the excitation can oscillate between the donor and the acceptor pigments and then result in the energy transfer (Renger, 2010).

PSs consist of an antenna system and a reaction centre, the antenna system collects the excitation energy and drives it to the reaction centre. In the reaction centre a special pair of chlorophylls is present, which catalyzes the photochemical reaction, consuming the energy of light to release an electron. The special pair are named P700 for PSI and P680 for PSII. The first photochemical reaction occurs inside the PSII, which exists in dimeric and monomeric form *in vivo* (Takahashi et al., 2009) containing chlorophylls, pheophytins and carotenoids (Guskov et al. 2009). The main structural domains are the transmembrane reaction centre, where is located the special pair P680, the two proteins CP43 and CP47 forming the inner light-harvesting antenna, and a set of proteins associated to the reaction centre in the luminal part of the thylakoids. The Oxygen-Evolving Complex (OEC) is connected to the reaction centre and performs the essential reaction of photo-oxidation of water, releasing O₂ and producing 4 electrons and 4 H⁺ ions.

The excitation energy is directed through the inner antenna to the P680 which release an electron (P680* → P680⁺ + e⁻; Bricker and Frankel, 2002). The electron is transferred through cofactors (pheophytin, quinones) inside the PSII and reaches the plastoquinone (PQ). After the reaction, the

special pair ($P680^+$) is neutralized thanks to an electron provided by water. An additional energy transfer to the P680 completes the reduction of PQ to plastoquinol, picking up 2 protons from the stroma (PQH_2 ; Satoh, 2008).

PQH_2 interacts with another transmembrane protein complex, the Cytochrome b_6f (Cyt b_6f). The Cyt b_6f has 3 binding sites, one for PQH_2 , another PQ and the third for plastocyanin (PC). The PQH_2 is oxidized by the Cyt b_6f , one electron reduces PC and the other an oxidized PQ, after two oxidation two PC are completely reduced, one plastoquinone is reduced and 4 H^+ are released in the thylakoid lumen. The release of protons contributes to the formation of a proton gradient across the thylakoid membranes. The reduced PC leaves the Cyt b_6f binding site and enter in the binding site of the PSI. PC is a 10 kDa soluble protein containing a copper ion and belonging to the cupredoxin family (Sigfridsson, 1998), it acts as electron carrier between the Cyt b_6f and the PSI in the lumen.

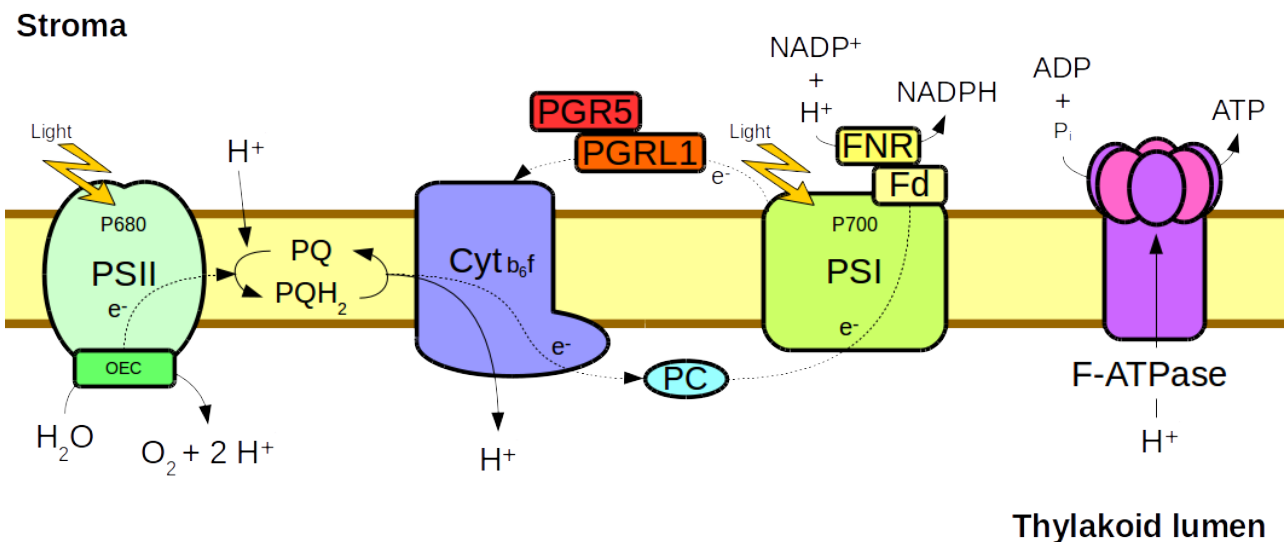


Figure 1.1 Photosynthetic electron transport chain. From left to right: PSII, photosystem II; PQ, oxidized plastoquinone; PQH_2 , reduced plastoquinone; Cyt b_6f , cytochrome b_6f ; PC, plastocyanin; PSI, photosystem ; Fd, ferredoxin; FNR, ferredoxin- $NADP^+$ reductase.

The PSI exists as monomeric complex in plants, diatoms, green and red algae (Gardian et al., 2007; Veith and Buchel, 2007; Germano et al., 2002; Amunts et al., 2007). On one side of the PSI the LHCI interacts with the core, in which more than 100 chlorophylls and 15 carotenoids collect the light energy and transfer it to the reaction centre (Amunts et al., 2007). The PC binds PSI on the luminal side whereas binding site for the terminal acceptor, the Ferredoxin (Fd), is localized on the stromal side of the complex (Busch and Hippler, 2011). The electron emitted by the $P700^+$ passes through a series of pigments and iron-sulfur clusters and reduces the ferredoxin (Fd). The positive charge on $P700^+$ is neutralized by reduced PC. In turn, the Fd is oxidized by FNR (Ferredoxin, $NADP^+$ Reductase), a FAD-enzyme conserved in all the photosynthetic organisms, and $NADP^+$ is reduced to NADPH.

The pathway above described is known as Linear Electron Flow (LEF), because the electrons are transferred from the PSII straight to the PSI leading to NADPH production. However, another pathway occurs inside the electron chain. Indeed the PSI electron flow can be directed to the Cyt b₆f thanks to the PGR5-PGRL1 complex resulting in a Cyclic Electron Flow (CEF; Shikanai and Yamamoto, 2017). The CEF specifically contributes to the proton gradient formation and does not lead to NADPH production. Then the gradient is consumed by the F-ATPase on the thylakoid membrane to produce ATP in the stroma. Therefore, the regulation of LEF and CEF contributes to the balance between the production of energy, as ATP, and reducing power, as NADPH, in function of the requirement of the carbon fixation.

1.2.2 The Calvin-Benson cycle

The Calvin-Benson cycle represents the main entrance of inorganic carbon into organic world and is the only pathway occurs in photosynthetic eukaryotes. The reductive pentose phosphate pathway comprises 11 enzymes catalysing 13 reactions that lead to the fixation and reduction of carbon dioxide into triose phosphates (Figure 1.2).

The cycle is classically divided in 3 stages, carboxylation, reduction and regeneration. During these stages the energy and the reducing power provided by PET are consumed to obtain organic carbon. The carboxylation is catalyzed by RuBisCO, acting as carboxylase. RuBisCO is found in eukaryotes and prokaryotes, it is a oligomeric enzymes consisting of 2 types of subunit, the large subunit (50-55 kDa) and small subunit (12-18 kDa), organized in a hexadecameric structure with 8 large and 8 small subunits (Andersson and Backlund, 2008). During the carboxylation, the CO₂ is added to C-2 of a 5-carbon molecule, the ribulose-1,5-bisphosphate (RuBP), which spontaneously splits in two molecules of 3-phosphoglycerate (3-PGA).

Entering in the reduction stage, the two molecules of 3-PGA are phosphorylated by the 3-phosphoglycerate kinase (PGK) consuming ATP producing 1,3-bisphosphoglycerate (1,3-BPGA). Then NADPH is oxidized by the photosynthetic isoform of glyceraldehyde-3-phosphate dehydrogenase to reduce 1,3-BPGA yielding glyceraldehyde-3-phosphate (G3P). The carbon fixed by the photosynthesis is mainly provided to the cell metabolism as triose phosphates, G3P or its isomer dihydroxy-acetone-3-phosphate (DHAP). During the day, the triose-phosphate/phosphate translocator (TPT) exports triose phosphates in exchange with inorganic phosphates. TPT is the most abundant integral protein in the chloroplast inner envelope (Flügge et al., 1991). Once in the cytosol, triose phosphates enter in the central metabolism and take part of gluconeogenesis and glycolysis.

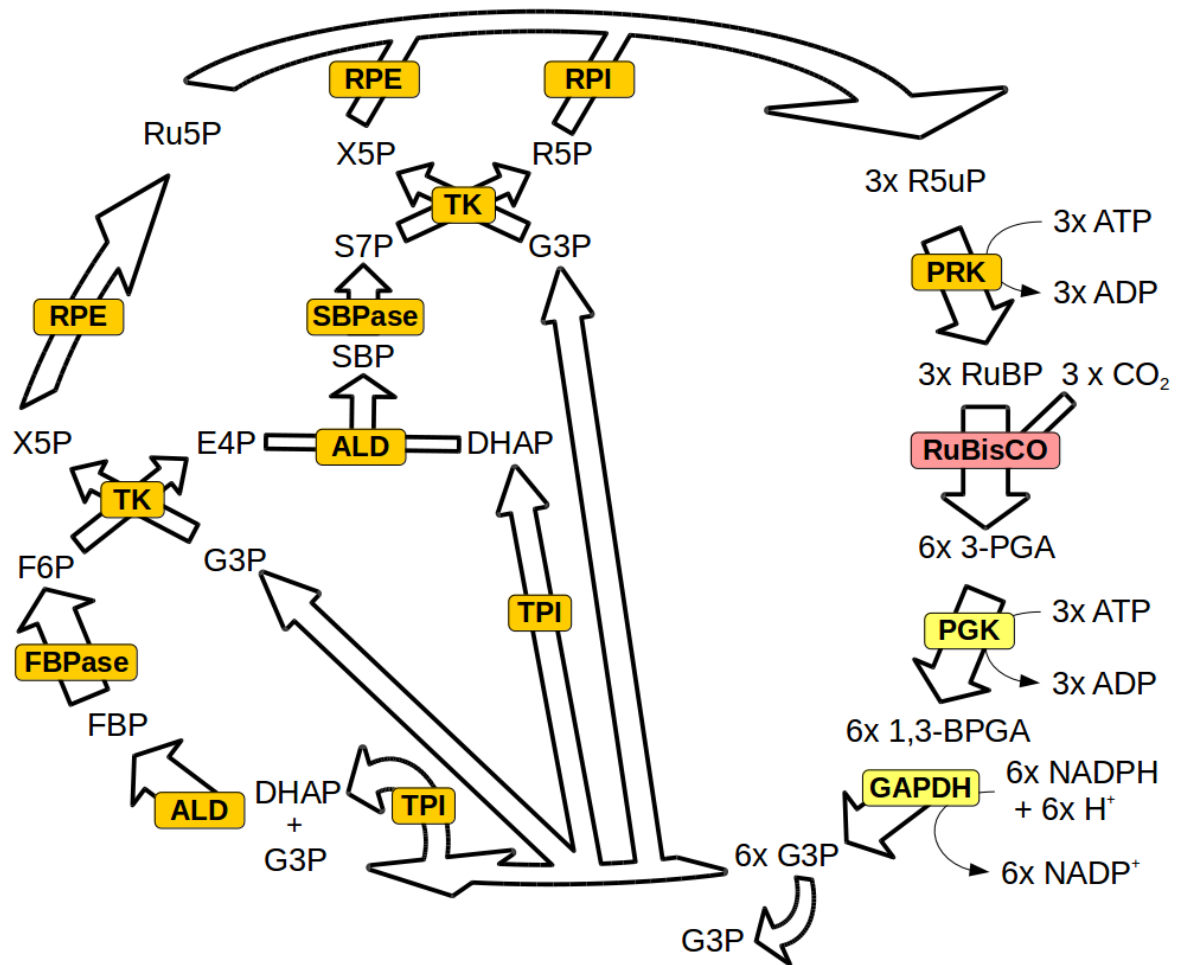


Figure 1.2 The Calvin-Benson cycle. Enzymes: RuBisCO, ribulose 1,5-bisphosphate carboxylase/oxygenase; PGK, phosphoglycerate kinase; GAPDH, glyceraldehyde 3-phosphate dehydrogenase; TPI, triose phosphate isomerase; ALD, aldolase; FBPase, fructose bisphosphate phosphatase; TK, transketolase; RPE, ribose phosphate epimerase; SBPase, sedoheptulose bisphosphate phosphatase; PRK, phosphoribulokinase. Intermediates: RuBP, ribulose bisphosphate; 3PGA, 3-phosphoglycerate; 1,3-BPGA, bisphosphoglycerate; G3P, glyceraldehyde 3-phosphate; DHAP, dihydroxyacetone phosphate; FBP, fructose bisphosphate; F6P, fructose 6-phosphate; E4P, erythrose 4-phosphate; SBP, sedoheptulose bisphosphate; S7P, sedoheptulose 7-phosphate; Xu5P, xylulose 5-phosphate; R5P, ribose 5-phosphate; ribulose 5-phosphate. Figure inspired by Michelet et al. (2013).

The regeneration stage is the longest of the cycle and provides the initial substrate, RuBP, allowing the cycle progression. Since the regeneration starts with 3-C molecules and ends with 5-C ones, the aim of the last stage is to rearrange carbon skeletons, thus 5 triose are necessary to yield 3 RuBP. The triose phosphate isomerase interconverts G3P in dihydroxyacetone-3-phosphate (DHAP), which is condensed with another G3P by the aldolase resulting in a molecule of fructose-1,6-bisphosphate (FBP). The fructose-1,6-bisphosphatase hydrolyzes the phosphate group on the C1 of FBP, then fructose-6-phosphate (F6P) is substrate of the transketolase (TK). The TK reaction transfers a 2-C unit from F6P to a third G3P molecule producing xylulose-5-phosphate (X5P) and erythrose-4-phosphate (E4P). Aldolase catalyzes a second reaction in the regeneration stage, E4P is condensed to a fourth G3P and sedoheptulose-1,7-bisphosphate (SBP) is produced. At this point another

phosphatase comes in to play and hydrolyzes the phosphate group on the C1 of SBP, the sedoheptulose-7-phosphate produced is the second substrate of the TK. A 2-C unit is moved to a fifth G3P, in this way the TK produces ribose-5-phosphate (R5P) and another X5P. R5P is isomerised by ribose-5-phosphate isomerase (RPI), whereas the two X5P obtained so far are epimerized by ribulose-5-phosphate epimerase (RPE), both reactions release ribulose-5-phosphate (Ru5P). The phosphoribulokinase (PRK) catalyzes the last reaction of the regeneration stage consuming ATP to produce RuBP from Ru5P.

1.2.3 Adaptations to improve CO₂ fixation

RuBisCO has double activity, as carboxylase participates of the carbon fixation through the Calvin-Benson cycle, but a side-reaction occurs in which the enzyme acts as oxygenase. The oxygenase activity leads to the production of 2-phosphoglycolate (2PG) and (3PG) and is facilitated by a variety of condition, *e.g.* high temperature (Jordan and Ogren, 1984). 2PG has not metabolic function and the photosynthetic organisms evolved a specific pathway to scavenge this compound and prevent its accumulation, the photorespiration. The photorespiration, so-named because consumes O₂ and releases carbon dioxide (and NH₃), probably represents the second most important metabolic flux of the biosphere, after the photosynthesis itself (Bauwe et al., 2010). The photorespiratory reactions involve about 10 enzymes located in chloroplasts, peroxisomes, mitochondria and cytoplasm.

In order to limit the oxygenation of RuBP, some organisms evolved CO₂ concentrating mechanisms. In this way, the carboxylation reaction is promoted due to the accumulation of its substrate. Three different strategies of CO₂ concentration were adopted to minimize photorespiration: 1) C4 plants, adapted to hot environments; 2) Crassulacean Acid Metabolism (CAM), adapted to dry environments, and 3) CO₂ pumps, a strategy adopted by aquatic photosynthetic organisms.

In hot environments, the concentration of CO₂ lowers more than the O₂ concentration (Sage, 2013), promoting the oxygenation reaction of RuBisCO. To avoid the side-reaction, C4 plants close in RuBisCO from the surrounding environment and concentrate CO₂. Indeed the peculiarity of C4 plants is the spatial separation between the site of CO₂ intake and the site of carbon fixation. In mesophyll cells the carbon dioxide (as bicarbonate ion HCO₃⁻) is bound to phosphoenolpyruvate (PEP) by the PEP-Carboxylase (PEPC) producing oxalacetate (OAA). These cells are more exposed to the atmosphere and so exposed to higher oxygen concentration. OAA is then converted to malate or aspartate, by malate dehydrogenase or aspartate aminotransferase respectively, and transported through the mesophyll to specialized cells in the inner part of the leaf, the bundle sheath cells. These

cells evolved a thicker and suberised cell wall, which becomes almost waterproof and all the exchanges are controlled by diffusion through the plasmodesmata (von Caemmerer and Furbank, 2003). In the bundle sheath aspartate or malate are converted to pyruvate releasing CO₂, that is fixed by the Calvin-Benson cycles while pyruvate returns to the mesophyll cells where is phosphorylated, producing PEP. By means of the C₄ strategy plants achieve a 90% reduction of photorespiration (Sage, 2013).

CAM plants adapted to hotter environments than C₄ plants. In fact their metabolism takes the name from plants adapted to desert, where the carbon fixation during the day would lead to massive water loss. For these reason CAM plants evolved a mechanism based on PEP caboxylase concentration of CO₂ but implemented with a temporal separation between the intake of carbon and its fixation. The stomata, which allow gas exchange between plant and environment, are open during the night, when the temperatures are lower. Stomata opening allow CO₂ diffusion in the photosynthetic tissue, where is bound to PEP by PEPC and accumulate in the vacuole as malate. During the day, the stomata are closed preventing water loss and malate is decarboxylated releasing CO₂ that is fixed consuming NADPH and ATP produced by the PET. Thanks to this temporal separation CAM plants lose 5-10 times less water than C₄ and C₃ plants (Taiz and Zeiger, 2010).

1.2.4 Other pathways for carbon fixation

Although all the economically relevant plant species fix CO₂ through the Calvin-Benson cycle, other five carbon fixation pathways are known to occur in different organisms (Ljungdahl, 1986; Buchanan and Arnon, 1990; Berg et al., 2007; Huber et al., 2008; Zarzycki et al., 2009).

Hydrogen (Hedderich and Forzi, 2005; Heim et al., 1998), sulphur, hydrogen sulphide (Friedrich et al., 2005) or sodium gradient are the most common sources of reducing power, while ATP is provided by a variety energetic reactions (Heise et al., 1989; Fuchs, 2011). The five cycles of CO₂ fixation take advantage of acetyl-CoA as molecule for carbon uptake, and then utilize it in different ways with different carbon yields and energy costs (Figure 1.3; Fuchs, 2011).

The reductive Coenzyme A pathway (also named Wood-Ljungdahl Pathway, WLP) is present in acetogenic bacteria and produces acetyl-CoA from CO₂ (Schuchmann and Müller, 2016). CO₂ is converted into methyl group and carbon monoxide, which are condensed to the acetyl group (Ragsdale and Pierce, 2008). Acetogens do not perform just WLP to sustain their growth because it is uncompetitive if compared to other metabolisms so it is probably integrated with other pathways (Schuchmann and Müller, 2016). Acetogenic bacteria are found in different kind of environments like soils, mammalian and termites gastrointestinal tracts, and high salt and temperature

environments (Simankova et al., 2000; Gössner et al., 1999; Küssel et al., 2001; Kamlage et al., 1997; Graber and Breznak, 2004; Küssel et al., 2000).

Green phototrophic sulfur bacteria are obligate anaerobe and fix CO₂ through the reductive citric acid cycle (RCA) generating acetyl-CoA. Irreversible steps of the Krebs cycle are catalyzed by enzymes with different activity, working in the reductive direction. For example, fumarate reductase replaces succinate dehydrogenase and 2-oxoglutarate dehydrogenase by 2-oxoglutarate synthase (Evans et al, 1966; Aoshima et al., 2007).

Anaerobic and microaerobic Archaea members of *Thermoproteales* and *Desulfurococcales* fix carbon via dicarboxylate/4-hydroxybutyrate cycle. The reactions are divided in two parts, the first utilize acetyl-CoA, CO₂ and bicarbonate to produce succinyl-CoA, which is converted to 4-hydroxybutyrate in the second part, then yielding two acetyl-CoA molecules (Ramos-Vera et al., 2009; Ramos-Vera et al., 2011).

In the Archaea order *Sulfolobales*, isolated in aerobic and microaerobic conditions, the 3-hydroxypropionate/4-hydroxybutyrate cycle converts two molecules of bicarbonate to acetyl-CoA. First the bicarbonate ions are fixed to 3-hydroxypropionate, which is processed leading to succinyl-CoA, further processing leads to acetyl-CoA release (Auernik et al., 2008; Ramos-Vera et al., 2011). The last acetyl-CoA utilizing cycle is the 3-hydroxypropionate bi-cycle (Herter et al., 2002; Zarzycki et al., 2009). In the first branch of the cycle glyoxylate is produced from acetyl-CoA and bicarbonate, then the second branch consumes propionyl-CoA produced by the first branch together with glyoxylate yielding pyruvate and again acetyl-CoA.

It is important to highlight how these five pathways are not the only ones possible, and other ways to fix carbon can still be discovered. An interesting example is the reductive hexulose-phosphate pathway (RHP) recently discovered in *Methanospirillum hungatei* by Kono et al. (2017). The RHP contains both archaeal RuBisCO and PRK allowing fixation of CO₂ and regeneration of the initial substrate. The newly fixed carbon is released as formaldehyde during the reactions in the regeneration phase, which are different from Calvin-Benson cycle. Final steps of the regeneration stage are catalyzed by 6-phospho-3-hexuloisomerase producing hexulose-6-phosphate and D-arabino-3-hexulose-6-phosphate synthase, producing Ru5P then phosphorylated by PRK.

Despite these procaryotic metabolisms do not largely contribute to the global fixation, those reactions are important for new biotechnological applications and in biological niches, in particular anaerobic niches where primary producers like plants and cyanobacteria cannot live (Friedrich et al 2005; Montoya et al., 2012).

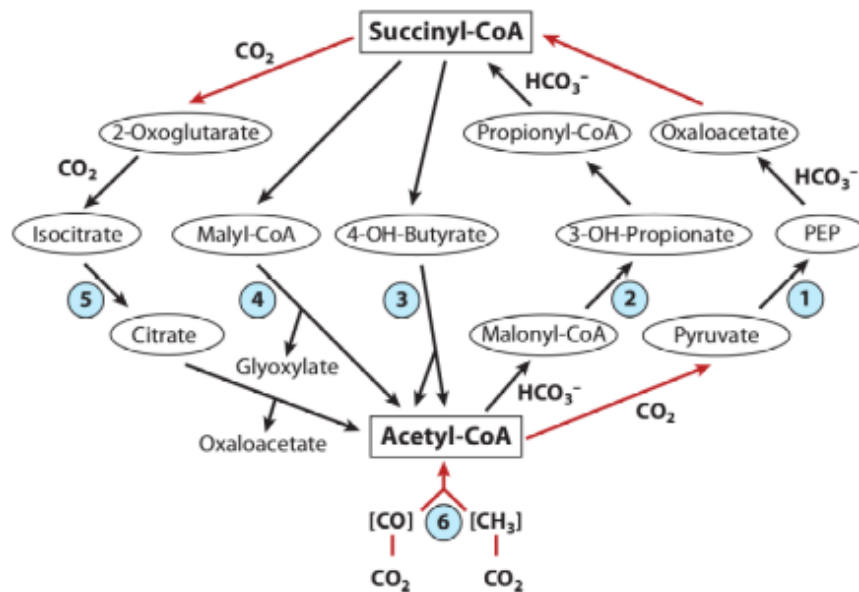


Figure 1.3 Schematic representation of carbon fixation pathways in prokaryotes. Combination of paths from 1 to 5 results in all the fixation pathways. Combining path 1 and 5 results in the reductive citric acid cycle. The combination of path 1 and path 3 yields the dicarboxylate/4-hydroxybutyrate cycle. Path 2 and 3 result in the 3-hydroxypropionate/4-hydroxybutyrate cycle, and combining path 2 and 4 generates the first cycle of the 3-hydroxypropionate bi-cycle, which requires an additional cycle for glyoxylate assimilation. The path 6 represents the reductive acetyl-CoA pathway, which requires the path 1 for the assimilation of acetyl-CoA. Oxygen-sensitive enzymes/reactions are represented by red arrows. The figure is adapted from Fuchs (2011).

1.3 The metabolism of starch in leaves

The CO_2 fixation in oxygenic photosynthetic organism is a light-driven process, meaning that from the dark onset until the next day the metabolism need to rest on a different carbon source. For this reason, freshly fixed carbon follows two different directions. Sugars can be immediately consumed to supply biosynthetic and energetic reactions, or they can be transiently immobilized in storage compounds that will be used during the night.

Depending on the plant species, a certain variability in transient carbon storage can be observed. The synthesis of starch in the chloroplast stroma during the day is a conserved feature in land plants (Weise et al., 2011). However, although species like *Arabidopsis thaliana*, sugar beet and soybean accumulate starch (Zeeman and ap Rees, 1999; Fondy et al., 1989; Upmeyer and Koller, 1973) other species, like *Phaseolus vulgaris* and spinach, store sucrose (Fondy et al., 1989; Stitt et al., 1983) and cereals and grasses can accumulate oligosaccharides such as fructans and raffinose (Pollock and Cairns, 1991; Bachmann and Keller, 1995; Zeeman et al., 2007).

Generally, starch granules are composed by 70-90% of amylopectin and 10-30% of amylose (Tester et al. 2004), which are both polymers of α -D-glucose but with different structural features (Figure 1.4). Amylopectin is made up of α -1,4-linked glucose units forming long chains with regularly arranged α -1,6 branching points. While amylose consists of α -1,4 glucose chains without branching

points. The linear chains are packed in double helices, producing a crystalline insoluble structures defined lamellae. Lamellae alternate with branching points that are grouped in amorphous regions (Santelia and Zeeman, 2011).

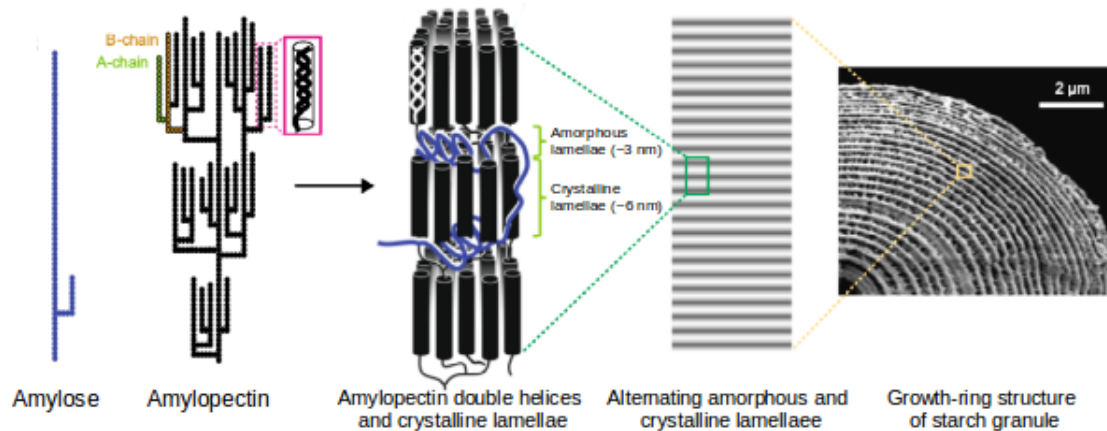


Figure 1.4 The structure of starch granule. Figure adapted from Pfister and Zeeman, 2016.

Starch granules are stored both in leaves and storage organs, like tubers and roots, and in seeds, like in grain crops as maize, rice and wheat. However, starch is always stored in plastids: chloroplasts in the leaf, amyloplasts in storage organs. Starch granules have always the same structure but the turnover changes depending on the organ, while leaf starch is degraded at night, starch from storage organs is degraded in specific conditions (*e.g.* in response to gibberellin during germination).

1.3.1 Diurnal starch biosynthesis

Transitory starch is synthesized in the daylight from photoassimilates. Then during the night, leaf starch content is almost depleted to fuel plant metabolism. Starch biosynthesis starts with F6P released by the FBP during the Calvin-Benson cycle (Figure 1.5). F6P is converted in glucose-6-phosphate (G6P) by the hexose phosphate isomerase (PGI). The phosphate group on C6 is then transferred on C1 by phosphoglucomutase (pPGM).

pPGM is crucial for starch biosynthesis and *ppgm* knock-out (KO) mutants are described almost starchless (0.3% of wild-type level) and, if starch granules are found, they are tiny compared to wild-type ones (Caspar et al., 1985; Hanson and McHale, 1988; Streb et al., 2009). Many data agree considering pPGM as the main gate for the carbon flux into starch biosynthesis.

Another important enzyme in the biosynthetic pathway is the ADP-glucose pyrophosphorylase (AGPase), an heterotetramer made up of two large subunits, with regulatory function, and two small catalytic subunits, that catalyzes the formation of ADP-glucose from ATP and glucose-1-phosphate, releasing pyrophosphate (PPi) (Streb et al., 2009; Ragel et al., 2013). PPi is then hydrolyzed by

chloroplast pyrophosphatase promoting the synthesis of ADPglucose (ADPglc). Indeed the pyrophosphatase was shown to be essential for chloroplast central metabolism (George et al., 2010). ADPglc is the building block of starch thanks to Starch Synthases (SSs), which add glucose units to the non-reducing end of glucans. In land plants five isoforms of SS have been found (Ball and Morrel, 2003). The Granule-Bound Starch Synthase (GBSS) is the unique starch synthase responsible for amylose synthesis. Indeed *gbss* knock-out mutants from several species show a full-amylopectin starch (Pfister and Zeeman, 2016). GBSS is embedded in the granule during starch biosynthesis and is not present in soluble form in the stroma (Denyer et al., 2001).

Contrary to GBSS, the other four SS are soluble enzyme. Three of them seem to act mainly on an already existing granule, thus contributing to the growth and the architecture of the starch granule. SS1, SS2 and SS3 elongate amylopectin chains, in contrast SS4 appears to play a crucial role in starch granule initiation, producing glucan primers afterwards elongated by the others SSs. Indeed, *ss4* KO lines have one or no starch granule in contrast to 5-8 granules of the wild-type, and accumulate almost 200-fold more ADPglc than wild-type plants (Roldán et al., 2007; Crumpton-Taylor et al., 2013; Ragel et al., 2013). Overall, these data reveal how the other SSs have extremely low activity without SS4.

In two recent papers (Seung et al., 2015; Seung et al., 2017) a new protein family named Protein Targeting to Starch (PTST) has been identified by phylogenetic analysis. PTSTs are characterized by coiled-coil domains and Carbohydrate Binding Module 48 (CBM48). First evidences suggest PTSTs support the activity of SSs enzymes, probably providing them substrates. The coiled-coils allow direct interactions with SSs while substrates are bound by PTSTs thanks to a CBM48 domain. In *Arabidopsis thaliana* 3 PTSTs have been found (Seung et al., 2015; Seung et al., 2017). PTST1 interacts with the unique GBSS, facilitating its amylose-elongating activity (Seung et al., 2015). KO lines for *ptst2*, and in part for *ptst3*, showed normal starch content. However, starch granules in *ptst2* are bigger and their number is lower (Seung et al., 2017), moreover these plants accumulate ADPglc at high levels, even if less than *ss4* KO. Considering all the available data, the initial model for PTST2 and 3 function hypothesize that PTST2 interacts with SS4 and provides malto-oligosaccharide subsequently elongated consuming ADPglc, in turn PTST3 binds PTST2 helping its activity. In Seung et al. (2017) was also hypothesised that PTST2 could improve the specificity of SS4 reaction recognising helical glucan chains, since SS4 seems to have no preference for malto-oligosaccharides (Cuesta-Seijo et al., 2016).

For proper amylopectin formation the activity of branching and debranching enzymes (BE and DBE, respectively) are required (Zeeman, Kossmann and Smith, 2010). DBEs hydrolyze α -1,6-

linkages and release linear chains. They can be divided in two classes: isoamylases (ISAs) and limit-dextrinase (LDA).

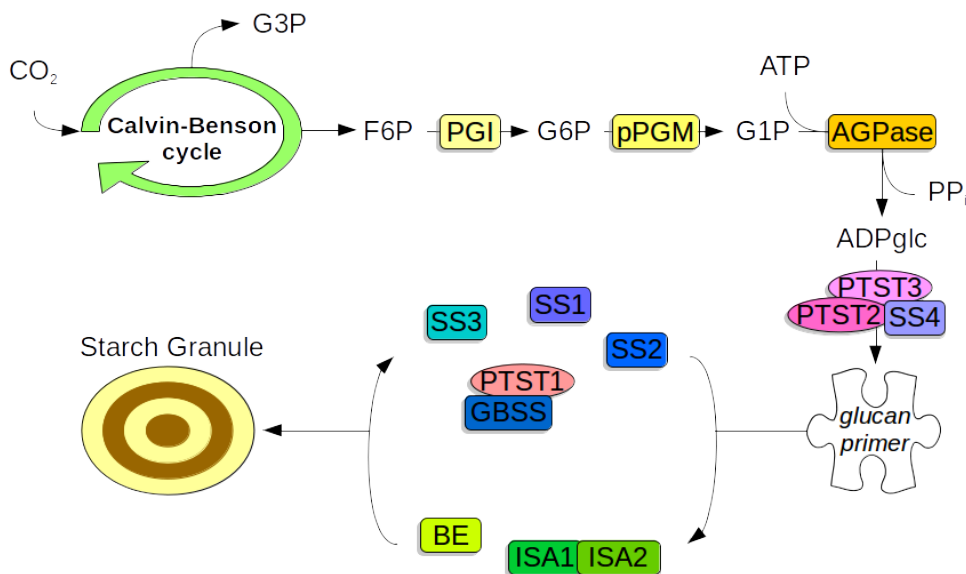


Figure 1.5 Transitory starch biosynthesis. ADPglc, ADP-glucose; AGPase, ADP-glucose Pyrophosphorylase; BE, Branching Enzyme; F6P, Fructose-6-phosphate; G1P, Glucose-1-phosphate; G3P, Glyceraldehyde-3-phosphate; G6P, Glucose-6-phosphate; GBSS, Granule-Bound Starch Synthase; ISA, Isoamylase (Debranching Enzyme); PGI, Phosphoglucoisomerase; pPGM, plastidial Phosphoglucomutase; PTST, Protein Targeting to Starch; SS, Starch Synthase.

In *Arabidopsis* ISA1 and ISA2 are involved in amylopectin elongation, while ISA3 and limit-dextrinase (LDA) are primarily involved in starch breakdown (Myers et al., 2000; Pfister and Zeeman, 2016). BEs cleave an α -1,4 glucan chain and transfer the cut to another chain, producing α -1,6 bond. BESs are grouped into two classes according to sequence similarities (Pfister and Zeeman, 2016). Branching activity is required for amylopectin synthesis, albeit BEs are not the sole determinants for the synthesis of crystallization-competent glucans (Pfister and Zeeman, 2016). Simultaneously to BE action, DBEs trim the excess of branching point, allowing SS to elongate just correctly localized branches. In fact, by abolishing the activity of DBEs, the formation of starch granules is impaired due to the impossibility of proper packing of amylopectin (Delatte et al., 2005; Wattedled et al., 2005).

The concurrent action of all these proteins contributes to the production of insoluble and highly ordered starch granules, two important features to improve compactness and allow accumulation of carbohydrates without affecting the osmotic balance.

1.3.2 Starch degradation at night

The breakdown of leaf starch has been mostly characterized in *Arabidopsis thaliana*, where the key reactions and enzymes have been discovered (Figure 1.6). Transitory starch degradation retains common features with the starch degradation in storage organs and non-photosynthetic tissues

(Zeeman et al., 2007). In fact the first step of the pathway is the phosphorylation of glucan chains on the granule surface. An enzyme called α -glucan, water dikinase (GWD1), initially found in potato and *Arabidopsis* (Nielsen et al., 1994; Yu et al., 2001), is responsible for this reaction. The phosphorylation occurs at low rate during day and at higher rate during the night (Ritte et al., 2004) and represents a crucial step for the subsequent glucan degradation (Edner et al., 2007). The reaction catalysed by GWD1 starts with the initial phosphorylation of a water molecule, resulting in a release of inorganic phosphate, then the β -phosphate of the ATP is transferred on the C6, preferentially, or on the C3 of the glucose units belonging to a glucan chain (Ritte et al., 2002). Another dikinase is involved downstream GWD1 and phosphorylates amylopectin exclusively in C3 position of C6-phosphorylated glucans, for this reason it has been called phosphoglucan, water dikinase (PWD; Kötting et al., 2005; Baunsgaard et al., 2005). The role of phosphorylation has still to be demonstrated, but a disrupting effect on amylopectin packing has been hypothesized (Yu et al., 2001). The disruption should be due to the hydrophilic properties of phosphates, as consequence glucans in starch become more soluble and accessible to degrading enzymes (Blennow and Engelsen, 2010).

Despite their essential role for glucan accessibility, phosphate groups inhibit the activity of glucan hydrolases involved in starch degradation (Fulton et al., 2008). For this reason, two phosphatases, Starch excess 4 (SEX4) and Like Sex Four 2 (LSF2) evolved to remove phosphate groups from C6 and C3, respectively (Kötting et al., 2009; Meekins et al., 2014; Santelia et al., 2011).

The β -amylases (BAMs) are responsible for most of the transitory starch degradation, they are exo-amylases that start degrading starch from the non-reducing end of linear glucans releasing β -maltose. In *Arabidopsis thaliana* BAM3 and BAM1 are the two main amylases. Their function is partially redundant, as highlighted by the double KO mutant *bam1bam3* which showed a stronger starch excess (*sex*) phenotype compared to single KO mutants (Fulton et al., 2008). Apparently the roles of the two BAMs do not overlap under stress conditions, BAM1 takes part to osmotic stress response (Zanella et al., 2016) while BAM3 to cold stress response (Kaplan and Guy, 2004).

Since BAMs cannot hydrolyze glucan chain at the branching point, debranching enzymes are required. ISA3 and LDA hydrolyze the branching points (Wattebled et al., 2005; Delatte et al., 2006) allowing the BAMs to continue. LDA seems to have a minor role in the debranching activity, as highlighted by *lda* KO lines, which do not display a *sex* phenotype (Streb et al., 2012).

The pathway for degradation of storage starch, like that in cereal endosperm and tubers, is different and typically performed by α -amylases (Lloyd and Kossmann, 2015). To clarify if α -amylases could have a role also in transitory starch degradation AMY3, the unique plastidial *Arabidopsis* α -amylases, has been frequently studied. In Yu et al. (2005) emerged as *Arabidopsis* plants lacking

AMY3 have no alteration of leaf starch content and only minor variations in the sugar amounts. In any case, AMY3 could release phospho-oligosaccharides from leaf starch *in vivo*, demonstrating that AMY3 attacks starch granules but is not essential for starch degradation (Kotting et al., 2004). Horrer and colleagues (2016) demonstrated that BAM1 and AMY3 have a specialized role in stomata opening, catalyzing the release of carbon in guard cells linked to the opening of stomata pores. On the whole, these data suggest a marginal role of BAM1 and AMY3 in starch degradation at night.

The product of debranching enzymes and α -amylase lead to linear and soluble glucans. Soluble glucans are further degraded by BAMs and by glucan phosphorylase, producing G1P (Smith et al., 2005). Glucan phosphorylase plays a secondary role in the overall degradation, whereas BAMs are the principal enzymes for transitory starch degradation.

The maltose released by BAMs activity is then exported in the cytoplasm by means of MEX1, a maltose transporter localized in the inner membrane of the chloroplast envelope (Niittyala et al., 2004).

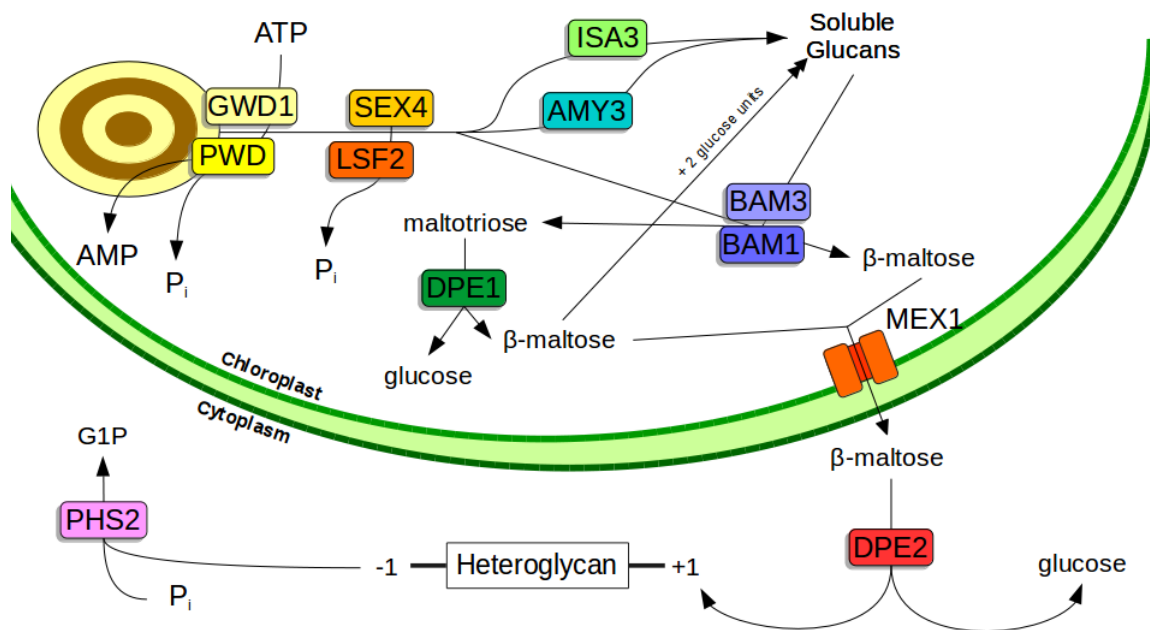


Figure 1.6 Transitory starch degradation. From left to right: GWD1, Glucan, Water Dikinase 1; PWD, Phosphoglucan, Water Dikinase; SEX4, Starch Excess 4 (phosphatase); LSF2, Like Sex Four 2 (phosphatase); ISA3, Isoamylase 3 (Debranching enzyme); AMY3, α -amylase 3; DPE1, Disproportionating Enzyme 1; BAM1, β -amylase 1; BAM3, β -amylase 3; MEX1, Maltose Excess 1 (transporter); DPE2, Disproportionating enzyme 2; PHS2, Glucan Phosphorylase 2.

Since BAMs are not active on glucans shorter than 4 glucose units, maltotriose is also produced as byproduct. Maltotriose is hydrolized by the chloroplast disproportionating enzymes (DPE1), an α -1,4-glucanotransferase (Critchley et al., 2001). DPE1 hydrolizes maltotriose into glucose and

maltose. While glucose is exported via glucose exporters, the maltose unit is transferred to another maltotriose molecule (Weber et al., 2000).

Variation on the turnover pathway are possible depending on the species, and homologous enzymes without a clear phenotype in Arabidopsis could have relevant role in other plants (Zeeman et al., 2007).

1.3.3 The cytosolic metabolism of starch-released sugars

Maltose and glucose are the end-products of the starch degradation in leaves, both are exported in the cytoplasm for further processing (respiration, biosynthetic reactions) and transport in other tissues. While the glucose can directly enter in the cell metabolism, maltose needs additional hydrolysis (Figure 1.6). In the cytoplasm two enzymes are responsible for the hydrolysis of maltose to glucose, exploiting cytosolic heteroglycans that act as a sugar buffer, *i.e.* as donor and acceptor of sugar units. The heteroglycans consist of glucose, galactose, arabinose, mannose, rhamnose and fucose with different abundance and kind of linkages (Lu and Sharkey, 2004; Fettke et al., 2005a). The maltose-processing enzyme is DPE2, a cytosolic isoform of the chloroplast disproportionating enzyme. DPE2 is an α -1,4-glucan transferase which transfers α -1,4-linked glucan from one glucan to another (Chia et al., 2004; Lu and Sharkey, 2004). In the current model maltose is splitted in two glucosyl residues, one is transferred to a heteroglycan while the other contributes to the glucose pool (Fettke et al., 2006). Then, the phosphorylase PHS2 (or PHO2) uses orthophosphate as acceptor molecule of a glucosyl residue from the heteroglycan, releasing glucose-1-phosphate (G1P). The PHS2 reaction is reversible, so it is possible that depending on metabolic conditions of the cell PHS2 catalyses heteroglycan elongation (Fettke et al., 2005b). Glucose molecules are phosphorylated by hexokinase to glucose-6-phosphate (G6P) while G1P can be isomerized to G6P and vice versa by cytosolic phosphoglucomutase (PGM). Additionally, PGI catalyses the interconversion of G6P to F6P. As active sugars, all these hexose phosphates can take part of the cellular metabolism.

G1P could be also converted to UDP-glucose by UDP-glucose pyrophosphorylase (UGPase) (van Rensburg and Van den Ende, 2018), replenishing biosynthetic pathways, like cell wall biosynthesis, although the physiological role of UGPase is still unclear (Meng et al., 2009).

The fate of the hexose pool relies on the metabolic requirements of cell/tissue, typically hexoses are consumed by sucrose synthesis or channelled through the central metabolism via glycolysis, Krebs cycle for biosynthesis or for energetic demands.

1.4 Sucrose metabolism

In photosynthetic tissues, triose phosphates deriving from diurnal carbon fixation and hexoses deriving from starch degradation at night converge in sucrose biosynthesis. Sucrose is transported through the phloem from source tissues (old leaves, storage tissues) to sink tissues (roots, meristems, fruits, flowers and young leaves). In sinks sucrose is degraded fuelling cell metabolism and tissue development providing carbon for the respiratory pathway, biosynthetic reactions and regulating gene expression by itself or through its degradation products by means of sugars sensors and sugar-responsive elements (Li and Sheen, 2016; Koch, 1996; Sheen et al., 1999).

1.4.1 Sucrose biosynthesis in photosynthetic tissues

Leaves constitute the primary carbon source, inside leaves the coupled action of two cytosolic enzymes produce sucrose for sink tissues (Figure 1.7, upper part). Sucrose phosphate synthase (SPS) condenses UDP-glucose and F6P to sucrose-6-phosphate subsequently hydrolyzed to sucrose by the sucrose-phosphate phosphatase (SPP). Another enzyme category can yield sucrose, starting from UDP-glucose and fructose, the sucrose synthase (SUS). Nevertheless it is generally accepted that SPS is responsible for synthesis and SUS preferentially catalyzes the breakdown of sucrose. Indeed several tissues mainly express just one of the two enzymes, but in some cases co-expression has been observed (Huber and Huber, 1996). Co-expression of SPS and sucrose degrading enzymes could lead to sucrose futile cycle which can help in tuning carbon partitioning (Nguyen-Quoc and Foyer, 2000; Ruan, 2014).

Plant SPSs are classified in three evolutionary groups: A, B and C (Langenkämper et al., 2002). From a phylogenetic point of view, specific isoforms for each group are found in dicotyledon and monocotyledon plants (Lutfiyya et al., 2007). The major isoform in tobacco leaves is SPSC (Chen et al., 2005), as well as in *Arabidopsis thaliana*, in which also SPSC1 acquired a relevant role (Volkert et al., 2014). In *Arabidopsis* all SPS have overlapping roles and, depending on the isoform, they can completely or partially compensate the absence of the other. In any case, different spatial and temporal expression patterns have been observed (Bahaji et al., 2015).

1.4.2 Phloem loading and sucrose transport

The link between source and sink tissues is the phloem, a vascular tissue constituted by specialized living cells. In flowering plants, the functional unit of phloem are sieve elements and companions cells. The sieve elements are stacked one over the other and connected internally, they contain an

endoplasmic reticulum, rudimentary plastids and mitochondria but no cytoskeleton and nucleus. Being without nucleus they depend on companion cells for maintenance of cellular components. Companion cells are tightly linked to sieve elements through plasmodesmata, providing essential elements like proteins and contributing to the phloem loading. Inside the sieve elements flows the phloem sap, which is loaded by source tissues and delivers nutrients and signals to sink tissues.

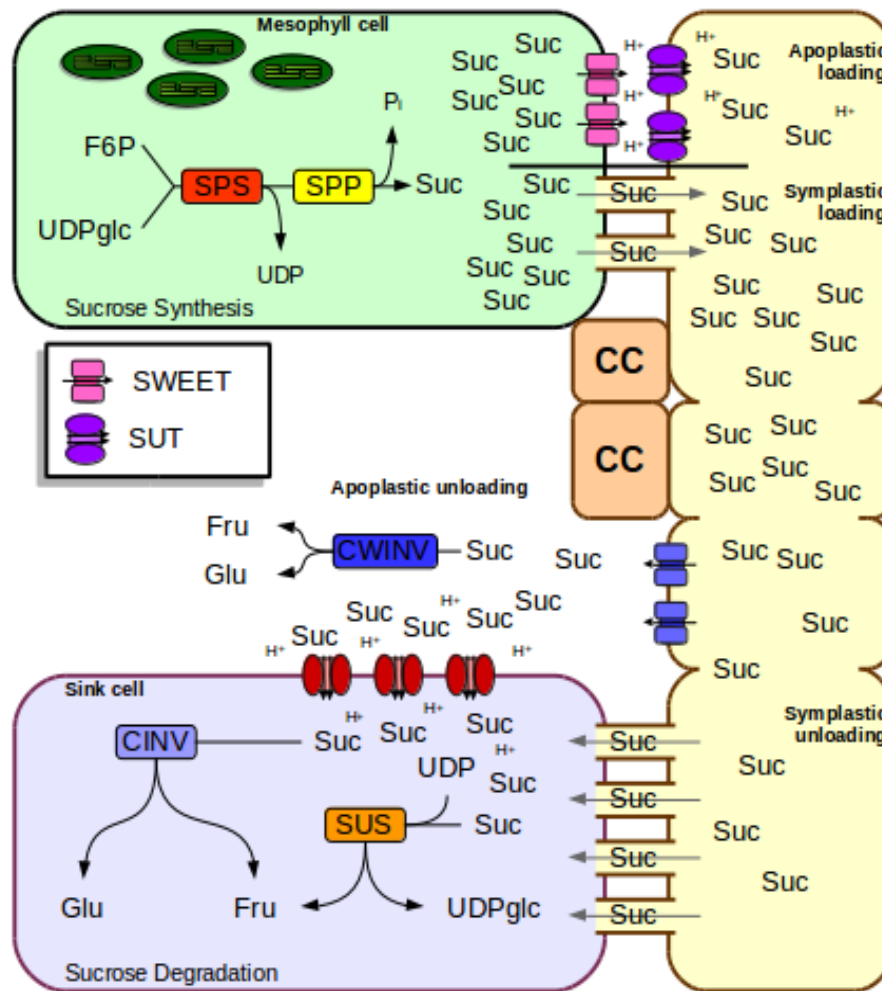


Figure 1.7 Sucrose metabolism and transport. Sucrose is synthesized in source tissues (e.g. mesophyll cells) by concerted activity of sucrose phosphate synthase (SPS) and sucrose phosphate phosphatase (SPP). Then sucrose is exported into sieve tube elements (pale yellow) via apoplastic loading thanks to coupled action of sucrose facilitators (SWEET) and sucrose/H⁺ symporter (SUT) or via symplastic loading through plasmodesmata. Phloem sap flows delivering sucrose to sink cells, where sucrose uptake occurs thanks to plasmodesmata (symplastic unloading) or transporters (SWEETs and SUTs). Sucrose degradation is then performed by Cytosolic Invertases (CINV), Cell Wall Invertases (CWINV) and Sucrose Synthases (SUS).

Sucrose produced in leaves is massively loaded in phloem following two possible mechanisms: apoplastic and symplastic loading (Figure 1.7, upper part). In apoplastic loading sucrose is first exported in the apoplast and then is loaded into the phloem against the concentration gradient. It is generally found in herbaceous species and it is the most studied because of agricultural interest (Zhang and Turgeon, 2018). The symplastic loading occurs by diffusion thanks to plasmodesmata

directly linked to the sieve elements of the phloem. Symplastic loading is generally ascribed to trees like poplar (Zhang et al., 2014). The two strategies are not exclusive and the same plant can load phloem in different ways depending on cell and tissue type or developmental stage (Slewinski et al., 2013). In *Arabidopsis* and crops, like rice, phloem is loaded from the apoplast through SWEET uniporters (Sugar Will Eventually be Exported Transporters) and sucrose/H⁺ symporters (SUT - Sucrose Transporter). The first exports sucrose in the apoplast (Chen et al., 2012; Eom et al., 2015), then the latter is localized on sieve elements membranes and loads sucrose together with a proton, consuming the energy of the proton gradient (Julius et al., 2017). SWEET uniporters were recently identified as a family of sugars transporters conserved in plants and animals (Chen et al., 2010), the clade 3 of SWEET family was demonstrated to be the key facilitator of sucrose efflux in the apoplast (Chen et al., 2012). SUTs are divided in 5 evolutionary clades (Kühn and Grof, 2010). SUT1 clade is specific of dicotyledons whereas SUT3 and 5 of monocotyledons, clades 2 and 4 are common of both groups of plants. Different affinities have been measured on these transporters, reflecting different plant- and tissue-related physiological role (Kühn and Grof, 2010). SUT1 has the highest affinity, SUT3 has intermediate values and together with SUT5 they localize in source tissues on plasma membrane of phloem elements. SUT2 showed the lowest affinity as well as SUT4, both localize on plasma membrane in sink tissues, but SUT4 is found in plastid and vacuole membrane inside the cell (Kühn and Grof, 2010). Apparently phloem loading from apoplast is an energy demanding process but transporters different from SUTs have been found, for example in legumes sucrose facilitators localize on sieve element membranes acting in pH- and energy-independent manner and suggesting variations on the classical model (Zhou et al., 2007).

1.4.3 Phloem unloading and sucrose degradation

Due to massive loading in source tissues, the concentration of solutes in sieve elements is higher enough to lower the osmotic potential of phloem in source tissues, in this way water moves into the sieve elements thanks to aquaporins passively driving the sap flow to sink organs, where the osmotic potential is higher as result of phloem unloading (Zhang and Turgeon, 2018). Two models illustrate the unloading process, the apoplasmic and the symplasmic unloading, and a combination of the two was also detected (Figure 1.7, lower part). The two strategies depend more on tissue type than plant type, in fact apoplasmic unloading occurs in stems and roots, and consists of transfer of sucrose from phloem to the apoplast and subsequent transfer into the sink cell. Usually a sucrose facilitator, like AtSWEET11 and 12 (Le Hir et al., 2015), permits sucrose efflux from sieve elements and an active transporter catalyzes the uptake of sucrose into the cell, for example SUT1 in *Arabidopsis* and SUC1 in *Zea mays* (Carpaneto et al., 2005; Sivitz et al., 2008). In the

symplasmic unloading the sucrose is directly delivered inside the sink cell through plasmodesmata, this latter case is found in meristems, tubers and root tip (Milne et al., 2018).

Once sucrose is exported, two enzymes are responsible for its degradation, invertases (INV) and sucrose synthases (SUS). INVs catalyze the hydrolysis of sucrose to fructose and glucose. INV are classified on the basis of their subcellular location. Cell wall INVs (CWINV) was demonstrated to be involved in the sucrose breakdown in sinks where the apoplasmic unloading takes place (Ruan, 2014). Apoplast degradation of sucrose leads to lower sucrose concentration, that drives the phloem unloading, and hexoses release. Cytosolic invertases (CINV) could be implicated in sucrose degradation during the symplasmic unloading, although SUSs reaction (see above, Paragraph 1.4.1) are more likely involved in cytosolic sucrose breakdown and are generally considered a marker of sink strength (Koch, 2004).

1.5 Carbon fluxes under abiotic stress

Importance of characterizing plant metabolism under abiotic stress is undoubted. Beyond its relevance for fundamental knowledge, understanding how plants set up their metabolism in adverse conditions is also crucial to select useful traits for crop resistance in challenging environments. Rearrangements in carbon metabolism are not equally studied for all stress conditions and so far most of the available information are from analysis on primary carbon metabolism under drought/osmotic stress. For this reason and for further interest in the thesis work, this paragraph will focus mainly on water deficiency and, when available, further details on other stress will be discussed.

Hummel and colleagues (2010) carried out an extensive survey on metabolites, enzymes and physiological traits in *Arabidopsis thaliana* under water deficiency. When *Arabidopsis* plants are exposed to moderate or severe drought (water potential equal to -0.6 MPa and -1.1 MPa respectively) they did not observe significant decrease of net photosynthesis or increase in respiration. Data on CO₂ fit well with data on enzyme activities from main carbon pathways like Calvin-Benson cycle, starch metabolism, sucrose metabolism and tricarboxylic acids cycle. Indeed, monitoring all enzymatic activities in optimal catalytic conditions, enzymes levels were globally stable or just slightly increased (Hummel et al., 2010; Bogaert-Triboulot et al., 2007; Pinhero et al., 2001). Underlining how metabolic response does not need massive changes but more definite and distinctive adaptations (Yu et al., 2003; Bogaert-Triboulot et al., 2007). At the same time enzymes activities can be modulated without affecting enzymes content, for example in *Trifolium*

subterraneum RuBisCO activity is decreased by drought, indicating some inhibitory effect induced by the stress (Medrano et al., 1997).

Transitory starch, deriving from recently fixed carbon, is emerging in the last few years as carbon source for abiotic stress response (Thalmann and Santelia, 2017), in addition to its role in carbon metabolism in the night. Indeed, in several challenging conditions transitory starch degradation has been reported in green algae, mosses, cereals and woody plants (Villadsen et al., 2005; Pressel et al., 2006; Goyal, 2007; Damour et al., 2008; Hummel et al., 2010). However, it should be noted that other studies reported increased starch accumulation under abiotic stress (Kaplan and Guy, 2004; Cuellar-Ortiz et al., 2008; Siaux et al., 2011; Wang et al., 2013). It is still unknown if the balance between starch synthesis and degradation is typical of each stress or it depends more on specific experimental conditions (Thalmann and Santelia, 2017). Despite all, several studies reported a positive correlations between stress tolerance and starch degradation (Nagao et al., 2005; Cuellar-Ortiz et al., 2008; Gonzalez-Cruz and Pastenes, 2012; Zanella et al., 2016; Thalmann et al., 2016). Yano et al. (2005) reported a concerted action of GWD1 and BAM3 in transitory starch mobilization in *Arabidopsis* plants exposed to cold stress.

Starch degradation pathway under stress does not necessarily follow the canonical pathway (see section 1.3.2). In fact under osmotic stress several experiments showed the importance of BAM1 and AMY3, which gene expression is driven by ABA signalling, typically activated under water stress (Zeller et al., 2009; Valerio et al., 2011; Zanella et al., 2016; Thalmann et al., 2016). Moreover a role for α -glucan phosphorylase PHS1 was suggested under drought and high salinity (Zeeman et al., 2004). These three enzymes are not essential for normal transitory starch degradation at night. It is noteworthy that selection of particular enzyme isoforms is not just a matter of gene expression and distinct biochemical properties should make BAM1 and AMY3 adapted to stress conditions. Indeed both the enzymes are activated by disulphide bond reduction *in vitro*, suggesting increased activity in the day, and also pH optima are shifted to more alkaline values, similar to stromal pH at light (Sparla et al., 2006; Seung et al., 2013).

When water levels are reduced *Arabidopsis* plants change the growth pattern of the rosette. The rosette expansion is distributed along both day and night, with almost 50% of expansion occurring at night. Under water deficiency the rosette expansion is 40% faster at day and inhibited at night (Hummel et al., 2010). In addition also leaf emergence-expansion rate is lower. In this way plants improve growth during the day when energy and carbon are available and store sources at night for the next day.

Although the rosette growth is decreased, the photosynthesis is not impaired thus a surplus of carbon is generated. Compounds with low molecular mass raise and are probably exported in roots,

since 30% more root mass is observed (Hummel et al., 2010). Raise of sugar content is observed also in maize kernels and seems to be of central importance for drought tolerance (Yang et al., 2018). Accumulation of compounds like sugars can help adjusting the osmotic balance in leaves (Xu et al., 2007; Hagemann and Pade, 2015), but also protect membranes and scavenge reactive species under cold, temperature and salt stress (Garg et al., 2002; Janska et al., 2010; Yuanyuan et al., 2009; Krasensky and Jonak, 2012). In fructan accumulating species, fructans provide freeze resistance thanks to their high solubility (Livingston et al., 2009; Pomerrenig et al., 2018). Sugars are also substrates for sugar alcohols synthesis, typically produced to enhance drought tolerance and scavenge ROS (Smirnoff and Cumber, 1989; Pomerrenig et al., 2018). The accumulation of sugars could be a consequence of several factors like reduced growth of photosynthetic tissues (Hummel et al., 2010), impaired catabolism in sinks and reduced sink strength (Quick et al., 1992) or reduced phloem sap flow due to compensatory water transfer from phloem to xylem (Sevanto et al., 2014). In response to drought Hummel et al. (2010) also describe accumulation of amino acids, fumarate, proline and sucrose, with more fumarate under severe drought. These metabolites are not simply accumulated and stored to recover the osmotic balance, they are also available to plant metabolism. In fact a clear decrease is observed at night for proline, malate and soluble sugars, probably consumed when other carbon sources are not available.

Since drought stress lead to water loss, Hummel et al. (2010) calculated the concentrating effect on osmolytes observed in *Arabidopsis* and reported that the 66% of the osmotic potential generated by the plant under stress is obtained thanks to the decrease in water content. Anyway, metabolic processes need physiological water levels to work properly and the plant synthesized osmolytes to further counteract the water loss. The osmolytes accumulation is responsible for the 33% of the osmotic potential generated under drought.

Considering the energetic balance of the whole plant, the carbon cost is estimated to be 1-3% of the daily photosynthetic yield (without considering the ATP consumed for biosynthetic reactions), so osmotic adjustment does not need high carbon cost or even lead to carbon depletion (Hummel et al., 2010).

1.6 Regulation of carbon metabolism

In absence of stress, plants manage their carbon to maximize growth (Rasse and Tocquin, 2006). In order to achieve this aim almost all the transitory starch fixed during the day is linearly degraded during the night (Smith, 2012). The nearly depletion of starch ensure the best exploitation of carbon

sources but excessive degradation speed would lead to carbon starvation at the end of the night. Environmental clues and circadian rhythms are complemented to control carbon mobilization and avoid starvation (Lu et al., 2005; Graf et al., 2010; Troein et al., 2009; Farre and Weise, 2012). Management of carbon sources takes place during all the day and is adjusted on the length of the photoperiod. For example, Arabidopsis plants grow preferentially during the light period, but 50% of growth is observed at night under 6 hours photoperiod (Sulpice et al., 2014). Not only the mobilization of carbon is modulated, in the case of starch the biosynthesis is more responsive in short daytime and suddenly starts at the beginning of the day, to ensure maximal exploitation of light energy, whereas when light is not limiting a lag in starch synthesis is observed (Sulpice et al., 2014). Several regulatory strategies are adopted to control carbon metabolism, regulation by redox modifications, circadian control, sugar-sensing and phosphorylation are the most known.

1.6.1 The redox regulation

The sensitivity of enzymes to the redox state of the cell is an important factor, especially in carbon fixation. The redox state is directly linked to the availability of reducing power in the plant and so to the energetic status of cell, tissue or organism. Redox regulation in proteins involves cysteine residues and its reaction with other thiols or reactive species of oxygen and nitrogen (ROS and RNS, respectively), only for RNS regulation other protein residues seem to be involved (Sevilla et al., 2015).

Protein cysteines form disulphide bonds, bind metal ligands, coordinate substrates, have catalytic functions and could be subjected to different post-translational modifications. The sensitivity to redox modifications lies on higher reactivity of specific cysteines, given by lower ionization constant (pK_a). Indeed if compared to free cysteines ($pK_a = 8.3$) reactive cysteines have more acidic constant and propensity to unprotonated form. Several features in the microenvironment determine a lower pK_a , like the presence of charged amino acids stabilizing unprotonated thiol, hydrogen bonds or dipole effect, often generated by N-terminal position of the reactive cysteine residue in α -helix (Couturier et al., 2013).

For what concerns primary carbon metabolism, it is fundamental to couple the photosynthetic energy production to carbon fixation and storage, avoiding energy waste and detrimental reactions. The synchronization is performed by the thioredoxin (TRX) system, which represents the first form of redox regulation discovered (Geigenberger et al., 2017). Further importance is given by the ability redox regulatory systems to react under developmental and stress conditions allowing carbon metabolism to set up in function of internal or external stimuli.

1.6.1.1 The thioredoxin system and NADPH-thioredoxin reductase in chloroplast

The basic principle of the TRX regulation is the possibility of thiol groups inside proteins to form reversible disulphide bonds. Regulatory thiols are localized in specific positions of enzymes and once oxidized typically inhibits catalytic activity, but one case of activation has been reported (Wenderoth et al., 1997; Gütle et al., 2017). The regulatory effect is obtained by closing the active site or preventing the access of substrates to the catalytic residues. Among the different ways to control enzyme activity the reversible formation of disulfide bond makes possible a fast control of the enzyme and avoids energy-demanding mechanisms like alternation of degradation and synthesis (Brandes et al., 2009).

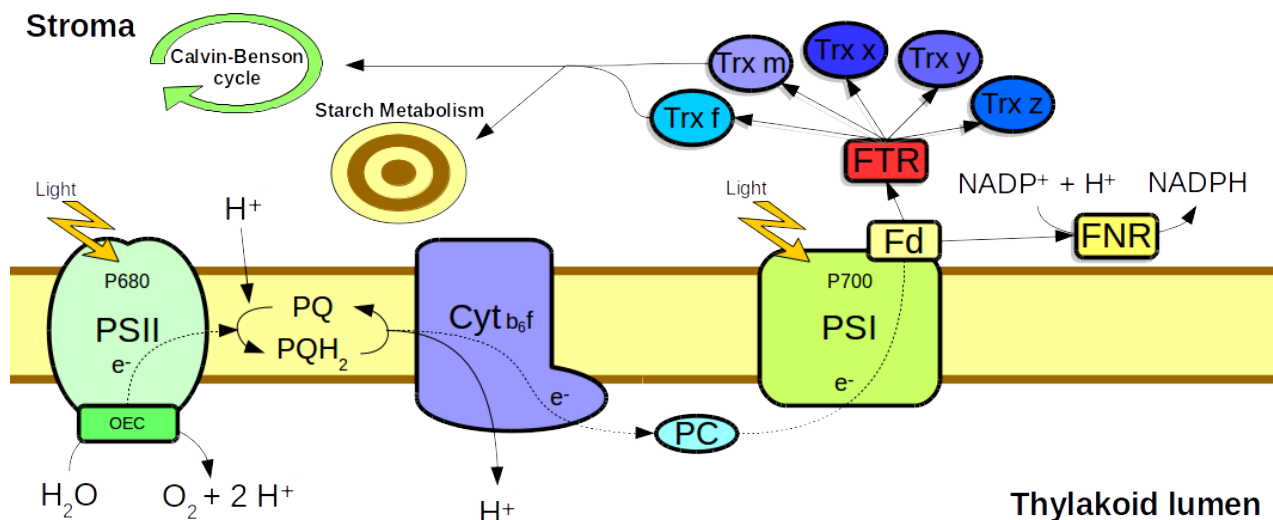


Figure 1.8 Thioredoxin system in chloroplast. Alternative electron flow to the Ferredoxin-Thioredoxin Reductase (FTR) allow reduction of thioredoxins. In turn thioredoxins control several targets in chloroplasts, in particular the carbon pathways like Calvin-Benson cycle and starch metabolism. From left to write: PSII, photosystem 2; PQ, oxidized plastoquinone; PQH₂, reduced plastoquinone; Cyt b₆f, cytochrome b₆f; PC, plastocyanin; PSI, photosystem 1; Fd, ferredoxin; FNR, ferredoxin-NADP⁺ reductase.

In chloroplasts, TRXs and NADP-dependent thioredoxin reductase C (NTRC) are the main redox regulators. Reduction of TRX is light-dependent through the small electron chain composed by ferredoxin (Fd), ferredoxin-thioredoxin reductase (FTR) and TRX (Figure 1.8). Plastidial classes of TRX are f, m, x, y and z, the first two are mainly involved in regulation of carbon metabolism enzymes (Geigenberger et al., 2017). The reduction of NTRC is light-independent, being a bimodular enzyme formed by a NTR module, containing FAD as cofactor, and a TRX module at the C-terminal domain of the enzyme. As a result, NTRC is reduced by NADPH and interacts directly with the target enzymes (Bernal-Bayard et al., 2012)

1.6.1.2 Redox modification by glutathione and oxygen and nitrogen reactive species

Redox modifications include also the glutathionylation and modifications by reactive oxygen and nitrogen species, ROS and RNS respectively, but functions of reactive sulphur species are emerging in the last years (Couturier et al., 2013; Kasamatsu et al., 2016).

Electron transport chain lead to reactive oxygen species production, indeed excited electrons and low redox potential carriers can react with molecular oxygen forming ROS (Mittler, 2017), RNS are instead produced as byproduct at enzymatic levels (Apel and Hirt, 2004; Umbreen et al., 2018). ROS are essentially hydrogen peroxide (H_2O_2) superoxide radical (O_2^-), hydroxyl radical (OH \cdot), and singlet oxygen (1O_2). RNS instead are especially nitric oxide and other derived molecules like nitrogen dioxide (NO_2), dinitrogen trioxide (N_2O_3) and peroxyxynitrite (ONOO \cdot) (Couturier et al., 2013). NO can alter protein function by metal nitrosylation of cofactors, tyrosine nitration or S-nitrosylation (Sevilla et al., 2015). S-nitrosylation occurs especially on cysteines modifying protein conformation, activity, localization and interaction (Sevilla et al., 2015). Both ROS and RNS effects depend on concentration, in sub-toxic amounts they work as signalling molecules, like secondary messengers, involved in plant physiology, immunity and development (Couturier et al., 2013; Farnese et al., 2016) or stimulating plant adaptation to stress condition (Foyer and Noctor, 2009). In stressing environments, production of ROS overcome the scavenging systems leading to an excess of radicals and cells, tissues or the entire organisms are subjected to oxidative stress. As consequence fundamental macromolecules are damaged by radical reactions and peroxidation, like proteins and lipids (Møller et al., 2007).

The glutathionylation is the formation of a mixed disulfide bond between a molecule of glutathione and a reactive thiol in a protein, the reaction is spontaneous and occurs without enzymatic catalysis. However the removal of glutathione needs an enzymatic reaction catalyzed by glutaredoxins, oxidoreductases belonging to the TRX family, and TRX (Zaffagnini et al., 2012).

Glutathionylation protects reactive cysteines from ROS over-oxidation to sulfinic and sulfonic acids that are irreversible thiol modifications (Zaffagnini et al., 2012). Considering the glutathionylation as a ROS-mediated process, alternating glutathionylation and deglutathionylation was also suggested as a ROS scavenging strategy performed by glutaredoxins (Zaffagnini et al., 2012). A signalling/regulatory function of glutathionylated proteins was also suggested (Zaffagnini et al., 2012), for example TRX f of *Arabidopsis thaliana* and *Chlamydomonas reinhardtii* is glutathionylated with possible consequences on carbon fixation enzymes (Michelet et al., 2005).

Glutathione is a tripeptide with a glutamate γ -bound to a cysteinylglycyl dipeptide. Specificity for glutathionylation is still unclear and it is unknown if it depends on accessibility, cysteine reactivity, physico-chemical properties of the microenvironment or a combined effect of them (Winterbourn

and Hampton, 2008). Reduced glutathione (GSH) is the glutathionylating form and also the most abundant under physiological conditions. As redox couple, GSH and oxidized glutathione (GSSG) they act as redox buffer inside cell compartments like mitochondria and plastids (Foyer and Noctor, 2005). Perturbations in glutathione redox state are reported in different stress conditions such as ozone, pathogen attack, chilling and drought (Jubany-Mari et al., 2010; Vanacker et al., 2000; Mou et al., 2003; Bick et al., 2001). GSH scavenges reactive species in excess (Foyer and Noctor, 2011), heavy metals (Cobbet and Goldsbrought, 2002) and xenobiotics (Edwards et al., 2000), and as consequence the GSSG level rises.

Crosstalk between glutathionylation and reactive species is also found, in fact GSH modification is usually promoted by ROS like hydrogen peroxide and S-nitrosylation is often catalyzed via trans-nitrosilation from nitrosoglutathion (Sevilla et al., 2015). The nitrosoglutathione is formed when NO and GSH react. The interplay between the ROS and RNS is also observed, since a common reactive species is peroxyxynitrite, formed by reaction of NO and O_2^- (Besson-Bard et al., 2008).

1.6.2 The circadian clock

Given the predictability of the changes linked to the day cycle, living beings evolved circadian regulation to coordinate molecular events and environmental rhythms. Since plant nourishment is deeply linked to environmental conditions plants evolved a tight circadian system, indeed in *Arabidopsis* plants approximately one third of gene transcripts oscillate with a circadian phasing (Covington et al., 2008). Circadian regulation allows plants to optimize biomass production and adapt under different climates (Böhlenius et al., 2006; Dodd et al., 2005; Kloosterman et al., 2013). Most of the plant clock characterization has been done in *Arabidopsis thaliana*, but homologue genes have been found in several cultivated crops (Hsu and Harmer, 2014).

The circadian regulation is based on three components: a self-sustaining central oscillator, *i.e.* the real clock; input signalling pathways to integrate the clock with the environment; output pathways to control biological processes. The oscillator is formed by interlaced loops of transcription and translation (Figure 1.9). Three sets of transcription factors generate the feedback loops, with alternated temporal expression during the day, morning-, day- and evening-phased. The morning components are two MYB-like transcription factors called CCA1 and LHY (Circadian Clock-Associated 1 and Late Elongated Hypocotyl, respectively), which are extensively transcribed in the morning and form homo- and heterodimers with each other, the heterodimeric form is more efficient (Lu et al., 2009; Yakir et al., 2009). CCA1 and LHY act as repressors and their main target is Time of CAB1 gene (*TOC1*), encoding an evening component of the clock. Other evening genes are repressed by CCA1 and LHY, like *GIGANTEA*, *LUX*, *BOA*, *ELF3* and *ELF4* (Dai et al., 2011;

Lu et al., 2012; Nagel and Kay., 2012). When expressed, TOC1 in turn regulated the expression of *CCA1* and *LHY*, this interlocked regulation represents the first feedback loop discovered in the clock (Hsu and Harmer, 2014). Evidences emerged for an activating function of *LHY* and *CCA1*, indeed expression of day-phased genes like *PRR7* and *PRR9* (Pseudo-Response Regulator) is enhanced by these two morning components (Nagel and Kay, 2012). *PRR9* is expressed as first day component, is found immediately after dawn, followed by *PRR7*, *PRR5* and *PRR3* (Farrè and Liu, 2013). A second feedback loop is now activated, because *PRR5*, together with *PRR7* and *PRR9*, represses the expression of *CCA1*, *LHY* and *RVE8* (*REVEILLE8*), an evening-phase component (Nakamichi et al., 2010; Nakamichi et al., 2012). Then *RVE* transcription factors are involved in dawn signalling and participate of the afternoon regulation of the clock in a feedback loop with *PRRs* (Rawat et al., 2011). Once expression of *CCA1* and *LHY* is finished, *TOC1* and other evening components like *LUX*, *ELF3* and *ELF4* are expressed, the last three form the so-called evening complex (Dixon et al. 2011; Helfer et al., 2011; Herrero et al., 2012). The evening complex represses *PRR9* and enhances the expression of *CCA1*. *BOA*, a *LUX* homologue, can also form a complex with *ELF3* and *ELF4* promoting the expression of *CCA1* (Daj et al., 2011). Regulation by *TOC1* and *PRR* proteins ensures that *LHY* and *CCA1* expression occurs in a small window at the beginning of the day (Gendron et al., 2012; Pokhilko et al., 2012).

Promoters of circadian components are enriched of sequences called Evening Elements that allow repression or activation of expression depending on the specific interactor (Hsu and Harmer; 2014). Control on clock pathway goes beyond transcriptional control and involves different levels of regulation. Several transcripts undergo alternative splicing (James et al., 2012), protein-protein interaction influence functioning and degradation (Baudry et al., 2010; Mas et al., 2003). Looking at post-translational modification, several clock components are subjected to ubiquitination and SUMOylation (Fujiwara et al., 2008; Mehra et al., 2009), while phosphorylation was observed on *PRR* proteins (Wan et al., 2010). Taken together all the regulatory levels work to guarantee the right functioning of the feedback loops inside the clock.

External inputs keep the clock synchronized with the environment. Two kind of inputs have been mainly studied: light and temperature. The light in particular has been demonstrated to influence gene transcription, RNA and protein stability and translation rates (Staiger and Green, 2011). Light sensors are *ZTL*, a circadian photoreceptor for blue light which regulates *TOC1* stability. *Phytochromes* (red and far-red light receptors) and *cryptochromes* (blue light receptors) are also involved in phasing the clock (Fankhauser et al., 2002). The clock is more temperature-tolerant and several temperature of physiological interest do not affect the clock (Salome et al., 2010), but

several clock genes are cold-responsive (James et al., 2012). Cold also triggers alternative splicing for all main clock components, *i.e.* CCA1, LHY, PRR3, PRR5, PRR7, PRR9 and TOC1.

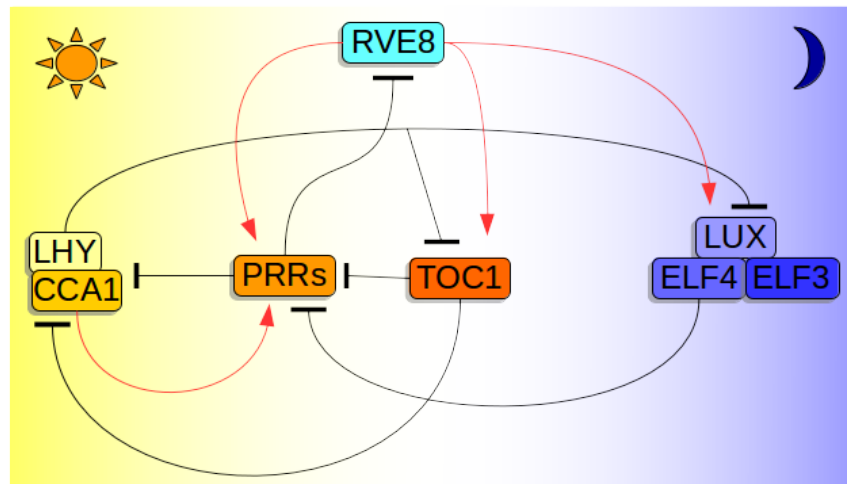


Figure 1.9 Central elements of circadian clock in *Arabidopsis thaliana*. LHY-CCA1 complex forms the morning loop, which control expression of day and evening elements. PRRs proteins constitute the second feedback loop, expressed during the day, while LUX-ELF3-ELF4 are the evening complex controlling the third feedback loop.

What makes the clock a circadian regulator for plant gene expression is the regulatory ability of each components, in fact transcription factors like TOC1, PRR5, PRR7 and RVE8 do not only regulate other clock genes but act as regulators for several plant genes. In this way, regulating each other they also give the timing of biological processes (Huang et al., 2012; Liu et al., 2013; Nakamichi et al., 2012).

1.6.3 Carbon metabolism controls growth by sugar sensing

Plant development relies on metabolic and environmental conditions. Since metabolic conditions rely on environmental availability of light and nutrients, signals from metabolism integrate the overall condition of the plant. In particular plants need carbon to synthesize new biomass, then pathways evolved to transmit signals of carbon availability and stimulate or inhibit growth as function of the overall metabolic status. Indeed signals from different metabolites are integrated, for example the response of the plant to sugar levels is influenced by nitrate and phosphate concentration (Martin et al., 2002; Müller et al., 2007).

Sugar signalling in plants is mainly performed by sucrose and glucose (Figure 1.10). Sucrose is the main carbon source transported toward sink tissues and its levels are proportional to carbon availability. Sucrose signalling is not performed by sucrose itself, in this regard another disaccharide, trehalose, carries out the sucrose signalling function and is found in extremely low amounts in plants (μM range, Zhang et al., 2009). The signalling is mediated by trehalose-6-phosphate (T6P), an intermediate of trehalose biosynthesis, which levels are proportional to sucrose

levels (Figuroa and Lunn, 2016). Trehalose biosynthesis is a two step pathway, analogous to sucrose biosynthesis, in which a Trehalose-6-Phosphate Synthase (TPS) uses UDP-glucose and G6P to synthesize T6P. Then Trehalose-6-Phosphate Phosphatase (TPP) hydrolyzes the phosphate group releasing trehalose, that can be degraded by the trehalase. From a metabolic point of view, T6P is a direct sensor of catabolic and anabolic reactions inside the cell, indeed UDP-glucose is the building block of polysaccharide biosynthesis, including cell wall and callose, whereas G6P is the starting point of energetic metabolism.

T6P relationship with sucrose has been studied in *Arabidopsis thaliana* at different developmental stages (Nunes et al., 2013; Wahl et al., 2013) and its levels undergoes ample fluctuations following sucrose levels (Lunn et al., 2006; Carillo et al., 2013). The same nexus between T6P and sucrose has been found in several plant species like cucumber (*Cucumis sativa*; Zhang et al., 2015), potato (*Solanum tuberosum*; Debast et al., 2011) and cereals like maize (*Zea mays*; Henry et al., 2014) and wheat (*Triticum aestivum*; Martinez-Barajas et al., 2013), reflecting how T6P signalling is a conserved mechanism at least in angiosperms.

However, the relationship between T6P and sucrose is not one-way and a T6P feedback inhibits sucrose biosynthesis (Yadav et al., 2014) working as a switch between carbon export and local biosynthesis. When sucrose levels exceeds the demand of sink tissues, T6P levels raise inhibiting sucrose synthesis and redirecting carbon toward biosynthetic pathways through tricarboxylic acid pathway, amino acid biosynthesis (Figuroa et al., 2016) and the anaplerotic reaction of PEPC (phosphoenolpyruvate carboxylase; O'Leary et al., 2011) yielding oxalacetate. In parallel, nitrate reductase, the final step of nitrogen assimilation, is activated allowing rise in amino acids synthesis (Figuroa et al., 2016). Moreover, T6P can have a strong impact on rates of starch degradation at night (Martins et al., 2013) tuning carbon release in function of the demand of sink tissues. Under high T6P levels a drop in maltose content is observed, pointing out as the inhibition should occur in the first degradation steps, maybe involving glucan dikinases or phosphatases. Despite it does not seem to influence diurnal starch biosynthesis in the leaves, it is worth to mention that artificial T6P levels activate carbon incorporation into starch (Kolbe et al., 2005; Zhang et al., 2009), probably acting on NTRC or other proteins upstream AGPase redox activation. In this scenario, T6P seems to coordinate, directly or indirectly, the allocation of carbon and nitrogen.

A crucial element of T6P signalling is the SnRK1 kinase (Sucrose-non-fermenting Related Kinase 1), which provides signals about nutrient and environmental status to regulate the growth (Radchuk et al., 2010). SnRK1 is specifically activated when the cell experience low energy, it inhibits biosynthetic processes and push catabolic reactions for energy production. In sink tissues, T6P stimulates growth by inhibiting SnRK1 (O'Hara et al., 2013; Delatte et al., 2011). The inhibition is

not direct and requires an intermediate factor (Zhang et al., 2009). Several processes are regulated by both T6P and SnRK1, like flowering (Wahl et al., 2013), starch metabolism (Kolbe et al., 2005; Lunn et al., 2009), senescence (Wingler et al., 2012) and anthocyanin biosynthesis (Baena-Gonzalez et al., 2007). So globally sucrose set plant metabolism and timing of development through the interaction between T6P and SnRK1 regulatory pathways.

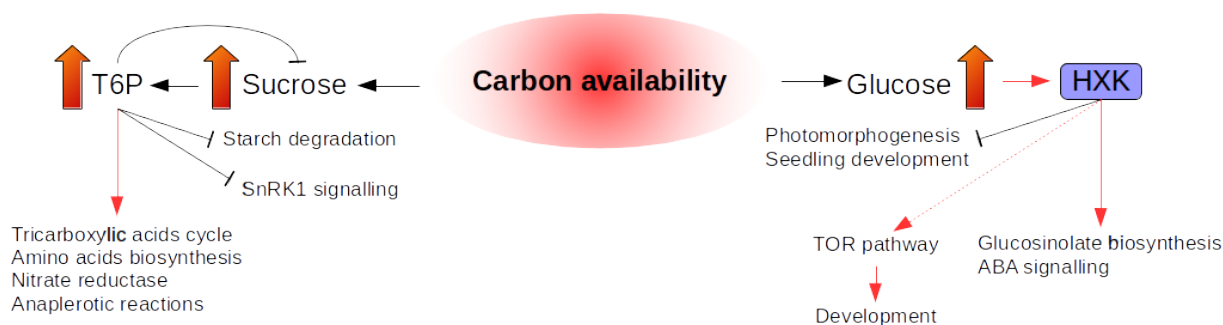


Figure 1.10 Sucrose and glucose signalling. Activation (Red arrows) and inhibitory (T-bar line) effects due to increase in carbon availability and consequent raise of sucrose and glucose levels.

Unlike sucrose, glucose levels are directly detected by hexokinases (HXKs). HXKs are conserved enzymes that in plants constitute a multigene family with proper HXKs and HXK-like proteins, some of these have both glucose sensor and catalytic function and other are just the latter (Dai et al., 1999; Veramendi et al., 2002; Cho et al., 2009; Kano et al., 2013; Kim et al., 2013; Li and Sheen, 2016; Aguilera-Alvarado and Sánchez-Nieto, 2017). In glucose signalling it is possible to distinguish direct and indirect HXK signalling. The direct signalling has been suggested to involve conformational movements, linked to glucose binding but not to phosphorylation, determining the interaction with signalling partners and even translocation into the nucleus (Moore et al., 2003; Feng et al., 2015). In the case of *Arabidopsis thaliana*, following high glucose concentration, HXK1 has been found in a repressor complex inside the nucleus with the subunit B of the atypical vacuolar H⁺-ATPase and the 19S regulatory particle of the proteasome (c). This complex binds *CAB* and *CAA* genes promoter repressing transcription, in this way high glucose levels affect photomorphogenesis and seedling development (Cho et al., 2006). HXKs sensors work as repressors or activators, probably depending on alternative interactors, and can repress genes involved in catabolism or anabolic reactions (Sheen, 1990; Graham et al., 1994; Jang and Sheen, 1994) but also upregulate genes expressing MYB transcription factors and glucosinolate biosynthesis genes (*CYP*, Miao et al., 2016). HXK can stimulate ABA signalling to control stomatal closure and lower water loss (Kelly et al., 2013; Lugassi et al., 2015).

HXK activity can regulate the metabolic flux through glycolysis, oxidative pentose phosphate pathway, nucleotides production, starch and fatty acid synthesis (Claeyssen and Rivoal, 2007). Indeed, metabolites downstream the G6P produced by HXK can be signals of the energetic status of

the cell and represent the indirect glucose signalling through HXK, independently of HXK as sensor. The most known influence of HXK indirect signalling is on the TOR pathway, which is regulated by glycolytic intermediates (Price et al., 2004; Villadsen and Smith, 2004; Xiong et al., 2013). TOR pathway then controls developmental transition and growth in function of the energy and metabolites supply (Xiong et al., 2013).

The global scenario is a complex net of sugar signals that allows coordination between photosynthetic and heterotrophic tissues of the plant. Thanks to diverse sugar sensors, localized in different tissues and subcellular environments, the metabolic status of the organism is monitored and the development regulated compatibly with carbon sources.

1.7 Regulation of Calvin-Benson cycle

The fixation of carbon dioxide is a process of fundamental importance for photosynthetic organisms, as such it is highly regulated by concomitant mechanisms following the day/night alternation.

RuBisCO is the key enzyme of the cycle and is responsible for the entry of carbon in the organic world. For this reason, RuBisCO activity is tightly regulated in different ways. Rubisco re-activation at light is catalyzed by the RuBisCO activase, a chaperon-like AAA+ ATPase which promotes the transition to the catalytically active carbamated state and the release of the 2-carboxyarabinitol-1-phosphate inhibitor (Zhang et al., 2002; Portis, 2003; Carmo-Silva et al., 2011). In turn, RuBisCO activase is regulated by ADP and ATP/ADP ratio and, depending on the isoform, it contains a redox-sensitive extension regulated by TRX f (Zhang and Portis, 1999; Zhang et al., 2001). Both mechanisms link the activase activity to the availability of ATP and reducing power in the chloroplasts, thus to the presence of light.

Since NADPH and ATP to fix CO₂ are provided by PET, the synchronization of PET and Calvin-Benson cycle is crucial. Different concerted mechanisms act to permit this process. A first way is the increase of both stromal pH to ~8 and Mg²⁺ concentration. Both conditions are directly linked to enzymes activity, indeed several enzymes of the cycle have alkaline pH optimum and RuBisCO, kinases and phosphatases activities need magnesium ions to work properly.

TRX-mediated redox regulation take part to the synchronization activating several enzymes during the day. Usually TRXs reduction make accessible the active site to substrates, indeed *in vitro* and *in vivo* studies demonstrated that GAPDH, FBPase, SBPase and PRK are activated by reduced TRXs (Bassham, 1971; Wolosiuk and Buchanan, 1978; Jaquot et al., 1995; Baalman et al., 1996; Jaquot et

al., 1997; Dunford et al., 1998; Sparla et al., 2002). For GAPDH two redox regulation have been found. The isoform A of GAPDH is indirectly redox regulated by the formation of an inhibitory complex with oxidized PRK (inactive), thanks to the intrinsically unfolded protein CP12 (Wedel and Soll, 1998; Trost et al., 2006), which works as scaffold for the assembly of the complex (Del Giudice et al., 2015). Furthermore, CP12 has been proposed to protect GAPDH and PRK from heat and oxidative stress (Erales et al., 2009; Marri et al., 2014), and stabilize PRK under physiological conditions (López-Calcano et al., 2017). The isoform B of GAPDH forms A₂B₂ heterotetramers with the subunit A and is directly regulated by TRX due to a C-terminal extension containing the two regulatory cysteines (Baalman et al., 1996; Sparla et al., 2002). Once oxidized, A₂B₂ heterotetramers oligomerize in A₈B₈ complexes in which the GAPDH activity is inhibited (Pupillo and Piccari, 1973). The C-terminal extension in B isoform is probably generated by a fusion of GAPDH-A gene with CP12 gene (Baalman et al., 1996), as highlighted by sequence homology.

Reactive cysteines inside Calvin-Benson cycle enzymes allow other redox modifications, like glutathionylation and nitrosylation. As mentioned above (section 1.6.1.2), glutathionylation have a protective function under stress. Proteomic studies pointed out all the Calvin-Benson cycle enzymes as putatively glutathionylated in *Chlamydomonas reinhardtii* (Zaffagnini et al., 2012; Zaffagnini et al., 2013). This result has been demonstrated *in vitro* for A₄-GAPDH, PRK, PGK, RPI and TPI in *C. reinhardtii* and FBPase in *A. thaliana* (Ito et al., 2003; Zaffagnini et al., 2007; Michelet et al., 2008; Zaffagnini et al., 2012; Zaffagnini et al., 2013). Thus cysteines modifications can interact and the same Calvin-Benson cycle enzyme can be modified by TRX, glutathione and nitrosylation (Lindemayr et al., 2005; Romero-Puertas et al., 2008; Abat et al 2008; Abat and Deswal, 2009; Zaffagnini et al., 2013).

Contributing to the intricate regulatory network of carbon fixation there are at least other three factors: calcium, phosphorylation and circadian clock. Calcium is a second messenger in all eukaryotes (Berridge et al., 2000; Clapham, 2007). In plants the number of calcium sensor proteins has increased, probably contributing to specificity and flexibility of signalling (Rocha and Votchnecht, 2012). Free calcium concentration has day/night fluctuations in the stroma, from 150 nM in light up to 5-10 μM in the dark, and can contribute to enzyme regulation (Johnson et al., 1995; Ettinger et al., 1999; Sai and Johnson, 2002). Accordingly, FBPase and SBPase showed activation at low calcium concentration and inhibition when calcium raises (Charles and Halliwell, 1980; Herting and Wolosiuk , 1983; Chardot and Meunier, 1990).

Phosphorylation and circadian regulation are still poorly studied on Calvin-Benson enzymes. Phosphorylation sites are found in Rubisco activase (*C. reinhardtii*; Lemeille et al., 2010) and PGK (*A. thaliana*, Reiland et al., 2009, Roitinger et al., 2015; *O. sativa*, Facette et al., 2013; *Z. mays*,

Baginsky, 2016). Interestingly, the main isoform of TK in Arabidopsis (TKL1) is subjected to calcium-dependent phosphorylation, with consequent loss of activity (Rocha et al., 2014).

Day/night control on Calvin-Benson cycle proteins has been highlighted by proteomic profiling done by Fox and colleagues (2015). The study reported that protein levels of PRK, GAPDH-B, RuBisCO activase and aldolase are lowered in quadruplet phytochrome and cryptochrome mutant (*phyA,phyB,cry1,cry2*). This downregulation correlates with lowered CO₂ fixation under high light conditions.

To conclude, different simultaneous mechanisms participate of CO₂ fixation cycle regulation in plants, the result is the integration of several information linked to internal and external factors to modulate CO₂ fixation.

1.8 Regulation of leaf starch metabolism

In physiological conditions, transitory starch represents both a carbon sink during the day and a carbon source during the night. Regulatory mechanisms for starch follow this distinctive trait determining the double behaviour of starch during the day-night cycle.

1.8.1 Regulation at protein level

Phosphorylation and phosphate (P_i) concentration have been involved especially in the biosynthetic pathway (MacNeill et al., 2017; White-Gloria et al., 2018). PGI, pPGM, SS2 and two subunits of AGPase resulted phosphorylated from phosphoproteomic analyses (Grimaud et al., 2008; Reinland et al., 2009). Interestingly SS2 phosphorylation is found only at the end of the light period (Reinland et al., 2009). The effects of phosphorylation are not known for starch enzymes in chloroplast, but in amyloplast starch synthase phosphorylation regulates the formation of a complex with debranching enzymes (Tetlow et al., 2004).

P_i levels are directly linked to ATP availability and TPT activity. When triose phosphates levels raise, due to high photosynthesis or reduced TPT activity, P_i levels lower (MacNeill et al., 2017). As consequence 3-PGA level raises and stimulates AGPase activity while low P_i releases allosteric inhibition from AGPase allowing concomitant activation of starch biosynthesis (Iglesias and Preiss, 1992; Sivak and Preiss, 1995).

Several enzymes of starch metabolism are redox regulated by TRX f and m in Arabidopsis plants, *i.e.* AGPase, BAM1, AMY3, SS1, GWD1 and SEX4 (Fu et al., 1998; Mikkelsen et al., 2005; Sparla

et al., 2006; Seung et al., 2013; Silver et al., 2013; Skryhan et al., 2015). Instead, SS3, ISA1/2/3, BAM3 and LDA have been suggested as redox regulated (Glaring et al., 2012).

AGPase is regulated by means of a single reactive cysteine conserved in all plants except for the monocot endosperm isoform (Ballicora et al., 1999). Oxidation of cysteine residue results in dimerization of AGPase tetramers and consequent inhibition (Fu et al., 1998; Ballicora et al., 2000; Tiessen et al., 2002). The reactivation is catalysed both by TRX f and m *in vitro* (Fu et al., 1998). Redox sensitivity of AGPase could be modulated by sugar-sensing since supplying T6P to isolated chloroplast results in upregulation of AGPase activity (Kolbe et al., 2005). Since reduction drives the activation of enzymes, both from synthetic (AGPase, SS1, SS3; ISA 1/3) and degradation (GWD1, BAM1/3, AMY3, SEX4, ISA2, LDA) pathways, redox properties of starch enzymes appear controversial. To clarify this aspect the importance of redox cysteines in starch enzymes has been investigated two times *in vivo*, for AGPase and GWD1. AGPase KO mutant has been transformed with a redox-insensitive AGPase gene, resulting in higher starch accumulation in long-days photoperiod (Hädrich et al., 2012). Surprisingly, AGPase protein level was lower than wild-type protein levels and suggesting protein turnover is affected by redox regulation. On the other hand, when *gwd* Arabidopsis plants are transformed with redox-insensitive GWD1 no difference is observed if compared to plants complemented with redox-regulated GWD1 (Skeffington et al., 2014).

Protein complexes usually can modify and control enzymatic activity, complexes in leaf starch metabolism are still unknown. Anyway several enzymes in the biosynthetic and the degradation pathways contain putative coiled-coil domains (Lohmeier-Vogel et al., 2008), which often mediate protein-protein interactions. The unique example of complex involves the two isoamylases ISA1 and 2, found in potato and Arabidopsis plants (Bustos et al., 2004; Wattedled et al., 2005). When one of the two ISA genes is knocked out the level of the remaining isoform are lowered due to protein instability or reduced gene expression (Delatte et al, 2005).

1.8.2 Time-dependent regulation of starch metabolism

In *Arabidopsis thaliana*, genes involved in starch metabolism in leaves have circadian expression. Circadian pattern is known for *BAM1/3/4*, *PHS1*, *GWD1*, *PWD*, *AMY3*, *DPE1* and *ISA1/2/3* (Smith et al., 2004; Lu et al., 2005; Covington et al., 2008). Despite this, when protein levels are analyzed no circadian fluctuations are observed, thus post-transcriptional and post-translational mechanisms could be involved in further regulation of enzyme activity (Kötting et al., 2010).

Regarding timing, a fundamental feature of starch degradation is the constant degradation rate at night (Smith and Stitt, 2007), which implies prediction of the night length and quantification of

starch amounts. How plants integrate information about time of the day and starch levels is still unknown but models have been hypothesised. Circadian clock should provide information about timing, in fact *Arabidopsis* double mutant lacking the morning loop (*cca1 lhy*) have a faster clock timing and also a faster starch degradation in a 24 hours light-dark cycle (Graf et al., 2010). Connection between clock and starch is underlined by plants exposed to short day and long night, which store more photoassimilates into starch avoiding carbon starvation in the dark period (Gibon et al., 2004). Anyway how plants can measure starch is still unknown, Scialdone et al. (2013) hypothesised different possible theoretical mechanisms and proposed PWD as key player in starch sensing. The loss of PWD leads to reduced starch degradation as well as other mutants for enzymes in the starch degradation pathway, but it interesting that *pwd* is the only mutant unable to lower the rate of degradation when exposed to an unexpected night. So PWD appears essential for the adaptation of degradation rate to unexpected night onset and could be involved in signalling starch amounts to set the right degradation rate.

Summing up the information available so far, our current knowledge of strategies to control leaf starch metabolism probably is just the tip of the iceberg and new players are emerging in the last few years. An example are non-enzyme proteins, which have been poorly considered so far. PTSTs together with MFP1 and MRC (MAR Binding Filament-Like Protein 1, Myosin-Resembling Chloroplast Protein) have been recently demonstrated to be important for starch granule initiation and growth (Seung et al., 2015; Seung et al., 2017; Seung et al., 2018). Other examples are proteins like BAM4, BAM8 and ESV1 that are supposed to have regulatory rather than catalytic function but their exact role is still unclear (Fulton et al., 2008; Soyk et al., 2014; Feike et al., 2016; Malinova et al., 2018).

1.9 Regulation of sucrose metabolism and phloem transport

Regulation of sucrose metabolism occurs at different levels in plants: controlling sucrose production in source tissues, sucrose loading, unloading and transport in the phloem and sucrose degradation in sink tissues. In apoplastic-loading species sugar transporters are regulated whereas in symplastic-loading species sink strength is the common regulatory strategy (Slewinski and Braun, 2010). In the first case, working at protein level in source tissues, is thought to allow faster regulation.

1.9.1 Sucrose-phosphate synthases are regulated at different levels

SPSs are the key enzymes of sucrose synthesis and as such SPSs are regulated by metabolic signals, like activation by G6P and inhibition by P_i , and environmental stimuli like osmotic stress and light (Huber and Huber, 1996). Early studies suggested a time-dependent regulation of SPSs activity, which peaks in the middle of the light-period and 12 hours later both in tomato and soybean plants (Kerr et al., 1985; Jones and Ort, 1997). Three phosphorylation sites have been found in SPSs, notably each isoform acquired variations in the phosphorylation site sequences allowing different kinase specificity (Huang and Huber, 2001; Chen et al., 2005). SPS also interacts with different isoforms of 14-3-3 proteins in a phosphorylation independent-manner (Börnke, 2004). Moreover, sucrose production is efficiently performed thanks to metabolic channelling through SPS and SPP, which interact *in vivo* in Arabidopsis plants (Maloney et al., 2015).

Hence SPSs appear to be highly regulated enzymes, tuning the sucrose production in response to developmental and environmental cues.

1.9.2 Control of sucrose transporters

SUT transporters are finely regulated at gene, transcript and protein level while regulation of SWEET sugars transporters is still largely unknown (Roblin et al., 1998; Ransom-Hodgkins et al., 2003; Nuhse et al., 2004; Niittyla et al., 2007, Fan et al., 2009, Eom et al., 2015). The only information concerning SWEET regulation regard the long non conserved C-terminal region (Eom et al 2015). This extension is phosphorylated in response to sucrose addition to the medium (Niittylä et al 2007) and involved interactions with other proteins (Eom et al., 2015).

SUTs have been studied for the last 10 years highlighting the post-transcriptional regulation acts on transcripts shortening the turnover to 60-130 minutes, as shown by He et al., 2008 and Liesche et al., 2011. In this regard, translational control is obtained by mRNA binding proteins for StSUT2 and 4 in *Solanum tuberosum* (He et al., 2008). The same regulation is probably conserved in Arabidopsis SUC2 and SUC4, which are the only two transporter family that are not regulated by miRNA (Lu et al., 2005; Kühn and Grof, 2010).

Also in sucrose transporters a sensitivity to redox state is found. Potato SUT1 dimerizes in oxidizing conditions and increasing of 10-fold the V_{max} . Dimerization is found also in SUT2 and 4 in *Solanum lycopersicum* (Reinders, 2002), while the distribution of S/SUT1 depends on redox conditions. It is homogeneously localized in reducing environment and under oxidizing conditions is found in highly localized areas of the membrane (Krügel et al., 2008).

A wide network of protein interaction is characteristic of SUT transporters (Krügel and Kühn 2013). S/SUT1 putative interactors include protein disulfide isomerase, pyrophosphatases, aldehyde

dehydrogenase and proteins for targeting. *Malus domestica* SUT1 and Arabidopsis SUC4 interact with cytochromes b5 negatively affecting germination (Fan et al., 2009; Li et al., 2012). Furthermore, *StSUT2* and 4 probably have regulatory rather than catalytic function, in fact they showed low affinity for sugars and have inhibitory effect on *StSUT1* (Chinciska et al., 2008; Kühn and Grof, 2010).

Phosphorylation occurs also for SUCs in Arabidopsis, despite the role of the modification is still unknown (Nühse et al., 2004; Niittyta et al., 2007; Durek et al., 2010).

1.9.3 Regulation of sucrose degradation

INVs and SUSs are generally considered part of the sucrose degradation pathway since usually localize in sink tissues. Thus controlling INV and SUS activities the plant can modulate sink strength and carbon flux.

Expression of *SUS* genes is controlled by metabolic factors like carbon starvation and hypoxia (Zeng et al., 1998; Koch, 1996; Koch et al., 2000), in these conditions mRNAs from *SUS* genes are preferentially loaded onto ribosomes increasing *SUS* protein translation and helping plant to survive (Clancy et al., 2002).

SUS proteins are subjected to phosphorylation by SnRK and likely other kinases (Purcell et al., 1998). Indeed all *SUS* proteins contain two conserved phosphorylation sites, the first enhances enzymatic activity depending on sugar levels (Huber et al., 1996; Zhang et al., 1999; Cheng et al., 2002) while the second site is phosphorylated depending on the first site and address to ubiquitin-dependent degradation (Hardin et al., 2003; Halford et al., 2003). The degradation can be blocked by the binding of ENOD40 protein, that stabilizes *SUSs* phosphorylated on the first site and contributes to vascular functioning and phloem unloading (Kouchi et al., 1999; Varkonyi-Gasic and White, 2002).

INVs are controlled mainly by transcriptional regulation and enzyme inhibitors. *INV* genes are responsive to environmental stimuli like gravity, water availability and pathogens infection (Long et al., 2002; Trouverie et al., 2003; Roitsch et al., 2000; Roitsch et al., 2003). In *Vitis vinifera* *CWINV* promoters have wound responsive elements, MYC recognition site, Sucrose-responsive element 1 (SURE1) and ABA-responsive (ABRE) element influencing gene expression (Hayes et al., 2010). Other evidences suggest circadian regulation of invertase gene *lin6* by CCA1-LHY, the morning loop of clock, in tomato plants (Proels and Roitsch, 2009). Transcripts are then controlled by increased turnover, indeed rice *VIN1* and *AtVINV2* mRNAs are destabilized by downstream elements and transcript decay is accelerated by glucose in Arabidopsis (Feldbrugge et al., 2002; Huang et al., 2007).

At protein level, enzymatic activity of CWINV and VIN is affected by inhibitor proteins (Ruan, 2014). Inhibitors are involved in senescence occurrence in tobacco plants (Lara et al., 2004; Jin et al., 2009). As SUSs, INVs are regulated by phosphorylation, for instance 14-3-3 proteins bind CIN1 after its phosphorylation in Arabidopsis, this process leads to a general increase in invertase activity in roots during the day (Gao et al., 2014).

The intersection of regulatory mechanisms for SPSs, sugar transporters, SUSs and INVs allows fine control of carbon partitioning adopting sugar metabolism and distribution to diurnal light cycle, developmental stage, environmental stimuli and stress.

2. Photosynthetic CO₂ assimilation: the last gap in the structural proteome is closed

The following chapter has been uploaded as preprint on bioRxiv and is available at <https://doi.org/10.1101/422709>.

Libero Gurrieri¹, Alessandra Del Giudice², Nicola Demitri³, Giuseppe Falini⁴, Nicolae Viorel Pavel², Mirko Zaffagnini¹, Maurizio Polentarutti³, Pierre Crozet⁵, Julien Henri⁵, Paolo Trost¹, Stéphane D. Lemaire⁵, Francesca Sparla¹, Simona Fermani⁴.

1 Department of Pharmacy and Biotechnology – FaBiT, University of Bologna, Bologna, Italy

2 Department of Chemistry, University of Rome ‘Sapienza’, Rome, Italy,

3 Elettra - Sincrotrone Trieste, S.S. 14 km 163.5 in Area Science Park, 34149, Basovizza - Trieste, Italy

4 Department of Chemistry ‘G. Ciamician’, University of Bologna, Bologna, Italy.

5 Institut de Biologie Physico-Chimique, UMR8226, CNRS, Sorbonne Université, 13 rue Pierre et Marie Curie, 75005 Paris, France.

2.1 Abstract

Photosynthetic CO₂ fixation supports life on Earth and is a fundamental source of food, fuels and chemicals for human society. In the vast majority of photosynthetic organisms, carbon fixation is operated by the Calvin-Benson (CB) cycle, a pathway that has been extensively studied at physiological, biochemical and structural level. It consists of 13 distinct reactions catalyzed by 11 enzymes (Michelet et al., 2013). In land plants and algae, the CB cycle takes place in the chloroplast, a specialized organelle operating the photosynthetic process. Despite decades of efforts, one last enzyme, the phosphoribulokinase (PRK), remains uncharacterized at atomic-scale while the structure of the other ten enzymes have been solved or confidentially modeled by close homology from the structure of isoforms found in other pathways. PRK together with ribulose-1,5-bisphosphate carboxylase/oxygenase (RuBisCO) enzyme, is exclusive of the CB cycle. In opposition to RuBisCO, whose structure has been solved from diverse sources, the structure of PRK remains unknown despite its characterization is crucial to better understand and control photosynthesis.

Here, we report for the first time the crystal structures of redox-sensitive PRK from two model species: the green alga *Chlamydomonas reinhardtii* (CrPRK) and the land plant *Arabidopsis thaliana* (AtPRK). The enzyme is an elongated homodimer characterized by a large central β -sheet of eighteen strands, extending between the two catalytic sites positioned at the dimer edges. The

structure was also studied in solution through the combination of size exclusion chromatography and small-angle X-ray scattering (SEC-SAXS) and no appreciable differences were found.

This study completes the description at atomic level of the 11 CB cycle enzymes providing a rational basis for catalytic improvement of carbon fixation in chloroplasts.

2.2 Results and Discussion

The challenge of support 9 billion people requires a multidisciplinary approach. Looking at food production only, several studies suggest that a 70-100% increase will be necessary by 2050 (Godfray et al., 2010). Different approaches have been made to improve crop yield trying to fill the gap between agricultural output and agricultural demand. Among them, the increase of photosynthetic carbon assimilation through the improvement of the efficiency of the CB cycle is regarded as a promising strategy and positive results have been obtained (Long et al., 2015). The CB cycle consists of 13 distinct reactions involving 11 different enzymes. By consuming ATP, phosphoribulokinase (PRK) catalyses the regeneration of the five-carbon sugar ribulose-1,5-bisphosphate (RuBP), exclusively used by Rubisco for CO₂ fixation.

So far, PRK is the only missing structure of the CB cycle enzymes. To fill this gap, the crystal structures of CrPRK and AtPRK have been determined at 2.6 Å and 2.5 Å, respectively. The enzyme is a dimer of two identical monomers related by a 2-fold non-crystallographic axis (Figure 2.1). Each monomer contains a nine-stranded mixed β-sheet (β1–β9) surrounded by height α-helices (α1, α3–α9), four additional β-strands (β1'–β4') and one helix α2 (Figure 2.2). The active sites (one for each monomer) are located in an elongated cavity at the edge of the dimer (Figure 2.1). Despite the exclusive role of PRK in photosynthesis, putative PRK sequences are also found in autotrophic organisms. Phylogenetic analysis performed on 69 PRK sequences including 31 from non-photosynthetic prokaryotes, clearly show a first evolutionary separation between Bacteria and Archaea (Figure 2.13 in Addendum).

A single structure of PRK from the photosynthetic bacterium *Rhodobacter sphaeroides* (RsPRK; PDB ID 1A7J, Harrison et al., 1998) and one from the non-photosynthetic Archaea *Methanospirillum hungatei* (MhPRK; PDB ID 5B3F; Kono et al., 2017) have been reported. Both Rs and MhPRK sequences are shorter compared to photosynthetic PRKs and they all share a very low sequence identity making impossible to infer reliable structural models for Cr and At enzymes (Figure 2.12 in Addendum).

Most of PRKs from bacteria (type I PRKs), including phototrophic ones, are octamers of about 32 kDa subunits allosterically activated by NADH and inhibited by AMP (Martin and Schnarrenberger,

1997; Kung et al., 1999). A third clade emerging from the Archaea, contains all cyanobacterial and eukaryotic PRKs. Archaea, cyanobacteria and cyanobacterial-derived (*i.e.* Plant-type) PRKs are dimers of about 40 kDa (type II PRKs; Martin and Schnarrenberger, 1997; Kono et al., 2017).

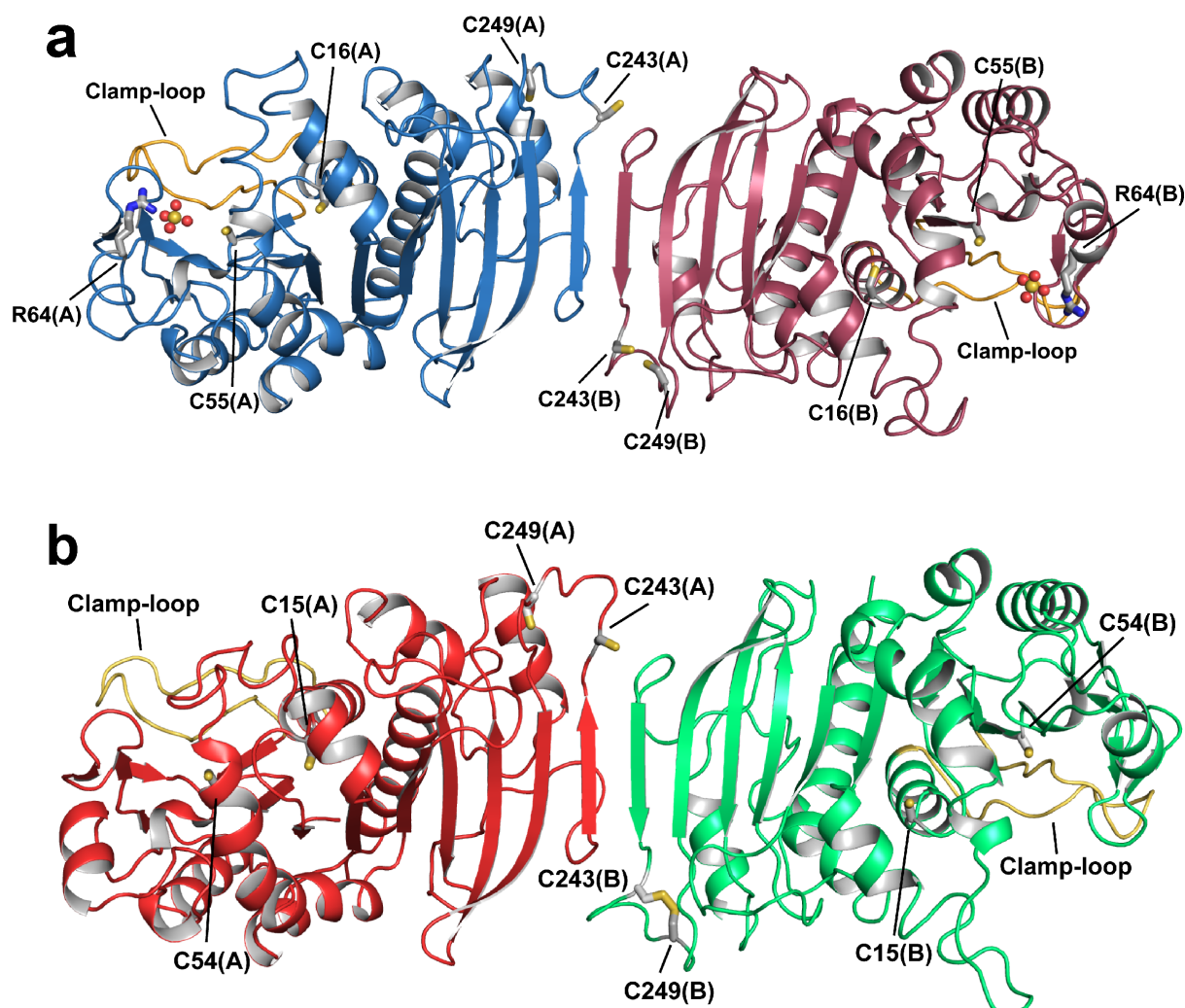


Figure 2.1 Crystal structure of photosynthetic PRK. Overall crystal structure in cartoon representation of reduced phosphoribulokinase (PRK) from a, *Chlamydomonas reinhardtii* and b, *Arabidopsis thaliana*. The two monomers are differently colored. The P-loop is highlighted in green and light-blue and the clamp-loop in orange and yellow. Each monomer contains two pairs of cysteines, one at the active site (Cys16 and Cys55 for CrPRK and Cys15 and Cys54 for AtPRK) and one at the dimer interface close to the C-terminal end of the protein chain (Cys243 and Cys249). Cysteine residues are indicated and represented as sticks. In AtPRK a pair of the C-terminal cysteines forms a disulfide bond. CrPRK binds two sulfate ions (one for each monomer) represented as spheres, coming from the crystallization solution. Arg64 represented as stick, is one of the residues stabilizing the anions.

While little is known about the regulation of dimeric and non-photosynthetic PRK, a fine tuning of photosynthetic PRK activity is achieved by the thioredoxin-dependent interconversion of a specific thiol-disulfide bridge (Porter et al., 1988; Porter and Hartman, 1990). The pair of cysteines involved in redox regulation and corresponding to Cys15/16 and Cys54/55 in At and CrPRK, are located into the P-loop (Walker A; responsible for ATP binding) and at the C-terminal end of strand $\beta 2$ (Figure 2.1 and 2.3), respectively. Both stick out from the catalytic cavity showing a considerable accessibility to facilitate thioredoxin interaction (Table 2.1).

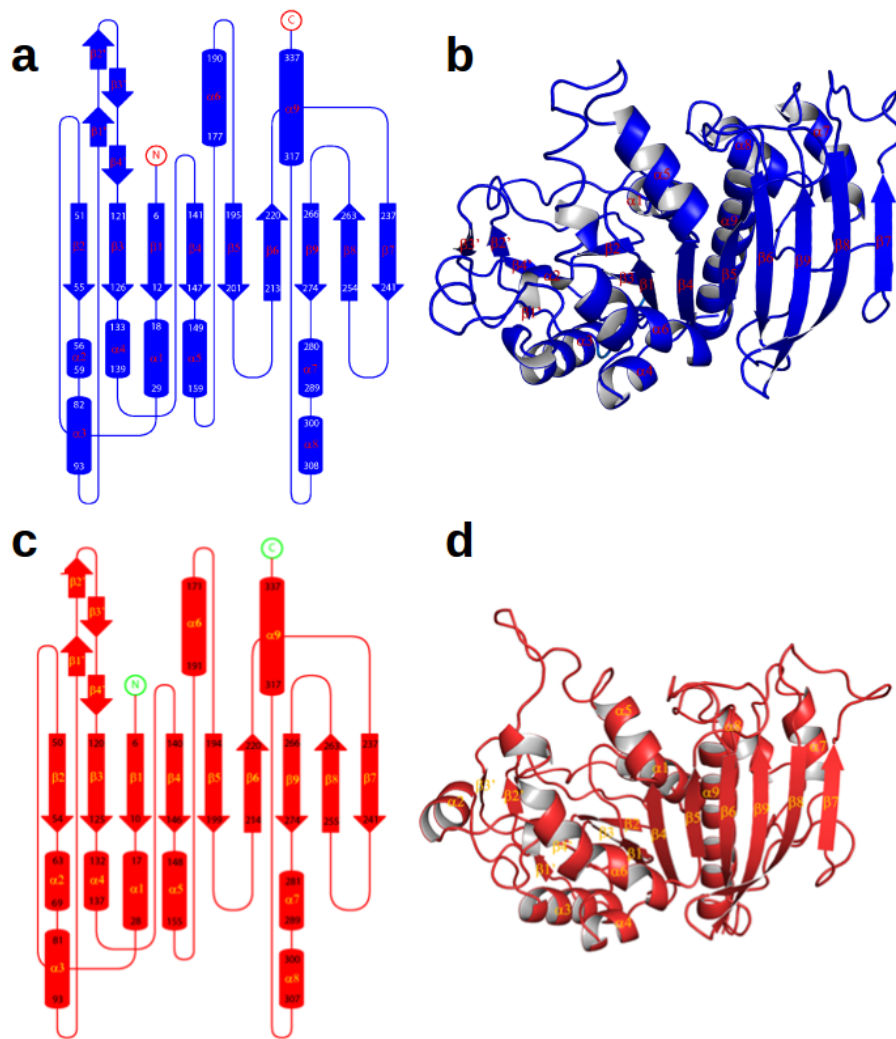


Figure 2.2 Topology and structures of PRK monomers. Topology diagram of CrPRK and AtPRK (a and c, respectively); the monomer is composed by a mixed β -sheet of nine strands, by nine α -helices and four additional small β -strands indicated by β' . b and d, Cartoon representation of the monomer structure of CrPRK and AtPRK, respectively; the central β -sheet is sandwiched between helices $\alpha 3$, $\alpha 4$ and $\alpha 6$ and helices $\alpha 1$, $\alpha 7$, $\alpha 8$ and $\alpha 9$. Strand $\beta 7$ is involved in dimer interface, while the four additional β -strands ($\beta 1'$ to $\beta 4'$) form the edge of the dimer.

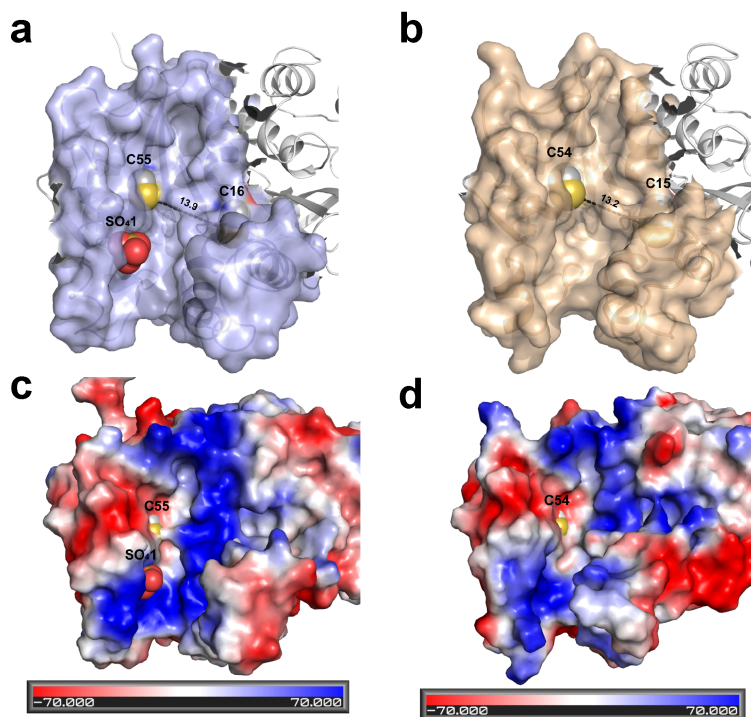


Figure 2.3 Active site of photosynthetic PRK. Catalytic cavity of a, CrPRK and b, AtPRK. The distance between the regulatory cysteines is higher than 13 Å, for both proteins. Catalytic cavity electrostatic surface potential of c, CrPRK and d, AtPRK. The positive potential observed at the bottom of the cavity is more intense and continuous in CrPRK than in AtPRK. A negative potential region observed in both proteins on the left side of the cavity, could be involved in the correct positioning of TRX close to regulatory cysteines.

Table 2.1 Accessibility values for cysteine residues and a strictly conserved arginine.

Residue (Cr/At)	ASA (Å ²)*			
	CrPRK		AtPRK	
	A	B	A	B
Cys16/15	14.5	8.5	7.6	10.6
Cys55/54	10.6	10.6	6.3	9.5
Cys61	55.9	58.7	/	/
Cys243	26.6	37.8	53.4	14.8
Cys249	42.4	31.1	14.8	50.6
Arg64/63	51.4	88.7	82.6	88.2

*Radius of the probe solvent molecule 1.4 Å

In addition, the similar midpoint redox potential (-312 ± 3 mV for CrPRK and -330 mV for AtPRK; Marri et al., 2005) and the slightly acidic pKa values (6.95 ± 0.13 for AtPRK and of 6.79 ± 0.01 for CrPRK) denote a similar susceptibility to redox-regulation for both PRKs (Figure 2.4). Retracing back the phylogenetic tree, the pair of cysteines involved in thioredoxin regulation appears from Cyanobacteria (Figure 2.13b in Addendum).

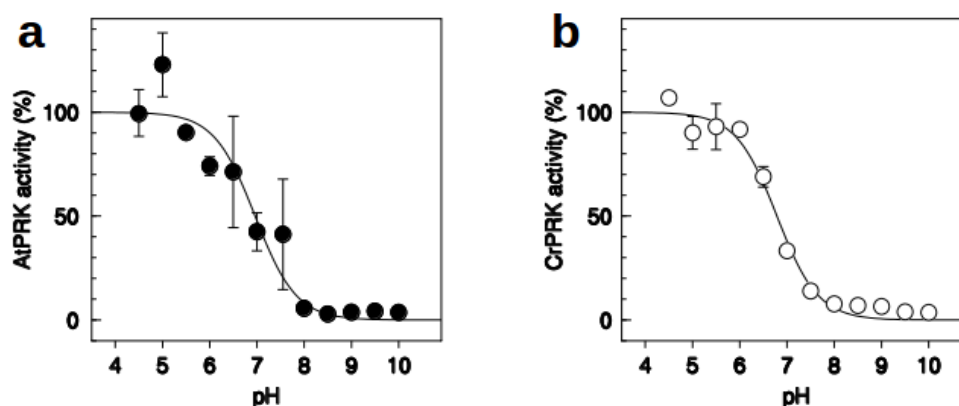


Figure 2.4 pK_a of the catalytic cysteine in photosynthetic PRK. The pK_a of catalytic relevant cysteine (Cys15/16) of a, AtPRK and b, CrPRK, was determined by measuring the IAM-mediated inactivation as a function of pH. Values are reported as mean \pm SD calculated considering 3 experimental replications.

However, ancient photosynthetic PRKs (*i.e.* Cyanobacteria) are deprived of an unstructured amino acid stretch (here named clamp-loop), compared to the most modern PRKs (*i.e.* Plant-type; Figure 2.13 in Addendum). The clamp-loop connects $\alpha 1$ and $\beta 2$ (Figure 2.1, 2.2 and 2.3), the two secondary-structure elements close to the regulatory cysteines, whose thiol groups lie at more than 13 Å (Figure 2.3). Thus, the formation of a disulphide bond necessarily requires conformational changes in the active site supposedly feasible thanks to the clamp-loop (Figure 2.5a).

The electrostatic surface potential of the catalytic cavity reveals an elongated positive region at the bottom and a negative portion on the side (Figure 2.3c,d), the former suitable for binding the phosphate groups of substrates, *i.e.* ATP and Ru5P, and the second relevant for recognition and positioning of thioredoxin as proposed for fructose-1,6-bisphosphatase (Mora-Garcia et al., 1997;

Gütle et al., 2016). Compared to TRX-m, TRX-f2 is more efficient in the reductive activation of both At (Marri et al., 2009) and PRKs (Figure 2.5b).

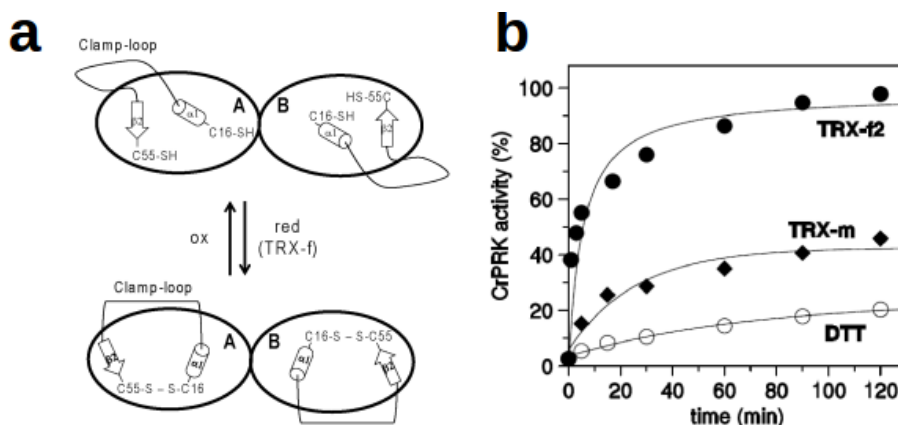


Figure 2.5 TRX-dependent regulation of photosynthetic PRK. a, Schematic representation of the proposed clamp-loop role and conformational changes occurring in chloroplast PRK, upon TRX interaction. b, Activation kinetics of CrPRK by plastidial *C. reinhardtii* TRX-f2 and m, and DTT.

Accordingly, the crystal structure of CrTRX-f2 (unpublished results) and the structural model of AtTRX-f1 show that the catalytic cysteines are surrounded by a large positive region, less extended or alternated with a negative one in TRX-m (Figure 2.6), suggesting that the stages of approaching and pairing between TRX and PRK are mainly governed by electrostatic interactions between exposed portions of the two proteins.

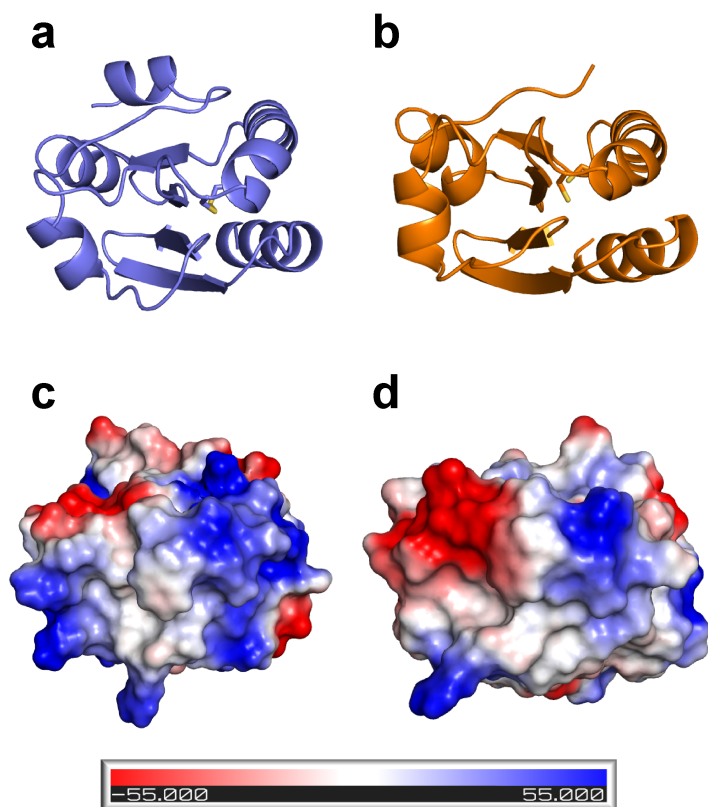


Figure 2.6 Structure represented as ribbon and electrostatic surface potential of the homology model of *Arabidopsis thaliana* TRX-f1 (a, c) and TRX-m2 (b, d). The crystal structures of *Spinacia oleracea* TRX-f and -m (PDB ID 1FAA and 1FB6) 60 have been used as template to model *Arabidopsis thaliana* TRX-f1 and TRX-m2, respectively. The sequence homology of *Arabidopsis thaliana* TRXs with spinach enzymes is 59% and 75% for TRX-f1 and TRX-m2, respectively. The homology modelling was performed with SWISS-MODEL 61.

However, it has been demonstrated that the oxidized-state of the target protein is an essential feature for TRX-target interaction, mainly because of the entropic contribution deriving from the reduction

of the disulfide bridge in the oxidized target (Palde and Carrol, 2015). Indeed, the disulfide bond between the two distant regulatory cysteines introduces a significant conformational restriction, decreasing the overall PRK's entropy.

Therefore, a favourable entropic contribution is proposed to be the main driven-force for TRX-targets interaction. The comparison of the atomic structures of the four PRKs known to date, provide useful information about how environmental conditions, like the climate and the ecological niches, shaped the chemistry and structure of these enzymes. Compared to Rs and Mh enzymes both Cr and At PRKs show a quite small dimer interface (545.6 and 560.3Å, respectively) exclusively formed by strand β 7 (Figure 2.1, 2.2a,c). This strand is absent in RsPRK, while in MhPRK the dimer interface is formed by two consecutive β -strands (Figure 2.14 in Addendum).

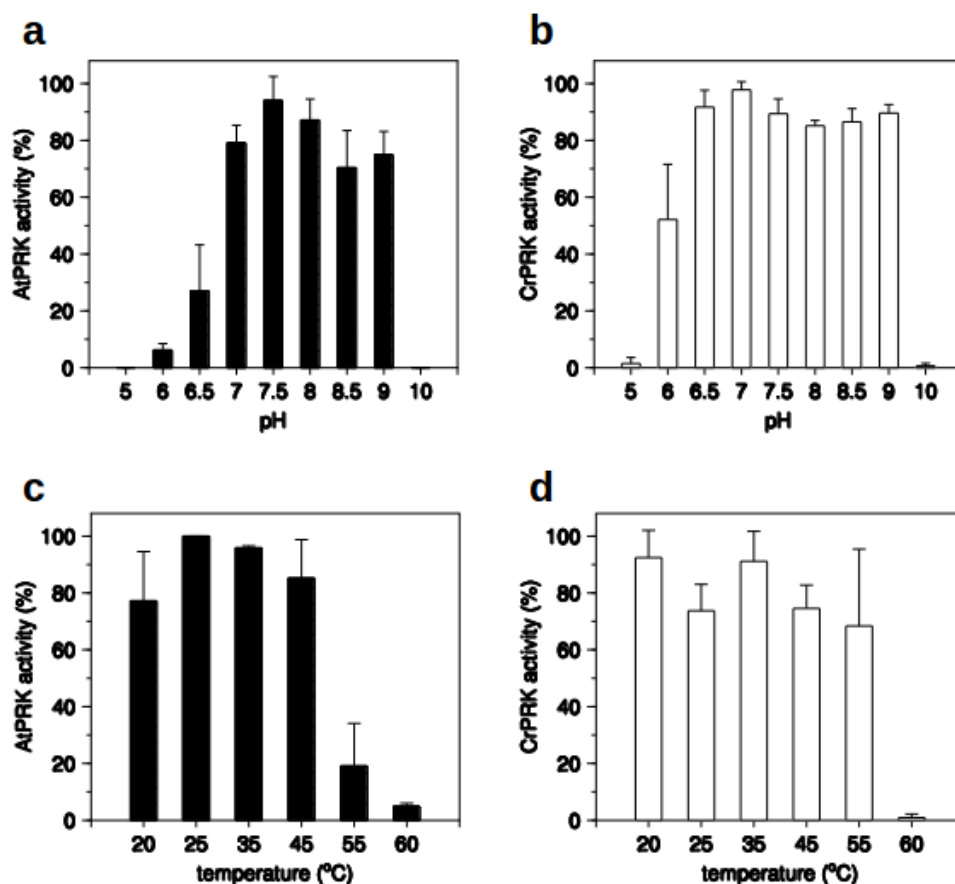


Figure 2.7 Inactivation temperatures and pHs of photosynthetic PRKs. The enzyme activity of a, c, AtPRK and b, d, CrPRK, was evaluated at different pHs (upper panels) and temperatures (lower panels). Values are reported as mean \pm SD calculated considering 3 experimental replications.

Following the evolution, it appears that PRK has undergone a decrease of the structural constraints. From Bacteria to Archaea deep changes in PRK quaternary structure occurred (*e.g.* from octamers to dimers) as well as the allosteric regulation was lost. Reasonably, temperature and acidity of the ancestor environment (Nisbet and Sleep, 2001; Gaucher et al., 2008) likewise the modern habitats of most Archea, did not require a specific regulation but rather functioning enzymes under extreme

conditions. Then, the activity of CrPRK in a wider range of temperature and pH compared to AtPRK (Figure 2.7) may be a heritage from the ancestor PRK.

Moreover, most of the Archaea are not photoautotrophic or at least they do not perform CB cycle, being depleted of genes encoding transketolase, sedoheptulose-1,7-bisphosphatase and ribulose-5-phosphate 3-epimerase (Kono et al., 2017). Consequently the harmonization of the two stages of photosynthesis would not be necessary. The structural evolution described above, is accompanied in photosynthetic PRK by an increase of exposed random coiled regions (Table 2.2). Certain of that, are characterized by a poor or absent electron density, thus being flexible and disordered. Two regions are common to algae and plant enzyme, while a third one is exclusive to AtPRK (Figure 2.8).

Table 2.2 Secondary structure element content in the structurally known PRKs.

PRK	Quaternary structure	Helix content (%)	Sheet content (%)	Other (%)
<i>C. reinhardtii</i>	Dimer	31.2	21.9	46.9
<i>A. thaliana</i>	Dimer	32.3	21.9	45.8
<i>M. hungatei</i>	Dimer	50.0	22.2	27.8
<i>R. sphaeroides</i>	Octamer	41.2	16.9	41.9

The long loop lasting from helices $\alpha 5$ and $\alpha 6$ (Figure 2.8) contains strictly conserved residues as the catalytic Asp160 or Arg159 and 164 involved in Ru5P binding (Charlier et al., 1994; Runquist et al., 1999). A second flexible region, corresponding to the loop between strands $\beta 7$ and $\beta 8$, contains Cys243 and Cys249 (Figure 2.2a,c and 2.8). In both PRK structures this portion is so flexible that the two thiol groups are far in one monomer and closer in the other, but differently from AtPRK they never get oxidized in CrPRK (Figure 2.1 and Figure 2.9), in agreement with the observation that in *Chlamydomonas* the disulfide bond between Cys243 and 249 occurs uniquely through a thiol disulfide exchange reaction with the small unstructured protein CP12 (Thieulin-Pardo et al., 2015). This interaction is an essential step of the assembling process between PRK and glyceraldehyde-3-phosphate dehydrogenase (GAPDH) leading to the regulatory complex GAPDH/CP12/PRK (Graciet et al., 2003; Marri et al., 2008; Del Giudice et al., 2015).

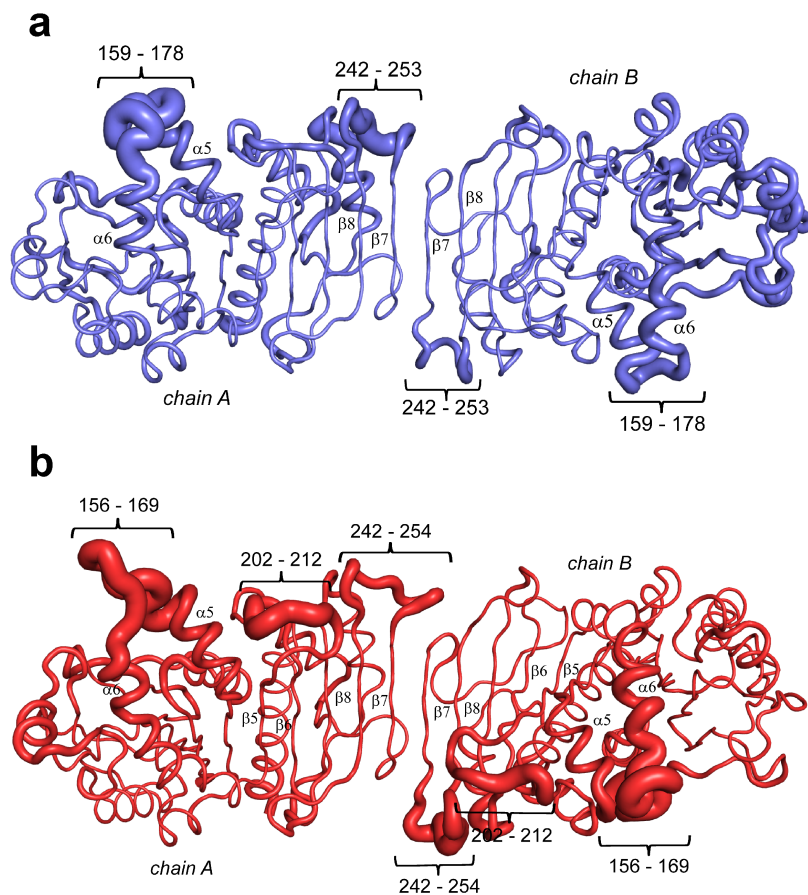


Figure 2.8 Flexible and disordered regions in photosynthetic PRKs. C_a trace of a, CrPRK and b, AtPRK. The trace thickness is proportional to the atomic B factor. AtPRK shows a higher number of flexible regions compared to CrPRK. The residues belonging to the flexible regions are reported.

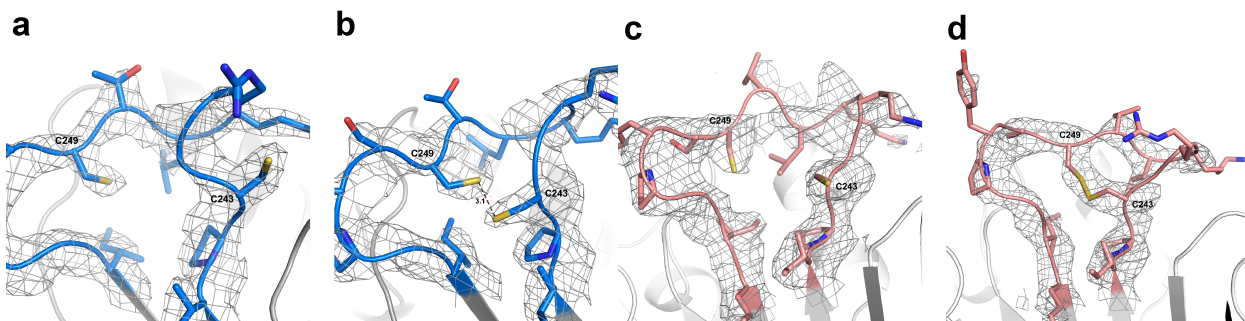


Figure 2.9 Electron density of the C-terminal cysteine pair. 2F_o - F_c electron density map contoured at 1.2 σ and associated to Cys243 and Cys249 in a, CrPRK subunit A b, CrPRK subunit B c, AtPRK subunit A and d, AtPRK subunit B. In CrPRK, both C-terminal cysteines are reduced even if in subunit B the thiol groups are only 3 Å apart. A disulfide bond is instead observed in subunits B of AtPRK, while the thiol groups of the other cysteine pair (subunit A) lie very distantly.

In CrPRK, in analogy to Rs and Mh PRKs, a sulphate ion coming from the crystallization solution is observed in the active site and stabilized by the side chains of Arg64, Arg67, Tyr103 and the main chain carbonyl group of His105 (Figure 2.10). Except for Arg67, all others residues are strictly conserved in PRKs and they form the binding site for phosphate groups of Ru5P (Brandes et al., 1996). The catalytic role of the invariant Arg64 was also confirmed in *C. reinhardtii* (Avilan et al., 1997). In addition, it was found that Arg64 plays a major role in the association of PRK and

GAPDH, in ternary complex formation (Avilan et al., 1997). Consistently, Arg64 faced out at the far end of the dimer (Figure 2.1; Table 2.1).

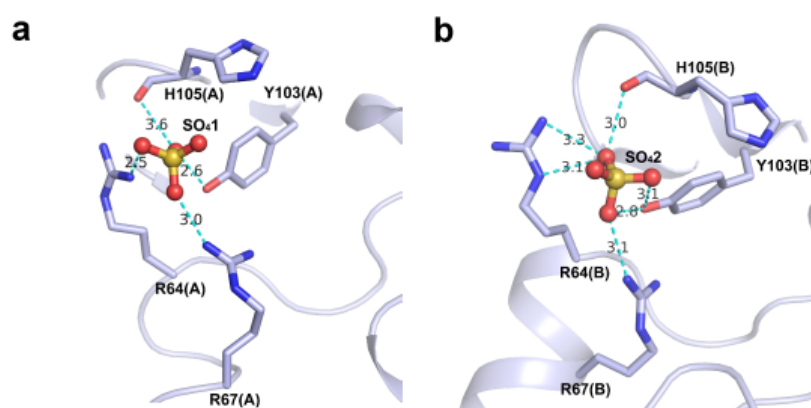


Figure 2.10 Binding site of the sulfate ion in CrPRK. The interactions between a sulfate ion coming from the crystallization solution, and protein residues in a, subunit A and b, subunit B, are represented. Salt-bridges are formed with Arg64 and Arg67, while hydrogen bonds with Tyr103 and His105.

The AtPRK crystal structure confirmed the elongated shape of the oxidized protein previously obtained by SAXS analysis (Del Giudice et al., 2015), but it appears less bent and screwed. Structural information of CrPRK in solution obtained by SEC-SAXS analysis provide a single recognizable species having an R_g value of 3.5 ± 0.1 Å and an estimated MW around 70 kDa (Figure 2.15 and Table 2.3 in Addendum).

The SAXS scattering profile well superimpose to the theoretical one calculated from CrPRK crystal structure (Figure 2.11a) allowing us to conclude that no relevant conformational change of the protein occurs in solution (Figure 2.11b).

In conclusion, our results provide the last structure of the 11 enzymes of the CB cycle, paving the way for a future improvement of the kinetic bottleneck within the CB cycle.

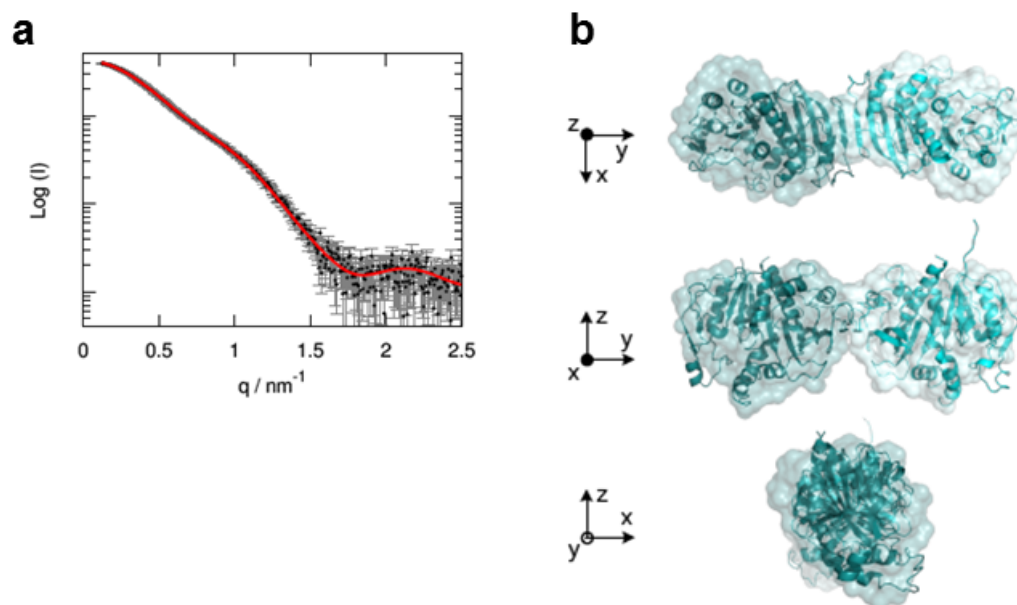


Figure 2.11 SAXS analysis of CrPRK. a, Superimposition between the experimental SAXS scattering profile (black) and the theoretical SAXS curve (red) calculated from CrPRK crystal structure (upper graph). The lower graph shows the residuals calculated by the difference of experimental and calculated intensities. b, Comparison between the ab-initio model (surface representation) and the crystal structure (ribbon representation) of CrPRK showing an excellent agreement between the two models.

2.3 Materials and methods

2.3.1 Protein expression and purification

Recombinant AtPRK and CrPRK were expressed in *E. coli* BL21(DE3) strain harboring the pET-28 expression vector (Novagen) containing the cDNA sequence of the mature form of both enzymes (Figure 3.12, 3.4 Addendum). AtPRK was expressed and purified as previously described (Marri et al., 2008). The cDNA coding for CrPRK was put in frame with a His-Tag and a thrombin cleavage site at the 5' end of the nucleotide sequence in order to purify the recombinant enzyme through a single chromatographic step performed loading the supernatant of the cellular lysate onto a Chelating Sepharose Fast Flow (GE Healthcare) column, following the manufacturer instruction. Immediately after elution, CrPRK was desalted in 30 mM Tris-HCl, 1 mM EDTA, pH 7.9 by PD-10 Desalting Columns (GE Healthcare). The His-Tag was removed by overnight digestion with thrombin protease. Samples purity was checked by 12.5% SDS-PAGE and purified proteins were quantified by absorbance at 280 nm (Nanodrop; Thermo Scientific) and stored at -80 °C.

When required, oxidized and reduced AtPRK and CrPRK were prepared by incubation at 25°C for 2/3 h in the presence of 40 mM trans-4,5-dihydroxy-1,2-dithiane (oxidized DTT) or 1,4-dithiothreitol (reduced DTT). Following incubation, samples were desalted in 30 mM Tris-HCl, pH 7.9, 1 mM EDTA through NAP-5 column (GE Healthcare) and brought to the desired concentration either by dilution or by concentration through Amicon-Ultra device (Millipore; cut-off 10 kDa).

2.3.2 Activity assay and determination of pH- and temperature-dependence

Phosphoribulokinase activity was measured spectrophotometrically (Cary 60 Uv-Vis; Agilent) as previously described (Roesler and Ogren, 1990). The pH dependence of purified enzymes was determined in Britton-Robinson buffer for pH values ranging from 4.0 to 8.5. For pH ranging from 9 to 10, 100 mM Glycine buffer was used. Activities were measured on two independent protein purifications and are expressed as percentage of the highest measured activity. Temperature-dependence was evaluated on aliquots of AtPRK and CrPRK incubated for 20 min at temperatures ranging from 20° to 60°C. Following incubation the activity was assayed at 25°C. Activities were measured on two independent protein purifications and are expressed as percentage of the highest measured activity.

2.3.3 Thioredoxin specificity and redox titration

Thioredoxin specificity was evaluated through the activation rate of oxidized CrPRK (2 μM) by 0.2 mM reduced DTT and thioredoxin f2, m, x, y and z (5 μM each), as previously described (Marri et al., 2009). At different incubation times, PRK activity was measured. To determine the midpoint redox potential of CrPRK, three independent redox titrations were performed. Briefly, a mixture containing pure recombinant CrPRK (0.5 mg ml⁻¹), commercial *E. coli* thioredoxin (1 mg ml⁻¹) and 20 mM DTT, at different reduced to oxidized ratios, were incubated for 3 h at 25°C before measuring PRK activity. The obtained curves were fitted by non-linear regression (CoStat, Co-Hort Software) to the Nernst equation.

2.3.4 Determination of the pK_a values of the catalytic cysteines

The determination of pK_a values for both CrPRK and AtPRK was performed as previously described (Bedhomme et al., 2012). Briefly, PRK activity was measured on reduced PRK samples (2 μM) following 20 min of incubation at 25°C in presence or in absence of 0.2 mM iodoacetamide (IAM). Incubations were performed in different buffers within a 4.5-10 pH range. Ten-20 μl aliquots were used to measure PRK activity in 1 ml of assay mixture. The residual activity was expressed as percentage of inhibition between IAM-treated and untreated samples, and expressed as a function of pH. The obtained curves were fitted by non-linear regression (CoStat, Co-Hort Software) to modified Henderson-Hasselbalch equation.

2.3.5 Crystallization and data collection

Reduced CrPRK and AtPRK were both concentrated at 10 mg ml⁻¹ in 30 mM Tris-HCl, pH 7.9, 1 mM EDTA, and 25 mM potassium phosphate buffer solution, pH 7.5, 20 mM reduced DTT, respectively. They were crystallized by the vapor diffusion method at 293 K with sitting drop for CrPRK and hanging drop for AtPRK. A protein solution aliquot of 2 μl was mixed to an equal volume of reservoir, and the prepared drop was equilibrated against 900 (CrPRK) and 750 (AtPRK) μl of reservoir.

CrPRK crystals appeared as elongated prisms and were obtained in different conditions of the Extension Kit from Hampton Research (solutions 22: 12 % w/v PEG 20K, 0.1 M MES, pH 6.5; 26: 30 % w/v PEG MME 5K, 0.1 M MES, pH 6.5, 0.2 M ammonium sulfate; 30: 10% w/v PEG 6K, 5% v/v MPD, 0.1 M HEPES, pH 7.5) and Structure screen 1 from Molecular Dimension (MD1-01-CF, solutions 35: 30 % w/v PEG 4K, 0.1 M Tris-HCl, pH 8.5, 0.2 M lithium sulfate; and 50: 15 % w/v PEG 8K, 0.5 M lithium sulfate). The conditions were optimized and the best diffracting crystal

grew in about 10 days, from 22 % w/v PEG MME 5K, 0.1 M MES, pH 6.5, 0.2 M ammonium sulfate.

AtPRK crystals showed a bipiramidal morphology and grew in three or five weeks from a reservoir solution containing 1.4 – 1.7 M sodium malonate, pH 5.0. The best diffracting crystal of AtPRK was obtained in 1.5 M sodium malonate, pH 5.0.

Crystals were mounted from the crystallization drop into cryo-loops, briefly soaked in a cryo-protectant solution containing 30 % w/v PEG MME and 20 % v/v PEG 200 for CrPRK and 1.7 M sodium malonate, pH 5.0, and 30% v/v glycerol for AtPRK, then frozen in liquid nitrogen. Diffraction images were recorded at 100 K using a synchrotron radiation at Elettra (Trieste, beam line XRD1) for CrPRK and at the European Synchrotron Radiation Facility (Grenoble, beam line ID14-4) for AtPRK. Data collection parameters are reported in Table 3.4, 3.4 Addendum. The data at a resolution of 2.5 Å for both CrPRK and AtPRK were processed using XDS (Kabsch, 2010) and scaled with SCALA (Evans, 2006). The correct space group was determined with POINTLESS (Evans et al., 2006) and confirmed in the structure solution stage. Data collection statistics are reported in Table 3.5, 3.4 Addendum.

2.3.6 Structure solution and refinement

CrPRK structure was solved by molecular replacement using the program PHASER (McCoy et al., 2007) from PHENIX (Adams et al., 2010). The coordinates of PRK from *Methanospirillum hungatei* (PDB code 5BF3; Kono et al., 2017) deprived of sulphate ions and water molecules, were used as search probe. The protein chain was traced by Autobuilt from PHENIX (Adams et al., 2010) and Buccaneer (Cowtan, 2006) from CCP4 package. The refinement was performed with REFMAC 5.8.0135 (Murshudov et al., 1997) selecting 5% of reflections for R_{free} . The manual rebuilding was performed with Coot (Emsley and Cowtan, 2004). The residual electron density map showed the position of a sulphate ion for each monomer coming from the crystallization solution, which was added to the model. Water molecules were automatically added and, after a visual inspection, they were conserved in the model only if contoured at 1.0 σ on the $(2F_o - F_c)$ map and if they fell into an appropriate hydrogen bonding environment. The structure of CrPRK without sulfate ions and waters, was used as probe to solve the AtPRK structure by molecular replacement using MOLREP (Vagin and Teplyakov, 2010). The refinement was performed as described for CrPRK. The refinement statistics are reported in Table 2.5 (2.4 Addendum). All structure figures were prepared using PyMOL (The PyMOL Molecular Graphics System, Schrödinger, LLC).

2.3.7 Small angle X-ray scattering data collection

Small angle X-ray scattering (SAXS) data were collected at the BioSAXS beamline BM29 (Pernot et al., 2013) at European Synchrotron Radiation Facility (ESRF, Grenoble) and the data collection parameters are reported in Table 2.4 (Addendum). A Size Exclusion Chromatography (SEC)-SAXS experiment was performed using a HPLC system (Shimadzu) directly connected to the measurement capillary. A volume of 100 μl of reduced CrPRK (6.1 mg ml^{-1}) was loaded onto a Superdex 200 10/300 GL column (GE Healthcare) pre-equilibrated in 50 mM Tris-HCl, pH 7.5, 150 mM KCl. The sample was eluted at a flow rate of 0.5 ml min^{-1} and SAXS frames obtained by 1 s exposure were collected continuously. The automatic pipeline for SEC-SAXS data analysis implemented at BM29 was used to assess the quality of the collected data (Brennich et al., 2016).

2.3.8 Small angle X-ray scattering data analysis

Afterwards, a classification of the collected frames as buffer (0-14 ml) or protein frames (14-17.75 ml) was performed on the basis of the SAXS intensity trace (Figure 2.16, Addendum 2.4). Statistical test implemented in CorrMap (Franke et al., 2015) aided by visual inspection, was used to choose the superimposable buffer intensity profiles. The averaging of the buffer profiles, the subtraction of the averaged buffer intensity from the protein data and an automatic analysis of the subtracted protein profiles was performed with a Matlab script. The script used the tools of the ATSAS package (Petoukhov et al., 2012) to automatically obtain from the subtracted intensity $I(q)$: (i) the $I(0)$ and the gyration radius (R_g) via the Guinier approximation (Guinier, 1939) $I(q) = I(0) \cdot \exp[-(qR_g)^2/3]$; (ii) the pair-distance $[p(r)]$ function, from which the maximum particle dimension (D_{max}) was estimated, in addition to an independent calculation of $I(0)$ and R_g . Estimates of the MW were also determined both from the Porod invariant (Porod, 1982) as 0.6 times the Porod volume (V_p) for roughly globular particles (Petoukhov et al., 2012) and by the invariant volume-of-correlation length (V_c), through a power-law relationship between V_c , R_g and MW that has been parametrized (Rambo and Tainer, 2013). The protein frames giving constant R_g values were scaled to the intensity of the elution maximum and averaged in order to obtain a single representative scattering profile with good signal to noise ratio, presented in the results and used for modelling.

2.3.9 Modelling from SAXS data

The experimental SAXS profile of the CrPRK dimer was fitted with the theoretical profile calculated from the atomic coordinates using CRY SOL3 (Franke et al., 2017) with default parameters. In addition, low-resolution models of the CrPRK dimer based on the SAXS profile were built using the ab-initio program GASBOR (Svergun et al., 2001). The sequence and the homodimeric state of

CrPRK were given as inputs in GASBOR and a 2-fold symmetry was imposed in the calculations. A series of 10 models was generated. The similarity of the structures obtained by repeated calculations was checked by DAMAVER (Volkov and Svergun, 2003) in which the superposition is performed by the SUPCOMB code (Kozin and Svergun, 2001).

All programs used for SAXS data analysis and reconstruction, belong to the ATSAS package 2.7 (Petoukhov et al., 2012). The graphical representations of the obtained three-dimensional models were built by using PyMOL (The PyMOL Molecular Graphics System, Schrödinger, LLC).

2.3.10 Data availability

Atomic coordinates and structure factors have been deposited in the Protein Data Bank (PDB) under accession codes 6H7G and 6H7H for Cr and AtPRK, respectively.

Addendum to Chapter 2

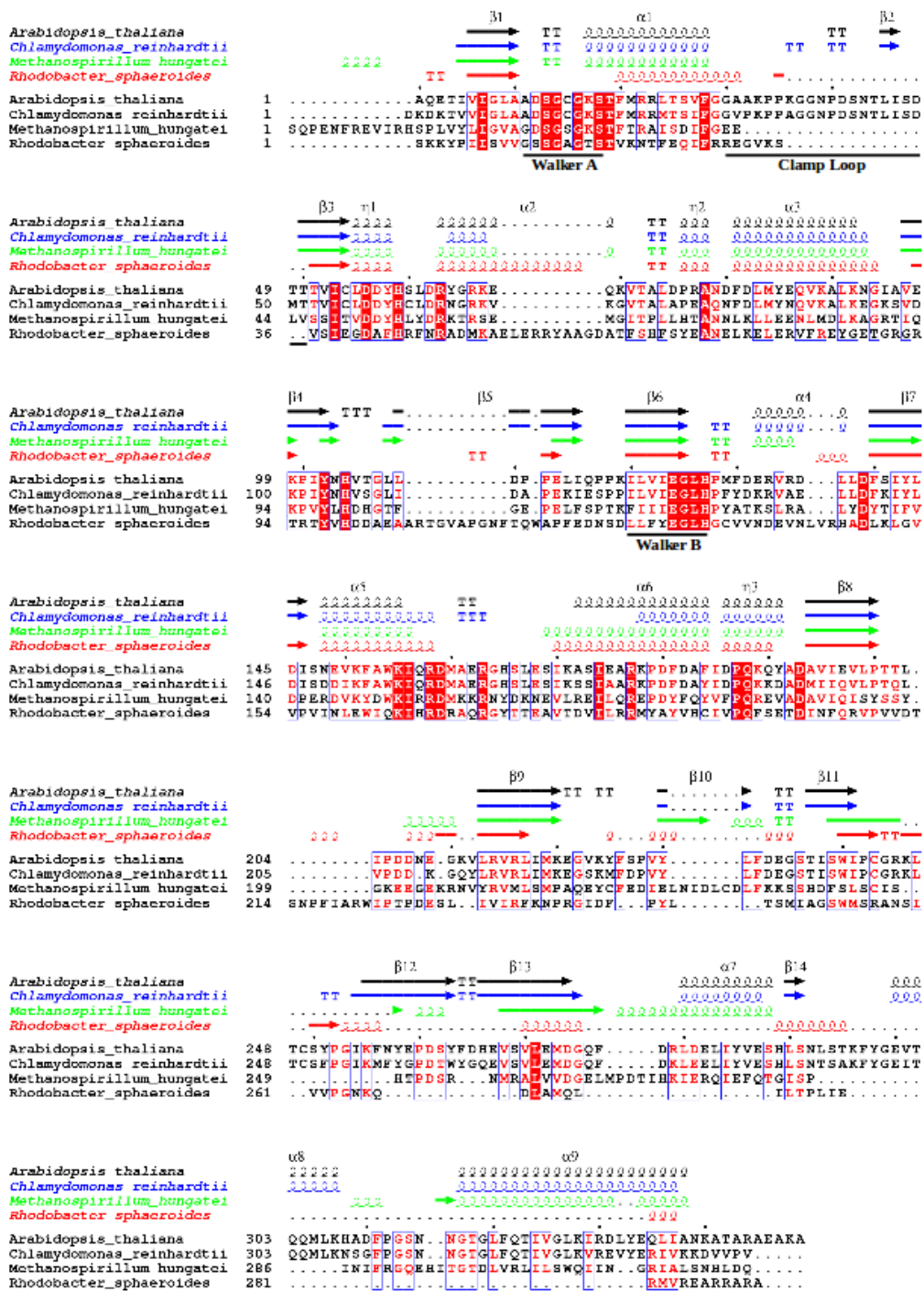
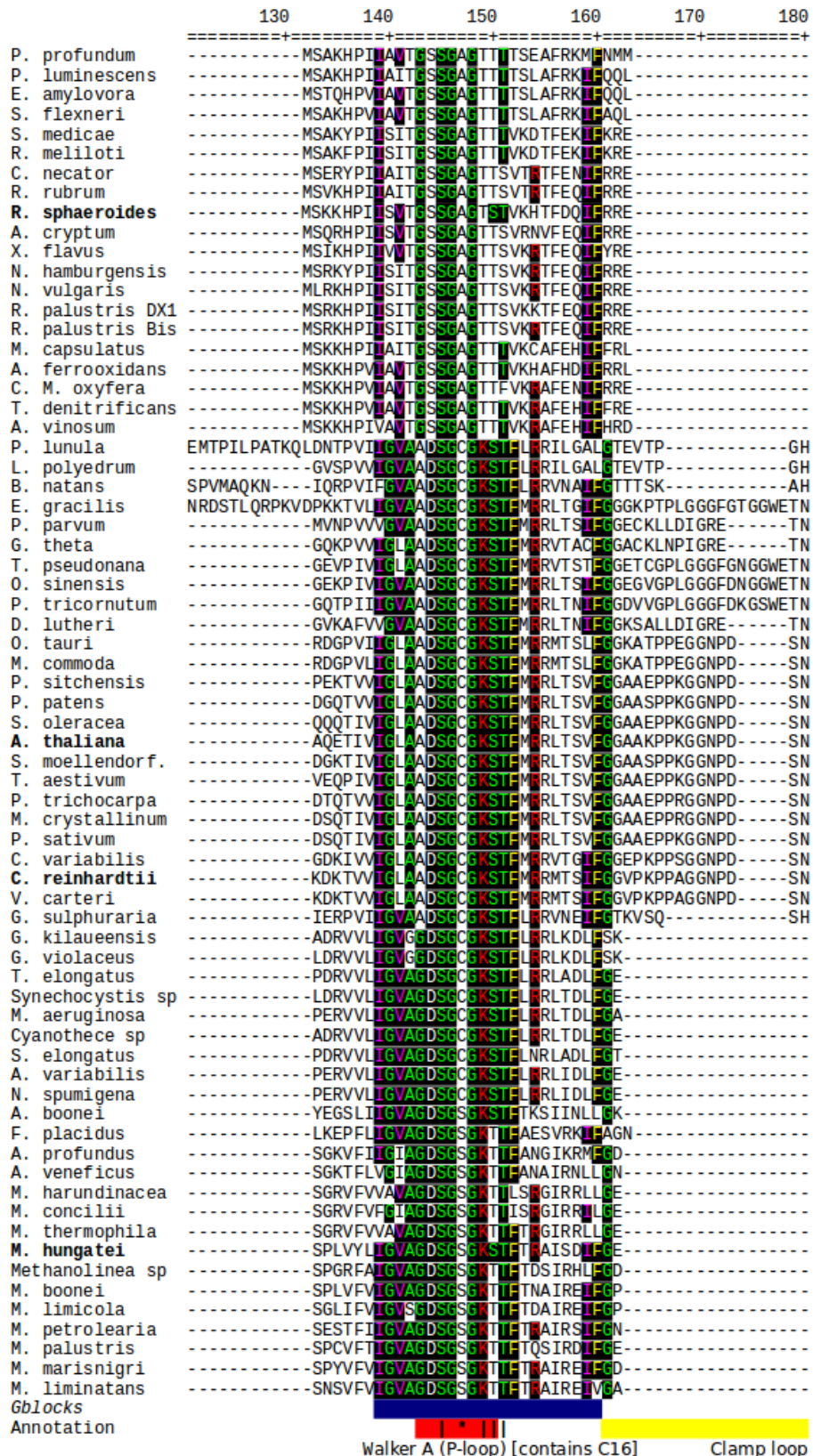


Figure 2.12 Sequence and structural alignment of the four structurally known PRKs. The alignment has been performed by Esript (<http://esript.ibcp.fr>) 58 using the sequence and the structure of AtPRK (Uniprot accession code P25697 and PDB ID 6H7H); CrPRK (Uniprot accession code P19824 and PDB ID 6H7G); RsPRK (Uniprot accession code P12033 and PDB ID1A7J, Harrison et al., 1998), MhPRK (Uniprot accession code Q2FUB5 and PDB ID 5B3F, Kono et al., 2017). The sequence of both photosynthetic PRKs is much longer (349 and 344 residues for AtPRK and CrPRK, respectively) than bacterial (290 residues) and Archae (323 residues) PRK. Sequence identities among considered PRKs are: 75% for AtvsCr; 35% for AtvsMh; 32% for CrvsMh; 22% for AtvsRs; 24% for CrvsRs. The sequence identities have been calculated by Clustal O (Bienert, S. et al.; 2017).

a

	10	20	30	40	50	60
P. profundum	-----	-----	-----	-----	-----	-----
P. luminescens	-----	-----	-----	-----	-----	-----
E. amylovora	-----	-----	-----	-----	-----	-----
S. flexneri	-----	-----	-----	-----	-----	-----
S. medicae	-----	-----	-----	-----	-----	-----
R. meliloti	-----	-----	-----	-----	-----	-----
C. necator	-----	-----	-----	-----	-----	-----
R. rubrum	-----	-----	-----	-----	-----	-----
R. sphaeroides	-----	-----	-----	-----	-----	-----
A. cryptum	-----	-----	-----	-----	-----	-----
X. flavus	-----	-----	-----	-----	-----	-----
N. hamburgensis	-----	-----	-----	-----	-----	-----
N. vulgaris	-----	-----	-----	-----	-----	-----
R. palustris DX1	-----	-----	-----	-----	-----	-----
R. palustris Bis	-----	-----	-----	-----	-----	-----
M. capsulatus	-----	-----	-----	-----	-----	-----
A. ferrooxidans	-----	-----	-----	-----	-----	-----
C. M. oxyfera	-----	-----	-----	-----	-----	-----
T. denitrificans	-----	-----	-----	-----	-----	-----
A. vinosum	-----	-----	-----	-----	-----	-----
P. lunula	-----	-----	-----	-----	-----	-----
L. polyedrum	-----	-----	-----	-----	-----	-----
B. natans	-----	-----	-----	-----	-----	-----
E. gracilis	-----	-----	-----	-----	-----	-----
P. parvum	-----	-----	-----	-----	-----	-----
G. theta	-----	-----	-----	-----	-----	-----
T. pseudonana	-----	-----	-----	-----	-----	-----
O. sinensis	-----	-----	-----	-----	-----	-----
P. tricornutum	-----	-----	-----	-----	-----	-----
D. lutheri	-----	-----	-----	-----	-----	-----
O. tauri	-----	-----	-----	-----	-----	-----
M. commoda	-----	-----	-----	-----	-----	-----
P. sitchensis	-----	-----	-----	-----	-----	-----
P. patens	-----	-----	-----	-----	-----	-----
S. oleracea	-----	-----	-----	-----	-----	-----
A. thaliana	-----	-----	-----	-----	-----	-----
S. moellendorff.	-----	-----	-----	-----	-----	-----
T. aestivum	-----	-----	-----	-----	-----	-----
P. trichocarpa	-----	-----	-----	-----	-----	-----
M. crystallinum	-----	-----	-----	-----	-----	-----
P. sativum	-----	-----	-----	-----	-----	-----
C. variabilis	-----	-----	-----	-----	-----	-----
C. reinhardtii	-----	-----	-----	-----	-----	-----
V. carteri	-----	-----	-----	-----	-----	-----
G. sulphuraria	MELRDSLSTMGVFLPSTTSVYVYKSSSTIKSKKYNKRNYSVSRVQVGGSKISSWSNRL	-----	-----	-----	-----	-----
G. kilaeensis	-----	-----	-----	-----	-----	-----
G. violaceus	-----	-----	-----	-----	-----	-----
T. elongatus	-----	-----	-----	-----	-----	-----
Synechocystis sp	-----	-----	-----	-----	-----	-----
M. aeruginosa	-----	-----	-----	-----	-----	-----
Cyanothece sp	-----	-----	-----	-----	-----	-----
S. elongatus	-----	-----	-----	-----	-----	-----
A. variabilis	-----	-----	-----	-----	-----	-----
N. spumigena	-----	-----	-----	-----	-----	-----
A. boonei	-----	-----	-----	-----	-----	-----
F. placidus	-----	-----	-----	-----	-----	-----
A. profundus	-----	-----	-----	-----	-----	-----
A. veneficus	-----	-----	-----	-----	-----	-----
M. harundinacea	-----	-----	-----	-----	-----	-----
M. concilii	-----	-----	-----	-----	-----	-----
M. thermophila	-----	-----	-----	-----	-----	-----
M. hungatei	-----	-----	-----	-----	-----	-----
Methanolinea sp	-----	-----	-----	-----	-----	-----
M. boonei	-----	-----	-----	-----	-----	-----
M. limicola	-----	-----	-----	-----	-----	-----
M. petrolearia	-----	-----	-----	-----	-----	-----
M. palustris	-----	-----	-----	-----	-----	-----
M. marisnigri	-----	-----	-----	-----	-----	-----
M. liminatans	-----	-----	-----	-----	-----	-----
Gblocks	-----	-----	-----	-----	-----	-----
Annotation	-----	-----	-----	-----	-----	-----

	70	80	90	100	110	120	
P. profundum	-----	-----	-----	-----	-----	-----	
P. luminescens	-----	-----	-----	-----	-----	-----	
E. amylovora	-----	-----	-----	-----	-----	-----	
S. flexneri	-----	-----	-----	-----	-----	-----	
S. medicae	-----	-----	-----	-----	-----	-----	
R. meliloti	-----	-----	-----	-----	-----	-----	
C. necator	-----	-----	-----	-----	-----	-----	
R. rubrum	-----	-----	-----	-----	-----	-----	
R. sphaeroides	-----	-----	-----	-----	-----	-----	
A. cryptum	-----	-----	-----	-----	-----	-----	
X. flavus	-----	-----	-----	-----	-----	-----	
N. hamburgensis	-----	-----	-----	-----	-----	-----	
N. vulgaris	-----	-----	-----	-----	-----	-----	
R. palustris DX1	-----	-----	-----	-----	-----	-----	
R. palustris Bis	-----	-----	-----	-----	-----	-----	
M. capsulatus	-----	-----	-----	-----	-----	-----	
A. ferrooxidans	-----	-----	-----	-----	-----	-----	
C. M. oxyfera	-----	-----	-----	-----	-----	-----	
T. denitrificans	-----	-----	-----	-----	-----	-----	
A. vinosum	-----	-----	-----	-----	-----	-----	
P. lunula	LPRSSPQAPRASSARV	PKVVALRAAADSQPT	GLWVPSPEAEAKLRE	VDGIKLYPTHAWTE			
L. polyedrum	RAARAL TAMRGAANSV	PTGLVWPSPEAEAKL	REEDG IKMYP THAWT	DDMMP IVPATKE--			
B. natans	RPAQREARVAAHGKGV	VSTVALDAPVATSEDS	SMTWS SAKGNEVDAG	MGQVH IEAAI SNEV			
E. gracilis	I GYTFSGGLVENYATT	RPVQTQPAAL ILPKA	VRYAGV SQGPQVES	REARTALHAAATGTV			
P. parvum	SPA-----	-----	-----	PSVVSQSRVAPRATV	VE--		
G. theta	-----	-----	-----	RVTNDKEMDVAIQQ	ISMSLAS--		
T. pseudonana	-----	-----	-----	MKFLVASLIASAFST	INTPT LRGNSALAAL	KD--	
O. sinensis	-----	-----	-----	MPANTL RAAAPASPSA	LNMAL KE--		
P. tricornutum	VPS-----	-----	-----	NLRGVAPSASSLNMAL	KE--		
D. lutheri	VPQ-----	-----	-----	TACTVLMATKT--			
O. tauri	-----	-----	-----	MSASLGFSTSVRAAP	VRATRDAVKPRATR	ARVVTTAK--	
M. commoda	RKFQGS-----	-----	-----	RVSGKSVVRAAKRNV	TVKAE--		
P. sitchensis	LAS-----	-----	-----	FSLAHTTRPRRALV	VCSVG--		
P. patens	KPARSARPVH-----	-----	-----	LTSAFHGQSVASVSQ	VAGFESSGVKYRS	AGRRVVVCKAA--	
S. oleracea	NKQVFFNYKR-----	-----	-----	SSSNNTLFTTRPSY	VITCS--		
A. thaliana	SSKQVF-----	-----	-----	LYRRQPQTNRFFNL	LITC--		
S. moellendorff.	SSNIGILQHHPWRGSH	ASSLFSFPKLGARIG	SSSGSGSGSGTSSSN	RVRVLVCCAAGG--			
T. aestivum	IPNSGFRQNG-----	-----	-----	VIFFTTRSSRRSNT	RHGARTFQVSCA--		
P. trichocarpa	KTHLGFNQRH-----	-----	-----	VVFYSTNKKTTKR	ASSAVITCSA--		
M. crystallinum	TSHLGFNQKK-----	-----	-----	QLFFCNKSAYKRV	SFSSRPCVITCLAG--		
P. sativum	-----	-----	-----	-----	AG--		
C. variabilis	APIARPTFSS-----	-----	-----	TLNQRTLKAGR	VASRVVVKAEG--		
C. reinhardtii	-----	-----	-----	MAFTMRAPAPRATA	QSRVTANRARRSLV	VRAD--	
V. carteri	-----	-----	-----	AQSRVTASRASRR	VLVKAQ--		
G. sulphuraria	L FQKKEINTTRKTTK	YWIIIVSSQTALEEF	VNCSGAKGVHESAGI	SRSKSKVLRNKG--			
G. kilaeensis	-----	-----	-----	-----	MVSK--		
G. violaceus	-----	-----	-----	-----	MVST--		
T. elongatus	-----	-----	-----	-----	MSSK--		
Synechocystis sp	-----	-----	-----	-----	MTTQ--		
M. aeruginosa	-----	-----	-----	-----	MANK--		
Cyanothece sp	-----	-----	-----	-----	MTTQ--		
S. elongatus	-----	-----	-----	-----	MSK--		
A. variabilis	-----	-----	-----	-----	MTTK--		
N. spumigena	-----	-----	-----	-----	MTTK--		
A. boonei	-----	-----	-----	-----	MLGEFRRL EE--		
F. placidus	-----	-----	-----	-----	MILEK--		
A. profundus	-----	-----	-----	-----	MLKEKL IK--		
A. veneficus	-----	-----	-----	-----	MTSNLKERL KE--		
M. harundinacea	-----	-----	-----	-----	MAERL KG--		
M. concilii	-----	-----	-----	-----	MRS LKDRI RE--		
M. thermophila	-----	-----	-----	-----	MR LLEKI RE--		
M. hungatei	-----	-----	-----	-----	MSQPENFRE VIRH--		
Methanolinea sp	-----	-----	-----	-----	MTSKPGFKEII KS--		
M. boonei	-----	-----	-----	-----	MPRTPPFKEII AR--		
M. limicola	-----	-----	-----	-----	MSCIDEYLSSESGKCR	NRFSGDDEYCFSSSG	KGINLKKI IEN--
M. petrolearia	-----	-----	-----	-----	MDYSHE TNLKNFR	HAVDS--	
M. palustris	-----	-----	-----	-----	MMQTEGKTGEKPD	LCPGTGGLNFKDRIAS--	
M. marisnigri	-----	-----	-----	-----	MPPSDFKRVI AE--		
M. liminatans	-----	-----	-----	-----	MDTPVFRDLISG--		
Gblocks							
Annotation							



	190	200	210	220	230	240	
P. profundum	----NINASWLEGSF	RYT	PEMDVEIRKAKEQGR	-HISYFG	PEAND	FPQLEKFFRQYG	
P. luminescens	----DISAAQIEGDSF	RYT	PEMDAAIRKAKEQGR	-HISYFG	PEAND	FGMLEKTMIDYG	
E. amylovora	----GLHAAEIEGDSF	RFT	PEMDAIRKARDMGK	-HVSYFG	PEAND	FALLERTFSEYG	
S. flexneri	----NLHAAEVEGDSF	RYT	PEMDAIRKARDAGR	-HISYFG	PEAND	FGLEQTFIEYG	
S. medicae	----NISASFIEGDAF	RYD	NETMRSKIAEEKARGV	-DFHFSAE	AN	ELEILESVFAEYG	
R. melliloti	----NISASFIEGDAF	RFD	NETMRSKIAEEKARGV	-DFHFSAE	AN	ELEILESVFAEYG	
C. necator	----GVKSYVIEGDSF	RYD	NAEMKVKMAEAEERTGNMNF	SHFGEEN	LL	GELENLFRSYA	
R. rubrum	----GVNAAVVEGDSF	RND	KAMKIAMAEAQKAGNAN	FSHFG	PEANL	FEELTLFRTYG	
R. sphaeroides	----GVKASIEGDAF	RFN	ADMKAELDRRYAAGDAT	FSHFSYE	AN	ELKELERLVFREYG	
A. cryptum	----KITAAHIEGDAF	RYD	NAEMKTKMAEAEAGNRHF	SHFS	PETN	LLAEELAAATFESYA	
X. flavus	----KVKAAFVEGDSF	RYD	RYEMRELMAAEAAKGNKHF	SHFS	PETN	RLLDLAQLFKDYG	
N. hamburgensis	----NVVAAIIEGDAF	RYN	ADMRTMAEESDRGNKHF	SHFS	PETN	LFELEAVFRSYS	
N. vulgaris	----NVVAAIIEGDAF	RYN	ADMRTMAEESDKGNKHF	SHFS	PETN	LFAELGVFRSYG	
R. palustris DX1	----NVNAAFIIEGDAF	RYN	VDMRNKMAEAEERGNRHF	SHFS	PETN	LFELEQTFKSYA	
R. palustris Bis	----NVNAAIIEGDAF	RYN	VDMRTMAEAEAKGNKTF	SHFS	PDTN	LFELETTFRDYS	
M. capsulatus	----GLKPLVIEGDSF	RYD	VMRAQIDKARREG	-RHF	SHFS	IEANILDELENVFRHYG	
A. ferrooxidans	----KIDPVVIEGDSF	RYN	NEMREAIKAAADG	-KTI	SHFG	PEGNDPEALERLFRFYG	
C. M. oxyfera	----EITSAVIEGDSF	SVT	NAQFVERSAVEH	----	NF	SHFGPEAND	
T. denitrificans	----KINAAVIEGDSF	SLA	VEFNAVKKAEAEGNFS	FSHFG	POANH	FDKLAELFKTYG	
A. vinosum	----NISAAVIEGDSF	SYD	NATMAEMAFAKRG	-SLSHFG	PVAN	RFDLEELFRFYG	
P. lunula	TAVGDMVVICLDD	YHTND	HAGRRK	-----	TGL	NALDARENDFALMGSQIEAL	
L. polyedrum	TAIGDMVVICLDD	YHTND	HAGRRK	-----	TGL	NALDAKENDFALMGVQIEAL	
B. natans	TPTGDLITVICLDD	FHTLD	TGTAD	-----	TGIS	ALDVRANFALMADQLKAL	
E. gracilis	TLVSDKTVVICLDD	YHLND	HAGRRV	-----	TGL	NALDQREINDFIMFQMSL	
P. parvum	TLVSDMTVICLDD	YFKWD	HTRKSNPEWPN	----	GTH	ALHEACQDMKMAADVL	
G. theta	TLISDMTVVICLDD	YHLND	HQGRK	-----	TGL	NALDPREINDFIMYEQVKAL	
T. pseudonana	TLVSDMATVICLDD	YHLND	REGRRV	-----	SGL	NALNTAEQKDFIMFHVKAL	
O. sinensis	SLVSDLTVVICLDD	YHLND	HNGRRV	-----	TQR	NALDPLEINDFIMYEQIAAL	
P. tricornutum	TLVSDLTVVICLDD	YHLND	HAGRRV	-----	TMR	NALDPEEINDFIMYEQVKAL	
D. lutheri	TLVSDKTVVICLDD	YHLYD	HKGKSA	-----	NKT	NALHKDCQKQDLMAGQVAAL	
O. tauri	TLISETTVVICLDD	YHLND	HAGRRK	-----	SGL	NALNLKEQDFIMYEQVKAL	
M. commoda	TLISDSTVICLDD	YHLND	HNGRKE	-----	SGL	NALNLKEQDFIMYEQTKAUM	
P. sitchensis	TLISDTTVICLDD	YHSLD	HNGRRD	-----	KGV	NALDPRANDFIMYEQVKAL	
P. patens	TLISDTTVICLDD	YHSLD	HNGRKE	-----	KAV	NALDPRANDFIMYEQVKAL	
S. oleracea	TLISDTTVICLDD	FHSLD	HNGRRV	-----	EKV	NALDPRANDFIMYEQVKAL	
A. thaliana	TLISDTTVICLDD	YHSLD	HNGRKE	-----	QKV	NALDPRANDFIMYEQVKAL	
S. moellendorff.	TLISDTTVICLDD	YHSLD	HNGRKE	-----	KGV	NALDPRANDFIMYEQVKAL	
T. aestivum	TLISDTTVICLDD	YHSLD	HNGRKE	-----	KGV	NALDPRANDFIMYEQVKAL	
P. trichocarpa	TLISDTTVICLDD	YHSLD	HNGRKE	-----	KGV	NALDPRANDFIMYEQVKAL	
M. crystallinum	TLISDTTVICLDD	YHSLD	HNGRKE	-----	KGV	NALDPRANDFIMYEQVKAL	
P. sativum	TLISDTTVICLDD	YHSLD	HNGRKE	-----	KGV	NALDPRANDFIMYEQVKAL	
C. variabilis	TLISDMTVVICLDD	YHSLD	HNGRKE	-----	AGV	NALDPRANDFIMYEQVKAL	
C. reinhardtii	TLISDMTVVICLDD	YHCLD	HNGRRV	-----	KGV	NALDPRANDFIMYQVKAL	
V. carteri	TLISDMTVVICLDD	YHCLD	HNGRRV	-----	KGV	NALDPRANDFIMYQVKAL	
G. sulphuraria	TPQGELVVICLDD	FHTLD	HKGKAE	-----	KKV	NALDPRANDFIMYQIAAL	
G. kilauensis	----ELVVICLDD	YHSLD	HNGRKE	-----	TGI	NALDPRANDFIMAEQAAAL	
G. violaceus	----ELVVICLDD	YHSLD	HNGRKE	-----	TGI	NALDPRANDFIMAEQATAL	
T. elongatus	----DFMVICLDD	YHSLD	HNGRKE	-----	MGI	NALDPRANDFIMYEQIKAL	
Synechocystis sp	----EFMVICLDD	YHSLD	HNGRKA	-----	AGV	NALDPRANDFIMYEQIKTL	
M. aeruginosa	----EFMVICLDD	YHCLD	HNGRKE	-----	VGV	NALDPRANDFIMYEQIKAL	
Cyanotheca sp	----EFMVICLDD	YHSLD	HNGRKA	-----	AGV	NALDPRANDFIMYEQIKAL	
S. elongatus	----ELMVICLDD	YHSLD	HNGRKE	-----	AGV	NALDPRANDFIMYEQVKAL	
A. variabilis	----EFMVICLDD	YHSLD	HNGRKE	-----	TGI	NALDPRANDFIMYEQIKAL	
N. spumigena	----EFMVICLDD	YHSLD	HNGRKE	-----	TGI	NALDPRANDFIMYEQIKAL	
A. boonei	----DLVSSFSLDD	YHTE	HETRRK	-----	TGHL	PDPKINLKLAAEHL	
F. placidus	----VATITLDD	YH	KYGRKE	RRK	----	LGI	PLNPEMNLDFRHLKLI
A. profundus	----DIVSHITLDD	YH	VYDHEMER	-----	LGI	PLHPSANLKLIVETHLYL	
A. veneficus	----DIVSSITLDD	YH	VYDQTK	RRK	----	LN	IPHPANLKLIVETHLM
M. harundinacea	----EAVSTFSMDD	YH	SLDHEE	RRV	----	RMI	PLNPEANRLDLAHLRS
M. concilii	----DMVATFSMDD	YH	SLDHRQ	RRKE	----	RN	IPHPANQDILAHLA
M. thermophila	----DVVSTFSMDD	YH	SLDHRQ	RRK	----	LS	IPHPANRFDILAHLAM
M. hungatei	----ELVSSITVDD	YH	LYDKT	RRSE	----	MGI	PLLHTANLKLLENLMD
Methanolinea sp	----SMVATITLDD	YH	IYNHTQ	RRDE	----	IQ	IPHPANLGLERDLRL
M. boonei	----DLVATITLDD	YH	TYDHEE	RRHH	----	LDI	IPHPANLGLADVHL
M. limicola	----SfVSTITLDD	YH	ILDHEE	RRKE	----	KN	IPHPANSLLEHLS
M. petrolearia	----NMVITLSD	YH	VLDHEE	RRR	----	TGI	IPHPANNSLLEHVAL
M. palustris	----DLVITLSD	YH	LYDHEE	RRV	----	RH	IPHPANRLDLEHDLVE
M. marisnigri	----DLVSTITLDD	YH	RYDQ	RRV	----	LS	IPHPANRFDLEHHLA
M. liminatans	----DLVATITLDD	YH	RYDK	RRD	----	LS	IPHPANRLDLADHIRA

Annotation * + # #

C55

	250	260	270	280	290	300
P. profundum	DDGSGQFRRYL	TFDEAVP	-----	YNQMP	SFTPWQKLPENTDV	IFYEGLRGGV
P. luminescens	ETGEGRRRKYL	TYDDAVP	-----	YNQLP	TFTPWESLPKQTDV	IFYEGLRGGV
E. amylovora	RSGKGKSRKYL	TYDEAVP	-----	WNQVP	TFTPWQPLAETDVI	IFYEGLRGGV
S. flexneri	QSGKGKSRKYL	TYDEAVP	-----	WNQVP	TFTPWQPLPEITDVI	IFYEGLRGGV
S. medicae	RRGVGRTRHYV	DDAEAVK	-----	FGSDP	TFTDWEFR - DSDL	IFYEGLRGCA
R. melliloti	RRGVGRTRHYV	DDAEAAK	-----	FGSDP	TFTDWEFR - DSDL	IFYEGLRGCA
C. necator	ETGTGMHRHYL	SPEEAAP	-----	FGQEP	TFTQWPLPADTDL	IFYEGLRGGV
R. rubrum	ETGGRRRRLYL	NDEEAAP	-----	FAQEP	TFTPWEDLP - ESDL	IFYEGLRGAV
R. sphaeroides	ETGQGRTRTYV	DDAEAAAR	-----	TGVAP	NFTDWRDFDSDSHL	IFYEGLRGAV
A. cryptum	ATGTGQYRHYL	DDDEAER	-----	YGGTP	TFTPWEDLPAITDVI	IFYEGLRGAV
X. flavus	ATGSGFRHYV	DDAGEAKL	-----	YNTEP	GRFTDWELEQGTDL	IFYEGLRGAV
N. hamburgensis	ESGTGNTRYVYV	DDVESAK	-----	HGVPP	TFTDWAQALPENSDL	IFYEGLRGAV
N. vulgaris	ETGTGNTRYVYV	DDAESAL	-----	HGVPP	TFTDWAQPLPADSL	IFYEGLRGAV
R. palustris DX1	ETGTGRTRHYV	DDDEAAL	-----	HGVPP	NFTGWRDLDPQSDL	IFYEGLRGAV
R. palustris Bis	ETGTGKTRYVYV	DDKEAAI	-----	HGVQP	NFTDWAQTLPEGSDL	IFYEGLRGAV
M. capsulatus	ETGTARRRFYV	NEAESQRL	-----	GGYKP	TFTPWEEVPAQTDL	IFYEGLRGGV
A. ferrooxidans	ESGHGMRYVYV	DELEAEL	-----	RGSAP	TFTPWQDIPLGTDL	IFYEGLRGGV
C. M. oxyfera	EAGVGKRYVYV	NAKEAAFHCKRLADAGVT	-----	CNADS	EFTPWEDIESNTDL	IFYEGLRGLV
T. denitrificans	ETGGGKRYVYV	SDSEADQHNKRLN	-----	TSLNP	EFTPWEDVPPGSDVI	IFYEGLRGLV
A. vinosum	ETGCGKRYVYV	SDSEARQLNARLG	-----	TSLNP	EFTPWEDLPAQTDL	IFYEGLRGLV
P. lunula	QKAVYKPIYNDT	-----	-----	FKDPP	ELIE - PNKVMVFEGLRPIY	
L. polyedrum	QKAVYKPIYNDT	-----	-----	GNKDP	ELIE - PNKVMVFEGLRPIY	
B. natans	QRAIKKPIYNDT	-----	-----	GAIDP	VEITIH - PNHIIIVFEGLRPMI	
E. gracilis	RGETIAKPIYNDV	-----	-----	GLDTP	EEIA - PASHMIIIEGLRPLL	
P. parvum	AKSVSKPIYNDV	-----	-----	GELDP	HYEVD - PTPVIVFEGLRPMY	
G. theta	EKKVMKPIYNDV	-----	-----	GLDPE	AEIIT - PTPVIVFEGLRPFY	
T. pseudonana	EKTIMKPIYNDV	-----	-----	GLDTP	EEIE - PTPVIVFEGLRPFV	
O. sinensis	NGESIEKPIYNDV	-----	-----	GLDTP	EIV - PTPVIVFEGLRPMY	
D. tricornutum	DKKTVEKPIYNDV	-----	-----	GLDTP	EIV - PTPVIVFEGLRPMH	
D. lutheri	AGNSVMKPIYNDV	-----	-----	GELDP	EIV - PTPVIVFEGLRPMI	
O. tauri	EKSVSKPIYNDV	-----	-----	GVFDP	AEKIE - SPEVIVFEGLRIFA	
M. commoda	EKAVDKPIYNDV	-----	-----	GVFDP	AEKIE - SPSVIVFEGLRIFA	
P. sitchensis	EKSDMKPIYNDV	-----	-----	GILDPAE	QIN - PPKLIVFEGLRPMF	
P. patens	EKSVSKPIYNDV	-----	-----	GLDPAE	TIH - PPKLIVFEGLRPMF	
S. oleracea	EKAVDKPIYNDV	-----	-----	GLDPAE	LIQ - PPKLIVFEGLRPMY	
A. thaliana	NGIAVEKPIYNDV	-----	-----	GLDPAE	LIQ - PPKLIVFEGLRPMF	
S. moellendorff.	EKAVDKPIYNDV	-----	-----	GLDPAE	LIQ - PPKLIVFEGLRPMF	
T. aestivum	EKAIEKPIYNDV	-----	-----	GLDPAE	LIQ - PPKLIVFEGLRPMY	
P. trichocarpa	DGTAVEKPIYNDV	-----	-----	GLDPAE	LIK - PPKLIVFEGLRPMY	
M. crystallinum	EKAVEKPIYNDV	-----	-----	GLDPAE	LIK - PPKLIVFEGLRPMF	
P. sativum	DKSVQKPIYNDV	-----	-----	GLDPAE	LIK - PPKLIVFEGLRPMY	
C. variabilis	EKAVDKPIYNDV	-----	-----	GLDPAE	PPTS - SPNTIVFEGLRPFY	
C. reinhardtii	EKSVSKPIYNDV	-----	-----	GLDPAE	KIE - SPPVIVFEGLRPFY	
V. carteri	EKAVDKPIYNDV	-----	-----	GLDPAE	KID - SPNTIVFEGLRPF	
G. sulphuraria	EYDIMKPIYNDV	-----	-----	GLDPAE	LIQ - PNHIIIVFEGLRPMY	
G. kilauensis	SGQSIQKPIYNDV	-----	-----	GKIDP	PERID - PTPVIVFEGLRPFY	
G. violaceus	VGQSIMKPIYNDV	-----	-----	GKIDP	PERIE - PTPVIVFEGLRPFY	
T. elongatus	NGESIMKPIYNDV	-----	-----	GTIDP	PEKVD - PNHVIVFEGLRPLY	
Synechocystis sp	SGQSIMKPIYNDV	-----	-----	GLDPAE	KVE - PNKVVIVFEGLRPLY	
M. aeruginosa	GGQAINKPIYNDV	-----	-----	GMDPP	EIE - PNKVVIVFEGLRPLY	
Cyanotheca sp	EQQIMKPIYNDV	-----	-----	GMDPP	ERIE - PNKVVIVFEGLRPLY	
S. elongatus	NGETIMKPIYNDV	-----	-----	GLDPAE	KIE - PNRIIVFEGLRPLY	
A. variabilis	EQTINKPIYNDV	-----	-----	GLDPAE	IVK - PNHVIVFEGLRPLY	
N. spumigena	EQQVIQKPIYNDV	-----	-----	GMDPP	ERVE - PNHIIIVFEGLRPLY	
A. boonei	KGNAIKPIYNDV	-----	-----	GKFDPP	EVFE - PPKLIVFEGLRPLY	
F. placidus	EWKEFEKPIYNDV	-----	-----	GEVCC	EIFK - PEKIVIVFEGLRVLY	
A. profundus	KBEKIKKPIYNDV	-----	-----	GTFGWE	DFFE - STPVIVFEGLRPLY	
A. veneficus	KMETIRKPIYNDV	-----	-----	GTFGWE	DFT - PTPVIVFEGLRPLY	
M. harundinacea	LGETIAKPIYNDV	-----	-----	GEFRE	VPFR - SGPVIVFEGLRPLY	
M. concilii	RNERIDKPIYNDV	-----	-----	GEISG	VPFG - PAVVIVFEGLRPLY	
M. thermophila	RGLAIEKPIYNDV	-----	-----	GEIRG	VPVIFK - PSPVIVFEGLRPFY	
M. hungatei	AGRTIQKPIYNDV	-----	-----	GTFGPE	PLFS - PTKVIVFEGLRPLY	
Methanolinea sp	QKGGIYKPIYNDV	-----	-----	GRLEGE	PYLA - PAKVIVFEGLRSLF	
M. boonei	QGYAIEKPIYNDV	-----	-----	GTFDPP	IPFP - SKKIVIVFEGLRSLF	
M. limicola	SGKEILKPIYNDV	-----	-----	GKFDPP	VPFS - SSKVIVFEGLRSLF	
M. petrolearia	EKSVSKPIYNDV	-----	-----	GKIEG	VPVRLS - PSTRVIVFEGLRSLF	
M. palustris	EGRIDKPIYNDV	-----	-----	GRFAP	PIRF - PPKLIVFEGLRSLF	
M. marisnigri	AGRTIEKPIYNDV	-----	-----	GRFDPP	VPFS - PTKVIVFEGLRSLF	
M. liminatans	SGNTVMKPIYNDV	-----	-----	GTFDPP	IPFR - PARVIVFEGLRSLF	
Gblocks						
Annotation	# #					Walker B

	310	320	330	340	350	360																																			
P. profundum	VD-----	GEVNAAEHV	LLIGMVP	PIVNL	EWIQ	KIVRDT	TRDRGHS	REAM	MESV	VRSMD																															
P. luminescens	VT-----	PQHNVASH	VLLVGV	PIVNL	EWIQ	LIKRT	GTGERGHS	QEA	MDS	VVRSMDD																															
E. amylovora	VT-----	PLHNV	AEVND	LLVGV	PIVNL	EWIQ	RLVRT	SEKRGHS	REAM	MDSVVRSMED																															
S. flexneri	VT-----	PQHNV	AQHV	LLVGV	PIVNL	EWIQ	LIKRT	SEKRGHS	REAM	MDSVVRSMED																															
S. medicae	VT-----	DTINLAQ	HCDL	KIGV	PIVNL	EWIQ	KIHRD	KAT	RGYST	TEATD	TDLR	FMPD																													
R. melliloti	VT-----	DTVNL	AQHCD	LKIGV	PIVNL	EWIQ	KIHRD	KAT	RGYST	TEATD	TDLR	FMPD																													
C. necator	VT-----	DSVNV	AQYP	NLLIGV	PIVNL	EWIQ	LWFRD	KKK	RGYST	TEATD	TDLR	FMPD																													
R. rubrum	VT-----	DTVD	AQHAD	LKIGV	PIVNL	EWIQ	LIHRD	RMA	RGYST	TEATD	TDLR	FMPD																													
R. sphaeroides	VN-----	SEVNI	AGLAD	LKIGV	PIVNL	EWIQ	KIHRD	RAT	RGYTT	TEATD	TVDLR	FMPD																													
A. cryptum	RH-----	GDIDT	GRHAD	VKIGV	PIVNL	EWIQ	KIHRD	RMA	RYST	TEAM	MDTDLR	FMPD																													
X. flavus	VT-----	DELNLAQ	HADL	KIGV	PIVNL	EWIQ	KIHRD	KAT	RGYTT	TEATD	TDLR	FMPD																													
N. hamburgensis	VT-----	DKVNV	AQYAD	LKIGV	PIVNL	EWIQ	LIHRD	RSA	RGYST	TEATD	TDLR	FMPD																													
N. vulgaris	VT-----	DKVNV	AQYAD	LKIGV	PIVNL	EWIQ	LIHRD	RMA	RGYST	TEATD	TDLR	FMPD																													
R. palustris DX1	IT-----	EKVN	AQHAD	LKIGV	PIVNL	EWIQ	LIHRD	RMA	RGYST	TEATD	TDLR	FMPD																													
R. palustris Bis	MT-----	ETVN	AQHAD	LKIGV	PIVNL	EWIQ	LIHRD	RSD	RGYST	TEATD	TDLR	FMPD																													
M. capsulatus	IT-----	DRINV	KYV	DLVGV	PIVNL	EWIQ	KIHRD	TAE	RGYK	PED	TETDLR	FMPD																													
A. ferrooxidans	KT-----	GAVD	V	TNYV	DLVGV	PIVNL	EWIQ	KIHRD	NAQ	RGYSA	EAIV	DTDLR	FMPD																												
C. M. oxyfera	KDISP	DQKYGGY	VAQYV	DLGIGV	PIVNL	EWIQ	KIHRD	HAE	RGYSP	EAIV	DTDLR	FMPD																													
T. denitrificans	KT-----	DTVD	AQHVD	LGVGV	PIVNL	EWIQ	KIHRD	GAE	RGYSA	ADV	IVDTDLR	FMPD																													
A. vinosum	VT-----	EDSN	AQHVD	LGVGV	PIVNL	EWIQ	KIHRD	NLE	RGYSA	EAIV	DTDLR	FMPD																													
P. lunula	DE-----	KAAQL	DLGLY	DI	VNDV	FANV	VQR	MAE	RGWTE	EQ	RAD	DKL	FMPD																												
L. polyedrum	DK-----	KARQD	DLGLY	DI	VNDV	FANV	VQR	MAE	RGWTE	EQ	RED	EK	FMPD																												
B. natans	DK-----	DVIES	LD	TFY	DI	VSDP	VKAW	K	ERD	MVER	GHKK	E	DI	IAS	ES	FMPD																									
E. gracilis	DD-----	RVAGL	LD	SLY	LD	ISDR	VFA	WK	IQR	MAE	RGW	AL	E	DI	KK	E	K	FMPD																							
P. parvum	DE-----	RVNKA	LD	TVY	LD	ITDE	VFA	W	QAQ	IAE	RGAT	M	E	Q	K	A	D	G	FMPD																						
G. theta	DK-----	RVEEL	MD	KLY	DI	ITPE	VFN	W	VQR	HEE	RGHS	E	SI	K	Q	E	A	G	FMPD																						
T. pseudonana	DE-----	RVELI	D	SLY	LD	ISPD	VNL	W	K	IQR	MEE	RGHS	E	SI	M	A	S	E	A	G	FMPD																				
O. sinensis	DE-----	RVDLL	D	SLY	LD	ISDE	VLN	W	K	IQR	MEE	RGHS	E	SI	L	A	S	E	A	G	FMPD																				
P. tricornutum	DK-----	RVDL	LD	SLY	LD	ISDD	VLN	W	VQR	MEE	RGHS	E	SI	L	A	S	E	A	G	FMPD																					
D. lutheri	DD-----	KVRSM	LD	SLY	LD	ISGX	VFA	WK	IQR	MQE	RGHS	E	SI	K	A	S	E	A	G	FMPD																					
O. tauri	DT-----	RVB	DMF	D	KLY	LD	ISDD	VFA	WK	IQR	MAE	RGHS	E	SI	K	A	S	E	A	G	FMPD																				
M. comoda	DE-----	RVB	DMF	D	KLY	LD	ISDD	VFA	WK	IQR	MAE	RGHS	E	SI	K	A	S	E	A	G	FMPD																				
P. sitichensis	DA-----	RVELL	D	SLY	LD	ISNE	VFA	WK	IQR	MAE	RGHS	E	SI	K	A	S	E	A	G	FMPD																					
P. patens	DE-----	RVELL	D	SLY	LD	ISDD	VFA	WK	IQR	MAE	RGHS	E	SI	K	A	S	E	A	G	FMPD																					
S. oleracea	DA-----	RVELL	D	SLY	LD	ISNE	VFA	WK	IQR	MKE	RGHS	E	SI	K	A	S	E	A	G	FMPD																					
A. thaliana	DE-----	RVELL	D	SLY	LD	ISNE	VFA	WK	IQR	MAE	RGHS	E	SI	K	A	S	E	A	G	FMPD																					
S. moellendorf.	DS-----	RVELL	D	SLY	LD	ISDA	VFA	WK	IQR	MAE	RGHS	E	SI	K	A	S	E	A	G	FMPD																					
T. aestivum	DE-----	RVELL	D	SLY	LD	ISNE	VFA	WK	IQR	MAE	RGHS	E	SI	K	A	S	E	A	G	FMPD																					
P. trichocarpa	DO-----	RVELL	D	SLY	LD	ISNE	VFA	WK	IQR	MAE	RGHS	E	SI	K	A	S	E	A	G	FMPD																					
M. crystallinum	DS-----	RVELL	D	SLY	LD	ISNE	VFA	WK	IQR	MAE	RGHS	E	SI	K	A	S	E	A	G	FMPD																					
P. sativum	DS-----	RVELL	D	SLY	LD	ISNE	VFA	WK	IQR	MAE	RGHS	E	SI	K	A	S	E	A	G	FMPD																					
C. variabilis	DE-----	RVNEL	V	FR	IY	LD	ISDEI	F	AW	K	IQR	MAE	RGHS	E	SI	K	A	S	E	A	G	FMPD																			
C. reinhardtii	DK-----	RV	AEL	LD	KLY	LD	ISDDI	F	AW	K	IQR	MAE	RGHS	E	SI	K	A	S	E	A	G	FMPD																			
V. carteri	DK-----	RV	ADL	LD	KLY	LD	ISDDI	F	AW	K	IQR	MAE	RGHS	E	SI	K	A	S	E	A	G	FMPD																			
G. sulphuraria	DA-----	RMK	QL	D	TFY	LD	ISDE	V	VA	W	K	IQR	MAE	RGH	K	L	E	N	I	L	A	S	E	A	G	FMPD															
G. kilauensis	DK-----	RV	DLL	D	KVY	F	LS	DPI	IQ	W	K	IQR	MAE	RGHS	E	Y	D	D	I	R	A	S	E	A	G	FMPD															
G. violaceus	DA-----	RV	NLF	D	KLY	F	LS	DPI	IQ	W	K	IQR	MAE	RGHTY	E	D	V	L	K	Q	E	S	E	A	G	FMPD															
T. elongatus	DE-----	RV	SLL	D	SVY	LD	ISDD	V	IA	W	K	IQR	MAE	RGHS	E	Y	E	D	I	A	S	E	A	G	FMPD																
Synechocystis sp	DE-----	RV	E	L	V	D	H	G	V	Y	LD	IS	E	V	I	N	W	K	IQR	MAE	RGHTY	E	D	I	A	S	E	A	G	FMPD											
M. aeruginosa	DE-----	RV	S	L	L	D	SVY	LD	IS	D	V	V	N	W	K	IQR	MAE	RGHTY	D	D	I	A	S	E	A	G	FMPD														
Cyanothecae sp	DE-----	RV	S	L	V	D	SVY	LD	IS	D	V	I	N	W	K	IQR	MAE	RGHTY	D	D	I	A	S	E	A	G	FMPD														
S. elongatus	DE-----	RV	S	L	L	D	SVY	LD	IS	D	V	I	A	W	K	IQR	MAE	RGHS	E	Y	E	D	I	A	S	E	A	G	FMPD												
A. variabilis	DE-----	RV	S	L	L	D	SVY	LD	IS	D	V	I	A	W	K	IQR	MAE	RGHRY	E	D	I	A	S	E	A	G	FMPD														
N. spumigena	DE-----	RV	S	L	L	D	SVY	LD	IS	D	V	I	A	W	K	IQR	MAE	RGHRY	E	D	I	A	S	E	A	G	FMPD														
A. boonei	DE-----	L	N	Y	L	D	R	I	F	V	D	P	A	R	I	R	R	W	K	IQR	V	E	E	R	G	Y	K	E	D	I	K	E	R	A	E	F					
F. placidus	DG-----	I	F	E	I	L	D	Y	K	I	F	V	D	P	A	R	I	R	W	K	IQR	M	E	K	R	G	Y	R	K	E	E	I	E	I	Q	E	S	D			
A. profundus	DG-----	I	R	O	Y	I	D	K	I	F	V	D	P	A	R	I	R	L	W	K	IQR	V	E	E	R	G	Y	D	R	D	K	I	R	E	I	R	E	P			
A. veneficus	DG-----	L	N	Y	L	D	R	I	F	V	D	P	A	R	I	R	R	W	K	IQR	V	E	E	R	G	Y	N	R	Q	K	V	E	E	I	R	E	S	D			
M. harundinacea	TQ-----	K	L	R	E	V	D	H	G	I	F	V	D	P	S	R	A	V	R	R	W	K	IQR	R	C	G	D	R	G	Y	Q	R	D	L	M	A	E	L	A	E	P
M. concilii	TE-----	R	L	S	Q	I	D	K	I	F	V	D	P	S	R	S	V	R	L	W	K	IQR	R	V	G	E	R	G	Y	E	T	G	O	M	A	E	L	Q	E	P	
M. thermophila	TE-----	E	L	S	K	L	D	H	K	I	F	V	D	P	S	R	A	V	R	R	W	K	IQR	R	D	V	G	E	R	G	Y	A	P	E	D	M	R	E	L	E	P
M. hungatei	TK-----	S	L	R	A	L	D	Y	T	I	F	V	D	P	E	R	D	V	R	Y	W	K	IQR	R	M	K	K	N	Y	D	K	N	E	L	R	E	L	Q	E	P	
Methanolinea sp	TP-----	G	L	S	L	L	D	SVY	LD	P	A	S	A	V	R	E	W	K	IQR	M	E	K	R	G	Y	E	R	E	R	D	A	R	A	R	E	N	D				
M. boonei	TP-----	A	L	S	D	L	V	D	S	V	F	V	D	P	R	E	V	R	Y	W	K	IQR	R	T	G	O	R	G	Y	S	P	E	I	N	G	E	A	R	E	A	D
M. limicola	TP-----	K	L	S	L	D	H	K	I	F	V	D	P	E	T	N	V	R	Y	W	K	IQR	V	N	A	R	G	Y	D	K	E	D	L	S	E	L	E	A	R	K	O
M. petrolearia	TE-----	K	L	S	L	L	D	SVY	LD	S	P	D	T	V	R	Y	W	K	IQR	V	N	L	R	G	Y	R	E	E	V	L	A	E	S	L	E	S	R	A	D		
M. palustris	TP-----	A	L	S	E	H	L	D	T	L	F	V	D	P	E	V	R	I	E	W	K	IQR	I	N	N	R	G	Y	T	R	E	Q	M	A	E	L	E	P	E	R	D
M. marisnigri	TG-----	T	L	R	I	D	H	K	I	F	V	D	P	P	D	V	R	A	W	K	IQR	V	E	R	G	Y	A	P	E	A	L	R	E	M	E	E	R	D			
M. liminatans	TP-----	E	L	S	L	L	D	SVY	LD	P	D	P	A	V	R	T	L	W	K	IQR	M	O	R	R	G	Y	S	R	A	E	V	L	A	E	M	E	E	R	D		

Gblocks
Annotation

|+

	370	380	390	400	410	420		
P. profundum	YLN	YTP	FSRTHIN	FRVPT	-----	VDTS---NPFSAKGLPSLD--ESFVVI		
P. luminescens	YIN	YTP	FSRTHIN	FRVPT	-----	VDTS---NPFSAKGLPSLD--ESFIVI		
E. amylovora	YIN	YTP	FSRTHIN	FRVPT	-----	VDTS---NPFSAKGLPSLD--ESFVWV		
S. flexneri	YIN	YTP	FSRTHLN	FRVPT	-----	VDTS---NPFSAKGLPSLD--ESFVVI		
S. medicae	YVH	YCP	FSLT	INFRVPT	-----	VDTS---NPFIAKGLIPTPA--ESILVI		
R. melliloti	YVY	YCP	FSLT	INFRVPT	-----	VDTS---NPFIAKGLIPTPA--ESILVI		
C. necator	YVY	YCP	FSRTHVNF	FRVPC	-----	VDTS---NPFISKGLIPAD--ESMVVI		
R. rubrum	YVH	YCP	FTRT	VNFRVPL	-----	VDTS---NPFVAKGLHVSAD--ESFVVI		
R. sphaeroides	YVH	YCP	FSQT	INFRVPT	-----	VDTS---NPFIAKGLIPTAD--ESVVI		
A. cryptum	YVH	YCP	FTET	INFRVPT	-----	VDTS---NPFIAKGLIPTAD--ESIIVI		
X. flavus	YVY	YCP	FTET	INFRVPT	-----	VDTS---NPFVAKGLIPTD--ESMVVI		
N. hamburgensis	YVY	YCP	FAET	INFRVPT	-----	VDTS---NPFIAKGLIPTD--ESMVVI		
N. vulgaris	YVY	YCP	FAET	INFRVPT	-----	VDTS---NPFISKGLIPTD--ESMVVI		
R. palustris DX1	YVH	YCP	FAET	INFRVPT	-----	VDTS---NPFIAKGLIPTAD--ESMVVI		
R. palustris Bis	YVH	YCP	FGET	INFRVPT	-----	VDTS---NPFIAKGLIPTD--ESMVVI		
M. capsulatus	YVK	YTP	FSQT	INFRVPT	-----	VDTS---NPFIAKGLIPTD--ESFVII		
A. ferrooxidans	YIH	YTP	FSRTHIN	FRVPL	-----	VDTS---NPFIAKGLIPTD--ESMVVI		
C. M. oxyfera	YIN	YTP	FSRTHVNF	FRVPT	-----	VDTS---NPFIAKGLIPSAD--ESFVVI		
T. denitrificans	YVY	YTP	FSRT	INFRVPT	-----	VDTS---NPFISKGLIPTD--ESFIVI		
A. vinosum	YIR	YTP	FSLT	INFRVPT	-----	VDTS---NPFIAKGLIPTD--ESFVII		
P. lunula	FSA	YVD	KAN	ADVILRYE	PS-----	DQGL---PYLKVKLIQKKG--GKFPPI		
L. polyedrum	FSA	YVD	KAN	ADVILRYE	PS-----	DQGL---PYLKVKLIQKKG--GKFPPI		
B. natans	FEK	FVE	PQK	AN	ADVILRYE	PS-----	DQGL---PYLKVKLIQKKG--GKFPPI	
E. gracilis	FDK	YVAP	RAK	AD	MVLEVL	PSRLAPP----	KDETAPL-EYLRVLIQKTTT-KHFDPV	
P. parvum	FAA	YVE	PQK	AK	AD	IIIVQLV	SDLI-----	DDPTG---KFLKVLITKNNL-KHISPA
G. theta	FDA	YDP	QK	AD	VVLEVL	PTQL-VA-----	DDNEG---KILRVLMIMKEV-ENFDAP	
T. pseudonana	FDA	YDP	QK	AD	VVLEVL	PTQL-----	DDNEG---KILRVLMIMKEV-ENFDAP	
O. sinensis	FDA	YDP	QK	AD	VVLEVL	PTQL-----	DDNEG---KILRVLMIMKEV-ENFDAP	
P. tricornutum	FDA	YDP	QK	AD	VVLEVL	PTQL-----	DDNEG---KILRVLMIMKEV-ENFDAP	
D. lutheri	FDA	YDP	QK	AD	VVLEVL	PTQL-V-----	DDNEG---KILRVLMIMKEV-ENFDAP	
O. tauri	FDA	YDP	QK	AD	VVLEVL	PTQL-IP-----	DDNEG---KILRVLMIMKEV-ENFDAP	
M. commoda	FDE	FVD	PQK	QY	AD	VVLEVL	PTQL-IP-----	DDNEG---KILRVLMIMKEV-ENFDAP
P. sitchensis	FDA	YDP	QK	AD	VVLEVL	PTQL-IP-----	DDNEG---KILRVLMIMKEV-ENFDAP	
P. patens	FDA	YDP	QK	AD	VVLEVL	PTQL-IP-----	DDNEG---KILRVLMIMKEV-ENFDAP	
S. oleracea	FDA	YDP	QK	AD	VVLEVL	PTQL-IP-----	DDNEG---KILRVLMIMKEV-ENFDAP	
A. thaliana	FDA	YDP	QK	AD	VVLEVL	PTQL-IP-----	DDNEG---KILRVLMIMKEV-ENFDAP	
S. moellendorf.	FDA	YDP	QK	AD	VVLEVL	PTQL-IP-----	DDNEG---KILRVLMIMKEV-ENFDAP	
T. aestivum	FDA	YDP	QK	AD	VVLEVL	PTQL-IP-----	DDNEG---KILRVLMIMKEV-ENFDAP	
P. trichocarpa	FDA	YDP	QK	AD	VVLEVL	PTQL-IP-----	DDNEG---KILRVLMIMKEV-ENFDAP	
M. crystallinum	FDA	YDP	QK	AD	VVLEVL	PTQL-IP-----	DDNEG---KILRVLMIMKEV-ENFDAP	
P. sativum	FEA	YDP	QK	AD	VVLEVL	PTQL-IP-----	DDNEG---KILRVLMIMKEV-ENFDAP	
C. variabilis	FDA	YDP	QK	AD	VVLEVL	PTQL-VP-----	DDNEG---KILRVLMIMKEV-ENFDAP	
C. reinhardtii	FDA	YDP	QK	AD	VVLEVL	PTQL-VP-----	DDNEG---KILRVLMIMKEV-ENFDAP	
V. carteri	FDA	YDP	QK	AD	VVLEVL	PTQL-VP-----	DDNEG---KILRVLMIMKEV-ENFDAP	
G. sulphuraria	FQY	YDP	QK	AD	VVLEVL	PTQL-IP-----	DDNEG---KILRVLMIMKEV-ENFDAP	
G. kilauensis	FSA	YDP	QK	AD	VVLEVL	PTQL-IP-----	DDNEG---KILRVLMIMKEV-ENFDAP	
G. violaceus	FSA	YDP	QK	AD	VVLEVL	PTQL-IP-----	DDNEG---KILRVLMIMKEV-ENFDAP	
T. elongatus	FMA	YDP	QK	AD	VVLEVL	PTQL-AK-----	DDNEG---KILRVLMIMKEV-ENFDAP	
Synechocystis sp	FTAY	YDP	QK	AD	VVLEVL	PTQL-IP-----	DDNEG---KILRVLMIMKEV-ENFDAP	
M. aeruginosa	FSA	YDP	QK	AD	VVLEVL	PTQL-IP-----	DDNEG---KILRVLMIMKEV-ENFDAP	
Cyanotheca sp	FSA	YDP	QK	AD	VVLEVL	PTQL-IE-----	DDNEG---KILRVLMIMKEV-ENFDAP	
S. elongatus	FKAY	YDP	QK	AD	VVLEVL	PTQL-IP-----	DDNEG---KILRVLMIMKEV-ENFDAP	
A. variabilis	FQY	YDP	QK	AD	VVLEVL	PTQL-IP-----	DDNEG---KILRVLMIMKEV-ENFDAP	
N. spumigena	FEK	FVE	PQK	AN	ADVILRYE	PS-----	DQGL---PYLKVKLIQKKG--GKFPPI	
A. boonei	YKRY	YDF	QK	AD	VVLEVL	PTQL-IP-----	DDNEG---KILRVLMIMKEV-ENFDAP	
F. placidus	YKRY	YDF	QK	AD	VVLEVL	PTQL-IP-----	DDNEG---KILRVLMIMKEV-ENFDAP	
A. profundus	YKRY	YDF	QK	AD	VVLEVL	PTQL-IP-----	DDNEG---KILRVLMIMKEV-ENFDAP	
A. veneficus	YKRY	YDF	QK	AD	VVLEVL	PTQL-IP-----	DDNEG---KILRVLMIMKEV-ENFDAP	
M. harundinacea	YKLY	YDV	QK	AD	VVLEVL	PTQL-IP-----	DDNEG---KILRVLMIMKEV-ENFDAP	
M. concilii	YKLY	YDV	QK	AD	VVLEVL	PTQL-IP-----	DDNEG---KILRVLMIMKEV-ENFDAP	
M. thermophila	YKLY	YDV	QK	AD	VVLEVL	PTQL-IP-----	DDNEG---KILRVLMIMKEV-ENFDAP	
M. hungatei	YFQ	YVFP	QK	AD	VVLEVL	PTQL-IP-----	DDNEG---KILRVLMIMKEV-ENFDAP	
Methanolinea sp	YRAY	YAP	QK	AD	VVLEVL	PTQL-IP-----	DDNEG---KILRVLMIMKEV-ENFDAP	
M. boonei	YATY	YEP	QK	AD	VVLEVL	PTQL-IP-----	DDNEG---KILRVLMIMKEV-ENFDAP	
M. limicola	YENF	YLP	QK	AD	VVLEVL	PTQL-IP-----	DDNEG---KILRVLMIMKEV-ENFDAP	
M. petrolearia	YENY	YHP	QK	AD	VVLEVL	PTQL-IP-----	DDNEG---KILRVLMIMKEV-ENFDAP	
M. palustris	YQRF	YAP	QK	AD	VVLEVL	PTQL-IP-----	DDNEG---KILRVLMIMKEV-ENFDAP	
M. marisnigri	YERY	YAP	QK	AD	VVLEVL	PTQL-IP-----	DDNEG---KILRVLMIMKEV-ENFDAP	
M. liminatans	YERY	YAP	QK	AD	VVLEVL	PTQL-IP-----	DDNEG---KILRVLMIMKEV-ENFDAP	
Gblocks								
Annotation								

	430	440	450	460	470	480	
P. profundum	RFRG	IEN	VDFP	YLLSMIQGSFMSRHNTLVVPGGKMS			
P. luminescens	RFRD	LTQ	IDFP	YLLAMLQGSFVSSINTIVVPGGKMG			
E. amylovora	HFGG	LED	IDFP	YLLSMLQGSFISHIKTLVVPGGKMG			
S. flexneri	HFRN	LEG	IDFP	WLLAMLQGSFISHINTLVVPGGKMG			
S. medicae	RFAK	PQS	IDFP	YLLSMLHNSYMSRANSTIVVPGDKLD			
R. melliloti	RFAK	PQS	IDFP	YLLSMLHNSYMSRANSTIVVPGDKLD			
C. necator	RFAN	PKG	IDFP	YLLSMIHDSFMSRANTIVVPGGKME			
R. rubrum	RFRD	PKG	IDFP	YLLNMLNDSFMSRPNTIVVPGGKME			
R. sphaeroides	RFRN	PRG	IDFP	YLTSMIHGSWMSRANSTIVVPGNKLD			
A. cryptum	RFRD	PHG	IDFP	YLLAMLHGSFMSRANSTAVPGNKFD			
X. flavus	RFRD	PHG	IDFP	YLLSMIHNSFMSRANSTIVVPGNKQD			
N. hamburgensis	RFKN	PRG	IDFP	YLLSMIPNSFMSRANSTIVIHGSKMD			
N. vulgaris	RFKN	PRG	IDFP	YLLSMIPSSFMSRANSTIVIHGSKLD			
R. palustris DX1	RFKN	PRG	IDFA	YLLSMIQGSFMSRANSTIVIHGAKLD			
R. palustris Bis	RFKS	PRG	IDFA	YLLSMIQGSFMSRANSTIVIHGSKMD			
M. capsulatus	RFKE	PGKFN	VDFP	YLLAMLQNSFMSRHNSTIVIPGGKMG			
A. ferrooxidans	RFRD	PKE	ENFP	TLLQMLPGSFMSRNTLVVPGTKMG			
C. M. oxyfera	RFVD	PKRFG	VDFP	TLLVMINGSFISRRNTIVVPGGKMV			
T. denitrificans	RFRN	PQG	VDFP	YLLNMCNSFMSRRNTIVVPGGKMG			
A. vinosum	RFKU	PKKLQ	IDFP	YLLSMIHDSFMSRRNMVVVPGGKMG			
P. lunula	SKKK	DLSLT	GSKP	GATMKMYDDWFFNPVTVVEMDGEIDMDNMA			
L. polyedrum	SKKK	DLTTL	GSKP	GATLKMYYDDWFFNAVTVVEMDGEIDMDNME			
B. natans	YMFE	EESTVDWPCAGPGAMA	CPYP	GTRVRYYNEMSGEKHAHVLEVDGQV			
E. gracilis	YIEKG	SSVTWKPC	GDNLQ	CEYP	GLQLAYYTEEYMHHPAEVLEMDGVIH		
P. parvum	YIMDEG	ASITWKPN	PNKLT	TSAP	GVLFSKYQDEWFFQSVLEMDGKID		
G. theta	YIMDEG	SDIEWVPP	RNKLA	SSAP	GAGLKIYQKTEKWAQKDAAVIGMDGKYD		
T. pseudonana	YIFDEG	SEIEWAPS	ADKLS	SPAP	GIKLSYKQEQYFADVAVEMDGTDF		
O. sinensis	YIFDEG	STIAWTPA	PSKLS	SSGP	GLTMAYGTEDYYKPAQVEMDGTDF		
P. tricornutum	YIFDEG	SSIEWTPA	PTKLS	SPAP	GIKLAYPEEFKDAQVLEMDGNF		
D. lutheri	YIFDEG	STIEWTPC	GKKLT	CAYP	GIKFRYGTMYMSEVTVLEMDGRFD		
O. tauri	YIFDEG	STISWIPC	GRKLT	CSYP	GIKFFYPGPTYFKEVTVLEMDGQFD		
M. comoda	YIFDEG	STISWIPC	GRKLT	CSYP	GIKFFYPGPTYFEEVTVLEMDGQFD		
P. sitchensis	YIFDEG	STISWIPC	GRKLT	CSYP	GIKFFYPGDIYYDNEVTVLEMDGQFD		
P. patens	YIFDEG	STISWIPC	GRKLT	CSYP	GIKFFYPGPTYFNEVTVLEMDGQFD		
S. oleracea	YIFDEG	STISWIPC	GRKLT	CSYP	GIKFSYGPDTFYNEVTVVEMDGMFD		
A. thaliana	YIFDEG	STISWIPC	GRKLT	CSYP	GIKFNYPDSYFDHEVTVLEMDGQFD		
S. moellendorf.	YIFDEG	STISWIPC	GRKLT	CSYP	GIKFFYPGPTYFDNEVTVLEMDGQFD		
T. aestivum	YIFDEG	STINWIPC	GRKLT	CSYP	GIKFSYGPDTYFQEVTVLEMDGQFD		
P. trichocarpa	YIFDEG	SSISWIPC	GRKLT	CSYP	GIKFSYGPDAYYGHEVTVLEMDGQFD		
M. crystallinum	YIFDEG	SSITWIPC	GRKLT	CSYP	GIKFFYPGPTYFNEVTVLEMDGQFD		
P. sativum	YIFDEG	STISWIPC	GRKLT	CSYP	GIKFFYPGPTYFNEVTVVEMDGMFD		
C. variabilis	YIFDQG	STVSWIPC	GRKLT	CSFP	GIKMFYGPDTYFEEVTVLEMDGQFD		
C. reinhardtii	YIFDEG	STISWIPC	GRKLT	CSFP	GIKMFYGPDTWYQEVTVLEMDGQFD		
V. carteri	YIFDEG	STISWIPC	GRKLT	CSFP	GIKMFYGPDTWYQEVTVLEMDGQFD		
G. sulphuraria	YIFDEG	STIDWIPC	GRKLT	CSYP	GIKFHYGPDNWNHADVTVLEVDGNFE		
G. kilauensis	YIFDRAISDVCW	KPNFP	NSDP	ELTFCYGTDDYFRPA	SYLSDIGFEFA		
G. violaceus	YIFDRAISDVCWK	PNFPN	SDEE	LTFCYGTQDYFRPA	SYLSDIGFEFA		
T. elongatus	YIFDEG	STITWIPC	GRKLT	CSYP	GIRLSYGPDEYYHPVTVLEVDGRFE		
Synechocystis sp	YIFDEG	STIDWRPC	GRKLT	CTYP	GIKMYYGPDNFMNEVTVLEVDGRFE		
M. aeruginosa	YIFDEG	STIDWRPC	GRKLT	CTYP	GIKLYYGPDGLNEVTVLELDGQFD		
Cyanothecae sp	YIFDEG	STIDWRPC	GRKLT	CAYP	GLKMYGPDNIFNEVTVLELDGQFD		
S. elongatus	YIFDEG	STIQWTPC	GRKLT	CSYP	GIRLAYGPDTYFHEVTVLEVDGQFE		
A. variabilis	YIFDEG	STINWTPC	GRKLT	CSYP	GMQLYYGSDVYYGRVYTVLEVDGQFD		
N. spumigena	YIFDEG	STINWTPC	GRKLT	CSYP	GMQVYYGSDVYYGRVYTVLEVDGQFD		
A. boonei	SEINT		SQKP	MMISYRDDFYMKRV	SRITFDGLIP		
F. placidus	TUNVDL		SRLIK	ASER	DFAISFSDYYYKRA	SFIDIDGFLN	
A. profundus	SUNIDI		SDLVK	ASER	DFSIGFSDYYYAEKA	SFIDIDGFLN	
A. veneficus	KIDIDL		SAFVR	ASEK	DFALGFSDYYYEKPA	SFIDIDGLMN	
M. harundinacea	DUKIDL		SAL	FSLP	DGEFISIFQRDDYYKRV	SVLTVDDELH	
M. concilii	SMNIDL		SKILR	RSEH	EFSIEFQRDDYYKRV	GIMTMDGEIH	
M. thermophila	DMTIDL		SRI MR	LTER	EFSIEFQRDDYYKRV	GVMTLDGEFP	
M. hungatei	ENIDL		CDL FK	KSSH	DFSLCSISHTPDSRNMRAL	VVDGELM	
Methanolinea sp	CGMDL		VSLMS	SFDH	NFMVEYRVVTEA	RRMGRVAFDGGIP	
M. boonei	SUNIDL		TSLLA	FHES	EFSIEFSTQRIECSFLRS	TFDGMEN	
M. limicola	CGFDL		FAINS	LADR	NFRFDFRVTERG	EKI GALSLDGEFQ	
M. petrolearia	NUNFDL		FAINS	LAER	GFSFDFSIIEKYKMGAL	SLDGEFR	
M. palustris	DUNIDL		FSLLS	LSDR	NFLIEFSHEQRNDERT	GEIILDGELS	
M. marisnigri	DSIDL		FGLLS	LSE	DFMVEFTIEDVGE	EAMGALTFDGLN	
M. liminatans	GUNIDL		GEIFRLCER		FLLEFGLSSLD	REL BALVLDGELA	

Gblocks
Annotation

* *
C243 C249

	490	500	510	520	530	540
P. profundum	-----	-----	-----	FAMEIVRPLIQQLIDTGKVG----		
P. luminescens	-----	-----	-----	LAMEIIMPLVQRLLLEGGKIS----		
E. amylovora	-----	-----	-----	LAMEIMGPLVKRLIEGKIG----		
S. flexneri	-----	-----	-----	LAMEIIMPLVQRLMEGKKIE----		
S. medicae	-----	-----	-----	LAMQIIFPLIHLLERKHRMS----		
R. meliloti	-----	-----	-----	LAMQIIFPLIHLLERKHRMS----		
C. necator	-----	-----	-----	LAMQIIFPFVLRMMERRKRAAQ--		
R. rubrum	-----	-----	-----	LSMQLIFPFVLRMMERRKRAAQ--		
R. sphaeroides	-----	-----	-----	LAMQIILPLIDRVVRESKVA----		
A. cryptum	-----	-----	-----	LAMQIILPIIMQLMDRKRRAQ----		
X. flavus	-----	-----	-----	LAMQILLPLIMQLMDRKRRAQ----		
N. hamburgensis	-----	-----	-----	LAMQIILPLILQLIDRKRRA-----		
N. vulgaris	-----	-----	-----	LAMQIILPLILQLIERKKRA-----		
R. palustris DX1	-----	-----	-----	LAMQIILPLIMQLIDRKRRAQ----		
R. palustris Bis	-----	-----	-----	LAMQIILPLIMQLIERKRRAQ----		
M. capsulatus	-----	-----	-----	LAMEIFRPIERMADREK-----		
A. ferrooxidans	-----	-----	-----	YAMEILGPRIERMLEDHMTI----		
C. M. oxyfera	-----	-----	-----	LAMEILAPIVHIMIENKLA-----		
T. denitrificans	-----	-----	-----	FAMEILAPLIQDMIANKKK-----		
A. vinosum	-----	-----	-----	FAMEILOPIIERMMDARRV-----		
P. lunula	DQLKEIEENLEGLAGS - PGELTEAMTKLRSSPGSQNGTGLDQVIAMVREVYERL TAKV					
L. polyedrum	AQLKEIEDNLEGLPSKTPGELTEAMVKLKSSPGSQNGTGLDQVIAMVREVYERL TGKK					
B. natans	EELFFIEERLSNTNTKYFGEITKQMLKNKAAPGSGDNGTGLDQVIAMVREVYERL TGR					
E. gracilis	KEGLVVEKFLHNTGAKFEFGEITQELLKGQNSPGGDNNGTGLDQVIAMVREVYERL TGE					
P. parvum	EELIYVESQLCNTGTYYGELTEQMVNKNKASPGSENGTGLDQVIAMVREVYERL TGE					
G. theta	DEMMYVEKQFASTGSKFVGEITKKMLEYEGQPGSNDNGTGLDQVIAMVREVYERL TGE					
T. pseudonana	QELVYVESNLGNTNSKFYGEVTQAML SLADSPGSNNGTGLDQVIAMVREVYERL TGE					
O. sinensis	QELVYVESQLSNTSTKFYGEITQAML KLADAPGSNNGTGLDQVIAMVREVYERL TGE					
P. tricornutum	QELVYVESALSNKTKFYGEMTQAMLALATAPGSNNGTGLDQVIAMVREVYERL TGE					
D. lutheri	DELIYVESALNTGAKFYGELTQQILKNKDAVGSNDNGTGLDQVIAMVREVYERL TGE					
O. tauri	EELIYVESHLNNTSSKFYGEITQQMLKYQNGPGSNNGTGLDQVIAMVREVYERL TGE					
M. commoda	EELIYVESHLNNTSSKFYGEITQQMLKYQNGPGSNNGTGLDQVIAMVREVYERL TGE					
P. trichocarpus	EELIYVESHLNNTSSKFYGEITQQMLKHADFPGSNNGTGLDQVIAMVREVYERL TGE					
P. patens	DELIYVESHLNNTSSKFYGEITQQMLKHADFPGSNNGTGLDQVIAMVREVYERL TGE					
S. oleracea	DELIYVESHLNNTSSKFYGEITQQMLKHADFPGSNNGTGLDQVIAMVREVYERL TGE					
A. thaliana	DELIYVESHLNNTSSKFYGEITQQMLKHADFPGSNNGTGLDQVIAMVREVYERL TGE					
S. moellendorff.	DELIYVESHLNNTSSKFYGEITQQMLKHADFPGSNNGTGLDQVIAMVREVYERL TGE					
T. aestivum	DELIYVESHLNNTSSKFYGEITQQMLKHADFPGSNNGTGLDQVIAMVREVYERL TGE					
P. trichocarpa	DELIYVESHLNNTSSKFYGEITQQMLKHADFPGSNNGTGLDQVIAMVREVYERL TGE					
M. crystallinum	DELIYVESHLNNTSSKFYGEITQQMLKHADFPGSNNGTGLDQVIAMVREVYERL TGE					
P. sativum	DELIYVESHLNNTSSKFYGEITQQMLKHADFPGSNNGTGLDQVIAMVREVYERL TGE					
C. variabilis	EELIYVESHLNNTSSKFYGEITQQMLKNSFPGSNNGTGLDQVIAMVREVYERL TGE					
C. reinhardtii	EELIYVESHLNNTSSKFYGEITQQMLKNSFPGSNNGTGLDQVIAMVREVYERL TGE					
V. carteri	EELIYVESHLNNTSSKFYGEITQQMLKNSFPGSNNGTGLDQVIAMVREVYERL TGE					
G. sulphuraria	EELIYVESHLNNTSSKFYGEITQQLRNSSAPGSNNGTGLDQVIAMVREVYERL TGE					
G. kiluaensis	DDSPLEQLRNTSETRYGELASLILKHTDYPGSRDNGTGLDQVIAMVREVYERL TGE					
G. violaceus	EDSPELEEKLRNTSETRYGELASLILKHTDYPGSRDNGTGLDQVIAMVREVYERL TGE					
T. elongatus	DELIYVESHLNNTSSKFYGEITQQLRNSSAPGSNNGTGLDQVIAMVREVYERL TGE					
Synechocystis sp	EEMVYVENHLSKTGTYYGEMTELLLKHKDYPGTDNGTGLDQVIAMVREVYERL TGE					
M. aeruginosa	EEMIYIESHLSKTGTYYGEMTELLLKHKDYPGTDNGTGLDQVIAMVREVYERL TGE					
Cyanothecce sp	EEMIYIEHLSRTGTYYGEMTHLLQHKDYPGSNNGTGLDQVIAMVREVYERL TGE					
S. elongatus	EEMIYIEGHLSKTDQYYGELTHLLLQHKDYPGSNNGTGLDQVIAMVREVYERL TGE					
A. variabilis	EEMIYIEHLSNTSTKYQGEITQQLRNSSAPGSNNGTGLDQVIAMVREVYERL TGE					
N. spumigena	DEVIYVETHLSKTSTKYEGEMTHLLLQHKDYPGSNNGTGLDQVIAMVREVYERL TGE					
A. boonei	-----HEAIDSLERRIMEYTGFEYILERSKYVNGTGLDQVIAMVREVYERL TGE					
F. placidus	---VEIFESLLDALRDETGYKVRW----EAREYVNSIEVAKLLLCWNLVEIIMKMG---					
A. profundus	---VDIFKSLFDSLRIEIGD-----EIKVSEYVNAIEFSKLLVCWNLVEIIMKMG---					
A. veneficus	---VELFSTLLDILKKEVGADVENKMT-----YVNAIEVAKLLVCWNLVEIIMKMG---					
M. harundinacea	SMVEGVEAKLKSLAG-----STAPICDRAGGDRVTSNGTGLDQVIAMVREVYERL TGE					
M. concilii	-----QSMISDLEKLLGSELTGDMISDRREEYVNAIEFSKLLVCWNLVEIIMKMG---					
M. thermophila	TMIKDLERKLCDFLGRDVPVTEG--CQEDHGSYVNAIEFSKLLVCWNLVEIIMKMG---					
M. hungatei	-----PDTIHKIERQIEFQTGISPINIFRGQEHITGDLVRLILSWQIINGRIALS NHL					
Methanolinea sp	-----REMAGDLRRKIEEQGTQPADMFRGNAMVTAEMVRLIVSWRIINHLANLA---					
M. boonei	-----YDTVRNLELSIEHTGIHPIEMFAGRKVTPINIVQLLSWRIINRRIFLQDHR					
M. limicola	DVIRCLLNIEEQTG-----VSPVSLFEGRDYVTAEMIQLLSWRIINRRIFLQDHR					
M. petrolearia	-----HEVVSLLLEKGIEMQTGIGPVSVYSRDSYVTAEMVRLILSWRIINRRIFLQDHR					
M. palustris	-----TRMVKRLETSIEEQTVRPIISDFHDHYMTAEMVRLILAWRIINRRIFLQDHR					
M. marisnigri	-----DAVARKLERNIEIQTQVEPIDLSQSDYLTAGDMAQLILAWRIINRRIFLQDHR					
M. liminatans	-----ASAIRRLARTIGRETREAVNLFADRQYVTAEMVRLILAWRIINRRIFLQDHR					

	550	560
	=====+=====+	
P. profundum	-----	-----
P. luminescens	-----	-----
E. amylovora	-----	-----
S. flexneri	-----	-----
S. medicae	-----	-----
R. meliloti	-----	-----
C. necator	-----	-----
R. rubrum	-----	-----
R. sphaeroides	-----	-----
A. cryptum	-----	-----
X. flavus	-----	-----
N. hamburgensis	-----	-----
N. vulgaris	-----	-----
R. palustris DX1	-----	-----
R. palustris Bis	-----	-----
M. capsulatus	-----	-----
A. ferrooxidans	-----	-----
C. M. oxyfera	-----	-----
T. denitrificans	-----	-----
A. vinosum	-----	-----
P. lunula	GA-----	-----
L. polyedrum	-----	-----
B. natans	IQIPKWGLFLDDY-----	-----
E. gracilis	KA-----	-----
P. parvum	-----	-----
G. theta	VPAQAN-----	-----
T. pseudonana	KLAATKETAASA-----	-----
O. sinensis	KLAVIEA-----	-----
P. tricornutum	KAKAGVSAAAA-----	-----
D. lutheri	VDASAAA-----	-----
O. tauri	VVAKA-----	-----
M. commoda	VVTAA-----	-----
P. sitchensis	TGASLEAAKA-----	-----
P. patens	KNAATLQSAKA-----	-----
S. oleracea	STATATAAKA-----	-----
A. thaliana	ATARAEAKA-----	-----
S. moellendorff.	GSPVGAATAATSKV-----	-----
T. aestivum	AGVPAEAAKV-----	-----
P. trichocarpa	AKTPVEATKA-----	-----
M. crystallinum	TAAPAAATKA-----	-----
P. sativum	RAETPVGAACA-----	-----
C. variabilis	-----	-----
C. reinhardtii	VVPV-----	-----
V. carteri	VVPA-----	-----
G. sulphuraria	IAPVLV-----	-----
G. kilaeensis	LAAAKV-----	-----
G. violaceus	LTASKAK-----	-----
T. elongatus	AATVTNR-----	-----
Synechocystis sp	KVPASV-----	-----
M. aeruginosa	AKVAASV-----	-----
Cyanothece sp	ESKVATQV-----	-----
S. elongatus	AAPVAASV-----	-----
A. variabilis	AKLAVQV-----	-----
N. spumigena	EAKLAVQV-----	-----
A. boonei	ENAREKNIY-----	-----
F. placidus	-----	-----
A. profundus	-----	-----
A. veneficus	L-----	-----
M. harundinacea	-----	-----
M. concilii	GY-----	-----
M. thermophila	-----	-----
M. hungatei	DQ-----	-----
Methanolinea sp	-----	-----
M. boonei	-----	-----
M. limicola	-----	-----
M. petrolearia	GVSS-----	-----
M. palustris	HQDHNK-----	-----
M. marisnigri	GAGGTGRTVTGNNGHGCGR	-----
M. liminatans	SAHAKG-----	-----
Gblocks		
Annotation		

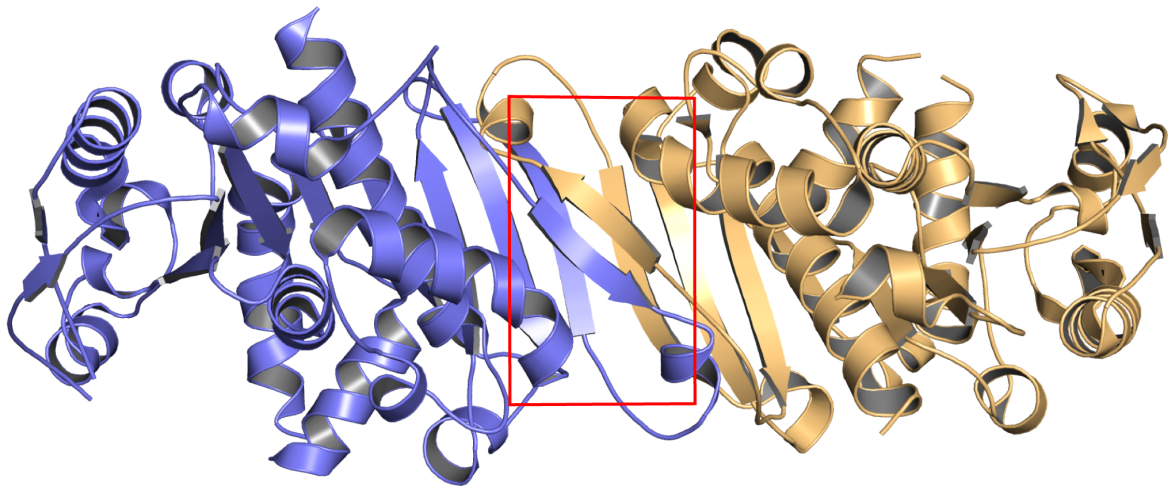
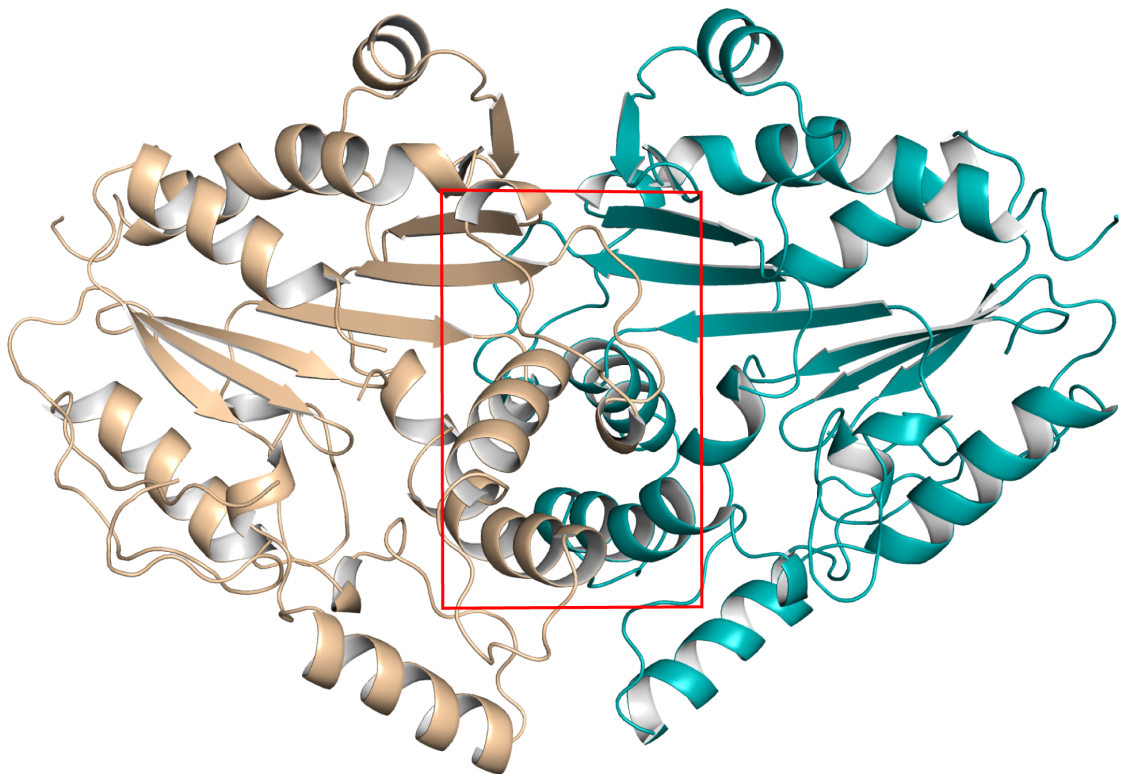
a**b**

Figure 2.14 Dimer interface of bacterial and Archaea PRKs. Dimer interface of a, octameric *Rhodobacter sphaeroides* PRK (PDB ID 1A7J) 6 and b, dimeric *Methanospirillum hungatei* PRK (PDB ID 5B3F) 7 is highlighted by a red box. The dimer interface of bacterial PRK is formed by three b-strands and one a-helix while in Archaea enzyme by two b-strands. The calculated dimer interface areas are 1667 and 1695 Å², respectively.

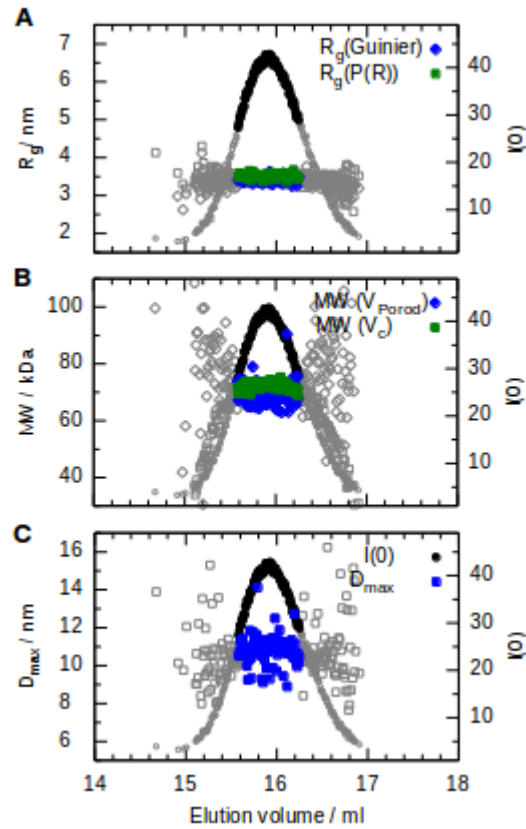


Figure 2.15 Parameters determined by SEC-SAXS analysis of CrPRK. a, $I(0)$ trace (dots) and R_g determined by the Guinier approximation (diamonds) and R_g calculated from the $P(r)$ function (squares). b, $I(0)$ trace (dots) and MW estimated from the Porod volume (diamonds) and from the volume-of-correlation (squares). c, $I(0)$ trace (dots) and D_{max} estimated from the $P(r)$ function (squares). The frames used in the average to obtain the representative scattering profile, are highlighted in black compared to the grey neglected frames.

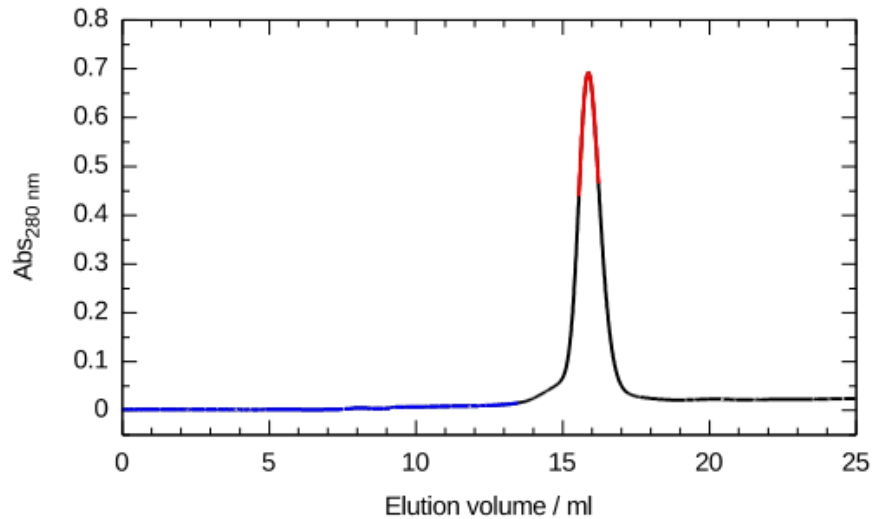


Figure 2.16 UV trace of the chromatogram profile of CrPRK analyzed in SEC-SAXS mode. Frames collected as buffer (from 0 to 14 ml) are highlighted in blue; frames collected as protein (from 14 to 17.5 ml) are highlighted in black; frames highlighted in red have been used for SAXS analysis.

Table 2.3 SEC-SAXS data analysis of reduced CrPRK.

Concentration (mg ml ⁻¹)	6.1 (injected)
Structural parameters⁴⁰	
q interval for Guinier linear fit (nm ⁻¹)	0.12-0.38
I(0) [from Guinier approximation]	42.0 ± 0.1
R _g (nm) [from Guinier approximation]	3.43 ± 0.01
q interval for Fourier inversion (nm ⁻¹)	0.12-3.5
I(0) [from P(R)]	42.4 ± 0.06
R _g (nm) [from P(R)]	3.55 ± 0.01
D _{max} (nm)	11.2±0.5
Porod volume estimate (nm ³)	115 ± 10
DAMMIN excluded volume (nm ³)	138 ± 1
Dry volume calculated from sequence (nm ³) (v=0.735 cm ³ g ⁻¹)	95
Molecular mass (kDa)	
From I(0)	70
From V _c ⁴⁰	70
From Porod invariant ⁶⁰	85
From Porod volume (x0.625) ³⁷	72
From excluded volume (x0.5) ³⁷	69
From sequence	77.8

* Maximum D_{max} allowed by the minimum q vector included, according to D_{max} = π/q_{min} (data truncated at low q).

Table 2.4 X-ray (CrPRK and AtPRK) and SEC-SAXS (CrPRK) data collection parameters.

	CrPRK	AtPRK	CrPRK SEC-mode
Detector	Pilatus 2M	ADSC Quantum Q315r	Pilatus 1M
Beam geometry (mm ²)	0.1 × 0.1	0.1 × 0.1	0.7 × 0.7
Wavelength (Å)	1.240	0.939	0.990
Capillary diameter (mm)	/	/	1.8
Sample-to-detector distance (mm)	239.85	393.43	2872
Δφ (°)	0.5	0.7	/
q* range (nm ⁻¹)	/	/	0.033-4.9
Exposure time (s)	5	5	1
Flow (ml/min)	/	/	0.5
Temperature (K)	100.0	100.0	277.15

* $q = 4\pi \sin(\theta)/\lambda$, where 2θ is the scattering angle and λ is the X-ray wavelength.

Table 2.5 X-ray data collection and refinement statistics.

	CrPRK	AtPRK
<i>Data collection</i>		
Unit cell (Å)	77.68, 83.55, 133.15, 90.00, 90.00, 90.00	116.30, 116.30, 106.81, 90.00, 90.00, 90.00
Space group	P2 ₁ 2 ₁ 2 ₁	I4 ₁
Resolution range* (Å)	44.39 – 2.50 (2.61 – 2.50)	82.23 – 2.47 (2.58 – 2.47)
Unique reflections	30406 (3329)	24824 (3107)
Completeness* (%)	99.4 (98.0)	97.6 (99.6)
R _{merge} *	0.082 (1.194)	0.091 (0.435)
I/σ(I) *	12.2 (1.1)	11.2 (2.3)
Multiplicity*	5.1 (5.2)	6.9 (6.5)
<i>Refinement</i>		
Resolution range* (Å)	39.86 – 2.60 (2.69 - 2.60)	46.77 – 2.47 (2.57 – 2.47)
Reflection used	27162 (2666)	24672 (2786)
R/R _{free} *	0.227/0.262	0.226/0.281
rmsd from ideality (Å, °)	0.004, 0.915	0.011, 1.128
<i>N° atoms</i>		
Non-hydrogen atoms	5360	5385
Protein atoms	5319	5355
Solvent molecules	31	30
Hetero atoms	10	/
<i>B value (Å²)</i>		
Mean	62.4	78.4
Wilson plot	59.0	52.5
Protein atoms	62.3	78.4
Hetero atoms	56.2	70.3
Solvent molecules	85.5	/
<i>Ramachandran plot (%) §</i>		
Most favoured	91.1	91.4
Allowed	7.4	6.0
Disallowed	1.5	2.7

*Values in parentheses refer to the last resolution shell

§ As defined by MolProbity (Bienert et al., 2017)

Organism	Organism - full description	Uniprot used	other Ref.	other Ref2	Kingdom	Phylum	Photosynthetic	Reference and/or status of the uniprot entry
<i>A. profilus</i>	Archaeoglobus profundus	D2RE9		AD55593	Archae	Euryarchaeota	no	Kono et al., 2017
<i>M. conalli</i>	Methanosarcina conalli	F4W63		AE68483	Archae	Euryarchaeota	no	Kono et al., 2017
<i>M. hungatei</i>	Methanospirillum hungatei	O2JL85		PDB: 5B3F	Archae	Euryarchaeota	no	Kono et al., 2017
<i>M. mansueti</i>	Methanococcus mansueti	A3CW0		ABN5780	Archae	Euryarchaeota	no	Kono et al., 2017
<i>M. thermophila</i>	Methanosarcina thermophila	AB947		ABK1521	Archae	Euryarchaeota	no	Kono et al., 2017
<i>A. boonei</i>	Acidilobum boonei (strain DSM 19572 / 7469)	B5C08			Archae	Euryarchaeota	no	Kono et al., 2017 / protein predicted
<i>A. veneficus</i>	Archaeoglobus veneficus (strain DSM 11195 / SNP6)	F2M18			Archae	Euryarchaeota	no	Kono et al., 2017 / protein predicted
<i>F. placidus</i>	Ferroglobus placidus (strain DSM 10642 / AED11200)	D3R22			Archae	Euryarchaeota	no	Kono et al., 2017 / protein predicted
<i>M. boonei</i>	Methanospirillum boonei (strain DSM 21154 / JOM 14080 / 648)	A74V6			Archae	Euryarchaeota	no	Kono et al., 2017 / protein predicted
<i>M. harundinacea</i>	Methanosarcina harundinacea (strain 64C)	G7W121			Archae	Euryarchaeota	no	Kono et al., 2017 / protein predicted
<i>M. limicola</i>	Methanoplanus limicola DSM 2279	HLX11			Archae	Euryarchaeota	no	Kono et al., 2017 / protein predicted
<i>M. limnatis</i>	Methanospirillum limnatis DSM 4140	J0518			Archae	Euryarchaeota	no	Kono et al., 2017 / protein predicted
<i>M. palustris</i>	Methanospirillum palustris (strain ATCC BAA-1556 / DSM 19958 / EL-9c)	B8G52			Archae	Euryarchaeota	no	Kono et al., 2017 / protein predicted
<i>M. petrolearia</i>	Methanospirillum petrolearia (strain DSM 11571 / OCM 486 / SEBR 4847) (Methanoplanus petrolearius)	ELR35			Archae	Euryarchaeota	no	Kono et al., 2017 / protein predicted
<i>Methanoplanus sp.</i>	Methanoplanus sp. SDB	A0A000VL5			Archae	Euryarchaeota	no	Kono et al., 2017 / protein predicted
<i>A. ferrooxidans</i>	Acidithiobacillus ferrooxidans (strain ATCC 23270 / DSM 14882 / CIP 104768 / NCIMB 9455)	B7555			Bacteria	Acidithiobacillia	no	Kono et al., 2017 / protein inferred from homology
<i>R. sphaeroides</i>	Rhodospirillum rubrum	AA42613	P12033	PDB: 1A7J	Bacteria	α-Proteobacteria	yes (purple non-sulfur)	Hallenbeck and Kaplan, 1987 inferred by homology
<i>N. vulgaris</i>	Nitrospira vulgaris	P37100			Bacteria	α-Proteobacteria	no	inferred by homology
<i>R. meliloti</i>	Rhizobium meliloti (strain 1021) (Ensifer meliloti) (Sinorhizobium meliloti)	P5847			Bacteria	α-Proteobacteria	no	inferred by homology
<i>S. melilicis</i>	Sinorhizobium meliloti (strain WSM419) (Ensifer melilicis)	P5887			Bacteria	α-Proteobacteria	no	inferred by homology
<i>R. palustris DX</i>	Rhodospirillum rubrum (strain DX-1)	AD146366	EA9W3		Bacteria	α-Proteobacteria	yes (purple non-sulfur)	Kono et al., 2017
<i>R. rubrum</i>	Rhodospirillum rubrum	ABC3204	Q2RRP1		Bacteria	α-Proteobacteria	yes (purple non-sulfur)	Kono et al., 2017
<i>A. cryptum</i>	Acidiphilium cryptum (strain JF-5)	AS9VQ9			Bacteria	α-Proteobacteria	no	Kono et al., 2017 / protein predicted
<i>N. hamburgensis</i>	Nitrospira hamburgensis (strain DSM 10229 / NCIMB 13809 / X14)	Q1LQD6			Bacteria	α-Proteobacteria	no	Kono et al., 2017 / protein inferred from homology
<i>R. palustris B1</i>	Rhodospirillum rubrum (strain B1A53)	O07M64			Bacteria	α-Proteobacteria	no	Kono et al., 2017 / protein inferred from homology
<i>X. flavus</i>	Xanthobacter flavus	P23015			Bacteria	α-Proteobacteria	yes (purple non-sulfur)	Meijer et al., 1991
<i>Synchrochlois sp.</i>	Synchrochlois sp. (strain PCC 6803 / Kazusa)	P37101			Bacteria	Cyanobacteria	yes	Experimental evidence at transcript level
<i>S. elongatus</i>	Synchrochlois elongatus PCC 7942	Q3JF2			Bacteria	Cyanobacteria	yes	Kobayashi et al., 2003
<i>A. variabilis</i>	Anabaena variabilis (strain ATCC 29413 / PCC 7937)	Q3JF31			Bacteria	Cyanobacteria	yes	Kono et al., 2017 / protein inferred from homology
<i>G. violaceus</i>	Gloeobacter violaceus (strain PCC 7421)	O7M87			Bacteria	Cyanobacteria	yes	Kono et al., 2017 / protein inferred from homology
<i>T. elongatus</i>	Thermosynechococcus elongatus (strain BP-1)	Q8DH2			Bacteria	Cyanobacteria	yes	Kono et al., 2017 / protein predicted
<i>Cyanothecae sp.</i>	Cyanothecae sp. (strain PCC 7424) (Synchrococcus sp. (strain ATCC 29155))	B7M62			Bacteria	Cyanobacteria	yes	Kono et al., 2017 / protein predicted
<i>G. klauensis</i>	Gloeobacter klauensis JS1	U920M9			Bacteria	Cyanobacteria	yes	Kono et al., 2017 / protein predicted
<i>M. aeruginosa</i>	Microcystis aeruginosa PCC 9701	MIW9			Bacteria	Cyanobacteria	yes	Kono et al., 2017 / protein predicted
<i>N. sputigena</i>	Nodularia sputigena CO9414	A0ZEL1			Bacteria	γ-Proteobacteria	no	inferred by homology
<i>E. amylovora</i>	Erwinia amylovora	ESB403			Bacteria	γ-Proteobacteria	no	inferred by homology
<i>S. flexneri</i>	Shigella flexneri	P049X6			Bacteria	γ-Proteobacteria	no	inferred by homology
<i>M. capsulatus</i>	Methylobacterium capsulatus (strain ATCC 33009 / NCIMB 11132 / Bath)	G602L2			Bacteria	γ-Proteobacteria	no	Kono et al., 2017 / protein predicted
<i>A. vinosum</i>	Altidrometium vinosum (strain ATCC 17899 / DSM 180 / NBRC 103801 / NCIMB 10441 / D) (Chromatium vinosum)	D3RR2			Bacteria	γ-Proteobacteria	yes (purple sulfur)	Kono et al., 2017 / protein inferred from homology
<i>P. luminescens</i>	Photobacterium luminescens (Xenorhabdus luminescens)	A0A1B8K0C5			Bacteria	γ-Proteobacteria	no	Kono et al., 2017 / protein inferred from homology
<i>P. profundum</i>	Photobacterium profundum (strain SS9)	O6LVE1			Bacteria	γ-Proteobacteria	no	Kono et al., 2017 / protein inferred from homology
<i>C. M. oxyfera</i>	Cardibacterium oxyfera	DSM104			Bacteria	unclassified	no	Kono et al., 2017 / protein inferred from homology
<i>T. denitrificans</i>	Thiobacillus denitrificans (strain ATCC 25259)	Q35C56			Bacteria	β-Proteobacteria	no	Kono et al., 2017 / protein predicted
<i>C. necator</i>	Cuptavidus necator	P19J23			Excavates	Euglenozoa	yes	Kossmann et al., 1989
<i>E. gracilis</i>	Euglena gracilis	Q24L70			Excavates	Cryptophyta	yes	Experimental evidence at transcript level
<i>G. theta</i>	Guillardia theta	Q24L74			Excavates	Cryptophyta	yes	Experimental evidence at transcript level
<i>D. lutheri</i>	Dicranonema lutheri (Monochrysis lutheri) Parvula lutheri	Q24L75			Excavates	Haptophyceae	yes	Experimental evidence at transcript level
<i>P. parvum</i>	Phymastrium parvum	Q24L58			Excavates	Haptophyceae	yes	Predicted/protein
<i>C. variabilis</i>	Chorella variabilis	ELZ77			Excavates	Chlorophyceae	yes	inferred by homology
<i>M. commoda</i>	Microcromes commoda	CI1FW3			Excavates	Chlorophyceae	yes	inferred by homology
<i>O. tauri</i>	Ostreococcus tauri	A0A090N369			Excavates	Chlorophyceae	yes	Predicted/protein
<i>V. carteri</i>	Volvox carteri f. naegariiensis	D18R77			Excavates	Chlorophyceae	yes	Predicted/protein
<i>C. reinhardtii</i>	Chlamydomonas reinhardtii	P19J24	A81Y4	AAE56402	Excavates	Chlorophyceae	yes	Roesler and Ogren, 1990
<i>G. sulphuraria</i>	Galdieria sulphuraria	M2324			Excavates	Rhodophyta	yes	Kono et al., 2017 / protein predicted
<i>P. sativum</i>	Psidium sativum	OP566			Excavates	Streptophyta	yes	Experimental evidence at transcript level
<i>P. sitchensis</i>	Picea sitchensis (Sitka spruce) (Pinus sitchensis)	OP566			Excavates	Streptophyta	yes	Experimental evidence at transcript level
<i>P. patens</i>	Physcomitrella patens	AG19N4			Excavates	Streptophyta	yes	inferred by homology
<i>P. trichocarpa</i>	Populus trichocarpa (Western balsam poplar) (Populus balsamifera subsp. trichocarpa)	B93275			Excavates	Streptophyta	yes	inferred by homology
<i>S. moellendorffii</i>	Selaginella moellendorffii	D8S148			Excavates	Streptophyta	yes	inferred by homology
<i>M. crystallinum</i>	Mesembryanthemum crystallinum	P27774			Excavates	Streptophyta	yes	inferred by homology
<i>S. oleacea</i>	Spizacia oleacea	P05539	CA30489		Excavates	Streptophyta	yes	Roesler and Ogren, 1990
<i>T. aestivum</i>	Triticum aestivum	P26502			Excavates	Streptophyta	yes	Roesler and Ogren, 1990
<i>A. thaliana</i>	Arabidopsis thaliana	P26597			Excavates	Streptophyta	yes	This Study and Roesler and Ogren, 1990
<i>L. polatum</i>	Lingulodinium polyedrum	O24L73			Excavates	SAR-Alveolates*	yes	Experimental evidence at transcript level
<i>P. lunula</i>	Pyrocypris lunula	O24L72			Excavates	SAR-Alveolates*	yes	Experimental evidence at transcript level
<i>B. natans</i>	Bigeloviella natans	Q24L57			Excavates	SAR-Rhizaria*	yes	Predicted/protein
<i>O. sinensis</i>	Oobrevia sinensis	B57503			Excavates	SAR-Stramenopiles*	yes	Experimental evidence at transcript level
<i>P. tricornutum</i>	Phaeodactylum tricornutum	B57503			Excavates	SAR-Stramenopiles*	yes	Experimental evidence at transcript level
<i>T. pseudonana</i>	Thalassiosira pseudonana	B85240			Excavates	SAR-Stramenopiles*	yes	inferred by homology

*Member of the SAR group (Burki et al., 2010); #Member of the Hacrobia Kingdom (Ogimoto et al., 2009)

Table 2.6 References of alignment sequences

3. Glutathionylation of *Arabidopsis thaliana* AMY3 and regulation by glutaredoxins and thioredoxin *in vitro*

3.1 Brief Introduction

In the last decades starch metabolism has been deeply studied and its biosynthetic and degradation pathways have been detailed, especially for leaf starch (Zeeman et al., 2010; Stitt and Zeeman, 2012). Several enzymes emerged as fundamental for starch turnover and when their genes are knocked out plants showed *starchless* or *starch excess* phenotypes (Yu et al., 2001; Fulton et al., 2008; Kötting et al., 2005; Kötting et al., 2009; Streb et al., 2009; Crumpton-Taylor et al., 2013). Another set of enzymes have been found which could potentially be involved in degradation pathway, however lack of these enzymes did not lead to any starch-related phenotype (Zeeman et al., 2004; Yu et al., 2005; Fulton et al., 2008). Their role is now being discovered studying plants exposed to abiotic stresses like drought, osmotic and salt stress (Zeeman et al., 2004; Zanella et al., 2016; Thalmann et al., 2016; Thalmann and Santelia, 2017). Indeed the demand of carbon backbones in adverse conditions can be fulfilled activating alternative enzymes to release sugars from starch (Thalmann and Santelia, 2017; MacNeil et al., 2017).

In *Arabidopsis thaliana* the α -amylase 3 (*AtAMY3*), together with the β -amylase 1 (*AtBAM1*), takes part to osmotic stress response (Valerio et al., 2011; Zanella et al., 2016; Thalmann et al., 2016). *AtAMY3* is the unique chloroplast-localized α -amylase encoded by *Arabidopsis* genome and is not required for normal starch breakdown (Yu et al., 2005). It is regulated by thioredoxins (TRXs) and activated under reducing conditions *in vitro* (Seung et al., 2013). The same feature is shared with other starch-related enzymes like GWD1, SEX4 and BAM1 (Mikkelsen et al., 2005; Sparla et al., 2006; Silver et al., 2013). Since reduction by TRXs occur during the day, thanks to the light-driven electron transport, the reductive activation of enzymes for transitory starch degradation is apparently in contrast with the typical nocturnal degradation pattern. However reductive activation perfectly fits the additional demand of carbon required under stress conditions during the day (Thalmann and Santelia, 2017; MacNeil et al., 2017; Pomerrenig et al., 2018). *AtAMY3* expression is induced by osmotic stress and stimulated by ABA (Thalmann et al., 2016), a typical drought stress hormone (Galldock et al., 2011; Vishwakarma et al., 2017; Kuromori et al., 2018). Moreover *AtAMY3* is required for starch degradation in guard cells (Horrer et al., 2016), a central process for

stomata movement during the day and under water deficiency (Daloso et al., 2017; Santelia and Lawson, 2016).

While TRXs turn on several enzymes at the onset of the day, under stress conditions proteins can be subjected to other redox post-translational modifications. Cellular processes, like respiration and photosynthesis, generate reactive oxygen species (ROS, Noctor et al., 2018). ROS production can raise in stress conditions and as consequence cysteine residues could undergo uncontrolled oxidation and loss of their functionality (Poole, 2015). Oxidation of cysteine thiols is usually carried out by H_2O_2 , which is the ROS with the longest half-life in cellular compartments and for this reason has a widespread physiological role in living cells (Mittler, 2017; Khan et al., 2018). The thiol oxidation occurs in 3 different steps, passing from thiol to sulphenic acid, then to sulphinic acid and at the end to sulphonic acid (Roos et al., 2013). The last two stages are not reversible and is not possible to recover proper functioning without synthesize new protein. In this regard, glutathionylation evolved to protect protein thiols from irreversible oxidation. The glutathione (GSH) is a cysteine-containing tripeptide which can form mixed disulfide bonds with cysteine residues inside proteins (Zaffagnini et al., 2012). Glutathione can be enzymatically removed by glutaredoxins (GRX) and TRXs restoring enzymatic activity (Zaffagnini et al., 2012). Glutathione is one of the cellular redox buffers, together with ascorbate and a set of ROS-scavenging enzymes, and contributes to maintaining redox homeostasis of cellular environments (Foyer and Noctor, 2016). In fact raise of H_2O_2 concentration in the cell causes accumulation of oxidized glutathione (GSSG) due to scavenging, GSSG is then accumulated in subcellular compartments like chloroplasts (Smith et al., 1985; Queval et al., 2011). The GSSG concentration reaches values of about 0.5 mM under stress conditions (Smith et al., 1985; Queval et al., 2011). These levels are high enough to allow protein glutathionylation by thiol-disulfide exchange with GSSG, preventing adverse reactions with reactive species. Glutathionylation can also regulate protein function influencing enzymatic activity, oligomeric state, and regenerating functional enzymes thanks to redox reactions (Michelet et al., 2005; Noguera-Mazon et al., 2006; Tarrago et al., 2009).

When plants are exposed to osmotic stress the photosynthesis is impaired producing higher amounts of ROS (Chaves et al., 2009; Farooq et al., 2009). Several proteins can be protected by glutathionylation in chloroplast (Ito et al., 2003; Dixon et al., 2005; Michelet et al., 2005; Zaffagnini et al., 2007), an important site of ROS production together with mitochondria and peroxisomes (Noctor et al., 2018). *AtAMY3* is required under osmotic stress for mobilization of carbon skeletons in the mesophyll cells and its activity should be regulated to control stomata movement. Considering the possible exposure to reactive species, recombinant *AtAMY3* was expressed and its biochemistry studied. The aim of the present set of experiments was to characterize the sensitivity

of *AtAMY3* to glutathione and hydrogen peroxide and the effect on its activity. Mechanisms to control the enzymatic activity *via* glutathionylation were studied together with the recovery of activity mediated by GSH, GRX and TRX.

3.2 Materials and Methods

3.2.1 Expression and purification of recombinant AMY3 from *Arabidopsis thaliana*

The expression vector pET-21 (Novagen) containing the cDNA coding for mature form of α -amylase 3 of *A. thaliana* cloned upstream a 6-histidine tag was kindly provided by Dr. D. Santelia (University of Zürich). Chemically competent *E. coli* BL21 (DE3) cells have been transformed by heat shock at 42 °C for 45 seconds. Cells were then cooled for 2 minutes on ice and then grown in shaking for 1 hour at 37 °C. After growth the culture was plated on agar/LB medium in presence of 100 μ g/ml ampicillin and incubated overnight (o.n.) at 37 °C. Bacterial stock was prepared using a sample of o.n. grown culture from a single picked colony and stored at - 80 °C in LB medium plus 5% glycerol.

For protein expression, o.n. culture from bacterial stock was transferred to fresh growth medium supplemented with 100 μ g/ml ampicillin and grown in 120 rpm shaking at 37 °C until 0.6 absorbance at 600 nm was reached. Then expression of *AtAMY3* was induced by addition of 1 mM isopropyl-thiogalactoside (IPTG) and the culture was grown o.n. at 20 °C under 120 rpm shaking. The next day cells were collected by centrifugation at 10,000 rpm (JA 14, Beckman) for 20 minutes and stored at - 80 °C.

In order to purify the protein, the bacterial pellet was resuspended in 30 ml of Binding buffer (20 mM Tris pH 7.9; 5 mM imidazole; 0.5 mM NaCl) and sonicated with 5 cycles of 2 minutes pulses with 8 μ m amplitude and 1 minute cooling on ice. Cellular debris were removed by spinning the lysate for 30 minutes at 15,000 rpm and 4 °C. The supernatant, containing soluble *AtAMY3*, was loaded into a column containing nickel-bound Chelating Sepharose Fast Flow resin (GE Healthcare). After complete loading, the flow-through was reloaded to ensure complete binding of His-tagged *AtAMY3*. Then the resin was washed with 8 column volumes of Binding buffer and 10 column volumes of Wash buffer (20 mM Tris pH 7.9 , 60 mM imidazole, 0.5 mM NaCl). *AtAMY3* was eluted by loading 5 column volumes of Elution buffer (20 mM Tris pH 7.9, 500 mM imidazole, 0.5 mM NaCl) and desalted in 100 mM Tricine-NaOH pH 7.9 through PD-10 Desalting Columns (GE Healthcare). Protein purity was verified on 12.5% SDS-PAGE. For protein quantification the absorbance at 280 nm was measured on Nanodrop system (Thermo Fisher Scientific). Extinction coefficient at 280 nm and molecular weight were calculated *in silico* using ProtParam (ExpPASy, <https://web.expasy.org/protparam/>, Gasteiger et al., 2005) and were 179,470 M⁻¹ cm⁻¹ and 93,691.9 g/mol respectively.

3.2.2 Biotinylated GSSG assay

Biotinylated GSSG (BioGSSG) assay was performed to verify *AtAMY3* glutathionylation *in vitro*. GSSG biotinylation was obtained incubating for 1 hour at room temperature (RT) 16 mM GSSG with 24 mM biotinylating agent (EZ-Link Sulfo-NHS-Biotin, Thermo Fisher Scientific) in 50 mM potassium phosphate buffer pH 7.2. The reaction was stopped by adding NH_4HCO_3 to a final concentration of 155 mM.

Reduced *AtAMY3* was obtained by 4 hours incubation at RT with 40 mM dithiothreitol (DTT) and desalted on a NAP-5 column (GE Healthcare) pre-equilibrated in 100 mM Tricine-NaOH pH 7.9. BioGSSG assay was performed incubating 2 μM reduced *AtAMY3* in presence of 2 mM BioGSSG at 25 °C. After 1 hour of incubation the sample was split in two, half sample was treated with 80 mM DTT for 30 minutes to assess reversibility of reaction, while the second part of the sample was transferred in a tube containing SDS-PAGE loading buffer without reducing agent (60 mM Tris-HCl pH 6.8, 2 % (w/v) SDS, 0.025 % (w/v), Bromophenol Blue, 10 % glycerol), 100 mM iodoacetamide (IAM) and 20 mM *N*-ethylmaleimide (NEM) to block free cysteine thiols. Control samples were incubated with 100 mM IAM and 20 mM NEM before incubation with 2 mM BioGSSG.

All samples were further divided in two and loaded by denaturing non-reducing 12.5% SDS-PAGE. One gel was stained with Coomassie brilliant blue R-250 and the other was transferred to nitrocellulose membrane and analyzed by western blot using 1:3800 diluted monoclonal anti-biotin antibodies (Sigma-Aldrich, B7633). Peroxidase-conjugated secondary antibodies were diluted 1:2000 and detected by enhanced chemiluminescence following manufacturer's instructions.

3.2.3 MALDI-ToF Mass Spectrometry

Pre-reduced *AtAMY3* (see below) was analysed by MALDI-ToF mass spectrometry at the Functional Genomics Center Zürich (<http://www.fgcz.ch/>). The protein was incubated in presence of 5 mM GSSG for 90 minutes at 25 °C. Before the analysis, samples were desalted in 100 mM Tricine-NaOH, pH 7.9 using NAP-5 columns (GE Healthcare). Protein samples were digested mixing 3 μl of sample with 20 μl of Tris-HCl pH 8.2 containing 0.1 μg of trypsin. Digestion was performed in the microwave for 30 minutes. Peptide digests were desalted using a C_{18} ZipTip (Millipore, Billerica, MA, USA) and spotted onto the MALDI target ((MTP 384 target polished steel TF, Bruker Daltonics, Bremen, Germany) with α -Cyano-4-hydroxycinnamic acid in 50:50:0.1 AVN/ H_2O /TFA (5 $\mu\text{g}/\mu\text{l}$) for subsequent MALDI-TOF measurements.

3.2.4 *At*AMY3 activity assay and oxidative treatments

*At*AMY3 activity was assayed using artificial substrate *p*-nitrophenyl maltoheptaoside (BPNPG7) following manufacturer's instructions (Megazyme, Ireland). A 4 μM concentration of *At*AMY3 was used in each assay.

All oxidative treatments were performed on fresh and fully reduced *At*AMY3 obtained by incubation with 40 mM DTT at 37°C for 90 minutes. Samples were then desalted on a NAP-5 column (GE Healthcare) pre-equilibrated with 100 mM Tricine-NaOH pH 7.9 and the absorbance was quantified as in 3.2.1. The protein was then brought to 20 μM concentration through Amicon-Ultra device (Millipore; cut-off 10 kDa). GSSG, H₂O₂ and H₂O₂ plus GSH treatments were performed by incubating reduced AMY3 at 25 °C in the absence (control) or in the presence (treated samples) of 50 μM, 0.25 mM, 1 mM or 5 mM GSSG for 30 min; 0.1 mM, 0.5 mM or 1 mM H₂O₂ for 60 minutes; 1 mM H₂O₂ and 5 mM GSH for 60 minutes. The reversibility of the oxidative treatments was tested by incubating the samples (both control and treated) with 80 mM DTT for an additional 30 minutes at 25 °C. After treatments, enzymes were diluted 5 times and the activity assayed. Data are plotted as percentage of control sample activity incubated under the same condition.

3.2.5 Determination of cysteines pK_a

pK_a determination was performed as described in Bedhomme et al., (2012). In brief, 8 μM *At*AMY3 was incubated at different pH values from 4 to 12 in different buffers (100 mM Na-Citrate pH 4, 100 mM Na-Acetate pH 5.0-5.5, 100 mM MES pH 6.0-6.5, 100 mM Tris pH 7.0-8.5, 100 mM Glycine pH 9.0-10). For each pH point the protein was incubated with 10-fold excess of alkylating reagent (IAM) in respect to the total thiol content. After 20 minutes incubation samples were 5-fold diluted and the activity assayed. The activity was expressed as percentage of inhibition between IAM-treated and untreated samples and plotted as function of pH values. The pK_a value was obtained by fitting experimental data to a derivation of Henderson-Hasselbalch equation (Gallogly et al., 2008):

$$\text{remaining activity} = 100 - 100 \times \left(\frac{10^{pH - pK_a}}{1 + 10^{(pH - pK_a)}} \right)$$

3.2.6 Reactivation of glutathionylated *At*AMY3 by GSH, GRX and TRX

Freshly reduced *At*AMY3 (see 3.2.4) was incubated in with 5 mM GSSG for 90 minutes at 25°C. GSSG-incubated samples were desalted in 100 mM Tricine-NaOH pH 7.9 through NAP-5 column

(GE Healthcare). *AtAMY3* was brought to 20 μM by concentrating (Amicon-Ultra device, Millipore, cut-off 10 kDa).

Reactivation experiments of glutathionylated *AtAMY3* were performed by incubating 30 minutes at 25 °C in presence of 50 μM , 0.2 mM, 1 mM, 2 mM, 5 mM and 7 mM GSH. Samples were then diluted 5 times and the activity assayed. Reactivation was also performed in presence of *Arabidopsis thaliana* GRX S12 and C5, and *E. coli* TRX (Sigma-Aldrich, T0910). GRX-dependent reactivation was assayed incubating 20 μM glutathionylated *AtAMY3* in presence of 2 mM GSH with or without 5 μM GRXs for 5, 15 and 30 minutes. For TRX-mediated reactivation 20 μM glutathionylated *AtAMY3* was incubated in presence of 0.2 mM DTT with or without 10 μM *E. coli* TRX for 5, 15 and 30 minutes. GRX S12 and C5 were kindly provided by N. Rouhier (University of Lorraine, France).

To assay if GRX and TRX act on different sites and their concerted action can lead to additional activation, samples were incubated 2 mM GSH plus 5 μM GRX S12 for 30 minutes. Once the activation plateaued, an additional incubation with 0.2 mM DTT with or without *E. coli* TRX was performed for 5 minutes. Upon incubation, enzyme samples were 5-fold diluted and the activity assayed. The activities are expressed as percentage of reduced sample obtained by incubating glutathionylated *AtAMY3* in presence of 80 mM DTT for 30 minutes at RT.

3.3 Results

3.3.1 AtAMY3 is target of glutathionylation *in vitro*

In order to investigate post-translational redox modification of AtAMY3 two approaches have been used: BioGSSG assay and mass spectrometry. Both techniques allow to visualize glutathionylation on proteins of interest. The binding of glutathione *in vivo* pass from an intermediate oxidized state of protein thiol (Noctor et al., 2012; Zhang et al., 2018b). Typically after H₂O₂ reacts with cysteines, reduced glutathione (GSH) forms a disulfide bond with the oxidized cysteine. *In vitro* protein glutathionylation is usually performed using the oxidized form of glutathione (GSSG).

To assess glutathionylation *in vitro* biotin-labeled GSSG (BioGSSG) was incubated with pre-reduced AtAMY3 and after immunoblotting the binding of BioGSSG was displayed using anti-biotin antibodies. As expected, no signal was observed in the negative control, prepared treating the sample with thiol-alkylating agents before BioGSSG treatment. On the contrary, protein treated with BioGSSG showed a clear signal removable by incubation with reduced DTT (Figure 3.1).

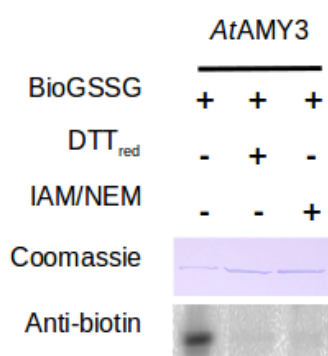


Figure 3.1 Glutathionylation of AtAMY3 *in vitro*. Pre-reduced AtAMY3 treated with biotinylated-GSSG (BioGSSG) and detected with anti-biotin antibodies. Reversibility of reaction was assessed by 30 minutes incubation with reduced DTT (DTT_{red}). As negative control, samples were alkylated before incubation with BioGSSG.

To identify the glutathionylation sites MALDI-ToF mass spectrometry experiments were performed on AtAMY3 after GSSG treatment. Three tryptic peptides showed a shift of 305.1-306.1 Da in the GSSG-treated sample (Table 3.1), these masses are compatible with the binding of a glutathione molecule (306.32 Da). The peptides contain the cysteine residues 310, 499 and 587.

Cysteine Residue	Peptide	Mass (Da)	Mass after treatment (Da)	Shift (Da)
310	NIVSIETDLPGDVTVHWGVCK	2282.1	2587.2	305.1
499	ISSGTGSGFEILCQGFNWESNK	2361.1	2666.2	305.1
587	VLGDAVLNHRCAHFK	1679.9	1986.0	306.1

Table 3.1 MALDI-ToF analysis on tryptic digestion of GSSG-treated AtAMY3.

Cys310 is found in the AtAMY3 N-terminal region lacking in the other α -amylases, its role is unknown despite a slight decrease in AtAMY3 activity is observed when Cys310 is mutated (Seung et al., 2013). Cys499 is not conserved and, together with Cys587, is important for catalysis and responsible for regulatory disulfide bond formation (Seung et al., 2013). In addition, Cys587 is

conserved in several plant α -amylases and found glutathionylated when recombinant barley AMY1 is purified from yeast (Søgaard et al., 1993; Juge et al., 1996).

3.3.2 Determination of catalytic cysteine pK_a

The possibility to form a disulfide bond, especially if reversible, is not common to all protein thiols. Cysteines involved in reversible bonds are generally exposed on protein surface and conserved only in closely related organisms (Cremers and Jakob, 2013). This position allows thiols to be modified by cellular components. Cysteine residues need to be deprotonated to be reactive and perform the nucleophilic attack at the basis of the disulfide formation. The propensity of a thiol group to be deprotonated is highlighted by acidic pK_a . Most of the cysteines have pK_a value around 8.5, similar to free cysteine, and are not suitable for disulfide bond (Roos et al., 2013). Reactive cysteines have peculiar microenvironments stabilizing the deprotonated form, *e.g.* hydrogen bond donors, proximal alkaline residues and N-terminal position in α -helix dipole (Poole, 2015), leading to a decrease in pK_a . IAM is an alkylating agent which binds cysteine thiols, if cysteines residues are present in the active site or directly involved in catalysis the alkylation can inhibit the activity. Since IAM specifically reacts with thiolate anion ($-S^-$), assaying the inhibitory effect at different pH values allows to determine the pK_a of catalytic relevant cysteines.

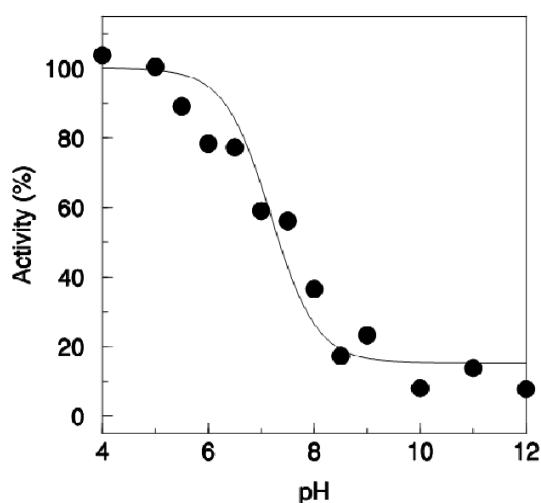


Figure 3.2 pK_a of *AtAMY3* cysteine involved in catalysis. Incubation of *AtAMY3* with or without alkylating agent (IAM) at different pH ranges. The percentages of activity were determined comparing the activity with and without IAM. Data are reported as mean \pm standard deviation ($n=3$).

In Figure 3.2 the pH dependency of IAM inactivation is shown. The fitting of experimental points resulted in a pK_a of 7.2 for *AtAMY3* thiol, this value is significantly lower than that of free cysteine pK_a (Paulsen and Carroll, 2013) indicating that a specific microenvironment is affecting the state of a cysteine important for catalysis. pK_a compatible with cysteine reactivity was in part expected since both Cys499 and 589 are important for both *AtAMY3* activity and regulatory disulfide (Seung et al., 2013).

3.3.3 Glutathione protects AtAMY3 from irreversible oxidation and inhibition

Glutathionylation, even if can lead to inhibition, has the advantage of being reversible and avoids irreversible oxidation of thiols, acting like a protective cap which can be removed when the physiological reducing environment is restored (Zaffagnini et al., 2012).

AtAMY3 is not required for normal starch turnover in mesophyll cells but it is involved in osmotic stress response and stomatal opening (Yu et al., 2005; Horrer et al., 2016; Thalmann et al., 2016). Especially under osmotic stress ROS production can exceed the scavenging ability of plants (Chaves et al., 2009). For this reason *AtAMY3* was incubated at different concentrations of H_2O_2 and the activity was assayed (Figure 3.3). Interestingly *AtAMY3* showed low susceptibility to H_2O_2 if compared to other enzymes (Liu et al., 2008; Bedhomme et al., 2009; Zaffagnini et al., 2016), being completely inactivated at high concentration of H_2O_2 (1 mM) and long incubation times (60 minutes).

Since glutathionylation is considered a protective modification against cysteine overoxidation, the protective role of GSH was tested on *AtAMY3* incubated with 1 mM H_2O_2 (Figure 3.3). After the incubation, *AtAMY3* showed inhibition of activity but also a complete recovery upon incubation with reduced DTT. Reversibility of inhibition strongly suggests that *AtAMY3* is glutathionylated after the incubation with GSH and H_2O_2 , supporting the hypothesis of a protective role of glutathionylation on *AtAMY3* in oxidizing environment.

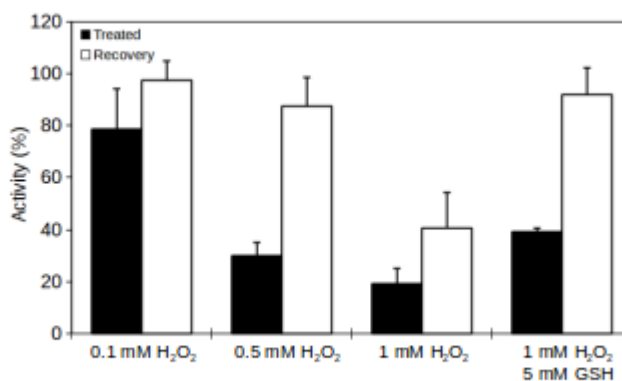


Figure 3.3 AtAMY3 sensitivity to hydrogen peroxide. Incubation at different concentrations of H_2O_2 for 1 hour. Strong and irreversible inhibition is observed in presence of 1 mM H_2O_2 . Presence of reduced glutathione (GSH) restore the reversibility of the inhibition, presumably inducing glutathionylation. Data are reported as mean \pm standard deviation (n=3).

GSSG was then used as glutathionylating agent and its effect on activity was tested. Incubating pre-reduced *AtAMY3* with GSSG led to inhibition of activity in 30 minutes (Figure 3.4). The inhibition is proportional to GSSG concentration and the addition of DTT after GSSG reaction completely restore the enzymatic activity. Considering the proportional effect of GSSG it is possible to speculate that *AtAMY3* is regulated by changing in GSH:GSSG ratio, typically altered under stress conditions.

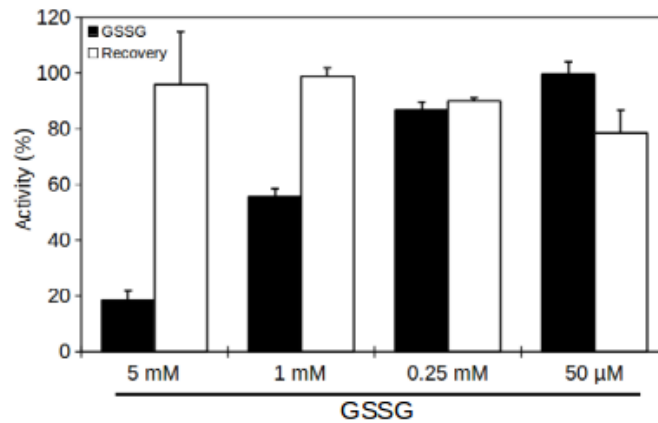


Figure 3.4 Inhibition of *AtAMY3* by GSSG treatment. Effects of increasing concentrations of oxidized glutathione on *AtAMY3* enzymatic activity. Recovery samples were treated with DTT 80 mM to verify the reversibility of the inhibition. Data are reported as mean \pm standard deviation (n=3).

To better understand the effect of glutathionylation on *AtAMY3* a structural model was obtained (Figure 3.5) by homology modeling thanks to I-TASSER online server (Zhang, 2008) using the barley AMY1 structure as template (PDB: 1AMY, Kadziola et al., 1994). The model contains only the carboxy-terminal catalytic domain (residues 441-832), which is conserved among all plant amylases. The amino-terminal region (residues 1-440) is specific for *AtAMY3* and contains a family 45 carbohydrate-binding module (CBM45) putatively involved in glucan recognition and binding (Seung et al., 2013). Surprisingly the two cysteines involved in the disulfide bond are distant (27.9 Å), underlining broad structural rearrangements upon oxidation. The inhibitory effect of glutathionylation can be ascribed to Cys589, which is near the highly conserved catalytic aspartate Asp666 (Figure 3.5).

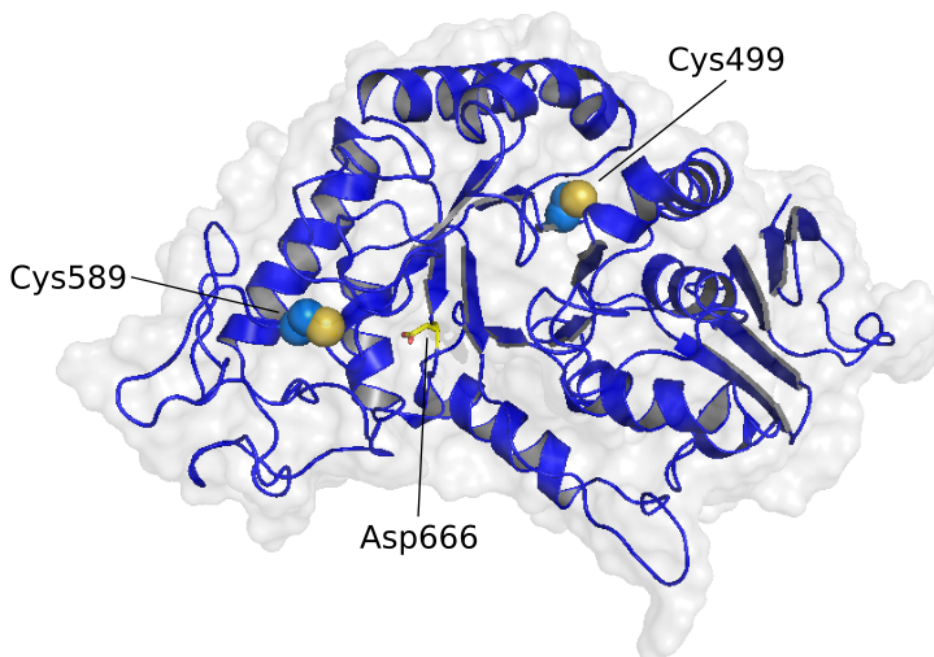


Figure 3.5 Structural model of *AtAMY3* catalytic domain. Cysteine residues, Cys499 and Cys589, identified by MALDI-ToF spectrometry as targets of glutathionylation are shown as spheres. The conserved catalytic aspartate residue (Asp666) is shown as sticks. The model by homology modelling with *Hordeum vulgare* AMY1 (PDB: 1AMY, homology 46%) was obtained using I-TASSER online server (Zhang, 2008).

Indeed, it is possible to hypothesize that glutathionylation of Cys589 results in steric hindrance, reducing the substrate accessibility to Asp666. It is difficult to predict the role Cys499 and Cys310 glutathionylation, but since Cys310 is inside the CBM45 it could prevent the binding of the glucan chain. Anyway no structural informations are available on Cys310.

3.3.4 GSH reactivates glutathionylated *At*AMY3 and redoxins speed up the process

In plants GSH is the main glutathione form and just small amounts of GSSG are found inside the cell. Under normal conditions, GSH is the main glutathione form and is continuously regenerated from GSSG consuming reducing power. High GSH/GSSG ratio contributes to the antioxidant ability of the cell (Rouhier et al., 2015). However under stress conditions concentration of both forms can be altered and often a decrease in GSH/GSSG ratio is observed (Noctor et al., 2012; Hasanuzzaman et al., 2017). GSH constitutes one of the reducing agents of the cell, in this regard the effect of GSH on glutathionylated *At*AMY3 was tested. Increasing concentration of GSH allow an almost complete reactivation of *At*AMY3 (Figure 3.6), suggesting that *At*AMY3 can be effectively regulated by modification of GSH/GSSG ratio.

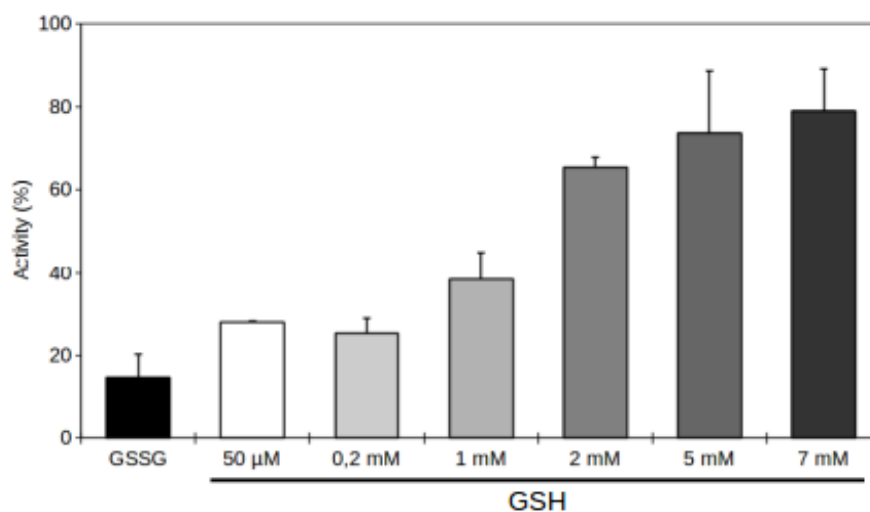


Figure 3.6 Release of glutathionylation inhibition by GSH treatment. Glutathionylated *At*AMY3 was incubated with increasing concentrations of reduced glutathione (GSH) to assess the recovery of catalytic activity. Activity are expressed as percentage of samples recovered after 30 minutes incubation with 80 mM DTT. Data are reported as mean \pm standard deviation (n=3).

In the redoxin family, two class of proteins have the ability to catalyze the reduction of disulfide bonds, thioredoxins (TRXs) and glutaredoxins (GRXs). TRXs act efficiently on protein disulfides but can reduce also mixed disulfides (Jung and Thomas, 1996; Lemaire et al., 2007; Ghezzi and Di Simplicio, 2007), whereas GRXs have been identified as specific for protein-glutathione disulfides (Meyer et al., 2008). The ability of GRXs and TRXs to revert inhibition of *At*AMY3 after GSSG treatment have been verified assaying catalytic activity upon incubation with Arabidopsis GRX S12

and GRX C5 plus GSH or *E. coli* TRX plus DTT (Figure 3.7). Both in presence of TRX or GRXs, a 5 minutes incubation is enough to obtain 2-2.5-fold higher activation than control samples, near to the reactivation obtained with GSH after 30 minutes (Figure 3.6). In addition, no preference for GRX type was observed in the recovery. Even if GSH/GSSG ratio can regulate *AtAMY3* activity, GRXs and TRX allow faster response, underlining the importance of catalyzed recovery.

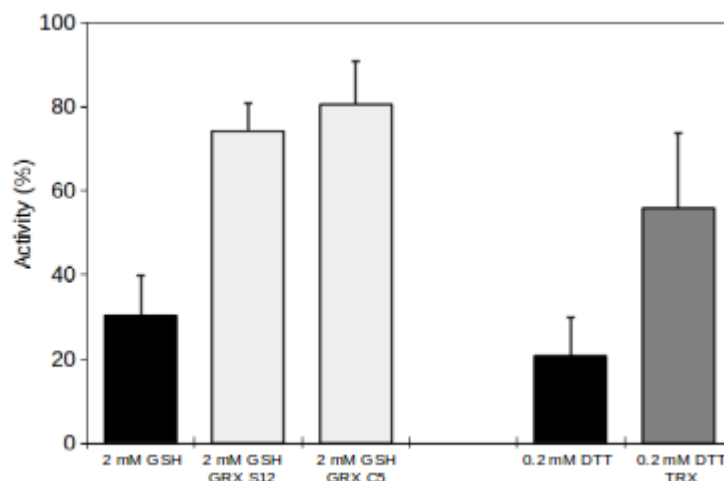


Figure 3.7 Glutathionylation inhibition is recovered incubating with GRXs and TRX. Glutathionylated *AtAMY3* was incubated with GSH and GRXs or DTT and TRX for 5 minutes, a faster rescue of the activity is observed. Activity are expressed as percentage of samples recovered after 30 minutes incubation with 80 mM DTT. Data are reported as mean \pm standard deviation (n=3).

3.3.5 Both GRX and TRX are required for complete recovery of *AtAMY3* activity

Notably, neither GRXs nor TRX were able to fully recover the activity of *AtAMY3* (Figure 3.7), resulting in 80% and 60% reactivation respectively. Since mixed disulfide could spontaneously evolve into a disulfide bridge, as observed for the small scaffold protein CP12 and for the CxxC GRXs (Marri et al., 2013; Gallogly et al., 2009), glutathionylated *AtAMY3* was first incubated with GRX S12 and GSH and, when activation plateaued (~ 30 minutes), TRX and DTT were added (Figure 3.7).

The activity of *AtAMY3* was completely restored only after incubation with both redoxins, supporting the hypothesis of the coexistence of both post-translational modifications (*i.e.* glutathionylation and disulfide bond).

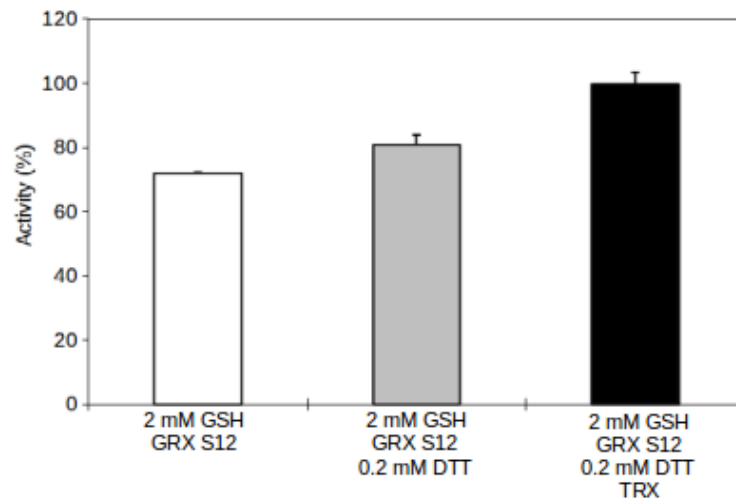


Figure 3.7 Glutathionylation inhibition is released after combined action of GRX and TRX. Glutathionylated AtAMY3 was incubated for 30 minutes with 2 mM GSH and GRX S12, then 0.2 mM DTT and *E. coli* TRX were added and a complete recovery is observed. Activity are expressed as percentage of samples recovered after 30 minutes incubation with 80 mM DTT. Data are reported as mean \pm standard deviation (n=2).

3.4 Discussion and concluding remarks

Despite the low sensitivity to H_2O_2 , the reactivity of *AtAMY3* to post-translational redox modifications is higher and different mechanisms are possible to modulate its activity *in vitro*. As highlighted by incubations with increasing concentrations of GSH and GSSG (Figure 3.3, Figure 3.5), *AtAMY3* glutathionylation is responsive to concentrations of both forms of glutathione. Since environmental stimuli altering photosynthesis, respiration and photorespiration as well as other ROS-generating systems modify the GSH:GSSG ratio and also total glutathione pool (Foyer and Noctor, 2003; Noctor et al., 2012), it is reasonable to hypothesize that *AtAMY3* could directly react to these alterations being inhibited or activated. Then *AtAMY3* activity can be restored faster by GRXs if required, and TRXs can recover its activity both after disulfide bond formation and partially after glutathionylation (Figure 3.7). In this regard, it is noteworthy that both redoxins are required for complete recovery of amylase activity (Figure 3.8), suggesting the formation of intra-protein disulfide bond. Since 3 glutathionylation sites are found (Table 3.1) and considering the propensity of Cys499 and 587 to form a disulfide bond and their importance for catalysis, it can be assumed that these residues are also involved in glutathione-induced disulfide bond. In this case two models could be hypothesized: the whole protein sample was both glutathionylated (on Cys310) and contained a disulfide bond (between Cys499 and Cys587) or alternatively two distinct populations were present, a great amount of protein was glutathionylated on the three sites while a smaller part had the disulfide and a single glutathionylation (Figure 3.8). These two parts can be assumed as 80% and 20%, considering the recover of the activity after GRXs and GRX + TRX incubations.

AtAMY3 is mainly involved in starch degradation during the day in guard cells (Horrer et al., 2016) and in response to osmotic stress (Thalmann et al., 2016). Considering that ROS are generated both under osmotic stress conditions and in stomata physiology (Chaves et al., 2009; Singh et al., 2017) it is not surprising that *AtAMY3* is tolerant to H_2O_2 and sensitive only at high levels (Figure 3.4). Moreover, guard cells are directly exposed to atmosphere and possibly higher oxidizing conditions affecting the GSH:GSSG ratio. In this hypothesis, *AtAMY3* could be regulated or preserved by glutathione.

Taken together, *in vivo* and *in vitro* evidences highlighted a complex regulatory network around *AtAMY3* which converges on two redox modifications, disulfide bridge and glutathionylation. These two modifications control and protect the activity of *AtAMY3* under physiological and stress conditions. TRXs, GRXs and the glutathione pool regulate *AtAMY3* possibly tuning the activity depending on cellular requirements.

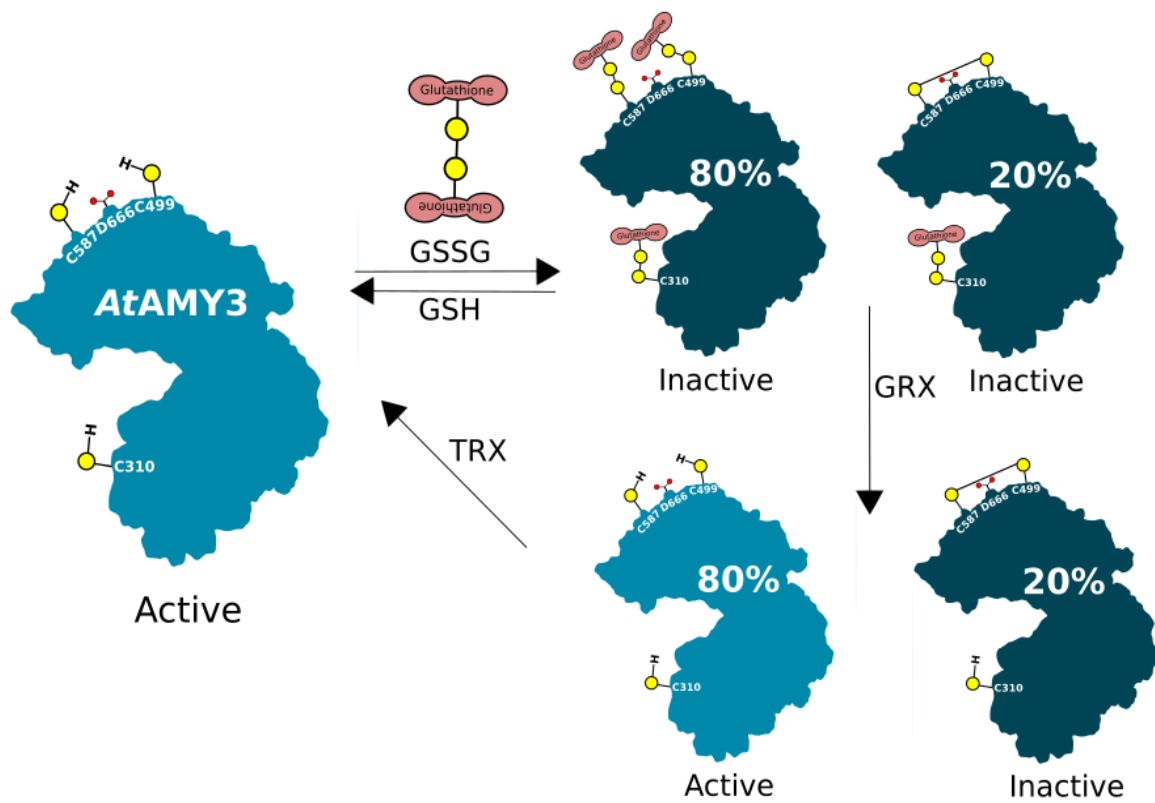


Figure 3.8 Model for GSSG inhibition and recovery of AtAMY3. Incubation with GSSG leads to modification of 3 cysteines (C310, C499, C587). Approximately 80% of AtAMY3 is glutathionylated on C310, C499 and C587 while the 20% is glutathionylated on C310 and GSSG causes the formation of a disulfide bond between C499 and C587. In both cases, modification of C499 and C587 could impair the accessibility of substrates to the catalytic aspartate (D666).

4. Enzymatic components involved in sugar and proline accumulation under osmotic stress in *Arabidopsis thaliana*

4.1 Brief Introduction

Along their life cycle plants have to face a variety of biotic and abiotic stresses. Among all, drought stress is increasing the mortality of crops and forests (Chaves et al., 2003; Bennet et al., 2015; Ding et al., 2018). Crop productivity is largely affected by water deficiency and is becoming an increasingly compelling issue (Farooq et al., 2009). Drought provokes osmotic imbalance caused by decreased water uptake from the soil. Lower water content increase the concentration of soluble compounds in the ground counteracting the osmotic potential generated by plants. Drought tolerance is acquired synthesizing huge amounts of compatible osmolytes to restore the osmotic balance (Singh et al., 2015). Osmolytes accumulation requires carbon backbones, to satisfy this demand different strategies have been reported, notably: arrest of shoot growth (Hummel et al., 2010) and transitory starch mobilization (Villadsen et al., 2005; Zanella et al., 2016; Thalmann and Santelia, 2017). The metabolism of transitory starch responds to a variety of abiotic stresses (Kaplan and Guy, 2005; Zanella et al., 2016; Thalmann et al., 2016; Thalmann and Santelia, 2017; Loreti et al., 2018), although enzymes involved in stress-induced starch degradation are not completely known. In *Arabidopsis thaliana* the β -amylase 1 (*AtBAM1*) takes part of starch mobilization in response to water deficiency (Zanella et al., 2016). In fact *AtBAM1* is not necessary for nocturnal starch degradation and its expression is induced by osmotic stress and ABA (Valerio et al., 2011; Thalmann et al., 2016). Interestingly, a positive correlation has been reported between the diurnal degradation of transitory starch by *AtBAM1* and proline accumulation in *Arabidopsis* plants subjected to osmotic stress (Zanella et al., 2016). Lack of *AtBAM1* in the *bam1* mutant leads to higher starch accumulation at the end of the day and reduced proline production (Zanella et al., 2016). Proline is a well-known and multi-functional osmolyte whose accumulation is widespread from bacteria to plants (Szabados and Savourè, 2010).

The partitioning of primary carbon into carbohydrates and nitrogen compounds for osmolyte production are poorly studied as yet. In order to fill this gap, a screening was performed on *Arabidopsis thaliana* T-DNA lines lacking enzymes from carbon metabolism which can potentially carry backbones from transitory starch to proline biosynthesis. The induction of expression under drought or osmotic stress was used as selective criteria and verified on eFP browser

(<http://bar.utoronto.ca/efp/cgi-bin/efpWeb.cgi>, Winter et al., 2007). Together with gene expression, oxidative stress levels were evaluated and T-DNA lines with significantly higher oxidation have been selected¹. Knock-out lines lacking the Sucrose-phosphate synthase A2 (*spsa2*), Sucrose Synthase 1 (*sus1*) and Glucan, water dikinase 2 (*gwd2*) showed high levels of oxidative stress and have been further characterized.

Sucrose-phosphate synthases (SPS) are master regulators of sucrose synthesis in source tissues (Winter and Huber, 2000). In *Arabidopsis thaliana* SPS family counts 4 members (Lutfiyya et al., 2007), among these SPSA2 is not necessary for normal growth even though appears to be essential for nectary secretions (Lin et al., 2014, Volkert et al., 2014; Bahaji et al., 2015). SPSA2 is expressed in roots of young seedlings but no expression was observed in leaves (Sun et al., 2011; Volkert et al., 2014), furthermore it is the unique SPS gene responding to cold and osmotic stress in *Arabidopsis* (Oono et al., 2006; Lehmann et al., 2008; Solís-Guzmán et al., 2017). On the contrary, sucrose synthases (SUS) are generally responsible for sucrose degradation in sink tissues and sink strength depends on their activity (Koch, 2004). *Arabidopsis* SUS family is formed by 6 genes (Baud et al., 2004), *SUS1* is moderately expressed in physiological conditions and *SUS1* transcript is found in buds, flowers, stems and roots especially in vascular tissues (Bieniawska et al., 2007). The same expression pattern is found in *SUS1* orthologous of *Nicotiana tabacum*, interestingly one of these orthologous showed increased expression under drought (Wang et al., 2015). Similarly to SPSA2, *SUS1* is not essential for growth and *sus1* do not show any abnormal phenotype (Bieniawska et al., 2007). However, *SUS1* was reported to be essential for tolerance of hypoxic stress (Bieniawska et al., 2007).

In dicotyledons the glucan dikinase family is constituted by 3 members (Mahlow et al., 2016). Two plastidial enzymes (GWD1 and PWD in *Arabidopsis*) catalyze the fundamental steps of glucan phosphorylation in the starch degrading pathway (Kötting et al., 2005; Baunsgaard et al., 2005; Edner et al., 2007). GWD2 is the third member of the family and it has a unique cytosolic localization (Glaring et al., 2007). Since starch is not present in cytoplasm, the role of GWD2 is still controversial and few studies focused on it. Glaring et al. (2007) reported GWD2 phosphorylates amylopectin on C-6 *in vitro* and found *GWD2* expressed in vascular tissues, mature flowers and siliques. Plants with *gwd2* background have reduced flower, silique and seed number and seeds contain lower lipid storage (Pirone et al., 2017).

In the present study a dissection of different carbon pools have been carried out on *spsa2*, *sus1* and *gwd2* together with amino acids and proline quantifications. The same experiments have been

¹ Primers for selection of homozygous T-DNA lines and lipid peroxidation assay for all the T-DNA lines not further analyzed are shown in the 4.5 Addendum.

performed on *p5cs1* plants, lacking the enzyme catalyzing the main reaction of proline biosynthesis under stress (Székely et al., 2008). The analysis of *p5cs1* should provide a better understanding of rearrangements of carbon metabolism in challenging water conditions. All the selected lines showed significant impairments in carbon and nitrogen pools, suggesting an involvement of SPSA2, SUS1 and GWD2 in improving tolerance to water deficiency.

4.2 Materials and Methods

4.2.1 Plant material and growth conditions

Plants carrying T-DNA insertions were grown in ground pots for selection of homozygous mutations. Seed were sown in pots, vernalized at 4 °C for 3 days and after germination 4-5 seedlings were distributed in each pot. For genomic DNA analysis leaves were harvested 2-3 weeks after germination.

For osmotic stress experiments, wild type and homozygous T-DNA plants of *Arabidopsis thaliana* (ecotype Columbia, Col-0) were hydroponically grown at 22 °C and in a 12 hours light/12 hours dark cycle. The photosynthetic photon flux density was 120 $\mu\text{mol m}^{-2} \text{s}^{-1}$. Seeds were sterilized on chlorine fumes for 5 hours and then stratified at 4 °C for 3 days in seedholders filled with 0.8% (w/v) agarose. Seedholders were inserted in dark polyethylene boxes filled with hydroponic medium (1.25 mM KNO₃, 1.5 mM Ca(NO₃)₂, 0.75 mM MgSO₄, 0.5 mM KH₂PO₄, 50 μM Fe(II)-EDTA, 50 μM H₃BO₃, 12 μM Na₂MoO₄, 1 μM ZnSO₄, 0.7 μM CuSO₄, 0.1 μM Na₂SiO₃). Seedholders were obtained cutting out cap and bottom from 0.5 ml test tubes. Osmotic stress treatment was performed transferring 35-days-old plants in hydroponic medium supplemented with 150 mM mannitol at the end of the dark period. Entire rosettes were then harvested at 12 hours of light at 0.5 days after treatment (DAT), 4.5 DAT and 6.5 DAT. Control samples were harvested together with 4.5 DAT samples.

4.2.2 Selection of homozygous lines

T-DNA lines *sus1* (At5g20830, SALK_014303C) and *sps2a* (At5g11110, SALK_064922C) were purchased from the European Arabidopsis Stock Centre (NASC, Nottingham, UK). T-DNA insertion site was confirmed by PCR on 400 ng of genomic DNA extracted from 2-4 leaves using a T-DNA primer together with gene specific primers (see below, Figure 4.1) designed by means of T-DNA Express (<http://signal-genet.salk.edu/cgi-bin/tdnaexpress>).

PCR reactions were performed using Taq LC (Fermentas; 1 U/ μl) on Biometra T-gradient thermocycler in the following conditions: 5 minutes at 94°C and 35 cycles of 30 seconds at 93°C, 30 seconds at 58 °C and 1 minute at 72°C.

gwd2 (At4g24450, SALK_080260C) T-DNA homozygous line was already available in the laboratory and selected in Pirone et al. (2017, *gwd2a*). *p5cs1* T-DNA homozygous line (At2g39800, SALK_063517) was kindly provided by Dr. M. Trovato ("Sapienza" - University of Rome).

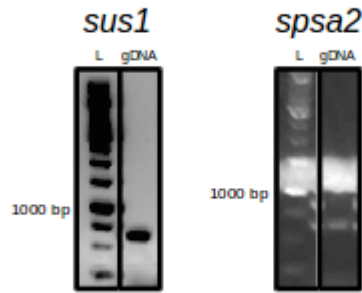


Figure 4.1 PCR products for selection of homozygous insertion on SUS1 and SPSA2 genes. In the left lane the DNA ladder (L) and in the right lane the genomic DNA sample amplified by PCR (gDNA). Single PCR product between 550 bp and 800 bp reveals homozygous T-DNA insertion in the respective gene.

Primers for selection of homozygous lines:

T-DNA 5'-ATTTTGCCGATTTTCGGAAC-3'

SUS1 forward (Fd) 5'-CTCAAGAGTGCAAGGATCAGG-3'

SUS1 reverse (Rv) 5'-ACGCTGAACGTATGATAACGC-3'

SPSA2 Fd 5'-TGCAAGACTTACAAGGTTTCGC-3'

SPSA2 Rv 5'-CCAGCTACTCTGAACCGTCTG-3'

4.2.3 Water content measures

In order to measure water content fresh weight (FW) values were taken by weighting single rosettes harvested at 12 hours of light just after the excision. Dry weight values were obtained by weighting the same plants after 24-48 hours drying at 80 °C. Water content was determined first as ratio of DW on FW, since this ratio is equivalent to the percentage of dry matter on the overall weight of the plant the water content (%) was then obtained using the following formula:

$$\text{Water Content} = \left(1 - \frac{DW}{FW}\right) \times 100$$

4.2.4 Lipid peroxidation measurements

Total lipid peroxidation was measured to evaluate the oxidative damage and quantified using the 2-thiobarbituric acid (TBA) assay (Guidi et al., 1999). About 100 mg of leaves were ground in liquid nitrogen, then vigorously mixed with 3 volumes (vol) of 0.1% (w/v) trichloroacetic acid (TCA). Samples were spun for 10 minutes at 13,000 rpm in a tabletop centrifuge and 200 µl of supernatant were added to 800 µl of 20% (w/v) TCA in a screw cap tube. After the addition of 5 µl of 0.5 % (w/v) TBA the mixture was incubated at 90 °C for 30 min in hot bath. The reaction was stopped in a

ice-water bath, then samples were centrifuged at 13,000 rpm for 10 minutes and the absorbance of the supernatants was read at 532 nm and 600 nm with a spectrophotometer (UV-Vis Cary60, Agilent Technologies). The absorbance of the empty cuvette was measured as blank sample. The concentration of malondialdehyde (MDA), the main product of lipid peroxidation, was calculated using an extinction coefficient ($\epsilon_{532\text{nm}}$) of $155 \text{ mM}^{-1}\text{cm}^{-1}$. The amount of MDA expressed on a FW basis was calculated using the following formula:

$$MDA \left(\frac{\text{nmol}}{\text{g FW}} \right) = \frac{\Delta 532 \text{ nm} - \Delta 600 \text{ nm}}{155 \text{ mM}^{-1}} \times \frac{\text{dilution} \times \text{resuspension volume}}{\text{FW mg}} \times 1000$$

4.2.5 Leaf starch quantification

Leaf starch content was quantified from samples of 3-5 rosettes as described in Smith and Zeeman (2006). In brief, 100-200 mg of leaf ground material were resuspended in 5 ml of 80% (v/v) ethanol and incubated in boiling water bath for 3 minutes, then spun at 5,000 rpm for 5 minutes at room temperature (RT). The supernatant was discarded and the ethanol extraction repeated until the pellet was clear from chlorophylls, typically 3 times. Ethanol was removed from the final pellet by evaporation. Pellets were then well resuspended in 5 ml of bidistilled water and for each sample 0.5 ml of suspension were transferred in two 1.5 ml tube and gelatinized by heating at $100 \text{ }^{\circ}\text{C}$ for 10 minutes. After cooling, 0.5 ml of 200 mM Na-Acetate pH 5.5 were added to each tube. For each sample 6 units of amyloglucosidase (Roche) and 0.5 units of α -amylase (Roche) were added to a 1.5 ml tube and an equivalent amount of water to an other tube (control), both were incubated at $37 \text{ }^{\circ}\text{C}$ overnight (o.n.).

Tubes were spun at 13,000 rpm for 5 minutes in a tabletop centrifuge and 10 to 200 μl were mixed with glucose assay mix (100 mM HEPES pH 7.5, 0.5 mM ATP, 1 mM NAD^+ , 4 mM MgCl_2) in a 1 ml cuvette. Background absorbance was measured at 340 nm and 1 unit of hexokinase (from yeast overproducer, Roche) and 1 unit of glucose 6-phosphate dehydrogenase (from *Leuconostoc mesenteroides*, Roche) were added. Absorbance at 340 nm was monitored until plateau was reached. Then glucose content in the cuvette was calculated using the following formula:

$$\text{Glucose}(\text{cuvette}, \mu\text{mol}) = \frac{A_s - A_c}{6.22 \text{ mM}^{-1} \text{ cm}^{-1}}$$

with A_s , absorbance of the sample with enzymes; A_c , absorbance of the sample without enzymes, and $6.22 \text{ mM}^{-1}\text{cm}^{-1}$ is the extinction coefficient at 340 nm of NADH.

Starch amounts as glucose equivalents were obtained on a FW basis using the following formula:

$$\text{Starch} (\mu g/mg FW) = \frac{\text{Glucose [mM]}}{\text{volume of sample assayed [ml]}} \times 2 \times \frac{5}{FW [mg]} \times 162 \frac{\mu g}{\mu mol}$$

with 162 $\mu\text{g}/\mu\text{mol}$ as mass of anhydroglucose.

4.2.6 Proline and amino acids quantifications

Amino acids and proline were quantified performing ninhydrin assay. Samples of Arabidopsis powders were mixed with 3% (w/v) 5-sulfosalicylic acid aqueous solution in a 1:2 ratio (eg. 100 mg + 200 μl). Samples were vortexed every minute for 5 minutes and then spun at 13,000 rpm for 10 minutes in a tabletop centrifuge. Without disturbing the pellet, supernatants were transferred in a clean tube and spun one more time to ensure complete removal of pellet residues. Then supernatants were transferred in a second clean tube. For each sample from 5 μl up to 15 μl were used on a 96-well plate. Typically for each sample two technical replicates of 5 μl and 12.5 μl has been done. After the addition of 15 μl of Na-Acetate 3 M and 200 μl of ninhydrin reagent (0.15% w/v ninhydrin dissolved in glacial acetic acid), the absorbance was read at both 352 nm for proline and 540 nm for total amino acid pool. This first value is considered the first time point of the measure (T_0) and constitutes the background absorbance. Then the plate was incubated at 50 °C for 12 minutes and allowed to cool for 3 minutes. Measures were repeated just after cooling (T_{15}) and after 2.5 and 5 minutes ($T_{17.5}$ and T_{20}).

T_0 was subtracted from T_{15} , $T_{17.5}$ and T_{20} , the average of the three points was compared with standard curves to calculate proline and amino acids content of samples. The standard solution was 3,8 mg/ml of amino acids mix (5 mM glutamine, 2 mM glutamic acid, 2 mM aspartic acid, 1 mM for all the other proteinogenic amino acids included proline). Volumes from 2,5 up to 15 μl of standard solution were utilized to obtain the curve. The same standard curve points were measured at 352 nm and 540 nm to quantify proline and amino acids, respectively.

4.2.7 Soluble sugar quantification

Total soluble sugars were quantified by means of the anthrone assay. Sugars were extracted by resuspending 100 mg of Arabidopsis powders from 3-5 rosettes in 200 μl bidistilled water. Powders were then vortexed for 1 minute then spun at 13,000 rpm for 5 minutes at RT in a tabletop centrifuge. Supernatants were collected and stored on ice and pellets were resuspended in the same way other two times. Supernatants for each sample were collected together.

CTR and 0.5 DAT samples were first diluted 4 times in bidistilled water while 4.5 DAT and 6.5 DAT samples 17 times. Dilutions were incubated at 70 °C for 45 minutes in a thermoblock and subsequently spun at 13,000 rpm for 20 minutes. Supernatants from all samples were further diluted 10 times and used for the assay. For each sample 350 µl were carefully mixed with 700 µl of anthrone solution (1 mg/ml anthrone, 96% H₂SO₄) and incubated 5 minutes at 100 °C. Blank samples were prepared mixing 350 µl of samples with 700 µl of bidistilled water. After cooling at RT, the absorbance at 630 nm of samples was measured in 1 ml cuvette on a standard spectrophotometer (UV-Vis Cary60, Agilent Technologies).

To calculate total soluble sugars a standard curve from 0 to 50 µg/µl of sucrose was assayed with anthrone. Concentration as µg/µl of sugars in samples was obtained from the standard curve equation and µg of soluble sugars were derived multiplying by dilutions and volume of sample, then normalized on FW.

4.2.8 Reducing sugar quantification

For reducing sugar quantifications samples were extracted as in 3.2.7. CTR and 0.5 DAT samples were directly used or diluted 2 times while for 4.5 DAT samples were diluted 8 times. 400 µl of samples were mixed with 600 µl of DNSA solution (1 mg/ml 3,5-Dinitrosalicylic acid, 0.8 M NaOH, 1.3 M Na-Tartrate dihydrate) or water for blank samples and incubated at 90 °C for 7 minutes. After incubations, samples were spun 10 minutes at 13,000 rpm in a tabletop centrifuge and absorbance at 550 nm was measured in a cuvette spectrophotometer (UV-Vis Cary60, Agilent Technologies). Reducing sugars in samples were calculated using a standard curve from 0 to 40 µg/µl of glucose assayed with 3,5-Dinitrosalicylic acid mix. µg of reducing sugars were derived multiplying by dilutions and volume of sample and normalized on FW.

4.2.9 Glucose and fructose assay

Soluble compounds for glucose and fructose quantification were extracted as in 3.2.7, using 100 µl each time instead of 200 µl. Extracts were incubated at 70 °C for 45 minutes and spun at 13,000 rpm for 10 minutes. Then supernatant were transferred in a clean tube and kept in ice.

All reagents for the assay were from Sucrose/D-Fructose/D-Glucose Assay Kit (Megazyme) and the assay was carried on 96-well plate reader (EnSpire Multimode Plate Reader, Perkin-Elmer). To assay both hexoses 15 µl for CTR and 0.5 DAT extracts, or 3 µl for 4.5 DAT and 6.5 DAT extracts and 12 µl of water were used. Extracts were mixed with ATP/NADP⁺ solution, bidistilled water and 24x buffer up to 198 µl and absorbance at 340 nm was measured as background value ($A_{\text{background}}$). Then 2 µl of hexokinase/glucose 6-phosphate dehydrogenase mix were added and after 15 minutes

the absorbance at 340 nm was measured (A_{glu}). After 15 minutes 2 μl of phosphoglucose isomerase were added and after 15 minutes the absorbance was recorded, this second value was comprehensive of glucose and fructose content (A_{glufru}). The absorbance of NADH corresponding to the two sugars were calculated in the following way:

$$\text{Glucose} = A_{\text{glu}} - A_{\text{background}} ; \text{Fructose} = A_{\text{glufru}} - A_{\text{glu}} - A_{\text{background}}$$

Sugar concentrations were obtained dividing corresponding absorbances by NADH extinction coefficient ($6.22 \text{ mM}^{-1}\text{cm}^{-1}$). Each concentration was multiplied by sugar molecular weight and divided by FW, expressing sugars as $\mu\text{g}/\text{mg}$ FW.

4.2.10 Quantification of carbohydrates in the cell wall

Cell wall carbohydrates quantification was performed on samples of 50-100 mg of Arabidopsis rosette powder from 3-5 plants. Powders were transferred in 2 ml tube and washed with 1.5 ml 80% (v/v) ethanol incubating 10 minutes at 80 °C and then spun at 13,000 rpm for 5 minutes, this wash was repeated 3 times. A second wash was performed 2 times with 1.5 ml 80% (v/v) acetone at RT for 10 minutes then samples were spun at 13,000 rpm for 5 minutes. To remove leaf starch from the insoluble part of the extract, pellets were resuspended in 0.5 ml of bidistilled water and gelified at 100 °C for 10 minutes in a thermoblock. Samples were spun at 13,000 rpm for 5 minutes, supernatant were discarded and the pellets were resuspended in 250 μl of water and 250 μl of 200 mM Na-Acetate pH 5.5. Leaf starch was degraded adding of 0.5 units of α -amylase (Roche) and 6 units of amyloglucosidase (Roche) and incubating o.n. at 37 °C.

After o.n. incubation, samples were kept at 100 °C for 10 minutes in order to denature enzymes and spun at 13,000 rpm for 20 minutes in a tabletop centrifuge. Supernatants were discarded and pellets dried at 70 °C. Dry pellets were resuspended in 1 ml of acetic acid:nitric acid (65% v/v):water (ration 8:1:2) and incubated at 100 °C for 30 minutes. After cooling, samples were spun at 13,000 rpm for 15 minutes. Supernatants were carefully discarded without disturbing the pellet. Then pellets were washed 1 time with 1.5 ml of bidistilled water and 3 times with acetone, each time samples were spun at 13,000 rpm for 5 minutes and supernatant was discarded without disturbing the pellet. Subsequently samples were dried o.n. at RT.

To release sugars from cell wall pellets an acid hydrolysis was performed adding 150 μl 72% (v/v) H_2SO_4 to dried pellets, vortexing and incubating for 30 minutes at RT. After, samples were vortexed again and incubated for additional 15 minutes at RT. Hydrolysis was stopped by addition of 600 μl of bidistilled water. Samples were spun at 13,000 rpm for 10 minutes and supernatants transferred

to a clean tube. Cell wall sugars quantification was performed by means of the anthrone assay, 100 µl of sample were mixed with 400 µl of anthrone solution (prepared as in 5.2.7) and incubated at 100 °C for 5 minutes. Standard curve samples was prepared in the same way using from 0 to 50 µg of glucose as standard sugar. After cooling, measurements were carried on 96-well plate reader (EnSpire Multimode Plate Reader, Perkin-Elmer) pipetting 250 µl for each sample or standard curve point.

4.2.11 Quantitative Real Time PCR analysis

Total RNA from wild-type plants (Columbia, Col-0) was purified from ground plant material using RNeasy Plant Mini Kit. DNA contaminations were removed using DNase I RNase-free (recombinant, ThermoFisher). RNA integrity and purity were verified on 1% (w/v) TAE-agar gel. Samples for gels were resuspended in loading buffer (0.025% w/v bromophenol blue, 0.025 w/v xylene cyanol FF, 0.025% SDS, 5 mM EDTA pH 8, 95% formamide). Genomic contaminations were checked performing Polymerase Chain Reaction (Phusion Hot Start II DNA Polymerase from ThermoFisher, Deoxynucleotide Kit from Sigma-Aldrich) using primer pair for *GWD2* transcript (see below), designed on intron-exon junction to allow the distinction from genomic DNA and mature mRNA.

Then, 1 µg of RNA for each sample was retrotranscribed using Easy Script™ Plus cDNA Synthesis Kit (ABM). Quantitative PCR was performed on optical 96-well plate on CFX Connect™ Real-Time PCR Detection System (BioRad) using 10 µl reactions with 1.5 µl cDNA, 400 nM of specific primer and SYBR® Green JumpStart™ Taq ReadyMix™ (Sigma-Aldrich) to monitor double strand DNA synthesis. Reactions were performed in triplicates for each gene on three samples for each point of the experiment (CTR, 0.5 DAT, 4.5 DAT, 6.5 DAT).

The following cycling profile was used for quantitative Real Time PCR reactions: 2 minutes at 95°C; 40 cycles of denaturation (95°C) for 5 seconds and 30 seconds at 60°C.

The relative expression of *GWD2*, *SUS1*, *SPSA2* and *P5CS1* genes were calculated following the ΔC_t method and normalized on *ACT2* housekeeping gene. For each cDNA sample the average C_t (threshold cycle) of the reference gene (*ACT2*) was subtracted from the average C_t of the gene of interest (ΔC_t). The relative expression was obtained calculating $2^{\Delta C_t}$ and normalizing on the expression fold of control samples.

Primers for quantitative Real Time PCR analysis:

GWD2 Fd 5'-CGCTCCTGGGTGGCAATTAAGAAG-3'
Rv 5'-GTCACCAGAGACCGGATTGTTTGTG-3'

P5CS1 Fd 5'-CGGGGTCGAAGGATTACTTACAACG-3'
Rv 5'-ATGGGAATGTCCTGATGGGTGTA AAA-3'

SUS1 Fd 5'-GGCCTGGTGT TTTGGGAATACTTACG-3'
Rv 5'-AGACGCATTGAATGGCTCGAAATCA-3'

SPSA2 Fd 5'-AGTGAAAGATCCCGCTTTGA-3'
Rv 5'-ACCTAAGGGCCTGAGATCGT-3'

Primer sequences were obtained using AtRTPrimer searching for amplicons of 100-200 bp. *SPSA2* primer sequences for quantitative Real Time PCR are taken from Volkert et al. (2014).

The primer efficiencies were calculated performing quantitative Real Time PCR on 4 serial dilution starting from 200 ng of *Arabidopsis thaliana* (Col-0) genomic DNA, the threshold cycle were plotted and the slope of the linear fit was used to obtain the efficiency using the following formula:

$$10^{((-1/slope)-1) \times 100}$$

4.3 Results

4.3.1 Water content under osmotic stress

Plants typically take up water from the ground thanks to a negative pressure generated through the entire organism by transpiration from stomata. When the water content decreases in the ground, roots are not able to preserve a physiological uptake of water and the plant undergoes osmotic stress. In the present set of experiments 150 mM mannitol was used to increase osmolarity of the hydroponic medium and generate osmotic stress. At this concentration the stress is generally considered to be mild, because it takes some day to establish and influence the physiology of the plant.

As showed in Figure 4.2, under osmotic stress conditions all genotypes fail to maintain normal water content. It is important to notice that water content is the same in all the genotypes analyzed but *p5cs1*, which contains 5% more water at 4.5 and 6.5 DAT. Water content is a fundamental parameter, because data normalized on FW of plants with the same water content can be directly compared without further calculations. For this reason, all the data in the present study will not be modified after normalization on FW. In this regard, compounds measured in *p5cs1* should be considered 5% more concentrated when compared to the other genotypes.

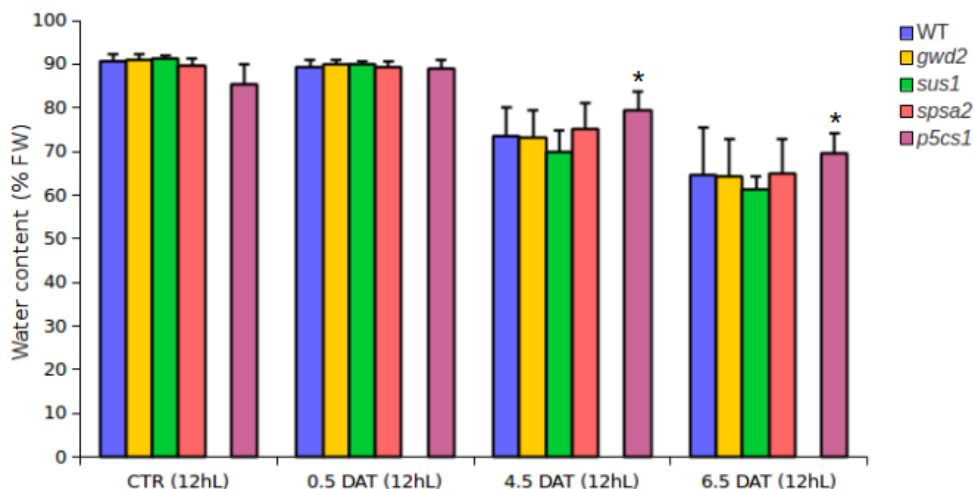


Figure 4.2 Water content along the treatment. Columns show mean \pm standard deviation ($n = 20$). Statistical analysis performed using Student's *t*-test, * $p \leq 0.05$. Plants harvested at 12 hours of light (12hL).

4.3.2 Generation of oxidative stress under osmotic stress

Reduced water content determines stomata closure to contain the loss of water despite the opening of stomata is essential for the entrance of carbon dioxide inside the leaf. After its entrance, CO_2 spreads in the mesophyll and is fixed by the Calvin-Benson cycle. As consequence of stomata

closure, CO₂ concentration inside leaves lowers and Calvin-Benson cycle slows down consuming less ATP and NADPH. Due to reduced regeneration of substrates, excited electrons in PET accidentally generates reactive species, especially ROS (Chaves et al., 2009). ROS are generated in low concentration under physiological conditions and contributes to photosynthesis signaling (Mittler, 2017), but under osmotic stress higher concentrations are produced causing oxidative stress (Aranjuelo et al., 2011; Wilhelm and Selmar, 2011). ROS reaction with saturated fatty acids results in peroxidation and malondialdehyde (MDA) production (Hernandez et al., 1993; Fadzilla et al., 1997).

MDA generation has been quantified to evaluate oxidative stress levels induced by osmotic treatment. Lipid peroxidation in T-DNA lines was not altered after 12 hours of stress (0.5 DAT) but raised after 4.5 DAT. At 6.5 DAT peroxidation levels in *gwd2* were 40% higher while *spsa2* increased to 60% more MDA if compared to wild-type (Figure 4.3). Curiously, in *sus1* lipid peroxidation had a 40% increase at 4.5 DAT and returned to wild-type values at 6.5 DAT, suggesting that the mutation is transiently affecting the adaptation to stress.

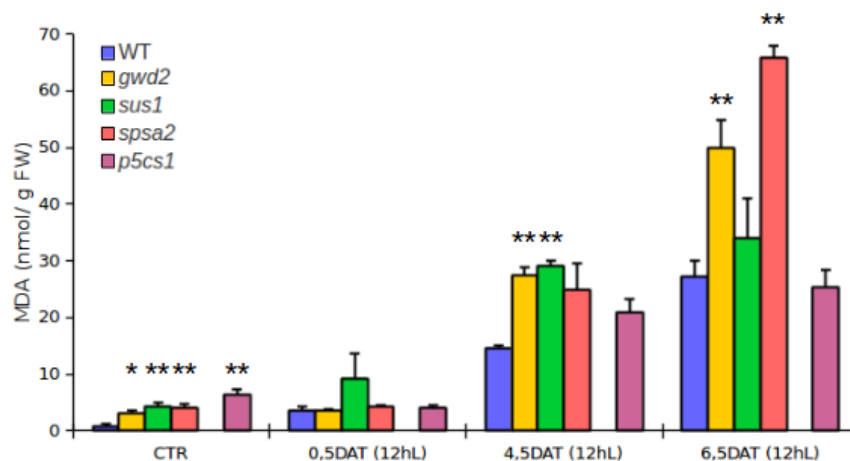


Figure 4.3 Oxidative stress levels under osmotic treatment. Oxidative levels are expressed as lipid peroxidation product malondialdehyde (nmol MDA/ g FW). Columns show mean ± standard error (n= 3-7). Statistical analysis performed with Student's *t*-test, * $p \leq 0.05$, ** $p \leq 0.01$. Plants harvested at 12 hours of light (12hL).

To note, *p5cs1* showed same amounts of MDA of wild-type plants. Several studies reported a fundamental role of P5CS1 as master regulator of stress-induced proline biosynthesis (Szabados and Savaouré, 2010). For example, knocking out *P5CS1* gene leads to higher oxidative stress after NaCl exposure (Székely et al., 2008). It is possible that *p5cs1* line adopted different mechanisms to tolerate stress, considering that P5CS1 is partially required for plant growth (Mattioli et al., 2008) and 5-weeks old plant could already have activated alternative mechanisms.

4.3.3 Proline accumulation under stress and amino acids levels

Proline is accumulated under several adverse conditions like after UV and heavy metals exposure or osmotic, salt and oxidative stress (Saradhi et al., 1995; Yoshiba et al., 1999; Schat et al., 1997; Choudhary et al., 2005; Székely et al., 2008; Shuang-Long et al., 2009). For this reason proline accumulation can be assumed as an indication of proper response to stress. Therefore, proline content was quantified in the attempt to connect the primary carbon metabolism to osmotic stress response. All genotypes but *p5cs1* accumulated proline in response to 150 mM mannitol (Figure 4.4). However, at 6.5 DAT *gwd2*, *sus1* and *spsa2* synthesized 44%, 52% and 57% of wild-type proline content respectively.

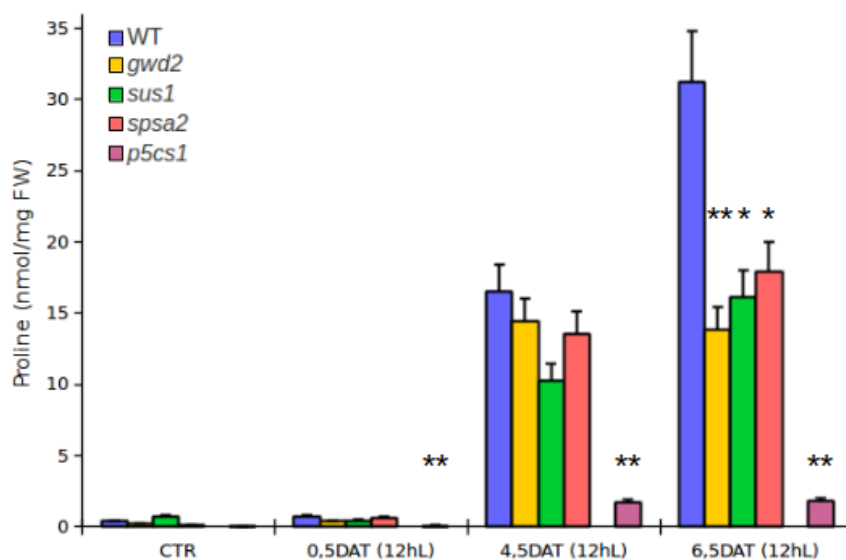


Figure 4.4 Proline accumulation under osmotic stress. Columns show mean \pm standard error (n= 3-4). Statistical analysis performed with Student's *t*-test, * $p \leq 0.05$, ** $p \leq 0.01$. Plants harvested at 12 hours of light (12hL).

Proline accumulation, together with proline addition to growth medium, has been correlated with a reduction in ROS levels and consequent oxidative damage in different organisms (Alia and Mohanty, 1997; Mehta and Gaur, 1999; Che and Dickman, 2005; Krishnan et al., 2008; Wang et al., 2009). Two hypothesis have been expressed to explain proline effect, proline can act as direct scavenger of ROS or can stabilize ROS-scavenging enzymes under stress conditions, but the first is still a matter of debate (Smirnioff and Cumber 1989; Rajendrakumar et al., 1994; Matysik et al., 2002; Sharma and Dubey, 2005; Signorelli et al., 2013). In our case, lower proline positively correlates with higher oxidative stress found in *gwd2*, *sus1* and *spsa2*. On the other hand the same correlation was not observed in *p5cs1*. It is attempting to speculate that adaptation to the absence of P5CS1 gene could occur leading to a better response to oxidative stress. In fact, P5CS1 is also

required during the development and, as already said in 3.3.2, given its absence compensatory mechanisms could come into play (Mattioli et al., 2008).

Lower proline levels could reflect a general impairment in amino acid biosynthesis or in nitrogen metabolism, to verify this possibility the amino acid pool was measured (Figure 4.5). Amino acids concentration has been reported to increase in osmotic stress (Gzik, 1996; Thu Hoai et al., 2003; Hummel et al., 2010), especially branched chain amino acids (Huang and Jander, 2017). Indeed *gwd2*, *spsa2* and *p5cs1* showed an increase in amino acid content equal to wild type, suggesting that amino acids metabolism is unaltered. Conversely *sus1* had a reduction of 2.1-2.3 $\mu\text{g}/\text{mg}$ FW starting from 4.5 DAT. Considering the lower proline content (~ 15 nmol/ mg FW = 1,7 $\mu\text{g}/\text{mg}$ FW), *sus1* had a approximately 4 $\mu\text{g}/\text{mg}$ FW less amino acids at 6.5 DAT, underlining a more complex impairment in amino acids biosynthesis under stress.

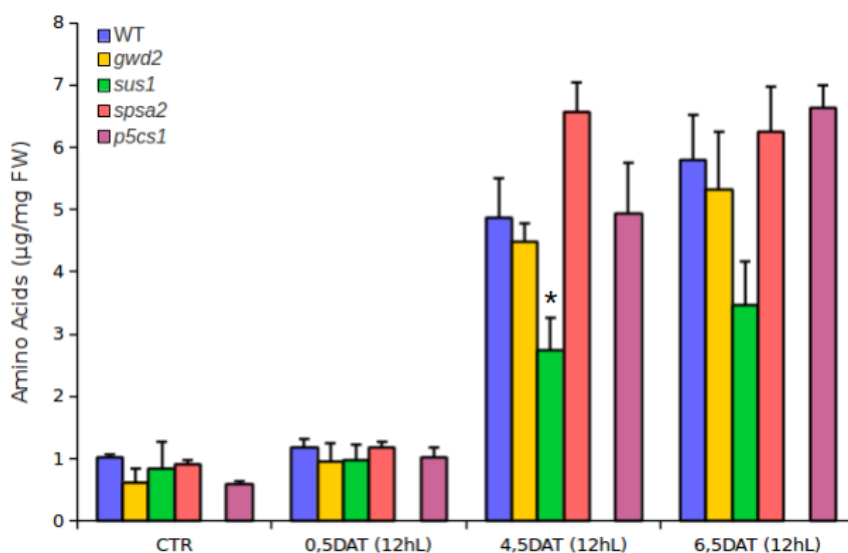


Figure 4.5 Amino acids accumulation under osmotic stress. Each column represent total amino acids amount except proline. Columns show mean \pm standard error (n= 3-4). Statistical analysis performed with Student's *t*-test, * $p \leq 0.05$. Plants harvested at 12 hours of light (12hL).

4.3.4 Transitory starch at the end of the day

In the following set of experiments carbon metabolism has been monitored quantifying a series of carbon compounds to highlight modification due to osmotic stress.

In the metabolic struggle to overcome stress, transitory starch mobilization is emerging as an important factor (see section 1.5 Carbon fluxes under abiotic stress). Thus starch accumulation has been assayed in *Arabidopsis* rosettes at the end of the day. All T-DNA lines had lower starch content in control conditions ($p < 0.05$), indeed wild-type plants had 10 mg/g FW while mutant lines have around 5-6 mg/g FW. During the treatment the ratio between starch and FW did not significantly change in wild-type, *gwd2* and *p5cs1* (Figure 4.6). Considering the decrease in water content along the treatment for all genotypes and the consequent decrease in FW, constant starch/FW ratios

pointed out that also leaf starch content is lowering along the treatment. Decrement of transitory starch has been observed in several photosynthetic organisms in response to stress (Nagao et al., 2005; Villadsen et al., 2005; Goyal, 2007; Zanella et al., 2016).

On the contrary the increased ratio in *spsa2* ($p < 0.05$) highlights the influence of the mutation on starch metabolism, e.g. impaired starch breakdown or increased starch accumulation, probably due to feedback mechanisms.

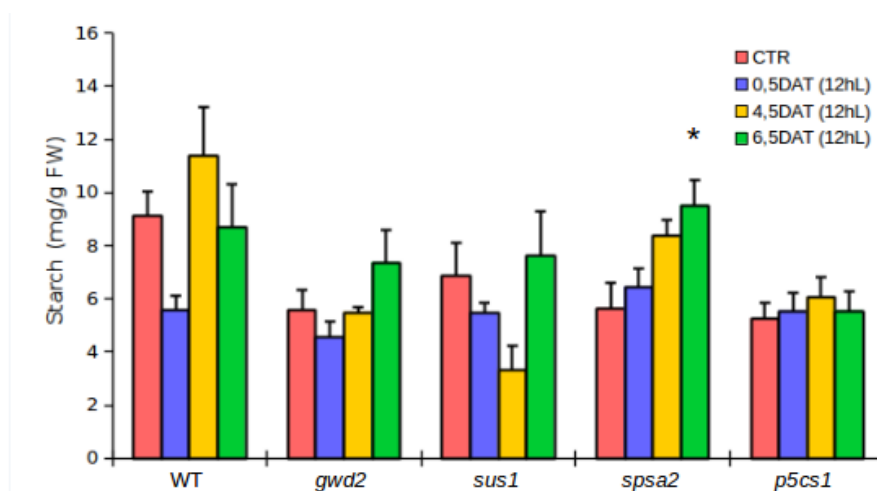


Figure 4.6 Starch levels at the end of the day. Columns show mean \pm standard error ($n = 3-10$). Statistical analysis performed with Student's *t*-test comparing treated and control samples of each genotype, * $p \leq 0.05$. Plants harvested at 12 hours of light (12hL).

4.3.5 Changing in soluble sugar levels

Sugars are central components of energetic and biosynthetic metabolism, but sugars can also be accumulated contributing to the re-establishment of osmotic balance, protect macromolecules and scavenge reactive species (Garg et al., 2002; Xu et al., 2007; Janska et al., 2009; Livingston et al., 2009; Yuanyuan et al., 2009; Krasensky and Jonak, 2012; Hagemann and Pade, 2015; Pomerrenig 2018).

For their central role soluble sugars were assayed, moreover sugar content is particularly interesting because SPSA2 and SUS1 catalyze reactions inside sugar metabolism (Bieniawska et al., 2007; Volkert et al., 2014). Assaying soluble sugars pointed out a significant reduction of soluble sugars in leaves, passing from 45 $\mu\text{g}/\text{mg}$ FW in wild-type to ~ 20 $\mu\text{g}/\text{mg}$ FW in T-DNA lines (Figure 4.7a). In this regard, lower starch content observed could be due to higher degradation stimulated by general decrease of sugars for *gwd2*, *sus1*, *spsa2* and *p5cs1*, however the fate of carbon backbones is not clear so far. Similar values are obtained for reducing sugars (Figure 4.7b), indicating that in the current growth condition the main part of soluble sugar pool is constituted by reducing sugars. Focusing on the two main hexoses of central metabolism, glucose resulted 40% and 70% lower than

wild-type in *gwd2* and in *p5cs1* respectively. Whereas glucose in *spsa2* was 30-36% less than wild-type (Figure 4.8a).

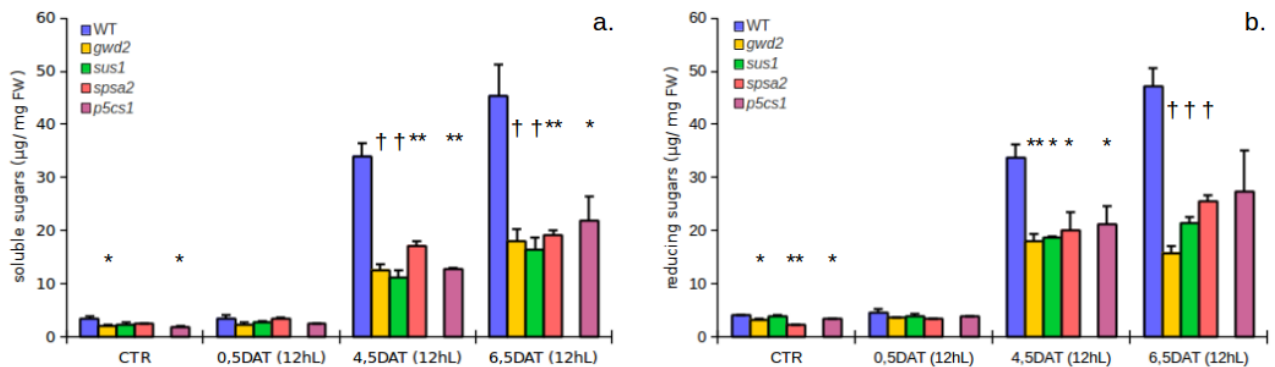


Figure 4.7 Soluble (a) and reducing (b) sugar accumulation under osmotic stress. Columns show mean \pm standard error (n= 3-7). Statistical analysis performed with Student's *t*-test, * $p \leq 0.05$; ** $p \leq 0.01$; † $p \leq 0.001$. Plants harvested at 12 hours of light (12hL).

Fructose content had stronger decrease, reaching 33% of wild-type content both in *gwd2* and *sus1* and 18% in *p5cs1* (Figure 4.8b). Interestingly *gwd2* and *p5cs1* glucose contents were constantly impaired in CTR and treated samples, while in *spsa2* the decrease occurs the last two days of treatment. Similarly, *gwd2*, *p5cs1* and even *sus1* showed decreased fructose amounts through all the experiment and *spsa2* only at 4.5 and 6.5 DAT. It is relevant to highlight that reducing sugars content in *p5cs1* is similar to wild-type if glucose and fructose are subtracted, indicating that the two hexoses were the unique sugars affected in *p5cs1* line.

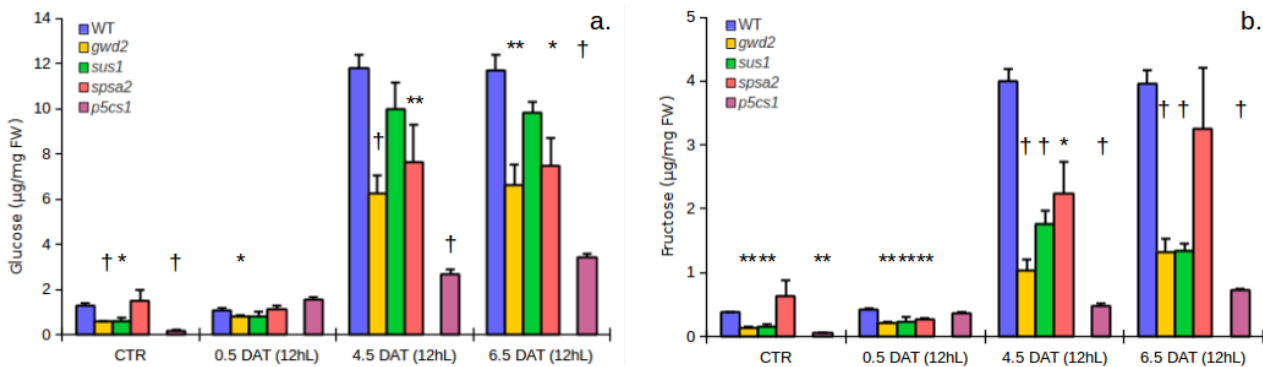


Figure 4.8 Glucose (a) and fructose (b) levels under osmotic stress. Columns show mean \pm standard error (n= 3-6). Statistical analysis performed with Student's *t*-test, * $p \leq 0.05$; ** $p \leq 0.01$; † $p \leq 0.001$. Plants harvested at 12 hours of light (12hL).

4.3.6 Carbohydrate content in the cell wall

The cell wall constitutes another pool of carbohydrates directly linked to central metabolism through sugar nucleotides, in particular UDP-glucose. Indeed, glucose units forms cellulose, the load-bearing polymer of the cell wall (Liepman et al., 2010). Cell wall rearrangements have been reported to take part to adaptation to diverse abiotic and biotic stresses (Moore et al., 2008; Houston et al., 2016), for this reason carbohydrates in cell wall were monitored during the treatment.

Cell wall carbohydrates have no alteration if compared to wild-type (Figure 4.9), thus it is possible to conclude that *GWD2*, *SUS1*, *SPSA2* and *P5CS1* have no influence on cell wall metabolism. Despite *SUS1* could potentially produce UDP-glucose and so be involved cellulose biosynthesis (Coleman et al., 2009).

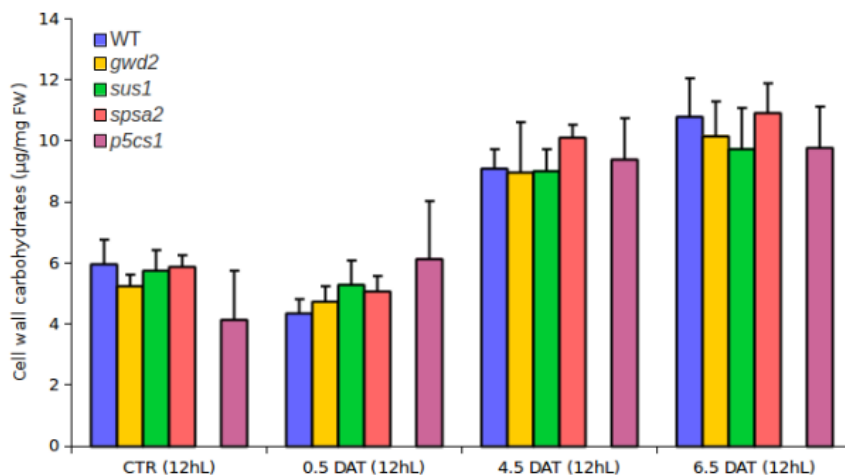


Figure 4.9 Carbohydrate content in the cell wall. Error bars show standard error (n= 3-5). Statistical analysis performed using Student's *t*-test comparing treated and control samples of each genotype. Plants harvested at 12 hours of light (12hL).

4.3.7 Gene expression profile of *GWD2*, *SUS1*, *SPSA2* and *P5CS1*

In the present study a parameter to identify enzymes of interest in the path from primary carbon to proline has been the induction of expression under osmotic stress. As starting point, the expression of genes of interest has been verified on eFP browser (<http://bar.utoronto.ca/efp/cgi-bin/efpWeb.cgi>) looking at reported expression during osmotic stress (300 mM mannitol) and drought (air stream). Once *gwd2*, *sus1*, *spsa2* emerged as interesting lines, the expression profile of corresponding genes was followed along the treatment to verify the expression pattern in current growth conditions.

Quantitative Real Time PCR experiments on wild-type samples reported 5-fold increase of expression for *SPSA2* (Figure 5.10), confirming the similar trend of expression recently reported in Solís-Guzmán et al. (2017) under osmotic stress. *P5CS1* induction varies from 12- to 20-fold, reflecting the well-known behavior under osmotic and salt stress (Yoshida et al., 1999; Székely et al 2008; Dai et al., 2018; Maghsoudi et al. 2018).

Differently *SUS1* and *GWD2* expression slowly turned off during the treatment, although *SUS1* expression is induced in *Arabidopsis thaliana* and *Hordeum vulgare* in response to several abiotic stresses like cold, hypoxia and osmotic stress (250 mannitol; Baud et al., 2004; Barrero-Sicilia et al., 2011).

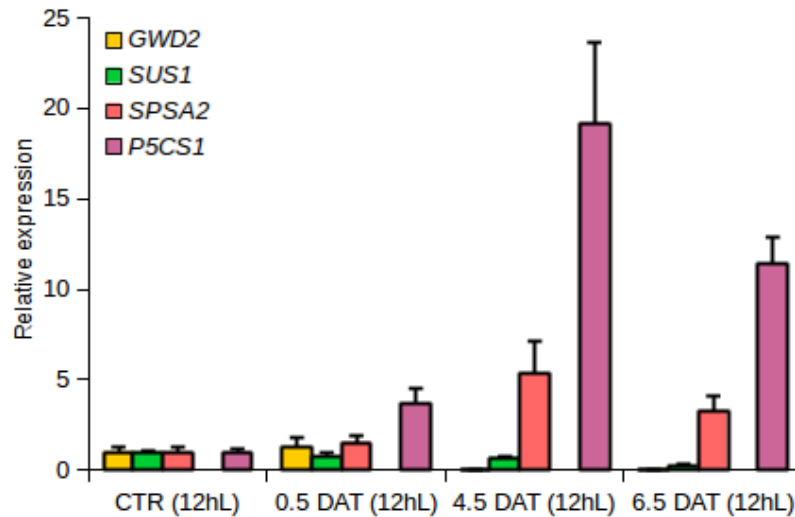


Figure 4.10 Relative gene expression during osmotic treatment. Expression levels of GWD2, SUS1, SPSA2 and P5CS1 in wild-type plants exposed to osmotic stress and harvested at the end of the day (12hL). Error bars show standard error.

It should be taken into account that gene expression was monitored at the end of the light period and gene expression could not be distributed uniformly during the day. In any case, considering only the current data these results are apparently in contrast with the data collected so far, but two interpretations can fit the actual data set. A first and simple interpretation could be a pleiotropic effect of the two mutations. Lack of SUS1 and GWD2 in the period before the treatment can influence metabolic pathways and then the expression of other genes causing a higher susceptibility to osmotic stress. The second hypothesis considers that both enzymes could be regulated at protein level by post-transcriptional modifications more than at gene or transcript level. Indeed it is well known that transcript levels do not necessarily correlates with protein abundance (Maier et al., 2009; Vogel and Marcotte, 2012) and further mechanisms regulate protein expression. All sucrose synthases are target of phosphorylation (see 1.9 Regulation of sucrose metabolism and phloem transport), regulating protein activity and stability. Phosphorylation of SUS-1 clade enzymes from *Zea mays* increase catalytic rate of sucrose-degrading reaction lowering the K_m (Nakai et al., 1998; Takeda et al., 2017). Cysteines in SUS are target of different regulations, indeed *Arabidopsis* SUS1 is found glutathionylated *in vivo* when plants are fed with biotinylated glutathione (Dixon et al., 2005). These data are in agreement with inhibition of sucrose-degrading activity of wheat germ SUS by GSSG and oxidized thioredoxin (Pontis et al., 1981). In addition, soybean SUS is thiolated by ENOD40, producing an inter-protein disulphide and stimulating sucrose-degrading activity (Röhrig et al., 2004).

For GWD2 is more difficult to speculate because it is poorly studied and no information are available on its *in vivo* function and regulation. However, several studies focused on the chloroplast homologous GWD1 for its importance in starch metabolism. GWD1 is a highly stable protein *in*

vivo with a 1.93 days half-life (Skeffington et al., 2014). Furthermore, GWD1 activity is regulated both by autophosphorylation (Reimann et al., 2004) and disulphide bond formation (Mikkelsen et al., 2005).

4.4 Discussion and concluding remarks

The current analysis aimed to discover enzymatic components involved in osmotic stress response in the metabolic machinery of *Arabidopsis thaliana*. Globally a correlation was observed between higher levels of oxidative stress and lower accumulation of proline and sugars in *gwd2*, *sus1* and *spsa2* genotypes. Lower accumulation of sugar and proline could prevent the re-establishment of osmotic potential leading to a weak adaptation to water deficiency. Reduced sugar concentrations mean also diminished carbon availability, slowing or impairing the ability to cope with stress. Furthermore diminished proline accumulation could overload photosynthetic electron transport through the reduction of NADP⁺ regeneration, decrease shoot-to-root transfer of reducing power for root elongation, prevent the protective effect of proline on macromolecules (Rajendrakumar et al., 1994; Sharma et al., 2005; Szabados et al., 2010; Sharma et al 2011; Signorelli et al., 2013). In this regard it is interesting that blocking the main step of proline accumulation at P5CS1 level have severe consequences on carbon metabolism. Indeed quantification of the primary carbon compounds in *p5cs1* highlighted a widespread impairment in starch and soluble sugars (Figure 4.5, 4.6 and 4.7).

Analyzing osmolytes amounts emerged that sugars are the main osmolyte in our set of experiments. Indeed, considering wild-type plants at 6.5 DAT soluble sugars were 260 nmols/ mg FW, while just 32 nmols/ mg FW of proline were accumulated. These results suggest sugars as the main determinant of osmotic potential under water deficiency whereas proline could affect stress tolerance in other ways.

A general phenotype observed among genotypes is the decreased accumulation of reducing sugars (~50%). GWD2, SUS1 and SPSA2 should be involved in sugar metabolism, thus a direct effect on carbohydrate pool could be hypothesized in *gwd2*, *sus1* and *spsa2* lines. Affecting glucose and fructose levels slows down carbon flux through glycolysis, providing less pyruvate to tricarboxylic acids cycle and so less precursors for glutamate production and consequent proline biosynthesis. Understanding phenotype of *gwd2* is complicated by the fact that GWD2 function is still unknown, but GWD2 is able to phosphorylate glucans *in vitro* (Glaring et al., 2007) similarly to its plastidial homologous GWD1, which is fundamental for glucose release from starch. If GWD2 was involved in sugar mobilization from carbohydrate chains, which is its substrate *in vivo* remains unknown. Among the different substrates phytyloglycogen and soluble heteroglycans can be hypothesized (Fettke et al., 2004; Malinova et al., 2011; Powell et al., 2014), as well as starch-like macromolecules found by Glaring et al. (2007) in companion cells. According to this function,

Pirone et al. (2017) suggested that GWD2 takes part of partitioning between soluble and insoluble carbohydrates, which under osmotic stress should tend toward the soluble pool.

SUS enzymes are involved in sucrose degradation in sink tissues, particularly SUS1 expression has been observed in vascular tissue of mature leaf in Arabidopsis and sink leaves and roots in rice and maize (Duncan et al., 2006; Bieniawska et al., 2007; Hirose et al., 2008). However SUS1 is not essential for sucrose degradation under control conditions (Bieniawska et al., 2007), but its activation upon osmotic stress can lead to higher sugar release in leaves and vascular tissues contributing to restoring the osmotic balance and fueling stress response. Biochemical analysis on SUS family in Arabidopsis reported the highest V_{max} and among the lowest K_m for SUS1 (Bieniawska et al., 2007), ensuring fast sucrose degradation. When SUS1 is lacking, like in *sus1* line, it could be hypothesized that sucrose cannot be consumed in the rosette and is completely exported to roots depleting sugars from shoot.

In the same way SPSA2 could be involved in sucrose production, which is then exported in vascular tissues where it can be degraded or transferred to sink tissues. Data from *spsa2* are controversial due to both slight but significant accumulation of leaf starch and decrease in glucose and fructose (Figure 4.5 and 4.7). Anyway the increase in transitory starch is too low to be responsible for sugar decrease. In *sps* T-DNA lines starch content can increase due to accumulation of degradation products caused by impaired sucrose biosynthesis (Volkert et al., 2014), but contrary hexoses are not accumulated in *spsa2*. Strand et al. (2000) observed a similar decrease in glucose, fructose and soluble carbohydrates content but also reduced starch levels when *SPSA1*, one of the two main isoforms in Arabidopsis leaves, is silenced. Based on further experimental evidences, Strand and colleagues proposed an alternative way to bypass SPS reaction and avoid metabolic block via PP_i degradation and stimulation of UDP-glucose production. UDP-glucose can be consumed as alternative substrate for sucrose production. Taken all together, these data and observations underline the complexity and plasticity of primary carbon metabolism.

For what concerns *p5cs1* knock-out, it is possible to speculate that the effect on sugar metabolism is indirect. Since proline accumulation is impaired, sugars provided for proline biosynthesis lead to the accumulation of precursors, which have not been assayed in the present set of experiments.

Taking into account the different compounds and pools assayed in the present study, it is important to notice that a general decrease in carbon content is found. Lower carbon can be simply caused by accumulation of other molecules that have not been quantified, for example organic acids from tricarboxylic acids cycle (Hummel et al., 2010) or lipids (Yang et al., 2018), but also alternative explanations are possible. Higher respiration rates under osmotic stress, when carbon fixation is reduced, can lead to diminished carbohydrates levels. On the other hand, sugar levels can be

directly decreased by lower carbon fixation rates. Alternatively, higher sugar export to the root, or increased root elongation, can deplete carbon from the shoot. All these factors are important and should be evaluated to guess the function of GWD2, SUS1, SPSA2 and P5CS1 and have a proper understanding of plant strategies to tolerate water deficiency.

4.5 Addendum

4.5.1 Selection of homozygous T-DNA lines

Plants carrying T-DNA insertions on *A/N-INVB* (Acid/Neutral Invertase B), *A/N-INVC* (Acid/Neutral Invertase C), *APL4* (AGPase Large subunit 4) and *SUS3* (Sucrose Synthase 3) lines were screened for homozygous T-DNA insertion using the same procedure described in 5.2.2 with the following specific primers (Figure 4.11):

A/N-INVB Fd 5'-CATGGCTTAAAGGGTTTAGGC-3'
Rv 5'-GAGACTCAAATCCAGGCTGTG-3'

A/N-INVC Fd 5'-AAACTAACGGAAGCTGGCAAGG-3'
Rv 5'-TGATTCCGATTCCATTAGCTG-3'

APL4 Fd 5'-CGAATTAGGACCTCAAGGGTC-3'
Rv 5'-GTGATCTCTTATGGCTGCAGG-3'

SUS3 Fd 5'-TTGGAGACCAGCGTCTGATAC-3'
Rv 5'-ATCGATGTGTTTGATCCGAAG-3'

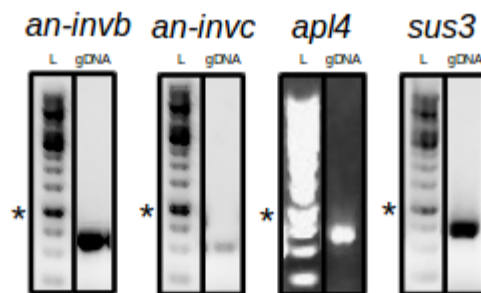


Figure 4.11 PCR products for selection of homozygous insertion. In the left lane the DNA ladder (L) and in the right lane the genomic DNA sample amplified by PCR (gDNA). Single PCR product between 550 bp and 800 bp reveals homozygous T-DNA insertion in the respective gene. The 1000 bp band in the ladder is marked with *.

4.5.2 Oxidative stress levels in T-DNA lines

Lipid peroxidation has been measured to assay oxidative stress in *an-invb*, *an-invc*, *apl4* and *sus3* T-DNA lines (Figure 4.12). All these genotypes did not show any significant difference

of MDA content if compared to wild-type plants, suggesting that lack of the corresponding enzymes did not alter the response to osmotic stress.

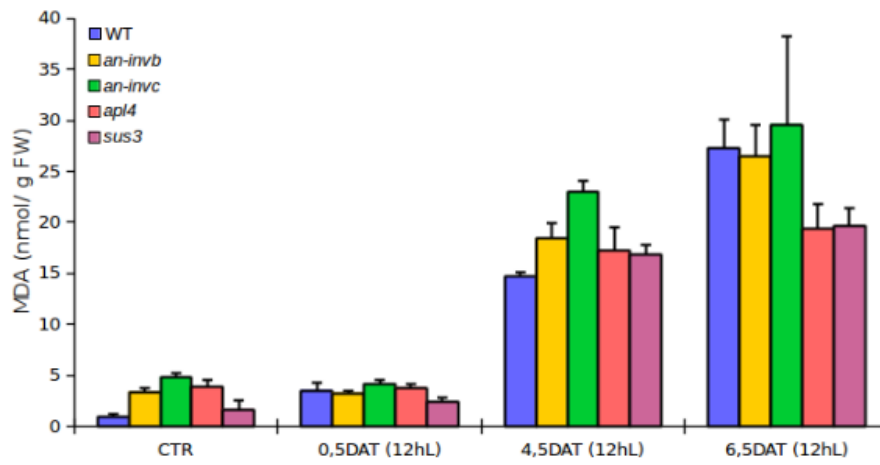


Figure 4.12 Oxidative stress levels under osmotic treatment. Oxidative levels are expressed as lipid peroxidation product malonedialdehyde (nmol MDA/ g FW). Columns show mean \pm standard error (n= 3). Plants harvested at 12 hours of light (12hL).

5. The analysis of the different functions of starch-phosphorylating enzymes during the development of *Arabidopsis thaliana* plants discloses an unexpected role for the cytosolic isoform GWD2

The following chapter has been published in *Physiologia Plantarum* 160: 447–457 (2017) and it is available at <https://doi.org/10.1111/ppl.12564>.

Claudia Pirone¹, Libero Gurrieri¹, Ivan Gaiba¹, Alessio Adamiano^{2,3}, Francesco Valle⁴, Paolo Trost¹, Francesca Sparla¹

1 Department of Pharmacy and Biotechnology FaBiT, University of Bologna, Bologna 40126, Italy

2 Department of Chemistry “G. Ciamician”, University of Bologna, Bologna 40126, Italy

3 Institute of Science and Technology for Ceramics (ISTEC), National Research Council (CNR), Faenza 48018, Italy

4 Institute for the Study of Nanostructured Materials (ISNM), National Research Council (CNR), Bologna 40129, Italy

Abbreviations – BAM5, β -amylase-5; GWD1, glucan, water dikinase-1; GWD2, glucan, water dikinase-2; MS, Murashige–Skoog; PCR, polymerase chain reaction; PWD, phosphoglucan, water dikinase; TZ, 2,3,5-triphenyl-tetrazolium chloride.

5.1 Abstract

The genome of *Arabidopsis thaliana* encodes three glucan, water dikinases. Glucan, water dikinase 1 (GWD1; EC 2.7.9.4) and phosphoglucan, water dikinase (PWD; EC 2.7.9.5) are chloroplastic enzymes, while glucan, water dikinase 2 (GWD2) is cytosolic. Both GWDs and PWD catalyze the addition of phosphate groups to amylopectin chains at the surface of starch granules, changing its physicochemical properties. As a result, GWD1 and PWD have a positive effect on transitory starch degradation at night. Because of its cytosolic localization, GWD2 does not have the same effect. Single T-DNA mutants of either GWD1 or PWD or GWD2 have been analyzed during the entire life cycle of *A. thaliana*. We report that the three dikinases are all important for proper seed development. Seeds from *gwd2* mutants are shrunken, with the epidermal cells of the seed coat irregularly shaped. Moreover, *gwd2* seeds contain a lower lipid to protein ratio and are impaired in germination. Similar seed phenotypes were observed in *pwd* and *gwd1* mutants, except for the normal morphology of epidermal cells in *gwd1* seed coats. The *gwd1*, *pwd* and *gwd2* mutants were also very similar in growth and flowering time when grown under continuous light and all three behaved differently from wild-type plants. Besides pinpointing a novel role of GWD2 and PWD in seed development, this analysis suggests that the phenotypic features of the dikinase mutants in *A. thaliana* cannot be explained solely in terms of defects in leaf starch degradation at night.

5.2 Introduction

Starch is a polymer of D-glucose that plants accumulate in nearly all organs, where it is synthesized inside plastids by the coordinated action of several enzymes. Different types of starch are found in plants: transitory starch in autotrophic tissues and storage starch in heterotrophic tissues. Starch biosynthesis is directly connected to the Calvin–Benson cycle in chloroplasts of photosynthetic tissues, whereas in plastids of heterotrophic tissues, starch biosynthesis relies on the cellular uptake of soluble sugars synthesized in other cells. The morphology of starch granules can vary significantly according to plant species (from spherical and discoidal in barley, to polyhedral in rice), but starch granules are invariably composed of two types of polymers: amylose and amylopectin (Buléon et al., 1998; Wani et al., 2012; Sparla et al., 2014). Amylose is an essentially linear polymer of several thousand D-glucose units linked by α -1,4-glucosidic bonds. Amylopectin is a highly branched polymer of D-glucose with α -1,6-glucosidic bonds stemming every 20–25 glucose units. Amylopectin accounts for about 70–90% of starch weight depending on the species (Ong et al., 1994; Roger and Colonna, 1996). Independently from morphology, amylose to amylopectin ratio and localization within the plant, starch granules are recalcitrant to degradation.

The turnover of starch granules is determined by the ratio between the rates of starch synthesis and starch degradation. Two main pathways of starch degradation are known to occur in plants, one is based on the endoamylolytic activity of α -amylases, the other on the exoamylolytic activity of β -amylases. In both cases starch needs to be previously phosphorylated in order to increase the accessibility of the granule surface to amylolytic enzymes (Blennow et al., 2000; Edner et al., 2007; Santelia et al., 2015). Dephosphorylation of phosphorylated amylopectin is also required to let amylases proceed freely in the depolymerization of the destabilized glucan chains (Kötting et al. 2009; Santelia et al. 2011). In short-term starch depositories, such as the transitory starch synthesized during the day in chloroplasts, starch phosphoesterification occurs at the hydroxyl groups of C-3 and C-6 of glucose monomers of amylopectin (Blennow et al., 2002). Phosphorylation at C-3 or C-6 has considerably different effects. C-6 bound phosphates have limited effects on starch granule crystallinity, whereas the C-3 modification significantly changes the packing of the double helices (O’Sullivan and Perez, 1999; Blennow et al., 2002). Glucan, water dikinase (GWD) and phosphoglucan, water dikinase (PWD) catalyze the formation of the glucosyl-phosphate esters by a dikinase mechanism in which the β -phosphate group of ATP is transferred to starch while the γ -phosphate group is transferred to water (for a deep characterization of the catalytic mechanism of GWD, see Hejazi et al., 2012). While GWDs phosphorylates the C-6 positions (Ritte et al., 2002), PWD transfers a phosphoryl residue to the C-3 position of a pre-phosphorylated amylopectin chain (Baunsgaard et al., 2005; Kötting et al., 2005). In *Arabidopsis*

thaliana, GWD1, GWD2 and PWD form a small protein family. GWD1 and PWD are localized in the chloroplast stroma (Ritte et al., 2000; Baunsgaard et al., 2005) whereas GWD2 is a cytosolic enzyme mainly expressed in the companion cells of the phloem in an age-dependent manner (Glaring et al., 2007). Strong experimental evidence supports the essential role of GWD1 and PWD in leaf starch degradation. Plants lacking GWD1 are unable to degrade leaf starch even after a prolonged dark period (Lorberth et al., 1998), and are characterized by a strong starch excess (*sex*) phenotype. A less severe *sex* phenotype is typically associated to *pwd* mutants (Baunsgaard et al., 2005; Kötting et al., 2005). In agreement with the extra-plastidial localization of GWD2, the lack of GWD2 gene does not cause the leaf-associated *sex* phenotype and the mutant appears indistinguishable from the wild-type (Glaring et al., 2007). It might be noted that GWD2 is not the only extra-plastidial enzyme that catalyzes a starch-related reaction. β -Amylase-5 (BAM5) is an active β -amylase and is cytosolic as well (Lin et al., 1988; Caspar et al. 1989). Similar to GWD2, BAM5 is also mainly associated to phloem tissues (Wang et al., 1995) and similar to *gwd2*, *bam5* mutants are also identical to wild-type plants (Laby et al., 2001; Monroe et al., 2014).

Several studies have been conducted on plants with altered expression of genes involved in starch metabolism (for a recent review see Lloyd and Kossmann, 2015; Mahlow et al., 2016). Much attention has been paid to severe phenotypes, as those of starch-less mutants (*e.g.* *pgm*) or starch-excess mutants (*e.g.* *sex1*). Less attention has been paid to mutations resulting in less severe phenotypes and most studies covered single developmental stages or specific organs. The aim of the present study is to analyze different phenotypic traits in single mutants of GWD1 (At1g10760), GWD2 (At4g24450) and PWD (At5g26570) during the entire life cycle and in different organs of *A. thaliana*. Although *gwd1* mutants have been thoroughly characterized already, *pwd* mutants are less characterized and almost nothing is known about *gwd2* mutants. Our systematic study of the three GWDs of *A. thaliana* demonstrates that cytosolic GWD2, and in part also plastidic PWD, play unexpected roles in proper seed development.

5.3 Materials and methods

5.3.1 Genotype analysis

T-DNA lines were searched for insertions in At1g10760 (SAIL_165_B11), At4g24450 (SALK_152327C; SALK_080260C already used in Glaring et al., 2007) and At5g26570 (SALK_110814 already used in Baunsgaard et al., 2005) genes. Stock seeds were purchased from the European Arabidopsis Stock Centre (NASC, Nottingham, UK; Table 6.1, Supporting information). Homozygous lines were selected by two independent polymerase chain reaction (PCR) amplifications on genomic DNA extracted from three to five leaves of T3 plants. One PCR reaction was performed utilizing a pair of primers both specific for the gene under study, while a second PCR reaction was performed utilizing a gene-specific primer and a T-DNA left border primer (Table 5.1).

Gene	NASC code	Mutant	¹ LP (5'-3')	² RP (5'-3')	³ LB (5'-3')
At1g10760	SAIL_165_B11	<i>gwd1</i>	CTGTTCTTGACAGAAGCCGAC	CAAAGAAATACTTGGAGGGGC	GCCTTTTCAGAAATGGATAAAT AGCCTTGCTTCC
At5g26570	SALK_110814	<i>pwd</i>	GCTAGGGTAGCCACCGTAAAG	TCCGATATGTCCTTTTCTGG	GCGTGGACCGCTTGCTGCAACT
At4g24450	SALK_152327C	<i>gwd2A</i>	AGACTCCTCCGTAGAAGCACC	GAAACTGGCGTTCTCAGATTG	GCGTGGACCGCTTGCTGCAACT
At4g24450	SALK_080260C	<i>gwd2B</i>	CAAATGTTCCGAATGGAAGAG	AGGTTATAAGAGCAGGGCCAG	GCGTGGACCGCTTGCTGCAACT

Table 5.1 Index of Arabidopsis thaliana T-DNA mutants under study. Homozygous lines were identified through two independent PCR reactions performed on genomic DNA. Utilized pairs of primers were LP+RP and LB+RP. ¹LP: gene specific, left border primer ²RP: gene specific, right border primer ³LB: T-DNA specific, left border primer.

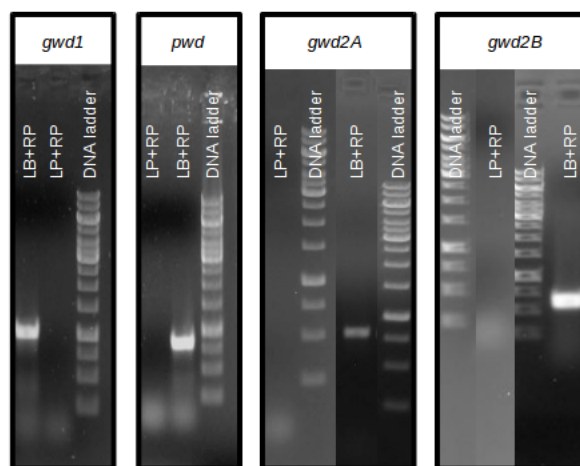


Figure 5.1 Selection of homozygous line by PCR analyses. PCR analyses were performed with 400 ng of DNA extracted from 30-day-old plants. Homozygous lines were selected using specific primers and 35 amplification cycles. Exclusively in homozygous lines, the pairs of primers LB+RP is expected to amplify a band of known length (typically around 300 bp) while on the same genome the pair LP+RP is expected unable to amplify. Representative results are reported.

PCR amplifications were performed on a Biometra T-gradient thermocycler under the following conditions: (1) 5 min at 94 °C, (2) 35 cycles of 30 s at 93 °C, 30 s at 58 °C and 1 min at 72 °C. PCR products were separated on 0.8% 40 mM Tris-acetate, 10 mM EDTA, pH 8.0 (TAE)-agarose gel and visualized with ethidium bromide (Figure 5.1). A total of 20–40 plants were analyzed for each T-

DNA line. Seeds were collected only from homozygous lines. All experiments were carried out on the T4 generation.

5.3.2 Plant growth conditions

Wild-type and T-DNA *A. thaliana* plants (ecotype Columbia) were grown on soil or on half-strength Murashige–Skoog medium (MS-agar medium; Micropoli, Milan, Italy), in a growth chamber at 22 °C either at a light intensity of 110 $\mu\text{mol photon m}^{-2} \text{s}^{-1}$ for 12 h day⁻¹ or at a light intensity of 60 $\mu\text{mol photon m}^{-2} \text{s}^{-1}$ for 24 h day⁻¹. Seeds grown in 1/2 MS-agar medium were sterilized with chlorine fumes for 5 h, and then transferred onto square Petri dishes. Cold stratification of about 4 days in the dark was applied. All experiments were conducted starting from seeds collected from mother plants grown at the same time and under the same conditions. Once collected, dry seeds were stored at 4 °C. All experiments were performed on seeds of the same age.

5.3.3 Phenotypic characterization

Leaves starch content was quantified from entire rosettes of 31- to 35-day-old plants and measured as described in Smith and Zeeman (2006). Starch quantification was performed at 12 h light and 12 h dark on four independent biological replicas. The percentage of germination was calculated by counting the seeds with radical protrusion 72 h after sowing. Permeability of the seed coat was tested through 2,3,5-triphenyl-tetrazolium chloride (TZ) assay as described in Wharton (1955). Briefly, following 15 min of incubation in aqueous solution of 20% (v/v) commercial bleach and 0.1% (v/v) Triton X-100, intact seeds were incubated in a 1% (w/v) aqueous solution of TZ (Sigma-Aldrich, Milan, Italy) at 30 °C in darkness for 48 h. Following incubation, seeds were rinsed with water and observed under a stereomicroscope (Nikon SMZ1000; Nikon, Firenze, Italy). Quantification of formazan was performed in triplicate, on pools of about 200 seeds that had been incubated for 48 h in 1% TZ aqueous solution in darkness at 30 °C. Following incubation, the supernatant was removed and the seeds were ground with a pestle in 200 μl of ethanol. The absorbance at 485 nm was measured in a Nanodrop (Thermo Scientific, Monza, Italy) spectrophotometer on the supernatants obtained after 3 min centrifugation at 15,000 g of the smashed seeds. The absorbance was normalized for the seeds weight and the absorbance of boiled seeds was used as a blank. Detection of mucilage was performed incubating approximately 250 seeds at room temperature for 15 min in an aqueous solution of 0.03% (w/v) ruthenium red. Seeds were rinsed with water before observation under a stereomicroscope (Nikon SMZ1000). The rate of primary root elongation was evaluated measuring the root length at regular intervals between 2 and 7 days of growth. The flowering time was defined as the time required by the primary inflorescence

to reach a height of 10 cm. The number of rosette leaves was taken at the flowering time. The number of flowers, siliques and seeds pertain to the primary inflorescence only. The seeds density was evaluated by counting seeds able to cross 100, 80 or 70% glycerol cushions after 15 min centrifugation at 15,000 g.

5.3.4 Scanning electron microscopy

Samples were dry mounted on stubs using carbon tape and subsequently coated with a 10 nm gold layer in a QR150R sputter system (Quorum Technologies, East Sussex, UK). Images were collected using a SEM-FEG Hitachi S4000 Scanning Electron Microscope ($V_{\text{ext}} = 20 \text{ keV}$; $i = \mu\text{A}$; Hitachi, Tokyo, Japan).

5.3.5 Quantification of starch, protein and lipids in seeds

For the quantification of seed proteins and seed starch content, about 30 mg of air-dried seeds were homogenized in a mortar at room temperature in the presence of three volumes of extraction buffer [50 mM 2-[4-(2-hydroxyethyl)piperazin-1-yl]ethanesulfonic acid (HEPES), 5 mM MgCl_2 , pH 7.5, 1% Triton X-100, 15% glycerol, 2% Sodium dodecyl sulfate (SDS), 1 mM according to the manufacturer's instructions. Pellets were washed once with 80% ethanol, three times with water and starch was quantified as described in Smith and Zeeman (2006). Total lipid quantification was performed gravimetrically as described in Wingenter et al. (2010) on 100 mg of mature and air-dried seeds for each genotype. The fatty acids composition of the lipid fraction was determined by means of base-catalyzed derivatization and gas chromatography–mass spectrometry (GC–MS) analysis as described in Torri et al. (2011).

5.4 Results

5.4.1 Isolation of homozygous T-DNA lines and leaf starch quantification

Selection of homozygous lines with T-DNA insertions in *GWD1*, *PWD* and *GWD2* coding sequences were carried out by PCR experiments on genomic DNA. Two PCR amplifications with T-DNA and gene-specific primers were performed (Table 5.1 and Figure 5.1). Only for *GWD2*, two independent T-DNA mutants were selected and named *gwd2A* and *gwd2B*.

Previously described *sex* phenotypes were confirmed by quantification of leaf starch concentration, measured at the end of the day and at the end of the night (Figure 5.2). As expected, starch content in *gwd1* was considerably higher than in wild-type plants both at 12 h light and 12 h dark (Yu et al. 2001). A weaker *sex* phenotype was observed in *pwd* mutant (Baunsgaard et al., 2005; Kötting et al., 2005), whereas in *gwd2* mutants starch concentration was not statistically different from that of the wild-type plants (Glaring et al., 2007; Figure 6.2).

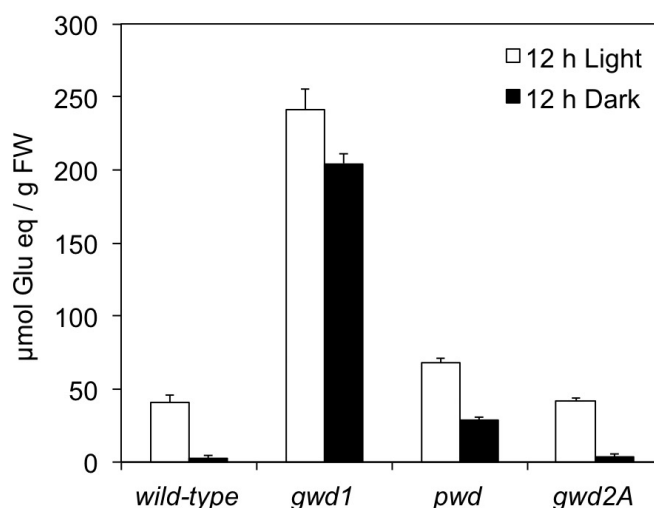


Figure 5.2 Transitory starch content measured at the end of the light (12 h Light) and at the end of the dark (12 h Dark) period in wild-type and mutant plants. Starch was extracted from entire rosette leaves of 31- to 35-day-old plants. Data are means \pm SE (n = 4).

Leaves starch	<i>wild-type</i>	<i>gwd2B</i>
12 h L ($\mu\text{mol Glu}_{\text{eq}} \text{ g FW}^{-1}$)	40.9 \pm 4.7	43.0 \pm 8.8
12 h D ($\mu\text{mol Glu}_{\text{eq}} \text{ g FW}^{-1}$)	2.3 \pm 1.8	6.8 \pm 3.9

Table 5.2 Transitory starch content measured at the end of the light (12 h Light) and at the end of the dark (12 h Dark) period in *gwd2B* plants. Starch was extracted from entire rosette leaves of 31- to 35-day-old plants. Data are means \pm SE (n = 4).

5.4.2 Seeds shape and composition

The effect of the T-DNA insertions was first evaluated on seeds. The 100-seed weight was not statistically different among lines (Table 5.3). Seed shape was analyzed by measuring the length and width of mature seeds (Table 5.3, Figure 5.3). Seeds belonging to mutant genotypes were all

reduced in length in respect to wild-type seeds. Width was reduced in *gwd1* and *pwd* seeds but not in *gwd2*.

	Seed dimension			Seed composition		
	* Weight (mg)	Length (μm)	Width (μm)	Lipids ($\mu\text{g seed}^{-1}$)	Proteins ($\mu\text{g seed}^{-1}$)	Starch (ng seed $^{-1}$)
wild-type	2.04 \pm 0.07	511 \pm 3.2	296 \pm 1.7	4.70 \pm 0.07	10.15 \pm 1.05	5.06 \pm 1.66
<i>gwd1</i>	1.94 \pm 0.04	481 \pm 3.9**	284 \pm 1.9**	3.36 \pm 0.22**	7.99 \pm 0.26	434 \pm 148**
<i>pwd</i>	1.80 \pm 0.06	488 \pm 3.7**	286 \pm 1.7**	3.00 \pm 0.29**	7.89 \pm 0.13	11.58 \pm 7.29
<i>gwd2A</i>	1.82 \pm 0.06	483 \pm 4.5**	296 \pm 1.9	3.40 \pm 0.08**	8.35 \pm 0.65	7.14 \pm 0.89
<i>gwd2B</i>	2.17 \pm 0.10	474 \pm 4.3**	291 \pm 2.4	4.05 \pm 0.14*	9.47 \pm 0.43	8.68 \pm 5.46

Table 56.3 Characterization of air-dried mature seeds collected from wild-type and mutant plants. Depending from the genotype, 31-52 pools composed by 100 seeds each were used to calculate seed weights. Seeds length and width were measured on 103-151 seeds (depending from the genotype) collected from 10 single plants; values are means \pm SE. Lipids, proteins and starch were quantified from mature seeds of wild-type and mutated lines; values are means \pm SD (n = 3). Statistical analyses were performed using Student's t-test. **P \leq 0.01. *Weight of seeds is referred to 100 seeds.

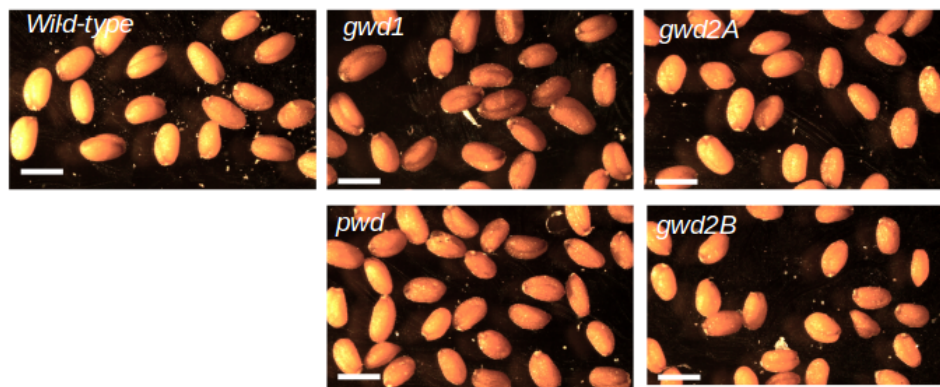


Figure 5.3 Appearance of wild-type and T-DNA mutants seeds. Batches of mature dry seeds were microscopic observed. Scale bar: 500 μm .

The very fact that mutant and wild-type seeds were similar in weight but different in size, suggests a difference in density that was further investigated by centrifugation of seeds on a step gradient of glycerol. Seeds of all mutants were confirmed to be denser than wild-type seeds (Table 5.4). In order to assess whether seed density depends on seed composition, the content of lipids, proteins and starch was evaluated (Table 5.3).

In comparison to wild-type seeds, lipid content (the lightest component of seeds) was statistically lower in all mutants, although no difference in fatty acid composition was observed (Figure 5.4). No statistical differences were observed in the protein content, hence the typical protein to lipid ratio of wild-type seeds (2.2) was slightly higher in mutants (between 2.4 and 2.6). This was apparently the reason for the difference in seed density. Starch is only a minor component of *A. thaliana* mature seeds (protein to starch ratio \approx 2,000) and differences in starch content could hardly affect seed density. Nevertheless, it is remarkable that *gwd1* seeds contained 90-fold more starch than wild type seeds, while starch levels in *pwd* and *gwd2* seeds were similar to wild-type (Table 5.3).

In sum, all three dikinase mutants make seeds that are slightly smaller and slightly denser than wild-type seeds because of their higher protein to lipid ratio, but only *gwd1* seeds compensate, although partially, the decrease of lipids with much more starch.

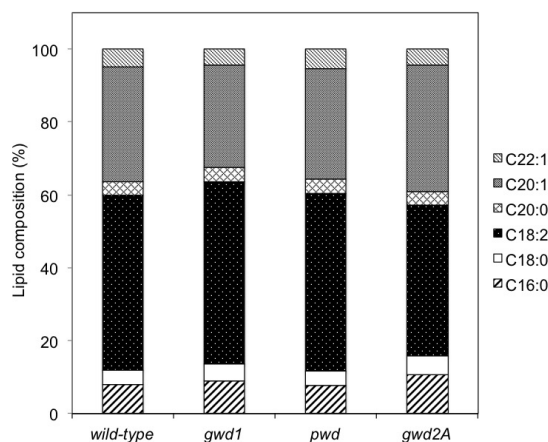


Figure 5.4 Fatty acid composition of *Arabidopsis thaliana* seeds lipid fraction of wild-type and mutant lines.

	Glycerol level		
	100%	80%	70%
wild-type	0%	0.8%	6.7%
<i>gwd1</i>	32.2%	---	---
<i>pwd</i>	---	84.4%	---
<i>gwd2A</i>	---	---	45.7%
<i>gwd2B</i>	---	---	42.2%

Table 5.4 Density of wild-type and mutated seeds evaluated by glycerol cushions. The seeds density was evaluated by counting seeds able to cross 100%, 80% or 70% glycerol cushions after 15 min centrifugation at 15,000 g. Data are expressed as percentage of the seeds able to cross the glycerol cushions.

5.4.3 Seed morphology and permeability

Scanning electron microscopy was used to investigate the morphology of whole seeds and seed coat details. Wild-type seed coats showed a regular morphology, characterized by the typical hexagonal epidermal cells with a volcano-shaped central columella. The same pattern was also observed in *gwd1* (Figure 5.5). On the contrary both *pwd* and *gwd2* seeds showed thin walled epidermal cells with a less clear hexagonal profile and irregularly shaped columella (Figure 5.5). In order to assess whether altered seed coats might affect seed permeability, a TZ assay was performed. This assay is based on the uptake of TZ by living cells and its subsequent reduction to formazan, a purple and non-diffusible salt. As shown in Figure 5.6, the uptake of TZ salt was much higher in *pwd* seeds and slightly increased in *gwd2*, as compared with *gwd1* and wild-type seeds. A correlation between altered seed coats and the increased permeability was therefore observed. Upon seed hydration, *Arabidopsis* epidermal cells release gelatinous material forming a mucilage capsule. Mucilage is

rich in pectin polymers, and relatively poor in cellulose and xyloglucan (North et al., 2014; Voiniciuc et al., 2015). Ruthenium red staining highlights the pectinaceous nature of the mucilage capsule. Upon ruthenium red staining (Figure 5.6) wild-type and *gwd2* mutants revealed the typical pink-stained capsule, with no macroscopic differences between the two genotypes. On the contrary, the mucilage capsules of *gwd1* and *pwd* mutants were less bright, suggesting a different mucilage composition (Voiniciuc et al., 2015).

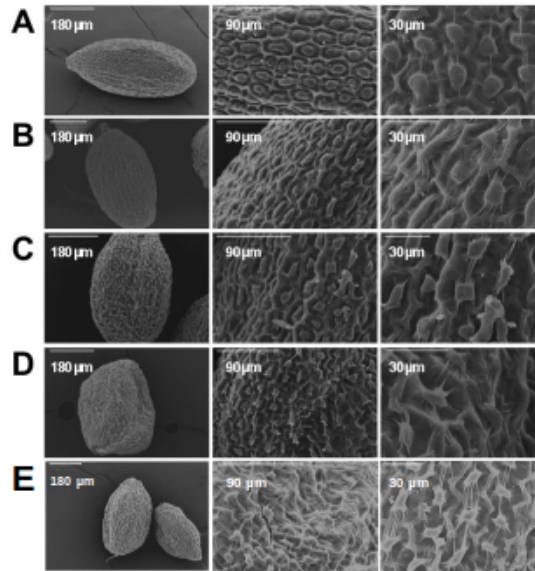


Figure 5.5 Scanning electron micrographs of dry seeds from wild-type (A), *gwd1* (B), *pwd* (C) and *gwd2A* (D), *gwd2B* (E).

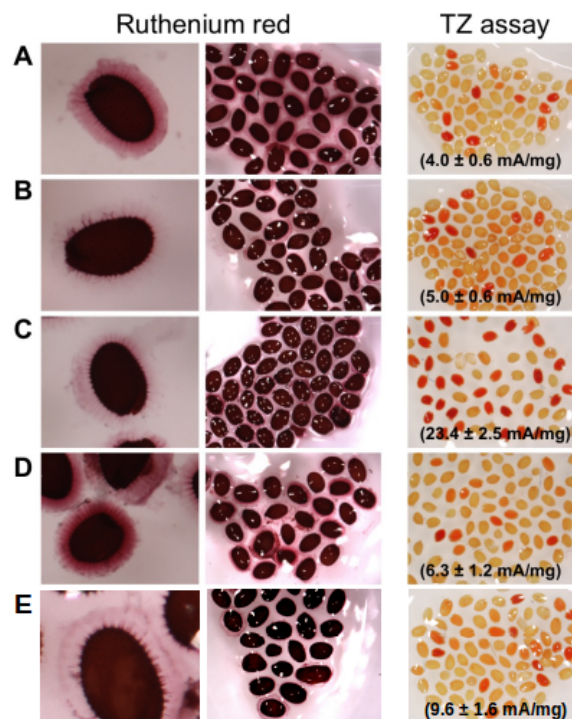


Figure 5.6 Ruthenium red and TZ staining of wild-type and mutant seeds. Measurements of absorbance at 485 nm, corresponding to the concentration of formazans, are reported in brackets as mA mg^{-1} of seeds

5.4.4 Seed viability and primary root growth

Seed viability was measured as the percentage of seeds showing the radical protrusion 72 h after sowing. The percentage of germination was statistically reduced in *pwd* and *gwd2*, but not in (Table 5.5), suggesting that the differences observed in the epidermal cells morphology and seed permeability in these two lines could inhibit germination. The rate of primary root elongation during the linear growth phase (between days 2 and 7) was much lower in all mutants in respect to wild-type (Table 5.5), pinpointing a positive correlation between lipid content of seeds and root growth during seedlings development (Table 5.5). Root growth was particularly inhibited in *gwd1* seedlings, possibly because of the strong inhibition of transitory starch degradation that is associated to this mutation. As the seedlings grow and acquire photosynthetic capacity, it is likely that the inability to mobilize starch synthesized in green cotyledons may further contribute to root growth inhibition.

	Germination (%)	Growth rate of primary root ($\mu\text{m h}^{-1}$)
wild-type	99.0 \pm 0.2	175 \pm 2
<i>gwd1</i>	97.9 \pm 1.5	76 \pm 1**
<i>pwd</i>	89.5 \pm 4.9**	94 \pm 3**
<i>gwd2A</i>	93.6 \pm 3.1**	94 \pm 3**
<i>gwd2B</i>	91.7 \pm 7.2**	105 \pm 3**

Table 5.5 Seed viability and rate of primary root elongation. The percentage of germination was evaluated scoring the number of germinated seeds in respect to the number of sowed seeds. Four independent biological replicas, each of which composed by 30 mutant and 30 wild-type seeds sown on the same 1/2MS-agar plate, were scored. Data are means \pm SE. Primary root elongation was obtained fitting data within the linear range of growth rate. Data are means \pm SE of single seedlings (n = 49 ~ 100). Statistical analyses were performed using Student's t-test. **P \leq 0.01.

5.4.5 Transition from vegetative to reproductive growth and plant fitness

The effect of mutations on the transition from vegetative to reproductive growth was evaluated by measuring the days required to reach flowering, assessed when the primary inflorescence was 10 cm tall. Wild-type plants and *pwd* and *gwd2* mutants reached the flowering time in about 70 days (Table 5.6), whereas more than 100 days were required by *gwd1*. Once they reached flowering time, rosette leaves were counted (Table 5.6). Consistent with the prolonged vegetative phase, an increased number of rosette leaves was counted in *gwd1* mutant, while *pwd* and *gwd2A* showed a small but statistically significant decrease (Table 5.6). Flowers, siliques and seeds of the primary inflorescence were counted in all four genotypes. Compared with wild-type, flowers, siliques and total seed production were reduced in both *pwd* and *gwd2* (Table 5.6). Interestingly, the *gwd1* mutant, characterized by the most severe sex phenotype, did not show a reduced number of flowers and siliques. And the reduction in seed production was less pronounced than in both *pwd* and

gwd2A mutants (–20% in *gwd1* vs approximately –40% in *pwd* and *gwd2A*; Table 5.6). Fitness was therefore decreased in all mutants, apparently with no correlation with the severity of the sex phenotype.

	Flowering time (day)	Rosette leaf	Flower (number)	Silique	Seed
wild-type	69.6 ± 2.3	21.7 ± 0.8	34.4 ± 1.4	25.7 ± 1.1	596 ± 30
<i>gwd1</i>	106.4 ± 2.3**	27.0 ± 0.6**	32.8 ± 1.1	27.2 ± 0.9	477 ± 25**
<i>pwd</i>	70.7 ± 2.4	18.9 ± 0.6**	22.9 ± 1.6**	14.5 ± 0.8**	349 ± 25**
<i>gwd2A</i>	72.6 ± 2.2	19.5 ± 0.5*	24.6 ± 1.4**	16.1 ± 0.8**	397 ± 23**
<i>gwd2B</i>	66.7 ± 2.2	20.7 ± 0.5	28.3 ± 1.4**	17.0 ± 0.9**	355 ± 24**

Table 6.6 Time of flowering and number of rosette leaves, flowers, siliques and seeds in wild-type and mutated lines. Plants were grown under 12 h light/ 12 h dark cycle. Time of flowering is defined by the length (10 cm) of the primary inflorescence (n = 60). The number of rosette leaves was assayed at the flowering time (n = 60). Flowers, siliques and seeds number pertain to the primary inflorescence (n = 80). Data are means ± SE. Statistical analyses were performed using Student’s t-test. **P ≤ 0.01; *P ≤ 0.05.

5.4.6 Rescue by light

Some of the above-mentioned phenotypic traits were also analyzed in plants grown under continuous low light intensity. The purpose of this experiment was to provide conditions in which the energy restriction that mutants unable to correctly degrade starch during the night necessarily experience, might be released. Exposure to continuous light conferred similar phenotypic traits to all mutants, clearly different from those of wild-type plants (Table 5.7). The rate of primary root elongation was approximately 70% of the wild-type rate, instead of 40–50% as observed under 12 h light cycle (Table 5.5). The time required to reach the transition to the reproductive phase was about 1 week delayed in all mutants compared with the wild-type, and the number of rosette leaves was about 40% greater in all mutants than in wild-type plants (Table 5.7). The appearance of identical phenotypic traits in all mutants strongly supports the view that transitory starch degradation is not exclusively restricted to the dark period (Valerio et al., 2011; Hejazi et al., 2014; Zanella et al., 2016) and that all three GWDs are required for the proper mobilization of sugars, although to different extent when plants are grown under a normal light/dark cycle.

	Growth rate of primary root ($\mu\text{m h}^{-1}$)	Flowering time (day)	Rosette leaf (number)
wild-type	164 ± 2	48.5 ± 1.2	8.3 ± 0.2
<i>gwd1</i>	111 ± 6**	54.7 ± 1.4**	11.0 ± 0.3**
<i>pwd</i>	119 ± 6**	54.6 ± 1.0**	11.8 ± 0.3**
<i>gwd2A</i>	114 ± 6**	52.8 ± 0.9**	11.8 ± 0.4**
<i>gwd2B</i>	114 ± 5**	58.8 ± 1.3**	12.1 ± 0.5**

Table 5.7 Rescue by light. Effects of the continuous low intensity light (60 $\mu\text{mol photon m}^{-2} \text{s}^{-1}$) on the rate of primary elongation (n = 30) and on the transition from vegetative to reproductive stage (n = 50). Data are means ± SE. Statistical analyses were performed using Student’s t-test. **P ≤ 0.01.

5.5 Discussion

In this study, single *A. thaliana* mutants lacking each of the three GWDs encoded by the Arabidopsis genome were phenotypically analyzed in parallel. The aim was to describe the morphological effects caused by such mutations during the entire life cycle of Arabidopsis plants.

The plastidic glucan, water dikinase isoforms, GWD1 and PWD, are important enzymes of starch metabolism. The third isoform, GWD2, catalyzes the same reaction of GWD1, but based on its extra-plastidial localization and low expression in leaves it was shown to play no role in transient starch metabolism, in Arabidopsis at least (Glaring et al., 2007). On the other hand, the evolutionary origin of starch metabolism may explain the existence of a starch-modifying enzyme in the cytosol of higher plants. Starch metabolism, in fact, has been acquired by plants following the endosymbiotic event that led to the evolution of modern plastids (Deschamps et al., 2008a; Comparot-Moss and Denyer, 2009; Li et al., 2012). Although the capacity to synthesize starch was a feature of the ancestor prokaryotic symbiont, phylogenetic analyses suggest that genes for starch metabolism were initially transferred to the nucleus of the host cell and only subsequently starch metabolism was relocated into the newly formed plastid (Deschamps et al., 2008b; 2008c). As a result, starch metabolism of present-day plants occurs almost exclusively in plastids, but some enzymes known to catalyze starch-related reactions are (still) located in the cytosol. These include GWD2, but also the isoform BAM5 of the family of β -amylases in Arabidopsis (Lin et al., 1988; Glaring et al., 2007). In the search of a physiological role for GWD2, *gwd2* mutants were thus included in our phenotypic analysis.

Because of the strong sex phenotype associated to the GWD1 mutation, *gwd1* mutants have been deeply investigated. The role of GWD1 on nocturnal mobilization of transitory starch is well established (for a recent review see Lloyd and Kossmann, 2015; Mahlow et al., 2016) and the knowledge acquired from the model plant Arabidopsis has been already transferred to some crops (Carciofi et al., 2011; Ral et al., 2012; Weise et al., 2012; Hirose et al., 2013), in some cases with unexpected results. In wheat, for instance, the endosperm-specific inhibition of GWD homologs by RNA interference (RNAi) caused the increase in vegetative biomass and grain yield compared with wild-type plants (Ral et al., 2012; Bowerman et al., 2016). Moreover, the very fact that GWD1-dependent transitory starch phosphorylation occurs also in the light (Hejazi et al., 2014; Skeffington et al., 2014) forced some authors to suggest that GWD1 exerts little control on starch degradation. In fact, a 70% reduction of GWD1 levels did not inhibit starch degradation in Arabidopsis leaves at night (Skeffington et al., 2014). Our results add further complexity to the general picture. Here we show that *gwd1* mutants have several phenotypic traits that distinguish them from wild-type plants:

fewer, smaller and denser seeds with less lipids and more starch, slower-growing primary root, delayed flowering time and increased vegetative growth (more rosette leaves). Many of these traits were already described in the literature and generally interpreted as the result of night-time starvation. In fact, these plants cannot mobilize the transitory starch properly to sustain the heterotrophic metabolism (Yu et al., 2001; Andriotis et al., 2012). According to this view, continuous light should revert the phenotypic traits of *gwd1*. We indeed observed a (partial) reversion of primary root growth inhibition and delayed flowering time in *gwd1* plants grown in continuous light but we also observed that *gwd1*, *pwd* and *gwd2* behaved the same under these conditions, and all were different from wild-type plants. Provided that GWD2 should not be involved in transitory starch mobilization, trying to explain these results exclusively in terms of energy starvation appears reductive. A complex integration of energetic signals (*e.g.* the ratio between starch and soluble sugars) (Lastdrager et al., 2014; Ruan, 2014) with hormonal signals appears a more reasonable hypothesis that could explain the different development of wild-type plants vs mutants of GWDs (Li et al., 2014; Ljung et al., 2015).

In comparison to *gwd1*, less is known about mutants *pwd* and *gwd2* (Mahlow et al. 2016). This is especially true for *gwd2*, presumably because of the lack of *sex* phenotype associated to leaves of this mutant (Glaring et al., 2007). However, *pwd* and *gwd2* showed several common phenotypic traits regarding the seeds: fewer, smaller and denser seeds containing less lipids but normal levels of protein and starch. Moreover, the percentage of germination in *pwd* and *gwd2* was statistically reduced in comparison to wild-type and *gwd1* mutants, a phenotypic trait that correlates with the altered morphology of seeds (shrunken seeds, particularly in *gwd2*), the altered morphology of seed coat epidermal cells and the increased seed permeability evaluated through the TZ assay. Plant productivity (evaluated as both leaves number and seed production) was also similarly impaired in *pwd* and *gwd2* mutants. Though plants do not contain starch in the cytosol, it may contain polysaccharides of various degree of polymerization and is tempting to speculate that GWD2 might favor polyglucans depolymerization. Incidentally, both GWD2 and BAM5 are particularly abundant in phloem cells and may well be involved in sustaining the phloem loading of soluble sugars in source organs. We suggest that GWD2, possibly in concert with BAM5, may thus contribute to controlling the ratio between soluble and insoluble polysaccharides in plants, and this parameter may in turn affect the phenotypic traits that are observed.

Taken together, these data demonstrate that despite their plastidial or extra-plastidial localization, all three GWDs are required for the proper development of *A. thaliana* plants, that only partially depends on the rate of leaf starch degradation at night. The complex phenotypes of the dikinase

mutants suggest that, besides being more or less impaired in leaf starch degradation at night, these plants may be altered in signaling pathways in manners that still have to be elucidated.

6. Ringraziamenti

Tre anni di dottorato sono rapidi e intensi al tempo stesso, tanti eventi si avvicendano dentro e fuori il laboratorio, si cresce scientificamente e si matura personalmente. Per questa terza ed ultima tesi voglio ringraziare sostanzialmente le stesse persone di sempre, che per mia fortuna mi sono state accanto dal primo giorno di Università.

Per la mia vita fuori dall'accademia il primo ringraziamento va, come sempre, a Silvia, che mi ha sopportato e supportato di persona nei momenti di crisi e di gioia. I miei genitori, Letizia e Pippo, che anche se a distanza mi hanno saputo sostenere e consigliare. Mia sorella Blanca, che quando ho cominciato l'Università era una bambina e adesso è una maggiorenne con cui si parla e ci si confronta su tutto.

Per quanto riguarda la vita accademica, il primo ringraziamento va sicuramente a Francesca Sparla, che mi ha allevato e insegnato sin da studentello e tirato su fino alla fine del dottorato (almeno). Un secondo importante grazie va a Simona Fermani, per avermi trasmesso i segreti della cristallografia di proteine e aver ottenuto la struttura che tanto abbiamo cercato. Devo ringraziare anche Mirko, per le utili discussioni e confronti, e anche Paolo, per i suoi consigli.

Oltre queste persone, sicuramente centrali e indispensabili, un elenco interminabile di amici si affianca. Tutti sono stati fonte di svago (soprattutto) ma anche di discussione e ispirazione, e per questo gli sono grato.

7. References

- Abat JK, Mattoo AK and Deswal R (2008) S-nitrosylated proteins of a medicinal CAM plant *Kalanchoe pinnata* – ribulose-1,5-bisphosphate carboxylase/oxygenase activity targeted for inhibition. *FEBS J* 275: 2862–2872.
- Abat JK and Deswal R (2009) Differential modulation of S-nitrosoproteome of *Brassica juncea* by low temperature: Change in S-nitrosylation of Rubisco is responsible for the inactivation of its carboxylase activity. *Proteomics* 9:4368–4380.
- Adams PD, Afonine PV, Bunkóczi G, Chen VB, Davis IA, Echols N, Headd JJ, Hung LW, Kapral GJ, Grosse-Kunstleve RW, McCoy AJ, Moriarty NW, Oeffner R, Read RJ, Richardson DC, Jane S. Richardson JS, Terwilliger TC and Zwart PH (2010) PHENIX: a comprehensive Python-based system for macromolecular structure solution. *Acta Cryst. D Biol. Cryst.* 66: 213–221.
- Aguilera-Alvarado GP and Sánchez-Nieto S (2017) Plant hexokinases are multifaceted proteins. *Plant Cell Physiol.* 58(7): 1151–1160 doi:10.1093/pcp/pcx062
- Alia, Saradhi PP, Mohanty P (1997) Involvement of proline in protecting thylakoid membranes against free radical-induced photodamage. *J Photoch. Photobio. B* 38: 253-257
- Amunts A, Drory O and Nelson N (2007) The structure of a plant photosystem I supercomplex at 3.4 Å resolution. *Nature* 447: 58-63.
- Andersson I and Backlund A (2008) Structure and function of Rubisco. *Plant Physiol Bioch* 46: 275-291.
- Andriotis VME, Pike MJ, Schwarz SL, Rawsthorne S, Wang TL, Smith AM (2012) Altered starch turnover in the maternal plant has major effects on Arabidopsis fruit growth and seed composition. *Plant Physiol* 160: 1175–1186.
- Aoshima M (2007) Novel enzyme reactions related to the tricarboxylic acid cycle: phylogenetic/functional implications and biotechnological applications. *Appl. Microbiol. Biotechnol* 75: 249–55.
- Apel K and Hirt H (2004) REACTIVE OXYGEN SPECIES : Metabolism, Oxidative Stress, and Signal Transduction *Annu. Rev. Plant Biol.* 55:373–99
- Aranjuelo I, Molero G, Erice G, Avice JC and Nogués S (2011) Plant physiology and proteomics reveals the leaf response to drought in alfalfa (*Medicago sativa* L.). *J Exp. Bot.* 62 (1): 111–123.
- Auernik KS, Maezato Y, Blum PH and Kelly RM (2008) The genome sequence of the metal-mobilizing, extremely thermoacidophilic archaeon *Metallosphaera sedula* provides insights into bioleaching-associated metabolism. *Appl. Environ. Microb.* 74 (3): 682-692.
- Avilan L, Gontero B, Lebreton S, Ricard J (1997) Information transfer in multienzyme complexes 2. The role of Arg64 of *Chlamydomonas reinhardtii* phosphoribulokinase in the information transfer between glyceraldehyde-3-phosphate dehydrogenase and phosphoribulokinase. *Eur. J. Biochem.* 250, 296–302.
- Baalman E, Scheibe R, Cerff R and Martin W (1996) Functional studies of chloroplast glyceraldehyde-3-phosphate dehydrogenase subunits A and B expressed in *Escherichia coli*: formation of highly active A4 and B4 homotetramers and evidence that aggregation of the B4 complex is mediated by the B subunit carboxy terminus. *Plant Mol. Biol.* 32: 505-513.
- Bachmann M and Keller F (1994) Metabolism of the raffinose family oligosaccharides in leaves of *Ajuga reptans* L. *Plant Physiol.* 109: 991-998
- Baena-Gonzalez E, Rolland F, Thevelein JM, Sheen J (2007) A central integrator of transcription networks in plant stress and energy signalling. *Nature* 448: 938-943

- Bahaji A, Baroja-Fernández E, Ricarte-Bermejo A, Sánchez-López AM, Muñoz FJ, Romero JM, Ruiz MT, Baslam M, Almagro G, Sesma MT, Pozueta-Romero J (2015) Characterization of multiple SPS knockout mutants reveals redundant functions of the four Arabidopsis sucrose phosphate synthase isoforms in plant viability, and strongly indicates that enhanced respiration and accelerated starch turnover can alleviate the blockage of sucrose biosynthesis. *Plant Sci.* 238: 135–147
- Ball SG and Morrel MK (2003) From bacterial glycogen to starch: understanding the biogenesis of the plant starch granule. *Annu. Rev. Plant Biol.* 54: 207–33
- Ballicora MA, Fu Y, Frueauf JB and Preiss J (1999) Heat stability of the potato tuber ADP-glucose pyrophosphorylase: role of cys residue 12 in the small subunit. *Biochem. Biophys. Res. Co.* 257: 782–786
- Ballicora MA, Frueauf JB, Fu Y, Schürmann P and Preiss J (2000) Activation of the potato tuber ADP-glucose pyrophosphorylase by thioredoxin. *J. Bio. Chem.* 275 (2): 1315–1320
- Baginsky S (2016) Protein phosphorylation in chloroplasts – a survey of phosphorylation targets. *J Exp. Bot.* 67 (13): 3873–3882.
- Barrero-Sicilia C, Hernando-Amado S, González-Melendi P, Carbonero P (2011) Structure, expression profile and subcellular localisation of four different sucrose synthase genes from barley. *Planta* 234: 391–403
- Bassham JA (1971) Photosynthetic carbon metabolism. *Proc. Nat. Acad. Sci. USA* 68(11): 2877–2882.
- Baud S, Vaultier MN and Rochat C (2004) Structure and expression profile of the sucrose synthase multigene family in Arabidopsis. *J Exp. Bot.* 55 (396): 397–409
- Baudry A, Ito S, Song YH, Strait AA, Kiba T, Lu S, Henriques R, Pruneda-Paz JL, Chua Nam-Hai, Tobin EM, Kay SA, Imaizumi T (2010) F-box proteins FKF1 and LKP2 act in concert with ZEITLUPE to control arabidopsis clock progression. *Plant Cell* 22: 606–622.
- Baunsgaard L, Lutken H, Mikkelsen R, Glaring MA, Pham TT, Blennow A (2005) A novel isoform of glucan, water dikinase phosphorylates pre-phosphorylated α -glucans and is involved in starch degradation in Arabidopsis. *Plant J* 41: 595–605
- Bauwe et al., 2010
- Bedhomme M, Zaffagnini M, Marchand GH, Gao XH, Moslonka-Lefebvre M, Michelet L, Decottignies P and Lemaire SD (2009) Regulation by glutathionylation of isocitrate lyase from *Chlamydomonas reinhardtii*. *J. Biol. Chem.* 284 (52): 36282–36291.
- Bedhomme M, Adamo M, Marchand CH, Couturier J, Rouhier N, Lemaire SD, Zaffagnini M and Trost P (2012). Glutathionylation of cytosolic glyceraldehyde-3-phosphate dehydrogenase from the model plant *Arabidopsis thaliana* is reversed by both glutaredoxins and thioredoxins *in vitro*. *Biochem. J.* 445: 337–347.
- Bennet AC, McDowell NG, Allen CG and Anderson-Teixeira KJ (2015) Larger trees suffer most during drought in forests worldwide. *Nature Plants* Article Number: 15139.
- Berg IA, Kockelkorn D, Buckel W, Fuchs G (2007). A 3-hydroxypropionate/4-hydroxybutyrate autotrophic carbon dioxide assimilation pathway in Archaea. *Science* 318:1782–86
- Bernal-Bayard P, Hervás M, Cejudo FJ and Navarro JA (2012) Electron transfer pathways and dynamics of chloroplast NADPH-dependent thioredoxin reductase C (NTRC). *J. Biol. Chem.* 287(40): 33865–33872.
- Berridge MJ, Lipp P and Bootman MD (2000) The versatility and universality of calcium signalling. *Nat. Rev. Mol. Cell. Bio.* 1: 11–21
- Bick JA, Setterdahl AT, Knaff DB, Chen Y, Pitcher LH, Zilinskas BA and Leustek T (2001) Regulation of the plant-type 5'-adenylyl sulfate reductase by oxidative stress. *Biochemistry-US* 40: 9040-9048.

- Bienert S, Waterhouse A, de Beer TAP, Tauriello G, Studer G, Bordoli L and Schwede T (2017) The SWISS-MODEL Repository - new features and functionality. *Nucleic Acids Res.* 45: D313-D319.
- Bieniawska Z, Barratt PDH, Garlick AP, Thole V, Kruger NJ, Cathie Martin C, Zrenner R and Smith AM (2007) Analysis of the sucrose synthase gene family in Arabidopsis. *Plant J.* 49: 810–828.
- Blennow A, Bay-Smidt AM, Olsen CE and Møller BL (2000) The distribution of covalently bound phosphate in the starch granule in relation to starch crystallinity. *Int J Biol Macromol* 27: 211–218.
- Blennow A, Engelsen SB, Nielsen TH, Baunsgaard L and Mikkelsen R (2002) Starch phosphorylation: a new front line in starch research. *Trends Plant Sci.* 7: 445–450.
- Blennow A and Engelsen SB (2010) Helix-breaking news: fighting crystalline starch energy deposits in the cell. *Trends Plant Sci.* 15(4): 236-240.
- Bogeat-Triboulot MB, Brosché M, Renaut J, Jouve L, Le Thiec D, Fayyaz P, Vinocur B, Witters E, Laukens K, Teichmann T, Altman A, Hausman JF, Polle A, Kangasjärvi J and Dreyer E (2007) Gradual soil water depletion results in reversible changes of gene expression, protein profiles, ecophysiology, and growth performance in *Populus euphratica*, a poplar growing in arid regions. *Plant Physiol.* 143: 876–892.
- Böhlenius H, Huang T, Charbonnel-Campaa L, Brunner AM, Jansson S, Strauss SH and Nilsson O (2006) CO/FT regulatory module controls timing of flowering and seasonal growth cessation in trees. *Science* 312 (5776): 1040-1043.
- Börnke F (2004) The variable C-terminus of 14-3-3 proteins mediates isoform-specific interaction with sucrose-phosphate synthase in the yeast two-hybrid system. *J. Plant Physiol.* 162: 161-168
- Bowerman AF, Newberry M, Dielen AS, Whan A, Larroque O, Pritchard J, Gubler F, Howitt CA, Pogson BJ, Morell MK and Ral JP (2016) Suppression of glucan, water dikinase in the endosperm alters wheat grain properties, germination and coleoptile growth. *Plant Biotechnol J* 14: 398–408
- Brandes HK, Hartman FC, Lu TYS and Larimer FW (1996) Efficient expression of the gene for spinach phosphoribulokinase in *Pichia pastoris* and utilization of the recombinant enzyme to explore the role of regulatory cysteinyl residues by site-directed mutagenesis. *J. Biol. Chem.* 271: 6490-6496.
- Brandes N, Schmitt S and Jakob U (2009) Thiol-based redox switches in eukaryotic proteins. *Antioxid. Redox Sign.* 11(5): 997-1014.
- Brennich ME, Kieffer J, Bonamis G, De Maria Antolinos A, Hutin S, Pernot P and Round A (2016) Online data analysis at the ESRF bioSAXS beamline, BM29. *J. Appl. Crystallogr.* 49: 203–212.
- Buchanan BB and Arnon DI (1990) A reverse KREBS cycle in photosynthesis: consensus at last. *Photosynth Res.* 24(1): 47–53.
- Buléon A, Colonna P, Planchota V, Ballb S (1998) Starch granules: structure and biosynthesis. *Int J Biol Macromol* 23: 85–112
- Burki, F, Kudryavtsev A, Matz MV, Aglyamova GV, Bulman S, Fiers M, Keeling PJ and Pawlowski J (2010) Evolution of Rhizaria: new insights from phylogenomic analysis of uncultivated protists. *BMC Evol. Biol.* 10: 377-395.
- Busch A and Hippler M (2011) The structure and function of eukaryotic photosystem I. *Biochim. Biophys. Acta* 1807:864–877.
- Bustos R, Fahy B, Hylton CM, Seale R, Nebane MN, Edwards A, Martin C and Smith AM (2004) *Proc. Natl. Acad. Sci. USA* 101(7):2215–2220
- von Caemmerer S and Furbank R (2003) The C 4 pathway: an efficient CO 2 pump. *Photosynth. Res.* 77: 191–207.
- Capitani G, Marković-Housley Z, DelVal G, Morris M, Jansonius JN and ürmann P (2000) Crystal structures of two functionally different thioredoxins in spinach chloroplasts. *J. Mol. Biol.* 302: 135-154.

- Carciofi M, Shaif SS, Jensen SL, Blennow A, Svensson JT, Vincze E and Hebelstrup KH (2011) Hyperphosphorylation of cereal starch. *J. Cereal Sci.* 54: 339–346.
- Carillo P, Feil R, Gibon Y, Satoh-Nagasawa N, Jackson D, Bläsing OE, Stitt M and Lunn JE (2013) A fluorometric assay for trehalose in the picomole range. *Plant Methods* 9:21.
- Carmo-Silva AE and Salvucci ME (2011) The activity of Rubisco's molecular chaperone, Rubisco activase, in leaf extracts. *Photosynth Res* 108:143–155.
- Carpaneto A, Geiger D, Bamberg E, Sauer N, Fromm J, Hedrich R (2005) Phloem-localized, proton-coupled sucrose carrier ZmSUT1 mediates sucrose efflux under the control of the sucrose gradient and the proton motive force. *J Biol. Chem.* 280(22): 21437–21443.
- Caspar T, Huber SC and Somerville C (1985) Alterations in growth, photosynthesis, and respiration in a starchless mutant of *Arabidopsis thaliana* (L.) deficient in chloroplast phosphoglucomutase activity *Plant Physiol.* 79: 11-17.
- Caspar T, Lin T-P, Monroe J, Bernhard W, Spilatro S, Preiss J, Somerville C (1989) Altered regulation of β -amylase activity in mutants of *Arabidopsis* with lesions in starch metabolism. *Proc. Natl. Acad. Sci. USA* 86: 5830–5833
- Chardot T and Meunier JC (1990) Fructose-1,6-bisphosphate and calcium activate oxidized spinach (*Spinacia oleracea*) chloroplast fructose-1,6-bisphosphatase. *Plant Sci.* 70:1-9.
- Charles SA and Halliwell B (1980) Action of calcium ions on spinach (*Spinacia oleracea*) chloroplast fructose bisphosphatase and other enzymes of the calvin cycle. *Biochem. J.* 188: 775-779.
- Charlier HA, Runquist JA and Mizioroko HM (1994) Evidence Supporting Catalytic Roles for Aspartate Residues in Phosphoribulokinase. *Biochemistry* 33:9343–9350.
- Chaves MM, Maroco JP and Pereira JS (2003) Understanding plant responses to drought - from genes to the whole plant. *Funct. Plant Biol.* 30: 239–264.
- Chaves MM, Flexas J and Pinheiro C (2009) Photosynthesis under drought and salt stress: regulation mechanisms from whole plant to cell. *Ann. Bot - London* 103: 551 –560.
- Chen C and Dickman MB (2005) Proline suppresses apoptosis in the fungal pathogen *Colletotrichum trifolii*. *Proc. Natl. Acad. Sci. USA* 102(9): 3459-3464.
- Chen S, Hajirezaei M and Börnke F (2005) Differential expression of sucrose-phosphate synthase isoenzymes in tobacco reflects their functional specialization during dark-governed starch mobilization in source leaves. *Plant Physiol.* 139: 1163–1174.
- Chen LQ, Hou BH, Lalonde S, Takanaga H, Hartung ML, Qu XQ, Guo WJ, Kim JG, Underwood W, Chaudhuri B, Chermak D, Antony G, White FF, Somerville SC, Mudgett MB and Frommer WB (2010a) Sugar transporters for intercellular exchange and nutrition of pathogens. *Nature* 468: 527-534.
- Chen VB, Arendall WB, Headd JJ, Keedy DA, Immormino RM, Kapral GJ, Murray LW, Richardson JS and Richardson DC (2010b) MolProbity: all-atom structure validation for macromolecular crystallography. *Acta Cryst. D Biol. Cryst.* 66: 12-21.
- Chen LQ, Qu XQ, Hou BH, Sosso D, Osorio S, Fernie AR and Frommer WB (2012) Sucrose efflux mediated by SWEET proteins as a key step for phloem transport. *Science* 335: 207-211.
- Cheng SH, Willmann WR, Chen HC and Sheen J (2002) Calcium signaling through protein kinases. The arabidopsis calcium-dependent protein kinase gene family. *Plant Physiol.* 129: 469-485.
- Chia T, Thorneycroft D, Chapple A, Messerli G, Chen J, Zeeman SC, Smith SM and Smith AM (2004) A cytosolic glucosyltransferase is required for conversion of starch to sucrose in *Arabidopsis* leaves at night. *Plant J.* 37: 853-863.
- Chiadmi M, Navaza A, Miginiac-Maslow M, Jacquot JP and Cherfils J (1999) Redox signalling in the chloroplast: structure of oxidized pea fructose-1,6- bisphosphate phosphatase. *EMBO J.* 18: 6809-6815

- Chinciska IA, Liesche J, Krügel U, Michalska J, Geigenberger P, Grimm B and Kühn C (2008) Sucrose transporter StSUT4 from potato affects flowering, tuberization, and shade avoidance response. *Plant Physiol.* 146: 515–528.
- Cho YH, Yoo SD and Sheen J (2006) Regulatory functions of nuclear hexokinase1 complex in glucose signaling. *Cell* 127:579–589.
- Cho JI, Ryoo N, JS Eom, Lee DW, Kim HB, Jeong SW, Lee YH, Kwon YK, Cho MH, Bhoo SH, Hahn TR, Park YI, Hwang I, Sheen J and Jeon JS (2009) Role of the rice hexokinases OsHXX5 and OsHXX6 as glucose sensors. *Plant Physiol.* 149: 745–759.
- Choudhary NL, Sairam RK and Tyagi A (2005) Expression of Δ 1-pyrroline-5-carboxylate synthetase gene during drought in rice (*Oryza sativa* L.). *Indian J. Biochem. Bio.* 42: 366-370.
- Ciais P, Denning AS, Tans PP, Berry JA, Randall DA, Collatz GJ, Sellers PJ, White SWC, Trolier M, Meijer HAJ, Francey RJ, Monfray P and Heimann M (1997) A three-dimensional synthesis study of δ^{18} of in atmospheric CO₂. *J. Geophys. Res.* 102(D5): 5857-5872.
- Claeysen E and Rivoal J (2007) Isozymes of plant hexokinase: Occurrence, properties and functions. *Phytochemistry* 68(6): 709-731.
- Clancy M and Hannah LC (2002) Splicing of the maize *Sh1* first intron is essential for enhancement of gene expression, and a T-rich motif increases expression without affecting splicing. *Plant Physiol.* 130: 918-929.
- Clapham DE (2007) Calcium Signaling. *Cell* 131: 147-158
- Cobbet C and Goldsbrought P (2002) Phytochelatins and Metallothioneins: Roles in heavy metal detoxification and homeostasis. *Annu. Rev. Plant Biol.* 53:159–82.
- Coleman HD, Yan J and Mansfield SD (2009) Sucrose synthase affects carbon partitioning to increase cellulose production and altered cell wall ultrastructure. *Proc. Natl. Acad. Sci. USA* 106 (31): 13118-13123.
- Comparot-Moss S and Denyer K (2009) The evolution of the starch biosynthetic pathway in cereals and other grasses. *J Exp. Bot.* 60: 2481–2492
- Covington MF, Maloof JB, Straume M, Kay SA and Harmer SL (2008) Global transcriptome analysis reveals circadian regulation of key pathways in plant growth and development. *Genom. Biol.* 9:R130.
- Couturier J, Chibani K, Jacquot JP and Rouhier N (2013) Cysteine-based redox regulation and signaling in plants. *Front. Plant Sci.* 4: 105.
- Cowtan, K. The Buccaneer software for automated model building. 1. Tracing protein chains. *Acta Cryst. D Biol. Cryst.* 62: 1002–1011.
- Cremers CM and Jakob U (2013) Oxidant sensing by reversible disulfide bond formation. *J. Biol. Chem.* 288 (37): 26489 –26496.
- Critchley JH, Zeeman SC, Takaha T, Smith AM and Smith SM (2001) A critical role for disproportionating enzyme in starch breakdown is revealed by a knock-out mutation in *Arabidopsis*. *Plant J.* 26(1): 89 - 100
- Crumpton-Taylor M, Pike M, Lu KL, Hylton CM, Feil R, Eicke S, Lunn JE, Zeeman SC and Smith SM (2013) Starch synthase 4 is essential for coordination of starch granule formation with chloroplast division during *Arabidopsis* leaf expansion. *New Phytol.* 200: 1064–1075.
- Cuellar-Ortiz SM, De La Paz Arrieta-Montiel M, Acosta-Gallegos J and Covarrubias AA (2008) Relationship between carbohydrate partitioning and drought resistance in common bean. *Plant Cell Environ.* 31: 1399-1409
- Cuesta-Seijo JA, Nielsen MM, Ruzanski C, Krucewicz K, Beeren SR, Rydhal MG, Yoshimura Y, Striebeck A, Motawia MS, Willats WGT and Palcic MM (2016) In vitro biochemical characterization of all barley endosperm starch synthases. *Front. Plant Sci.* 6:1265.

- Dai N, Schaffer A, Petreikov M, Shahak Y, Giller Y, Ratner K, Levine A, and Granot D (1999) Overexpression of arabidopsis hexokinase in tomato plants inhibits growth, reduces photosynthesis, and induces rapid senescence. *Plant Cell* 11: 1253–1266.
- Dai S, Wei X, Pei L, Thompson RL, Liu Y, Heard JE, Thomas G. Ruff and Beachy RN (2011) BROTHER OF LUX ARRHYTHMO is a component of the *Arabidopsis* circadian clock. *Plant Cell* 23(3): 961-971.
- Daloso DM, Medeiros DB, dos Anjos L, Yoshida T, Araujo WL and Fernie AR (2017) Metabolism within the specialized guard cells of plants. *New Phytol.* 216: 1018–1033.
- Damour G, Vandame M and Urban L (2008) Long-term drought modifies the fundamental relationships between light exposure, leaf nitrogen content and photosynthetic capacity in leaves of the lychee tree (*Litchi chinensis*). *J Plant Physiol.* 165: 1370—1378.
- Davies GJ, Gamblin SJ and Littlechild JA (1994) Structure of the ADP complex of the 3-phosphoglycerate kinase from *Bacillus stearothermophilus* at 1.65 Å. *Acta Cryst. D Biol. Cryst.* 50, 202-209.
- Debast S, Nunes-Nesi A, Hajirezaei MR, Hofmann J, Sonnewald U, Fernie AR and Börnke F (2011) Altering trehalose-6-phosphate content in transgenic potato tubers affects tuber growth and alters responsiveness to hormones during sprouting. *Plant Physiol.* 156: 1754-1771.
- Delatte T, Trevisan M, Parker ML and Zeeman SC (2005) Arabidopsis mutants Atisa1 and Atisa2 have identical phenotypes and lack the same multimeric isoamylase, which influences the branch point distribution of amylopectin during starch synthesis. *Plant J.* 41: 815-830.
- Delatte TL, Sedijani P, Kondou Y, Matsui M, de Jong GJ, Somsen GW, Wiese-Klinkenberg A, Primavesi LF, Paul MJ and Schluepmann H (2011) growth arrest by trehalose-6-phosphate: an astonishing case of primary metabolite control over growth by way of the SnRK1 signaling pathway. *Plant Physiol.* 157: 160-174.
- Del Giudice A, Pavel NV, Galantini L, Falini G, Trost P, Fermani S, Sparla F (2015) Unravelling the shape and structural assembly of the photosynthetic GAPDH-CP12-PRK complex from Arabidopsis thaliana by small-angle X-ray scattering analysis. *Acta Cryst. D Biol. Cryst.* 71: 2372–2385.
- Denyer K, Johnson P, Zeeman S, Smith AM (2001) The control of amylose synthesis. *J. Plant Physiol.* 158: 479-487.
- Dereeper A, Guignon V, Blanc G, Audic S, Buffet S, Chevenet F, Dufayard JF, Guindon S, Lefort V, Lescot M, Claverie JM, Gascuel O (2008) Phylogeny.fr: robust phylogenetic analysis for the non-specialist. *Nucleic Acids Res.* 36: 465-469.
- Deschamps P, Colleoni C, Nakamura Y, Suzuki E, Putaux JL, Buléon A, Haebel S, Ritte G, Steup M, Falcón LI, Moreira D, Löffelhardt W, Raj JN, Plancke C, d’Hulst C, Dauvillée D, Ball S (2008a) Metabolic symbiosis and the birth of the plant kingdom. *Mol. Biol. Evol.* 25: 536-548
- Deschamps P, Haferkamp I, d’Hulst C, Neuhaus HE, Ball SG (2008b) The relocation of starch metabolism to chloroplasts: when, why and how. *Trends Plant Sci* 13: 574-582
- Deschamps P, Moreau H, Worden AZ, Dauvillée D, Ball SG (2008c) Early gene duplication within chloroplastida and its correspondence with relocation of starch metabolism to chloroplasts. *Genetics* 178: 2373-2387
- Ding L, Lu Z, Gao L, Guo S and Shen Q (2018) Is Nitrogen a Key Determinant of Water Transport and Photosynthesis in Higher Plants Upon Drought Stress? *Front. Plant Sci.* 9:1143.
- Dixon DP, Skipsey M, Grundy NM and Edwards R (2005) Stress-induced protein S-Glutathionylation in Arabidopsis. *Plant Physiol.* 138(4): 2233-2244.
- Dixon LE, Knox K, Kozma-Bognar L, Southern MM, Pokhilko A and Millar AJ (2011) Temporal repression of core circadian genes is mediated through EARLY FLOWERING 3 in Arabidopsis. *Curr. Biol.* 21(2):120-125.
- Dodd AN, Salathia N, Hall A, Kévei E, Tóth R, Nagy F, Hibberd JM, Millar AJ and Webb AA (2005) Plant circadian clocks increase photosynthesis, growth, survival, and competitive advantage. *Science* 309(5734): 630-3.

- Duncan KA, Hardin SC and Huber SC (2006) The three maize sucrose synthase isoforms differ in distribution, localization, and phosphorylation. *Plant Cell Physiol.* 47(7): 959-71.
- Dunford RP, Durrant MC, Catley MA and Dyer TA (1998) Location of the redox-active cysteines in chloroplast sedoheptulose-1,7-bisphosphatase indicates that its allosteric regulation is similar but not identical to that of fructose-1,6-bisphosphatase
- Durek P, Schmidt R, Heazlewood JL, Jones A, MacLean D, Nagel A, Kersten B and Schulze WX (2010) PhosPhAt: the *Arabidopsis thaliana* phosphorylation site database. An update. *Nucleic Acids Res.* 38: D828-34.
- Edner C, Li J, Albrecht T, Mahlow S, Hejazi M, Hussain H, Kaplan F, Guy C, Smith SM, Steup M and Ritte G (2007) Glucan, water dikinase activity stimulates breakdown of starch granules by plastidial beta-amylases. *Plant Physiol.* 145: 17–28.
- Edwards R, Dixon DP, Walbot V (2000) Plant glutathione S-transferases: enzymes with multiple functions in sickness and in health. *Trends Plant Sci.* 5(5):193-198.
- Emsley P and Cowtan K (2004) Coot: model-building tools for molecular graphics. *Acta Cryst. D Biol. Cryst.* 60, 2126–2132 .
- Eom JS, Chen LQ, Sosso D, Julius BT, Lin IW, Qu XQ, Braun DM and Frommer WB (2015) SWEETs, transporters for intracellular and intercellular sugar translocation. *Curr. Opin. Plant Biol.* 25: 53-62.
- Erales J, Lignon S and Gontero B (2009) CP12 from *Chlamydomonas reinhardtii*, a permanent specific "chaperone-like" protein of glyceraldehyde-3-phosphate dehydrogenase. *J. Biol. Chem.* 284(19): 12735-12744.
- Ettinger WF, Clear AM, Fanning KJ and Peck ML (1991) Identification of a Ca²⁺/H⁺ antiport in the plant chloroplast thylakoid membrane. *Plant Physiol.* 119(4): 1379-86.
- Evans MCW, Buchanan BB and Arnon DI (1966) A new ferredoxin-dependent carbon reduction cycle in a photosynthetic bacterium. *Biochemistry* 55: 928-034.
- Evans P (2006) Scaling and assessment of data quality. *Acta Cryst. D Biol. Cryst.* 62, 72–82.
- Facette MR, Shen Z, Björnsdóttir FR, Briggs SP and Smith LG. (2013) Parallel proteomic and phosphoproteomic analyses of successive stages of maize leaf development. *Plant Cell.* 25(8): 2798-812.
- Fadzilla NM, Finch RP and Burdon RH (1997) Salinity, oxidative stress and antioxidant responses in shoot cultures of rice. *J. Exp. Bot.* 48(307): 325-331.
- Fan RC, Peng CC, Xu YH, Wang XF, Li Y, Shang Y, Du SY, Zhao R, Zhang XY, Zhang LY and Zhang DP (2009) Apple sucrose transporter SUT1 and sorbitol transporter SOT6 interact with cytochrome b5 to regulate their affinity for substrate sugars. *Plant Physiol.* 150(4):1880-901.
- Fankhauser C and Staiger D (2002) Photoreceptors in *Arabidopsis thaliana* : light perception, signal transduction and entrainment of the endogenous clock. *Planta* 216: 1–16.
- Farnese FS, Menezes-Silva PE, Gusman GS and Oliveira JA (2016) When bad guys become good ones: the key role of reactive oxygen species and nitric oxide in the plant responses to abiotic stress. *Front. Plant Sci.* 7:471.
- Farooq M, Wahid A, Kobayashi N, Fujita D and Basra SMA(2009) Plant drought stress: effects, mechanisms and management. *Agron. Sustain. Dev.* 29: 185–212
- Farré EM and Weise SE (2012) The interactions between the circadian clock and primary metabolism. *Curr. Opin. Plant Biol.* 15(3): 293-300.
- Farré EM and Liu T (2013) The PRR family of transcriptional regulators reflects the complexity and evolution of plant circadian clocks. *Curr. Opin. Plant Biol.* 16(5):621-629.

- Feike D, Seung D, Graf A, Bischof S, Ellick T, Coiro M, Soyk S, Eicke S, Mettler-Altmann T, Lu KJ, Trick M, Zeeman SC and Smith AM (2016) The Starch Granule-Associated Protein EARLY STARVATION1 Is Required for the Control of Starch Degradation in *Arabidopsis thaliana* Leaves. *Plant Cell* 28(6):1472-89
- Feldbrügge M, Arizti P, Sullivan ML, Zamore PD, Belasco JG and Green PJ (2002) Comparative analysis of the plant mRNA-destabilizing element, DST, in mammalian and tobacco cells. *Plant Mol Biol.* 49(2): 215-23.
- Feng J, Zhao S, Chen X, Wang W, Dong W, Chen J, Shen JR, Liu L and Kuang T (2015) Biochemical and structural study of *Arabidopsis* hexokinase 1. *Acta Cryst. D Biol. Cryst.* 71(Pt 2): 367-75.
- Fermani S, Sparla F, Marri L, Thumiger A, Pupillo P, Falini G, Trost P (2010) The crystal structure of photosynthetic glyceraldehyde-3-phosphate dehydrogenase (isoform A4) from *Arabidopsis thaliana* in complex with NAD. *Acta Crystallog. F* 66: 621-626.
- Fettke J, Eckermann N, Poeste S, Pauly M and Steup M (2004) The glycan substrate of the cytosolic (Pho 2) phosphorylase isozyme from *Pisum sativum* L.: identification, linkage analysis and subcellular localization. *Plant J.* 39(6):933-46.
- Fettke J, Eckermann N, Tiessen A, Geigenberger P and Steup M (2005a) Identification, subcellular localization and biochemical characterization of water-soluble heteroglycans (SHG) in leaves of *Arabidopsis thaliana* L.: distinct SHG reside in the cytosol and in the apoplast. *Plant J.* 43(4):568-85.
- Fettke J, Poeste S, Eckermann N, Tiessen A, Pauly M, Geigenberger P and Steup M. (2005b) Analysis of cytosolic heteroglycans from leaves of transgenic potato (*Solanum tuberosum* L.) plants that under- or overexpress the Pho 2 phosphorylase isozyme. *Plant Cell Physiol.* 46(12):1987-2004.
- Fettke J, Chia T, Eckermann N, Smith A and Steup M (2006) A transglucosidase necessary for starch degradation and maltose metabolism in leaves at night acts on cytosolic heteroglycans (SHG). *Plant J.* 46(4):668-84.
- Figueroa CM, Feil R, Ishihara H, Watanabe M, Kölling K, Krause U, Höhne M, Encke B, Plaxton WC, Zeeman SC, Li Z, Schulze WX, Hoefgen R, Stitt M and Lunn JE (2016) Trehalose 6-phosphate coordinates organic and amino acid metabolism with carbon availability. *Plant J.*85(3): 410-423.
- Figueroa CM and Lunn JE (2016) A Tale of Two Sugars: Trehalose 6-Phosphate and Sucrose. *Plant Physiol.* 172(1): 7-27.
- Flügge UI, Weber A, Fischer K, Lottspeich F, Eckerskorn C, Waegemann K and Soll J (1991) The major chloroplast envelope polypeptide is the phosphate translocator and not the protein import receptor. *Nature* 353: 364-367.
- Fondy BR, Geiger DR and Servaites JC (1989) Photosynthesis, Carbohydrate Metabolism, and Export in *Beta vulgaris* L. and *Phaseolus vulgaris* L. during Square and Sinusoidal Light Regimes. *Plant Physiol.* 89(2):396-402.
- Fox AR, Barberini ML, Ploschuk EL, Muschietti JP and Mazzella MA (2015) A proteome map of a quadruple photoreceptor mutant sustains its severe photosynthetic deficient phenotype. *J. Plant Physiol.* 185:13-23.
- Foyer CH and Noctor G (2003) Redox sensing and signalling associated with reactive oxygen in chloroplasts, peroxisomes and mitochondria. *Physiol. Plantarum* 119(3): 55-364
- Foyer CH and Noctor G (2005) Redox homeostasis and antioxidant signaling: a metabolic interface between stress perception and physiological responses. *Plant Cell* 17: 1866-1875
- Foyer CH and Noctor G (2009) Redox regulation in photosynthetic organisms: signaling, acclimation, and practical implications. *Antioxid. Redox Sign.* 11(4): 861-905
- Foyer CH and Noctor G (2011) Ascorbate and glutathione: the heart of the redox hub. *Plant Physiol.*155: 2-18.
- Foyer CH and Noctor G (2016) Stress-triggered redox signalling: what's in pROSpect? *Plant Cell Environ.* 39(56): 951-964

- Franke D, Jeffries CM and Svergun DI (2015) Correlation Map, a goodness-of-fit test for one-dimensional X-ray scattering spectra. *Nat. Methods* 12: 419-422.
- Franke D, Petoukhov MV, Konarev PV, Panjkovich A, Tuukkanen A, Mertens HDT, Kikhney AG, Hajizadeh NR, Franklin JM, Jeffries CM and Svergun DI (2017) ATSAS 2.8: A comprehensive data analysis suite for small-angle scattering from macromolecular solutions. *J. Appl. Crystallogr.* 50: 1212-1225.
- Friedrich CG, Bardischewsky F, Rother D, Quentmeier A and Fischer J (2005) Prokaryotic sulfur oxidation. *Curr. Opin. Microbiol.* 8(3): 253-9.
- Fu Y, Ballicora MA, Leykam JF and Preiss J (1998) Mechanism of reductive activation of potato tuber ADP-glucose pyrophosphorylase. *J. Biol. Chem.* 273(39): 25045-52.
- Fuchs G (2011) Alternative pathways of carbon dioxide fixation: insights into the early evolution of life? *Annu. Rev. Microbiol.* 65: 631-658
- Fujiwara S, Wang L, Han L, Suh SS, Salomé PA, McClung CR and Somers DE (2008) Post-translational regulation of the Arabidopsis circadian clock through selective proteolysis and phosphorylation of pseudo-response regulator proteins. *J. Biol. Chem.* 283(34): 23073-23083.
- Fulton DC, Stettler M, Mettler T, Vaughan CK, Li J, Francisco P, Gil M, Reinhold H, Eicke S, Messerli G, Dorken G, Halliday K, Smith AM, Smith SM and Zeeman SC (2008) Beta-AMYLASE4, a noncatalytic protein required for starch breakdown, acts upstream of three active beta-amylases in Arabidopsis chloroplasts. *Plant Cell.* 20(4): 1040-1058
- Gallogly MM, Starke DW, Leonberg AK, Ospina SM and Mieyal JJ (2008) Kinetic and mechanistic characterization and versatile catalytic properties of mammalian glutaredoxin 2: implications for intracellular roles. *Biochemistry* 47(42): 11144-11157
- Gao J, van Kleeff PJ, Oecking C, Li KW, Erban A, Kopka J, Hinch DK and de Boer AH (2014) Light-modulated activity of root alkaline/neutral invertase involves the interaction with 14-3-3 proteins. *Plant J.* 80: 785-796.
- Gardian Z, Bumba L, Schrofel A, Herbstova M, Nebesarova J and Vacha F (2007) Organisation of Photosystem I and Photosystem II in red alga *Cyanidium caldarium*: encounter of cyanobacterial and higher plant concepts. *Biochim. Biophys. Acta.* 1767(6): 725-31.
- Garg AK, Kim JK, Owens TG, Ranwala AP, Choi YD, Kochian LV and Wu RJ (2002) Trehalose accumulation in rice plants confers high tolerance levels to different abiotic stresses. *Proc. Natl. Acad. Sci. USA* 99(25):15898-903.
- Geigenberger P, Thormählen I, Daloso DM and Fernie AR (2017) The unprecedented versatility of the plant thioredoxin system. *Trends Plant Sci.* 22(3): 249-262. *Plant Physiol.* 154(1): 55-66.
- George GM, van der Merwe MJ, Nunes-Nesi A, Bauer R, Fernie AR, Kossmann J and Lloyd JR (2010) Virus-induced gene silencing of plastidial soluble inorganic pyrophosphatase impairs essential leaf anabolic pathways and reduces drought stress tolerance in *Nicotiana benthamiana*.
- Gendron JM, Pruneda-Paz JL, Doherty CJ, Gross AM, Kang SE and Kay SA (2012) Arabidopsis circadian clock protein, TOC1, is a DNA-binding transcription factor. *Proc. Natl. Acad. Sci. USA* 109(8): 3167-72.
- Germano M, Yakushevskaya AE, Keegstra W, van Gorkom HJ, Dekker JP and Boekema EJ (2002) Supramolecular organization of photosystem I and light-harvesting complex I in *Chlamydomonas reinhardtii*. *FEBS Lett.* 525(1-3): 121-125.
- Gibon Y, Bläsing OE, Palacios-Rojas N, Pankovic D, Hendriks JH, Fisahn J, Höhne M, Günther M and Stitt M. (2004) Adjustment of diurnal starch turnover to short days: depletion of sugar during the night leads to a temporary inhibition of carbohydrate utilization, accumulation of sugars and post-translational activation of ADP-glucose pyrophosphorylase in the following light period. *Plant J.* 39(6): 847-862.
- Glaring MA, Zygadlo A, Thorneycroft D, Schulz A, Smith SM, Blennow A, Baunsgaard L (2007) An extra-plastidial alpha-glucan, water dikinase from Arabidopsis phosphorylates amylopectin in vitro and is not necessary for transient starch degradation. *J. Exp. Bot.* 58: 3949-3960

- Glaring MA, Skryhan K, Kötting O, Zeeman SC and Blennow A. (2012) Comprehensive survey of redox sensitive starch metabolising enzymes in *Arabidopsis thaliana*. *Plant Physiol. Biochem.* 58: 89-97.
- Godfray HC1, Beddington JR, Crute IR, Haddad L, Lawrence D, Muir JF, Pretty J, Robinson S, Thomas SM and Toulmin C (2010) Food security: the challenge of feeding 9 billion people. *Science* 327: 812–818.
- Gonzales-Cruz J and Pastenes C (2012) Water-stress-induced thermotolerance of photosynthesis in bean (*Phaseolus vulgaris* L.) plants: The possible involvement of lipid composition and xanthophyll cycle pigments. *Environ. Exp. Bot.* 77: 127–140.
- Gössner AS, Devereux R, Ohnemüller N, Acker G, Stackebrandt E and Drake HL (1999) *Thermicanus aegyptius* gen. nov., sp. nov., isolated from oxic soil, a fermentative microaerophile that grows commensally with the thermophilic acetogen *Moorella thermoacetica*. *Appl. Environ. Microbiol.* 65(11): 5124-33.
- Goyal A (2007) Osmoregulation in *Dunaliella*, Part II: Photosynthesis and starch contribute carbon for glycerol synthesis during a salt stress in *Dunaliella tertiolecta*. *Plant Physiol. Biochem.* 45(9): 705-10.
- Graber JR and Breznak JA (2004) Physiology and nutrition of *Treponema primitia*, an H₂/CO₂-acetogenic spirochete from termite hindguts. *Appl. Environ. Microbiol.* 70(3): 1307-14.
- Graciet E, Gans P, Wedel N, Lebreton S, Camadro JM and Gontero B. (2003) The small protein CP12: a protein linker for supramolecular complex assembly *Biochemistry* 42: 8163–8170.
- Graf A, Schlereth A, Stitt M and Smith AM (2010) Circadian control of carbohydrate availability for growth in *Arabidopsis* plants at night. *Proc. Natl. Acad. Sci. USA* 107(20): 9458-9463.
- Graham IA, Denby KJ and Leaver CJ (1994) Carbon Catabolite Repression Regulates Glyoxylate Cycle Gene Expression in Cucumber. *Plant Cell.* 6(5): 761-772.
- Grimaud F, Rogniaux H, James MG, Myers AM and Planchot V (2008) Proteome and phosphoproteome analysis of starch granule-associated proteins from normal maize and mutants affected in starch biosynthesis. *J. Exp. Bot.* 59(12): 3395-3406.
- Guidi L, Bonghi G, Ciompi S, Soldatini GF (1999) In *Vicia faba* leaves photoinhibition from ozone fumigation in light precedes a decrease in quantum yield of functional PSII centres. *J. Plant Physiol.* 154: 167-172.
- Guinier A (1939) La Diffraction des rayons x aux très petits angles: application à l'étude des phénomènes ultramicroscopiques. *Ann. Phys.* 12: 161–237.
- Güttele DD, Roret T, Müller SJ, Couturier J, Lemaire SD, Hecker A, Dhalleine T, Buchanan BB, Reski R, Einsle O and Jacquot JP (2016) Chloroplast FBPase and SBPase are thioredoxin-linked enzymes with similar architecture but different evolutionary histories. *Proc. Natl. Acad. Sci. USA* 113: 6779–6784.
- Gzik A (1996) Accumulation of proline and pattern of α -amino acids in sugar beet plants in response to osmotic, water and salt stress. *Environ. Exp. Bot.* 36(1): 29-38.
- Hackenberg C, Hakanpää J, Cai F, Antonyuk S, Eigner C, Meissner S, Laitaoja M, Jänis J, Kerfeld CA, Dittmann E, Lamzin VS (2018) Structural and functional insights into the unique CBS-CP12 fusion protein family in cyanobacteria. *Proc. Natl. Acad. Sci. USA* 115(27): 7141-7146.
- Hädrich N, Hendriks JH, Kötting O, Arrivault S, Feil R, Zeeman SC, Gibon Y, Schulze WX, Stitt M and Lunn JE (2012) Mutagenesis of cysteine 81 prevents dimerization of the APS1 subunit of ADP-glucose pyrophosphorylase and alters diurnal starch turnover in *Arabidopsis thaliana* leaves. *Plant J.* 70(2): 231-242.
- Hagemann M and Pade N (2015) Heterosides - compatible solutes occurring in prokaryotic and eukaryotic phototrophs. *Plant. Biol. (Stuttg)* 17(5): 927-934.
- Halford NG, Hey S, Jhurrea D, Laurie S, McKibbin RS, Paul M and Zhang Y. (2003) Metabolic signalling and carbon partitioning: role of Snf1-related (SnRK1) protein kinase. *J. Exp. Bot.* 54(382): 467-475.

- Hallenbeck PL and Kaplan S (1987) Cloning of the gene for phosphoribulokinase activity from *Rhodobacter sphaeroides* and its expression in *Escherichia coli*. *J. Bacteriol.* 169: 3669-3678.
- Hanson KR and McHale NA (1988) A starchless mutant of *Nicotiana sylvestris* containing a modified plastid phosphoglucomutase. *Plant Physiol.* 88(3): 838-844.
- Hardin SC, Tang GQ, Scholz A, Holtgraewe D, Winter H and Huber SC (2003) Phosphorylation of sucrose synthase at serine 170: occurrence and possible role as a signal for proteolysis. *Plant J.* 35(5): 588-603.
- Harrison DH, Runquist JA, Holub A and Mizioro HM (1998) The crystal structure of phosphoribulokinase from *Rhodobacter sphaeroides* reveals a fold similar to that of adenylate kinase. *Biochemistry* 37: 5074–5085.
- Hasanuzzaman M, Nahar K, Anee TI and Fujita M (2017) Glutathione in plants: biosynthesis and physiological role in environmental stress tolerance. *Physiol. Mol. Biol. Plants* 23(2): 249-268.
- Hayes MA, Feechan A and Dry IB (2010) Involvement of abscisic acid in the coordinated regulation of a stress-inducible hexose transporter (VvHT5) and a cell wall invertase in grapevine in response to biotrophic fungal infection. *Plant Physiol.* 153(1): 211-21.
- He H, Chincinska I, Hackel A, Grimm B and Christina Kühn C (2008) Phloem mobility and stability of sucrose transporter transcripts. *The Open Plant Science Journal* 2: 1-14.
- Hedderich R and Forzi L (2005) Energy-converting [NiFe] hydrogenases: more than just H₂ activation. *J. Mol. Microbiol. Biotechnol.* 10(2-4):92-104.
- Heim S, Künkel A, Thauer RK and Hedderich R (1998) Thiol: fumarate reductase (Tfr) from *Methanobacterium thermoautotrophicum* Identification of the catalytic sites for fumarate reduction and thiol oxidation. *Eur. J. Biochem.* 253: 292-299.
- Heise R, Müller V and Gottschalk G (1989) Sodium dependence of acetate formation by the acetogenic bacterium *Acetobacterium woodii*. *J. Bacteriol.* 171(10):5473-8.
- Hejazi M, Steup M, Fettke J (2012) The plastidial glucan, water dikinase (GWD) catalyses multiple phosphotransfer reactions. *FEBS J* 279: 1953–1966.
- Hejazi M, Mahlow S, Fettke J (2014) The glucan phosphorylation mediated by α -glucan, water dikinase (GWD) is also essential in the light phase for a functional transitory starch turn-over. *Plant Signal. Behav.* 9: e28892.
- Helfer A, Nusinow DA, Chow BY, Gehrke AR, Bulyk ML and Kay SA (2011) LUX ARRHYTHMO encodes a nighttime repressor of circadian gene expression in the Arabidopsis core clock. *Curr. Biol.* 21(2): 126-33.
- Henry C, Bledsoe SW, Siekman A, Kollman A, Waters BM, Feil R, Stitt M and Lagrimini LM (2014) The trehalose pathway in maize: conservation and gene regulation in response to the diurnal cycle and extended darkness. *J. Exp. Bot.* 65(20): 5959-73.
- Hernandez JA, Corpass FJ, Gomez M, del Rio LA and Sevilla F (1993) Salt-induced oxidative stress mediated by active oxygen species in pea leaf mitochondria. *Physiol. Plant.* 89: 103–110.
- Heron PW and Sygusch J (2017) Isomer activation controls stereospecificity of class I fructose-1,6-bisphosphate aldolases. *J. Biol. Chem.* 292: 19849-19860.
- Herrero E, Kolmos E, Bujdoso N, Yuan Y, Wang M, Berns MC, Uhlworm H, Coupland G, Saini R, Jaskolski M, Webb A, Gonçalves J and Davis SJ (2012) EARLY FLOWERING4 recruitment of EARLY FLOWERING3 in the nucleus sustains the Arabidopsis circadian clock. *Plant Cell.* 24(2): 428-443.
- Herter S, Fuchs G, Bacher A, Eisenreich W (2002) A bicyclic autotrophic CO₂ fixation pathway in *Chloroflexus aurantiacus*. *J. Biol. Chem.* 277(23): 20277-20283.
- Herting CM and Wolosiuk RA (1983) Studies on the hysteretic properties of chloroplast fructose-1,6-bisphosphatase. *J. Biol. Chem.* 258(2): 984-989.

- Hirose T, Scofield GN and Terao T (2008) An expression analysis profile for the entire sucrose synthase gene family in rice. *Plant Sci.* 174: 534–543.
- Hirose T, Aoki N, Harada Y, Okamura M, Hashida Y, Ohsugi R, Akio M, Hirochika H and Terao T (2013) Disruption of a rice gene for alpha-glucan water dikinase, OsGWD1, leads to hyperaccumulation of starch in leaves but exhibits limited effects on growth. *Front. Plant Sci.* 4: 147
- Hohmann-Marriott MF and Blankenship RE (2011) Evolution of photosynthesis. *Annu. Rev. Plant Biol.* 62: 515–548.
- Horrer D, Flütsch S, Pazmino D, Matthews JS, Thalmann M, Nigro A, Leonhardt N, Lawson T and Santelia D (2016) Blue light induces a distinct starch degradation pathway in guard cells for stomatal opening. *Curr. Biol.* 26(3): 362-370.
- Houston K, Tucker MR, Chowdhury J, Shirley N and Little A (2016) The plant cell wall: a complex and dynamic structure as revealed by the responses of genes under stress conditions. *Front. Plant Sci.* 7:984.
- Hsu PY and Harmer SL (2014) Wheels within wheels: the plant circadian system. *Trends Plant Sci.* 19(4): 240-9.
- Huang JZ and Huber SC (2001) phosphorylation of synthetic peptides by a cdpk and plant snf1-related protein kinase. Influence of proline and basic amino acid residues at selected positions. *Plant Cell Physiol.* 42(10): 1079–1087.
- Huang LF, Bocock PN, Davis JM and Koch KE (2007) Regulation of invertase: a suite of transcriptional and post-transcriptional mechanisms. *Funct Plant Biol* 34:499–507.
- Huang T and Jander G (2017) Abscisic acid-regulated protein degradation causes osmotic stress-induced accumulation of branched-chain amino acids in *Arabidopsis thaliana*. *Planta* 246(4): 737-747.
- Huber SC, Huber JL, Liao PC, Gage DA, McMichael RW Jr, Chourey PS, Hannah LC and Koch K (1996) Phosphorylation of serine-15 of maize leaf sucrose synthase. Occurrence in vivo and possible regulatory significance. *Plant Physiol.* 112(2): 793-802.
- Huber SC and Huber JL (1996) Role and regulation of sucrose-phosphate synthase in higher plants. *Annu. Rev. Plant Physiol. Plant Mol. Biol.* 47: 431–444.
- Huber H, Gallenberger M, Jahn U, Eylert E, Berg IA, Kockelkorn D, Eisenreich W and Fuchs G (2008) A dicarboxylate/4-hydroxybutyrate autotrophic carbon assimilation cycle in the hyperthermophilic archaeum *Ignicoccus hospitalis*. *Proc. Natl. Acad. Sci. USA* 105: 7851–56.
- Huang W, Pérez-García P, Pokhilko A, Millar AJ, Antoshechkin I, Riechmann JL and Mas P (2012) Mapping the core of the Arabidopsis circadian clock defines the network structure of the oscillator. *Science* 336(6077): 75-79.
- Hummel I, Pantin F, Sulpice R, Piques M, Rolland G, Dauzat M, Christophe A, Pervent M, Bouteillé M, Stitt M, Gibon Y and Muller B (2010) Arabidopsis plants acclimate to water deficit at low cost through changes of carbon usage: an integrated perspective using growth, metabolite, enzyme, and gene expression analysis. *Plant Physiol.* 154(1): 357-372.
- Iglesias aa and preiss j (1992) Characterization of the allosteric activatory site(s) of ADP-glucose pyrophosphorylase from *Synechocystis* PCC 6803. *FASEB J.* 6(1): A62-A62
- Ito H, Iwabuchi M and Ogawa K. (2003) The sugar-metabolic enzymes aldolase and triose-phosphate isomerase are targets of glutathionylation in *Arabidopsis thaliana*: detection using biotinylated glutathione. *Plant Cell Physiol.* 44(7): 655-60.
- James AB, Syed NH, Bordage S, Marshall J, Nimmo GA, Jenkins GI, Herzyk P, Brown JW and Nimmo HG (2012) Alternative splicing mediates responses of the arabidopsis circadian clock to temperature changes. *Plant Cell* 24(3): 961-981.
- Jang JC and Sheen J (1994) Sugar sensing in higher plants. *Plant Cell* 6(11): 1665-1679.
- Janská A, Marsík P, Zelenková S and Ovesná J (2010) Cold stress and acclimation – what is important for metabolic adjustment? *Plant Biol. (Stuttg)* 12(3): 395-405.

- Jacquot JP, Lopez-Jaramillo J, Chueca A, Cherfils J, Lemaire S, Chedozeau B, Miginiac-Maslow M, Decottignies P, Wolosiuk R and Lopez-Gorge J (1995) High-level expression of recombinant pea chloroplast fructose-1,6-bisphosphatase and mutagenesis of its regulatory site. *Eur. J. Biochem.* 229(3): 675-681.
- Jacquot JP, Lopez-Jaramillo J, Miginiac-Maslow M, Lemaire S, Cherfils J, Chueca A and Lopez-Gorge J (1997) *FEBS Lett.* 401(2-3): 143-647.
- Jin Y1, Ni DA and Ruan YL (2009) Posttranslational elevation of cell wall invertase activity by silencing its inhibitor in tomato delays leaf senescence and increases seed weight and fruit hexose level. *Plant Cell* 21(7): 2072-2089.
- Johnson CH, Knight MR, Kondo T, Masson P, Sedbrook J, Haley A and Trewavas A (1995) Circadian oscillations of cytosolic and chloroplastic free calcium in plants. *Science* 269(5232):1863-1865.
- Jones TL and Ort DR (1997) Circadian regulation of sucrose phosphate synthase activity in tomato by protein phosphatase activity. *Plant Physiol.* 113(4): 1167-1175.
- Jordan DB and Ogren WL (1984) The CO₂/O₂ specificity of ribulose 1,5-bisphosphate carboxylase/oxygenase. *Planta* 161(4): 308-313.
- Jubany-Mari T, Alegre-Batlle L, Jiang K and Feldman LJ (2010) Use of a redox-sensing GFP (c-roGFP1) for real-time monitoring of cytosol redox status in Arabidopsis thaliana water-stressed plants. *FEBS Lett.* 584(5): 889-897.
- Juge N, Andersen JS, Tull D, Roepstorff P and Svensson B (1996) Overexpression, purification, and characterization of recombinant barley alpha-amylases 1 and 2 secreted by the methylotrophic yeast *Pichia pastoris*. *Protein Expr. Purif.* 8(2): 204-14.
- Julius BT, Leach KA, Tran TM1, Mertz RA and Braun DM (2017) Sugar transporters in plants: new insights and discoveries. *Plant Cell Physiol.* 58(9): 1442-1460.
- Kabsch W (2010) XDS. *Acta Cryst. D Biol. Cryst.* 66: 125-132.
- Kadziola A, Abe J, Svensson B and Haser R (1994) Crystal and molecular structure of barley alpha-amylase. *J. Mol. Biol.* 239: 104-121.
- Kamlage B, Gruhl B and Blaut M (1997) Isolation and characterization of two new homoacetogenic hydrogen-utilizing bacteria from the human intestinal tract that are closely related to *Clostridium coccooides*. *Appl. Environ. Microbiol.* 63(5): 1732-8.
- Kano A, Fukumoto T, Ohtani K, Yoshihara A, Ohara T, Tajima S, Izumori K, Tanaka K, Ohkouchi T, Ishida Y, Nishizawa Y, Ichimura K, Tada Y, Gomi K, Akimitsu K (2013) The rare sugar D-allose acts as a triggering molecule of rice defense via ROS generation. *J. Exp. Bot.* 64: 4939-4951.
- Kaplan F and Guy CL (2004) β -Amylase induction and the protective role of maltose during temperature shock. *Plant Physiol.* 135(3): 1674-1684.
- Kaplan F and Guy CL (2005) RNA interference of Arabidopsis beta-amylase8 prevents maltose accumulation upon cold shock and increases sensitivity of PSII photochemical efficiency to freezing stress. *Plant J.* 44(5):730-743.
- Kasamatsu S, Nishimura A, Morita M, Matsunaga T, Abdul Hamid H and Akaike T (2016) Redox Signaling Regulated by Cysteine Persulfide and Protein Polysulfidation. *Molecules* 21(12) pii: E1721.
- Kelly G, Moshelion M, David-Schwartz R, Halperin O, Wallach R, Attia Z, Belausov E and Granot D (2013) Hexokinase mediates stomatal closure. *Plant J.* 75(6): 977-88.
- Kerr PS, Rufty TW and Huber SC. (1985) Endogenous rhythms in photosynthesis, sucrose phosphate synthase activity, and stomatal resistance in leaves of soybean (*Glycine max* [L.] Merr.). *Plant Physiol.* 77(2): 275-80
- Khan TA, Yusuf M and Fariduddin Q (2018) Hydrogen peroxide in regulation of plant metabolism: Signalling and its effect under abiotic stress. *Photosynthetica* 56 (4): 1237-1248.

- Kim YM, Heinzel N, Giese JO, Koeber J, Melzer M, Rutten T, von Wirén N, Sonnewald U and Hajirezaei MR (2013) A dual role of tobacco hexokinase 1 in primary metabolism and sugar sensing. *Plant Cell Environ.* 36: 1311–1327
- Kloosterman B, Abelenda JA, Gomez Mdel M, Oortwijn M, de Boer JM, Kowitzanich K, Horvath BM, van Eck HJ, Smaczniak C, Prat S, Visser RG and Bachem CW (2013) Naturally occurring allele diversity allows potato cultivation in northern latitudes. *Nature* 495(7440): 246–50.
- Kobayashi D, Tamoi M, Iwaki T, Shigeoka S and Wadano A (2003) Molecular characterization and redox regulation of phosphoribulokinase from the cyanobacterium *Synechococcus* sp. PCC 7942. *Plant Cell Physiol.* 44: 269–276.
- Koch KE (1996) Carbohydrate-modulated gene expression in plants. *Annu. Rev. Plant Physiol. Plant Mol. Biol.* 47:509–40.
- Koch KE, Ying Z, Wu Y and Avigne WT (2000) Multiple paths of sugar-sensing and a sugar/oxygen overlap for genes of sucrose and ethanol metabolism. *J. Exp. Bot.* 51 Spec No: 417–27.
- Koch K (2004) Sucrose metabolism: regulatory mechanisms and pivotal roles in sugar sensing and plant development. *Curr. Opin. Plant Biol.* 7(3): 235–46.
- Kolbe A, Tiessen A, Schluempmann H, Paul M, Ulrich S and Geigenberger P (2005) Trehalose 6-phosphate regulates starch synthesis via posttranslational redox activation of ADP-glucose pyrophosphorylase. *Proc Natl Acad Sci USA* 102(31): 11118–11123.
- Kono T, Mehrotra S, Endo C, Kizu N, Matusda M, Kimura H, Mizohata E, Inoue T, Hasunuma T, Yokota A, Matsumura H and Ashida H. (2017) A RuBisCO-mediated carbon metabolic pathway in methanogenic archaea. *Nat. Commun.* 8: 14007.
- Kopp J, Kopriva S, Süß KH and Schulz GE (1999) Structure and mechanism of the amphibolic enzyme D-ribulose-5-phosphate 3- epimerase from potato chloroplasts. *J. Mol. Biol.* 287: 761–771.
- Kossmann J, Klintworth R and Bowien B (1989) Sequence analysis of the chromosomal and plasmid genes encoding phosphoribulokinase from *Alcaligenes eutrophus*. *Gene* 85: 247–252.
- Kötting O, Santelia D, Edner C, Eicke S, Marthaler T, Gentry MS, Comparot-Moss S, Chen J, Smith AM, Steup M, Ritte G and Zeeman SC (2004) STARCH-EXCESS4 is a laforin-like Phosphoglucan phosphatase required for starch degradation in *Arabidopsis thaliana*. *Plant Cell* 21(1): 334–46.
- Kötting O, Pusch K, Tiessen A, Geigenberger P, Steup M and Ritte G (2005) Identification of a novel enzyme required for starch metabolism in *Arabidopsis* leaves. The phosphoglucan, water dikinase. *Plant Physiol.* 137: 242–252
- Kötting O, Santelia D, Edner C, Eicke S, Marthaler T, Gentry MS, Comparot-Moss S, Chen J, Smith AM, Steup M, Ritte G and Zeeman SC (2009) STARCH-EXCESS4 is a laforin-like phosphoglucan phosphatase required for starch degradation in *Arabidopsis thaliana*. *Plant Cell* 21: 334–346.
- Kozin MB and Svergun DI (2001) Automated matching of high- and low-resolution structural models. *J. Appl. Crystallogr.* 34: 33–41.
- Kouchi H, Takane K, So RB, Ladha JK, Reddy PM (1999) Rice ENOD40: isolation and expression analysis in rice and transgenic soybean root nodules. *Plant J.* 18(2): 121–9.
- Krasensky J and Jonak C (2012) Drought, salt, and temperature stress-induced metabolic rearrangements and regulatory networks. *J. Exp. Bot.* 63(4): 1593–1608.
- Krishnan N, Dickman MB and Becker DF (2008) Proline modulates the intracellular redox environment and protects mammalian cells against oxidative stress. *Free Radic. Biol. Med.* 44(4): 671–81.
- Krügel U, Veenhoff LM, Langbein J, Wiederhold E, Liesche J, Friedrich T, Grimm B, Martinoia E, Poolman B and Kühn C (2008) Transport and sorting of the solanum tuberosum sucrose transporter SUT1 is affected by posttranslational modification. *Plant Cell* 20(9):2497–2513.

- Krügel U and Kühn C (2013) Post-translational regulation of sucrose transporters by direct protein–protein interactions. *Front. Plant Sci.* 4:237.
- Kühn C and Grof CP (2010) Sucrose transporters of higher plants. *Curr. Opin. Plant Biol.* 13(3): 288-298.
- Kung G, Runquist JA, Mizioroko HM and Harrison DH (1999) Identification of the allosteric regulatory site in bacterial phosphoribulokinase. *Biochemistry* 38: 15157–15165.
- Kuromori T, Seo M and Shinozaki K (2018) ABA transport and plant water stress responses. *Trends Plant Sci.* 23(6):513-522.
- Küsel K, Dorsch T, Acker G, Stackebrandt E and Drake HL (2000) *Clostridium scatologenes* strain SL1 isolated as an acetogenic bacterium from acidic sediments. *Int. J. Syst. Evol. Microbiol.* 50(2): 537-546.
- Küsel K, Karnholz A, Trinkwalter T, Devereux R, Acker G and Drake HL (2001) Physiological ecology of *Clostridium glycolicum* RD-1, an aerotolerant acetogen isolated from sea grass roots. *Appl. Environ. Microbiol.* 67(10): 4734-4741.
- Laby RJ, Kim D, Gibson SI (2001) The ram1 mutant of *Arabidopsis* exhibits severely decreased β -amylase activity. *Plant Physiol.* 127: 1798–1807.
- Langenkämper G, Fung RW, Newcomb RD, Atkinson RG, Gardner RC and MacRae EA (2002) Sucrose phosphate synthase genes in plants belong to three different families. *J. Mol. Evol.* 54(3): 322-332.
- Lara ME, Gonzalez Garcia MC, Fatima T, Ehness R, Lee TK, Proels R, Tanner W and Roitsch T (2004) Extracellular invertase is an essential component of cytokinin-mediated delay of senescence. *Plant Cell* 16(5): 1276-1287.
- Lastdrager J, Hanson J and Smeekens S (2014) Sugar signals and the control of plant growth and development. *J. Exp. Bot.* 65: 799–807.
- Le Hir R, Spinner L, Klemens PA, Chakraborti D, de Marco F, Vilaine F, Wolff N, Lemoine R, Porcheron B, Géry C, Téoulé E, Chabout S, Mouille G, Neuhaus HE, Dinant S and Bellini C (2015) Disruption of the sugar transporters AtSWEET11 and AtSWEET12 affects vascular development and freezing tolerance in *Arabidopsis*. *Mol. Plant* 8(11): 1687-1690.
- Lehmann U, Wienkoop S, Tschöep H and Weckwerth W (2008) If the antibody fails - a mass Western approach. *Plant J.* 55(6): 1039-1046.
- Lemeille S, Turkina MV, Vener AV and Rochaix JD (2010) Stt7-dependent phosphorylation during state transitions in the green alga *Chlamydomonas reinhardtii*. *Mol. Cell Proteomics* 9(6): 1281-1295.
- Letunic I and Bork P (2016) Interactive tree of life (iTOL) v3: an online tool for the display and annotation of phylogenetic and other trees. *Nucleic Acids Res.* 44: 242-245.
- Li C, Li QG, Dunwell JM and Zhang YM (2012) Divergent evolutionary pattern of starch biosynthetic pathway genes in grasses and dicots. *Mol. Biol. Evol.* 29: 3227–3236.
- Li Y, Van den Ende W and Rolland F (2014) Sucrose induction of anthocyanin biosynthesis is mediated by DELLA. *Mol. Plant* 7: 570–572.
- Li L and Sheen J (2016) Dynamic and diverse sugar signaling. *Curr. Opin. Plant Biol.* 33: 116-125.
- Liepman AH, Wightman R, Geshi N, Turner SR and Scheller HV (2010) *Arabidopsis* – a powerful model system for plant cell wall research. *Plant J.* 61(6): 1107-21.
- Liesche J, Krügel U, He H, Chincinska I, Hackel A and Kühn C (2011) Sucrose transporter regulation at the transcriptional, post-transcriptional and post-translational level. *J. Plant Physiol.* 168(12): 1426-33.
- Lin TP, Spilatro SR and Preiss J (1988) Subcellular localization and characterization of amylases in *Arabidopsis* leaf. *Plant Physiol.* 86: 251–259.

- Lin IW, Sosso D, Chen LQ, Gase K, Kim SG, Kessler D, Klinkenberg PM, Gorder MK, Hou BH, Qu XQ, Carter CJ, Baldwin IT and Frommer WB (2014) Nectar secretion requires sucrose phosphate synthases and the sugar transporter SWEET9. *Nature* 508(7497): 546-549.
- Lindermayr C, Saalbach G and Durner J (2005) Proteomic identification of S-nitrosylated proteins in Arabidopsis. *Plant Physiol.* 137(3): 921-930.
- Liu KL, Shen L, Wang JQ and Sheng JP (2008) Rapid inactivation of chloroplastic ascorbate peroxidase is responsible for oxidative modification to Rubisco in tomato (*Lycopersicon esculentum*) under cadmium stress. *J. Integr. Plant Biol.* 50(4): 415-426.
- Liu T, Carlsson J, Takeuchi T, Newton L and Farré EM (2013) Direct regulation of abiotic responses by the Arabidopsis circadian clock component PRR7. *Plant J.* 76(1): 101-114.
- Livingston DP 3rd, Hinch DK and Heyer AG (2009) Fructan and its relationship to abiotic stress tolerance in plants. *Cell. Mol. Life Sci.* 66(13): 2007-2023.
- Ljung K, Nemhauser JL and Perata P (2015) New mechanistic links between sugar and hormone signalling networks. *Curr. Opin. Plant Biol.* 25: 130–137
- Ljungdahl LG (1986) The autotrophic pathway of acetate synthesis in acetogenic bacteria. *Annu. Rev. Microbiol.* 40:415-450.
- Lloyd JR and Kossmann J (2015) Transitory and storage starch metabolism: two sides of the same coin? *Curr. Opin. Biotechnol.* 32: 143–148
- Lohmeier-Vogel EM, Kerk D, Nimick M, Wrobel S, Vickerman L, Muench DG and Moorhead GB (2008) Arabidopsis At5g39790 encodes a chloroplast-localized, carbohydrate-binding, coiled-coil domain-containing putative scaffold protein. *BMC Plant Biol.* 8:120.
- Long JC, Zhao W, Rashotte AM, Muday GK and Huber SC (2002) Gravity-stimulated changes in auxin and invertase gene expression in maize pulvinal cells. *Plant Physiol.* 128(2): 591-602.
- Long SP, Marshall-Colon A and Zhu XG (2015) Meeting the global food demand of the future by engineering crop photosynthesis and yield potential. *Cell* 161: 56–66.
- Elena López-Calcano P, Omar Abuzaid A, Lawson T and Anne Raines C. (2017) Arabidopsis CP12 mutants have reduced levels of phosphoribulokinase and impaired function of the Calvin–Benson cycle. *J. Exp. Bot.* 268(9): 2285-2298.
- Lorberth R, Ritte G, Willmitzer L and Kossmann J (1998) Inhibition of a starch-granule-bound protein leads to modified starch and repression of cold-induced sweetening. *Nat. Biotechnol.* 16: 473–477.
- Loreti E, Valeri MC, Novi G and Perata P (2018) Gene regulation and survival under hypoxia requires starch availability and metabolism. *Plant Physiol.* 176(2): 1286-1298.
- Lu Y and Sharkey TD (2004) The role of amyloamylase in maltose metabolism in the cytosol of photosynthetic cells. *Planta* 218(3): 466-473.
- Lu C, Tej SS, Luo S, Haudenschild CD, Meyers BC and Green PJ (2005) Elucidation of the small RNA component of the transcriptome. *Science* 309(5740): 1567-1579.
- Lu SX, Knowles SM, Andronis C, Ong MS and Tobin EM (2009) CIRCADIAN CLOCK ASSOCIATED1 and LATE ELONGATED HYPOCOTYL function synergistically in the circadian clock of Arabidopsis. *Plant Physiol.* 150(2): 834-43.
- Lu SX, Webb CJ, Knowles SM, Kim SH, Wang Z and Tobin EM (2012) CCA1 and ELF3 interact in the control of hypocotyl length and flowering time in Arabidopsis. *Plant Physiol.* 158(2): 1079-88.
- Lugassi N, Kelly G, Fidel L, Yaniv Y, Attia Z, Levi A, Alchanatis V,

- Moshelion M, Raveh E, Carmi N and Granot D (2015) Expression of Arabidopsis hexokinase in citrus guard cells controls stomatal aperture and reduces transpiration. *Front. Plant Sci.* 6: 1114.
- Lunn JE, Feil R, Hendriks JH, Gibon Y, Morcuende R, Osuna D, Scheible WR, Carillo P, Hajirezaei MR and Stitt M (2006) Sugar-induced increases in trehalose 6-phosphate are correlated with redox activation of ADPglucose pyrophosphorylase and higher rates of starch synthesis in *Arabidopsis thaliana*. *Biochem J.* 397(1): 139-148.
- Lutfiyya LL, Xu N, D'Ordine RL, Morrell JA, Miller PW and Duff SM (2007) Phylogenetic and expression analysis of sucrose phosphate synthase isozymes in plants. *J. Plant Physiol.* 164(7): 923-33.
- MacNeill GJ, Mehrpouyan S, Minow MAA, Patterson JA, Tetlow IJ and Emes MJ (2017) Starch as a source, starch as a sink: the bifunctional role of starch in carbon allocation. *J Exp Bot.* 2017 68(16): 4433-4453.
- Maghsoudi K, Emam Y, Niazi A, Pessarakli M and Arvin MJ (2018) P5CS expression level and proline accumulation in the sensitive and tolerant wheat cultivars under control and drought stress conditions in the presence/absence of silicon and salicylic acid. *J. Plant Interact.* 13(1): 461-471.
- Mahlow S, Orzechowski S and Fettke J (2016) Starch phosphorylation: insights and perspectives. *Cell. Mol. Life Sci.* 73: 2753–2764.
- Maier T1, Güell M and Serrano L (2009) Correlation of mRNA and protein in complex biological samples. *FEBS Lett.* 583(24): 3966-3973.
- Malinova I, Steup M and Fettke J (2011) Starch-related cytosolic heteroglycans in roots from *Arabidopsis thaliana*. *J. Plant Physiol.* 168(12): 1406-14.
- Malinova I, Mahto H, Brandt F, Al-Rawi S, Qasim H, Brust H, Hejazi M and Fettke J (2018) EARLY STARVATION1 specifically affects the phosphorylation action of starch-related dikinases. *Plant J.* 95(1): 126-137.
- Maloney VJ, Park JY and Unda F and Mansfield SD (2015) Sucrose phosphate synthase and sucrose phosphate phosphatase interact in planta and promote plant growth and biomass accumulation. *J. Exp. Bot.* 66(14): 4383-4394.
- Marri L, Trost P, Pupillo P and Sparla F (2005) Reconstitution and properties of the recombinant glyceraldehyde-3-phosphate dehydrogenase/CP12/phosphoribulokinase supramolecular complex of Arabidopsis. *Plant Physiol.* 139: 1433–1443.
- Marri L, Trost P, Trivelli X, Gonnelli L, Pupillo P and Sparla F (2008) Spontaneous assembly of photosynthetic supramolecular complexes as mediated by the intrinsically unstructured protein CP12. *J. Biol. Chem.* 283: 1831–1838.
- Marri L, Zaffagnini M, Collin V, Issakidis-Bourguet E, Lemaire SD, Pupillo P, Sparla F, Miginiac-Maslow M and Trost P (2009) Prompt and easy activation by specific thioredoxins of Calvin cycle enzymes of *Arabidopsis thaliana* associated in the GAPDH/CP12/PRK supramolecular complex. *Mol. Plant.* 2: 259–269.
- Marri L, Thieulin-Pardo G, Lebrun R, Puppo R, Zaffagnini M, Trost P, Gontero B and Sparla F (2014) CP12-mediated protection of Calvin-Benson cycle enzymes from oxidative stress. *Biochimie* 97: 228-37.
- Martin, W and Schnarrenberger C (1997) The evolution of the Calvin cycle from prokaryotic to eukaryotic chromosomes: a case study of functional redundancy in ancient pathways through endosymbiosis. *Curr. Genet.* 32: 1–18.
- Martin T, Oswald O and Graham IA (2002) Arabidopsis seedling growth, storage lipid mobilization, and photosynthetic gene expression are regulated by carbon:nitrogen availability. *Plant Physiol.* 128(2): 472-81.
- Martinez-Barajas E, Delatte T, Schluepmann H, de Jong GJ, Somsen GW, Nunes C, Primavesi LF, Coello P, Mitchell RAC and Paul MJ (2013) Wheat grain development is characterized by remarkable trehalose 6-phosphate accumulation pregrain filling: tissue distribution and relationship to SNF1-Related Protein Kinase1 activity. *Plant Physiol.* 156(1): 373-381

- Martins MC, Hejazi M, Fettke J, Steup M, Feil R, Krause U, Arrivault S, Vosloh D, Figueroa CM, Ivakov A, Yadav UP, Piques M, Metzner D, Stitt M and Lunn JE (2013) Feedback inhibition of starch degradation in Arabidopsis leaves mediated by trehalose 6-phosphate. *Plant Physiol.* 163(3): 1142-1163.
- Más P, Kim WY, Somers DE and Kay SA (2003) Targeted degradation of TOC1 by ZTL modulates circadian function in *Arabidopsis thaliana*. *Nature* 426(6966): 567-570.
- Mattioli R, Marchese D, D'Angeli S, Altamura MM, Costantino P and Trovato M. (2008) Modulation of intracellular proline levels affects flowering time and inflorescence architecture in Arabidopsis. *Plant Mol. Biol.* 66: 277-288.
- Matysik J, Alia A, Bhalu B and Mohanty P (2002) Molecular mechanisms of quenching of reactive oxygen species by proline under stress in plants. *Curr. Sci.* 82: 525-532.
- McCoy AJ, Grosse-Kunstleve RW, Adams PD, Winn MD, Storoni LC and Read RJ (2007) Phaser crystallographic software. *J. Appl. Crystallogr.* 40: 658-674.
- Medrano H, Parry MAJ, Socias X and Lawlor DW (1997) Long term water stress inactivates Rubisco in subterranean clover. *Ann. Appl. Biol.* 131: 491-501.
- Meekins DA, Raththagala M, Husodo S, White CJ, Guo HF, Kötting O, Vander Kooi CW, Gentry MS (2014) Phosphoglucan-bound structure of starch phosphatase Starch Excess4 reveals the mechanism for C6 specificity. *Proc. Natl. Acad. Sci. USA* 111(20): 7272-7277
- Mehra A, Baker CL, Loros JJ and Dunlap JC (2009) Post-translational modifications in circadian rhythms. *Trends Biochem. Sci.* 34(10): 483-90.
- Mehta SK and Gaur JP (1999) Heavy-metal-induced proline accumulation and its role in ameliorating metal toxicity in *Chlorella vulgaris*. *New Phytol.* 143: 253-259
- Meijer WG, Arnberg AC, Enequist HG, Terpstra P, Lidstrom ME and Dijkhuizen L (1991) Identification and organization of carbon dioxide fixation genes in *Xanthobacter flavus* H4-14. *Mol. Gen. Genet.* 225: 320-330.
- Meng M, Geisler M, Johansson H, Harholt J, Scheller HV, Mellerowicz EJ and Kleczkowski LA (2009) UDP-glucose pyrophosphorylase is not rate limiting, but is essential in Arabidopsis. *Plant Cell Physiol.* 50(5): 998-1011.
- Meyer Y, Siala W, Bashandy T, Riondet C, Vignols F and Reichheld JP (2008) Glutaredoxins and thioredoxins in plants. *Biochim. Biophys. Acta* 1783(4): 589-600.
- Miao H, Cai C, Wei J, Huang J, Chang J, Qian H, Zhang X, Zhao Y, Sun B, Wang B and Wang Q (2016) Glucose enhances indolic glucosinolate biosynthesis without reducing primary sulfur assimilation. *Sci. Rep.* 6: 31854.
- Michalowski CB, Derocher EJ, Bohnert HJ, and Salvucci M (1992) Phosphoribulokinase from ice plant: Transcription, transcripts and protein expression during environmental stress. *Photosynth. Res.* 31: 27-38.
- Michelet L, Zaffagnini M, Marchand C, Collin V, Decottignies P, Tsan P, Lancelin JM, Trost P, Miginiac-Maslow M, Noctor G and Lemaire SD (2005) Glutathionylation of chloroplast thioredoxin f is a redox signaling mechanism in plants. *Proc. Natl. Acad. Sci. USA* 102(45): 16478-16483.
- Michelet L, Zaffagnini M, Vanacker H, Le Maréchal P, Marchand C, Schroda M, Lemaire SD and Decottignies P (2008) In Vivo Targets of S-Thiolation in *Chlamydomonas reinhardtii*. *J. Biol. Chem.* 283(31): 21571- 21578.
- Michelet L, Zaffagnini M, Morisse S, Sparla F, Pérez-Pérez ME, Francia F, Danon A, Marchand CH, Fermani S, Trost P and Lemaire SD (2013) Redox regulation of the Calvin-Benson cycle: Something old, something new. *Front. Plant Sci.* 4: 470.
- Mikkelsen R, Mutenda KE, Mant A, Schürmann P and Blennow A (2005) α -Glucan, water dikinase (GWD): A plastidic enzyme with redox-regulated and coordinated catalytic activity and binding affinity. *Proc Natl Acad Sci USA* 102(5): 1785-1790.
- Mittler R (2017) ROS Are Good. *Trends Plant Sci.* 22(1): 11-19

- Møller IM, Jensen PE and Hansson A (2007) Oxidative Modifications to cellular components in plants. *Annu. Rev. Plant Biol.* 58: 459-481.
- Monroe JD, Storm AR, Badley EM, Lehman MD, Platt SM, Saunders LK, Schmitz JM and Torres CE (2014) β -amylase1 and β -amylase3 are plastidic starch hydrolases in Arabidopsis that appear to be adapted for different thermal, pH, and stress conditions. *Plant Physiol.* 166: 1748-1763.
- Montoya et al., 2012
- Mora-Garcia S, Rodríguez-Suárez R and Wolosiuk RA (1997) Role of electrostatic interactions on the affinity of thioredoxin for target proteins. Recognition of chloroplast fructose-1,6-bisphosphatase by mutant *Escherichia coli* thioredoxins. *J. Biol. Chem.* 273: 16273-16280.
- Moore B, Zhou L, Rolland F, Hall Q, Cheng WH, Liu YX, Hwang I, Jones T and Sheen J (2003) Role of the Arabidopsis glucose sensor HXK1 in nutrient, light, and hormonal signaling. *Science* 300(5617): 332-326.
- Moore JP, Vitré-Gibouin M, Farrant JM and Driouch A (2008) Adaptations of higher plant cell walls to water loss: drought vs desiccation. *Physiol Plant.* 134(2): 237-245.
- Mou Z, Fan W and Dong X (2003) Inducers of plant systemic acquired resistance regulate NPR1 function through redox changes. *Cell* 113(7): 935-944.
- Müller R, Morant M, Jarmer H, Nilsson L and Nielsen TH (2007) Genome-wide analysis of the Arabidopsis leaf transcriptome reveals interaction of phosphate and sugar metabolism. *Plant Physiol.* 143(1): 156-171.
- Murshudov GN, Vagin AA and Dodson EJ (1997) Refinement of macromolecular structures by the maximum-likelihood method. *Acta Cryst. D Biol. Cryst.* 53: 240–255.
- Myers AM, Morell MK, James MG and Ball SG (2000) Recent progress toward understanding biosynthesis of the amylopectin crystal. *Plant Physiol.* 122(4): 989-997.
- Nagao M, Minami A, Arakawa K, Fujikawa S and Takezawa D (2005) Rapid degradation of starch in chloroplasts and concomitant accumulation of soluble sugars associated with ABA-induced freezing tolerance in the moss *Physcomitrella patens*. *J. Plant Physiol.* 162(2): 169-180.
- Nagel DH and Kay SA (2012) Complexity in the wiring and regulation of plant circadian networks. *Curr. Biol.* 22(16):R648-57.
- Nakai T, Konishi T, Zhang XQ, Chollet R, Tonouchi N, Tsuchida T, Yoshinaga F, Mori H, Sakai F and Hayashi T (1998) An increase in apparent affinity for sucrose of mung bean sucrose synthase is caused by in vitro phosphorylation or directed mutagenesis of Ser11. *Plant Cell Physiol.* 39(12):1337-1341.
- Nakamichi N, Kiba T, Henriques R, Mizuno T, Chua NH and Sakakibara H (2010) PSEUDO-RESPONSE REGULATORS 9, 7, and 5 are transcriptional repressors in the Arabidopsis circadian clock. *Plant Cell* 22(3): 594-605.
- Nakamichi N, Kiba T, Kamioka M, Suzuki T, Yamashino T, Higashiyama T, Sakakibara H and Mizuno T (2012) Transcriptional repressor PRR5 directly regulates clock-output pathways. *Proc. Natl. Acad. Sci. USA* 109(42):17123-17128.
- Nielsen TH, Wischmann B, Enevoldsen K and Møller BL (1994) Starch phosphorylation in potato tubers proceeds concurrently with *de novo* biosynthesis of starch. *Plant Physiol.* 105(1): 111-117.
- Niittylä T, Messerli G, Trevisan M, Chen J, Smith AM and Zeeman SC (2004) A previously unknown maltose transporter essential for starch degradation in leaves. *Science* 303(5654): 87-89.
- Niittylä T, Fuglsang AT, Palmgren MG, Frommer WB and Schulze WX (2007) Temporal analysis of sucrose-induced phosphorylation changes in plasma membrane proteins of Arabidopsis. *Mol Cell Proteomics* 6(10): 1711-1726.
- Nguyen-Quoc B and Foyer CH (2000) A role for 'futile cycles' involving invertase and sucrose synthase in sucrose metabolism of tomato fruit. *J. Exp. Bot.* 52(358): 881-889.

- Noctor G, Mhamdi A, Chaouch S, Han Y, Neukermans J, Marquez-Garcia B, Queval G and Foyer CH (2012) Glutathione in plants: an integrated overview. *Plant Cell Environ.* 35(2): 454-484.
- Noctor G, Reichheld JP and Foyer CH (2018) ROS-related redox regulation and signaling in plants. *Semin. Cell. Dev. Biol.* 80: 3-12.
- Noguera-Mazon V, Lemoine J, Walker O, Rouhier N, Salvador A, Jacquot JP, Lancelin JM and Krimm I (2006) Glutathionylation induces the dissociation of 1-Cys D-peroxiredoxin non-covalent homodimer. *J. Biol. Chem.* 281(42): 31736-31743.
- North HM, Berger A, Saez-Aguayo S and Ralet MC (2014) Understanding polysaccharide production and properties using seed coat mutants: future perspectives for the exploitation of natural variants. *Ann. Bot.* 114: 1251–1263
- Nühse TS, Stensballe A, Jensen ON and Peck SC.(2004) Phosphoproteomics of the Arabidopsis plasma membrane and a new phosphorylation site database. *Plant Cell.* 16(9): 2394-2405.
- Nunes C, Schluepmann H, Delatte TL, Wingler A, Silva AB, Fevereiro PS, Jansen M, Fiorani F, Wiese-Klinkenberg A and Paul M (2013) Regulation of growth by the trehalose pathway. *Plant Signal. Behav.* 8(12): e26626.
- O'Hara LE, Matthew JP and Wingler A (2013) How do sugars regulate plant growth and development? new insight into the role of trehalose-6-phosphate. *Mol. Plant* 6(2): 261-274.
- O'Leary B, Park J and Plaxton WC (2011) The remarkable diversity of plant PEPC (phosphoenolpyruvate carboxylase): recent insights into the physiological functions and post-translational controls of non-photosynthetic PEPCs. *Biochem. J.* 436: 15–34.
- O'Sullivan AC and Perez S (1999) The relationship between internal chain length of amylopectin and crystallinity in starch. *Biopolymers* 50: 381–390
- Okamoto K, Kondo-Okamoto N and Ohsumi Y(2009) A landmark protein essential for mitophagy. *Autophagy* 5: 1203-1205.
- Ong MH, Jumel K, Tokarczuk PF, Blanshard JMV and Harding SE (1994) Simultaneous determinations of the molecular weight distributions of amyloses and the fine structures of amylopectins of native starches. *Carbohydr. Res.* 260: 99–117.
- Oono Y, Seki M, Satou M, Iida K, Akiyama K, Sakurai T, Fujita M, Yamaguchi-Shinozaki K and Shinozaki K (2006) Monitoring expression profiles of Arabidopsis genes during cold acclimation and deacclimation using DNA microarrays. *Funct. Integr. Genomics* 6(3): 212-234.
- Palde PB and Carroll KS (2015) A universal entropy-driven mechanism for thioredoxin-target recognition. *Proc. Natl. Acad. Sci. USA* 112: 7960–7965.
- Pasquini M, Fermani S, Tedesco D, Sciabolini C, Crozet P, Naldi M, Henri J, Vothknecht U, Bertucci C, Lemaire SD, Zaffagnini M and Francia F (2017) Structural basis for the magnesium-dependent activation of transketolase from *Chlamydomonas reinhardtii*. *Biochim. Biophys. Acta* 1861: 2132-2145.
- Paulsen CE and Carroll KS (2013) Cysteine-mediated redox signaling: chemistry, biology, and tools for discovery. *Chem Rev.* 113(7): 4633-79.
- Payne JL, Boyer AG, Brown JH, Finnegan S, Kowalewski M, Krause RA Jr, Lyons SK, McClain CR, McShea DW, Novack-Gottshall PM, Smith FA, Stempien JA and Wang SC (2009) Two-phase increase in the maximum size of life over 3.5 billion years reflects biological innovation and environmental opportunity. *Proc. Natl. Acad. Sci. USA* 106(1): 24-27.
- Pernot P, Round A, Barrett R, De Maria Antolinos A, Gobbo A, Gordon E, Huet J, Kieffer J, Lentini M, Mattenet M, Morawe C, Mueller-Dieckmann C, Ohlsson S, Schmid W, Surr J, Theveneau P, Zerrad L and McSweeney S (2013) Upgraded ESRF BM29 beamline for SAXS on macromolecules in solution. *J. Synchrotron Radiat.* 20: 660–664.

- Petoukhov MV, Franke D, Shkumatov AV, Tria G, Kikhney AG, Gajda M, Gorba C, Mertens HD, Konarev PV and Svergun DI (2012) New developments in the ATSAS program package for small-angle scattering data analysis. *J. Appl. Crystallogr.* 45: 342–350.
- Pfister B and Zeeman SC (2016) Formation of starch in plant cells. *Cell. Mol. Life Sci.* 73: 2781-2807.
- Pinheiro C, Chaves MM and Ricardo CP (2001) Alterations in carbon and nitrogen metabolism induced by water deficit in the stems and leaves of *Lupinus albus* L. *J. Exp. Bot.* 52(358):1063-1070.
- Pirone C, Gurrieri L, Gaiba I, Adamiano A, Valle F, Trost P and Sparla F (2017) The analysis of the different functions of starch-phosphorylating enzymes during the development of *Arabidopsis thaliana* plants discloses an unexpected role for the cytosolic isoform GWD2. *Physiol Plant.* 160(4):447-457.
- Pokhilko A, Fernández AP, Edwards KD, Southern MM, Halliday KJ and Millar AJ (2012) The clock gene circuit in *Arabidopsis* includes a repressilator with additional feedback loop. *Mol. Syst. Biol.* 8:574.
- Pollock CJ and Cairns AJ (1991) Fructan metabolism in grasses and cereals. *Annu. Rev. Plant Phys.* 42:77-101.
- Pommerrenig B, Ludewig F, Cvetkovic J, Trentmann O, Klemens PAW and Neuhaus HE (2018) In concert: orchestrated changes in carbohydrate homeostasis are critical for plant abiotic stress tolerance. *Plant Cell Physiol.* 59(7): 1290-1299.
- Pontis HG, Babio JR and Salerno G (1981) Reversible unidirectional inhibition of sucrose synthase activity by disulfides. *Proc. Natl. Acad. Sci. USA* 78(11) 6667-6669.
- Poole LB (2015) The basics of thiols and cysteines in redox biology and chemistry. *Free Rad. Bio. Med.* 80: 148–157.
- Porod G (1982) General theory, in: Glatter O and Kratky O (Eds.), *Small-Angle X-Ray Scatt.*, Academic Press, London, UK, 514.
- Porter MA and Hartman FC (1990) Exploration of the function of a regulatory sulfhydryl of phosphoribulokinase from spinach. *Arch. Biochem. Biophys.* 281: 330–334.
- Portis AR Jr. (2003) Rubisco activase – Rubisco’s catalytic chaperone. *Photosynth Res.* 75(1): 11-27.
- Powell PO, Sullivan MA, Sweedman MC, Stapleton DI, Hasjim J and Gilbert RG (2014) Extraction, isolation and characterisation of phytylglycogen from su-1 maize leaves and grain. *Carbohydr. Polym.* 101: 423– 431.
- Price J, Laxmi A, St Martin SK and Jang JC (2004) Global transcription profiling reveals multiple sugar signal transduction mechanisms in *Arabidopsis*. *Plant Cell* 16(8): 2128-2150.
- Pressel S, Ligrone R and Duckett JG (2006) Effects of de- and rehydration on food-conducting cells in the moss *Polytrichum formosum*: a cytological study. *Ann. Bot.* 98(1): 67-76.
- Proels RK and Roitsch T (2009) Extracellular invertase LIN6 of tomato: a pivotal enzyme for integration of metabolic, hormonal, and stress signals is regulated by a diurnal rhythm. *J. Exp. Bot.* 60(6): 1555-1567.
- Pupillo P and Piccari GG (1973) The effect of NADP on the subunit structure and activity of spinach chloroplast glyceraldehyde-3-phosphate dehydrogenase. *Arch. Biochem. Biophys.* 154(1): 324-31.
- Purcell PC, Smith AM and Halford NG (1998) Antisense expression of a sucrose non-fermenting-1-related protein kinase sequence in potato results in decreased expression of sucrose synthase in tubers and loss of sucrose-inducibility of sucrose synthase transcripts in leaves. *Plant J.* 14(2): 195-202.
- Queval G, Jaillard D, Zechmann B and Noctor G (2011) Increased intracellular H₂O₂ availability preferentially drives glutathione accumulation in vacuoles and chloroplasts. *Plant Cell Environ.* 34(1): 21-32.
- Quick WP, Chaves MM, Wendler R, David MM, Rodrigues ML, Passarinho JA, Pereira JS, Adcock MD, Leegood RC and Stitt M (1992) The effect of water stress on photosynthetic carbon metabolism in four species grown under field conditions. *Plant Cell and Environ.* 15: 25–35.

- Radchuk R, Emery RJ, Weier D, Vigeolas H, Geigenberger P, Lunn JE, Feil R, Weschke W and Weber H (2010) Sucrose non-fermenting kinase 1 (SnRK1) coordinates metabolic and hormonal signals during pea cotyledon growth and differentiation. *Plant J.* 61(2): 324-38.
- Ragel P, Streb S, Feil R, Sahrawy M, Annunziata MG, Lunn JE, Zeeman S and Mérida Á (2013) Loss of starch granule initiation has a deleterious effect on the growth of Arabidopsis plants due to an accumulation of ADP-glucose. *Plant Physiol.* 163(1): 75-85.
- Ragsdale SW and Pierce E (2008) Acetogenesis and the Wood-Ljungdahl pathway of CO₂ fixation. *Biochim. Biophys. Acta.* 1784(12): 1873-1898.
- Rajendrakumar CS, Reddy BV and Reddy AR (1994) Proline-protein interactions: protection of structural and functional integrity of M4 lactate dehydrogenase. *Biochem. Biophys. Res. Commun.* 201(2):957-63.
- Ral JP, Bowerman AF, Li Z, Sirault X, Furbank R, Pritchard JR, Bloemsma M, Cavanagh CR, Howitt CA and Morell MK (2012) Downregulation of glucan, water-dikinase activity in wheat endosperm increases vegetative biomass and yield. *Plant Biotechnol. J.* 10: 871–882.
- Rambo RP and Tainer JA (2013) Accurate assessment of mass, models and resolution by small-angle scattering. *Nature* 496: 477-481.
- Ramos-Vera WH, Berg IA and Fuchs G (2009) Autotrophic carbon dioxide assimilation in Thermoproteales revisited. *J. Bacteriol.* 191(13): 4286-4297.
- Ransom-Hodgkins WD, Vaughn MW and Bush DR (2003) Protein phosphorylation plays a key role in sucrose-mediated transcriptional regulation of a phloem-specific proton-sucrose symporter. *Planta.* 217(3): 483-9.
- Rasse DP and Tocquin P (2006) Leaf carbohydrate controls over Arabidopsis growth and response to elevated CO₂: an experimentally based model. *New Phytol.* 172(3): 500-513.
- Rawat R, Takahashi N, Hsu PY, Jones MA, Schwartz J, Salemi MR, Phinney BS and Harmer SL (2011) REVEILLE8 and PSEUDO-REPONSE REGULATOR5 form a negative feedback loop within the Arabidopsis circadian clock. *PLoS Genet.* 7(3): e1001350.
- Reiland S, Messerli G, Baerenfaller K, Gerrits B, Endler A, Grossmann J, Gruissem W and Baginsky S (2009) Large-scale Arabidopsis phosphoproteome profiling reveals novel chloroplast kinase substrates and phosphorylation networks. *Plant Physiol.* 150(2): 889-903.
- Reinders A, Schulze W, Kühn C, Barker L, Schulz A, Ward JM and Frommer WB (2002) Protein-protein interactions between sucrose transporters of different affinities colocalized in the same enucleate sieve element. *Plant Cell.* 14(7): 1567-1577.
- Reimann R, Hippler M, Machelett B and Appenroth KJ (2004) Light induces phosphorylation of glucan water dikinase, which precedes starch degradation in turions of the duckweed *Spirodela polyrhiza*. *Plant Physiol.* 135(1): 121-128.
- Renger G (2010) The light reactions of photosynthesis. *Curr. Sci.* 98(10): 1305-1319.
- Janse van Rensburg HC and Van den Ende W (2018) UDP-Glucose: A potential signaling molecule in plants? *Front. Plant Sci.* 8: 2230.
- Ritte G, Lorberth R, Steup M (2000) Reversible binding of the starch-related R1 protein to the surface of transitory starch granules. *Plant J.* 21: 387–391
- Ritte G, Lloyd JR, Eckermann N, Rottmann A, Kossmann J, Steup M (2002) The starch-related R1 protein is an α -glucan, water dikinase. *Proc Natl Acad Sci USA* 99: 7166–717
- Ritte G, Scharf A, Eckermann N, Haebel S and Steup M (2004) Phosphorylation of transitory starch is increased during degradation. *Plant Physiol.* 135(4): 2068-2077.

- Robert X and Gouet P (2014) Deciphering key features in protein structures with the new ENDscript server. *Nucl. Acids Res.* 42: W320-W324.
- Roblin G, Sakr S, Bonmort J and Delrot S (1998) Regulation of a plant plasma membrane sucrose transporter by phosphorylation. *FEBS Lett.* 424(3): 165-168.
- Rocha AG, Mehlmer N, Stael S, Mair A, Parvin N, Chigri F, Teige M and Vothknecht UC (2014) Phosphorylation of Arabidopsis transketolase at Ser428 provides a potential paradigm for the metabolic control of chloroplast carbon metabolism. *Biochem J.* 458(2): 313-322.
- Rocha AG and Vothknecht UC (2012) The role of calcium in chloroplasts—an intriguing and unresolved puzzle. *Protoplasma* 249(4): 957-966.
- Roesler, KR and Ogren WL (1990) *Chlamydomonas reinhardtii* phosphoribulokinase: sequence, purification and kinetics. *Plant Physiol.* 93: 188–193.
- Roger P and Colonna P (1996) Molecular weight distribution of amylose fractions obtained by aqueous leaching of corn starch. *Int. J. Biol. Macromol.* 19: 51–61
- Röhrig H, John M and Schmidt J (2004) Modification of soybean sucrose synthase by S-thiolation with ENOD40 peptide A. *Biochem. Biophys. Res. Commun.* 325(3): 864-870.
- Roitinger E, Hofer M, Köcher T, Pichler P, Novatchkova M, Yang J, Schlögelhofer P and Mechtler K (2015) Quantitative phosphoproteomics of the ataxia telangiectasia-mutated (ATM) and ataxia telangiectasia-mutated and rad3-related (ATR) dependent DNA damage response in *Arabidopsis thaliana*. *Mol. Cell. Proteomics* 14(3): 556-571
- Roitsch T, Ehneû R, Goetz M, Hause B, Hofmann M and Sinha AK (2000) Regulation and function of extracellular invertase from higher plants in relation to assimilate partitioning, stress responses and sugar signalling. *Aust. J. Plant Physiol.* 27: 815-825.
- Roitsch T, Balibrea ME, Hofmann M, Proels R and Sinha AK (2003) Extracellular invertase: key metabolic enzyme and PR protein. *J. Exp. Bot.* 54(382): 513-524.
- Roldán I, Wattedled F, Mercedes Lucas M, Delvallé D, Planchot V, Jiménez S, Pérez R, Ball S, D'Hulst C and Mérida A (2007) The phenotype of soluble starch synthase IV defective mutants of *Arabidopsis thaliana* suggests a novel function of elongation enzymes in the control of starch granule formation. *Plant J.* 49(3): 492-504.
- Romero-Puertas MC, Camprostrini N, Mattè A, Righetti PG, Perazzolli M, Zolla L, Roepstorff P and Delledonne M (2008) Proteomic analysis of S-nitrosylated proteins in *Arabidopsis thaliana* undergoing hypersensitive response. *Proteomics* 8(7): 1459- 1469.
- Roos G, Foloppe N and Messens J (2013) Understanding the pK_a of redox cysteines: the key role of hydrogen bonding. *Antioxid. Redox Signal.* 18(1): 94-127.
- Rouhier N, Cerveau D, Couturier J, Reichheld JP and Rey P (2015) Involvement of thiol-based mechanisms in plant development. *Biochim. Biophys. Acta* 1850(8): 1479-1496.
- Ruan YL (2014) Sucrose metabolism: gateway to diverse carbon use and sugar signaling. *Annu. Rev. Plant Biol.* 65: 33–67.
- Runquist JA, Harrison DH and Mizioroko HM (1999) *Rhodobacter sphaeroides* phosphoribulokinase: identification of lysine-165 as a catalytic residue and evaluation of the contributions of invariant basic amino acids to ribulose 5-phosphate binding. *Biochemistry* 38: 13999-14005.
- Sage RF (2013) Photorespiratory compensation: a driver for biological diversity. *Plant Biol.* 15: 624–638.
- Sai J and Johnson CH (2002) Dark-stimulated calcium ion fluxes in the chloroplast stroma and cytosol. *Plant Cell.* 14(6): 1279-1291.

- Salomé PA, Weigel D and McClung CR (2010) The role of the Arabidopsis morning loop components CCA1, LHY, PRR7, and PRR9 in temperature compensation. *Plant Cell*. 22(11): 3650-3661.
- Santelia D, Kötting O, Seung D, Schubert M, Thalmann M, Bischof S, Meekins DA, Lutz A, Patron N, Gentry MS, Allain FH and Zeeman SC (2011) The phosphoglucan phosphatase like sex Four2 dephosphorylates starch at the C3-position in Arabidopsis. *Plant Cell* 23: 4096-40111
- Santelia D, Trost P and Sparla F (2015) New insights into redox control of starch degradation. *Curr. Opin. Plant Biol.* 25: 1–9.
- Santelia D and Lawson T (2016) Rethinking guard cell metabolism. *Plant Physiol.* 172(3): 1371-1392.
- Santelia D and Zeeman SC (2011) Progress in Arabidopsis starch research and potential biotechnological applications. *Curr. Opin. Biotechnol.* 22(2):271-80.
- Saradhi PP, Alia, Arora S and Prasad KV. (1995) Proline accumulates in plants exposed to UV radiation and protects them against UV induced peroxidation. *Biochem. Biophys. Res. Commun.* 209(1): 1-5.
- Schuchmann K and Müller V (2016) Energetics and Application of Heterotrophy in Acetogenic Bacteria. *Appl. Environ. Microbiol.* 82(14):4 056-4069.
- Scialdone A, Mugford ST, Feike D, Skeffington A, Borrill P, Graf A, Smith AM and Howard M (2013) Arabidopsis plants perform arithmetic division to prevent starvation at night. *Elife* 2: e00669.
- Sevanto S (2014) Phloem transport and drought. *J. Exp. Bot.* 65(7): 1751-1759.
- Seung D, Soyk S, Coiro M1, Maier BA, Eicke S and Zeeman SC (2015) PROTEIN TARGETING TO STARCH is required for localising GRANULE-BOUND STARCH SYNTHASE to starch granules and for normal amylose synthesis in Arabidopsis. *PLoS Biol.* 13(2): e1002080.
- Seung D, Boudet J, Monroe J, Schreier TB, David LC, Abt M, Lu KJ, Zanella M and Zeeman SC (2017) Homologs of PROTEIN TARGETING TO STARCH control starch granule initiation in Arabidopsis leaves. *Plant Cell* 29(7): 1657-1677.
- Seung D, Schreier TB, Bürgy L, Eicke S and Zeeman SC (2018) Two Plastidial Coiled-Coil Proteins Are Essential for Normal Starch Granule Initiation in Arabidopsis. *Plant Cell* 30(7): 1523-1542.
- Sevilla F, Camejo D, Ortiz-Espín A, Calderón A, Lázaro JJ and Jiménez A (2015) The thioredoxin/peroxiredoxin/sulfiredoxin system: current overview on its redox function in plants and regulation by reactive oxygen and nitrogen species. *J. Exp. Bot.* 66(10): 2945-2955.
- Sharma P and Dubey RS (2005) Modulation of nitrate reductase activity in rice seedlings under aluminium toxicity and water stress: role of osmolytes as enzyme protectant. *J. Plant Physiol.* 162(8): 854-864.
- Sharma S, Villamor JG and Verslues PE (2011) Essential role of tissue-specific proline synthesis and catabolism in growth and redox balance at low water potential. *Plant Physiol.* 157(1): 292-304.
- Schat H, Sharma SS and Vooijs R (1997) Heavy metal-induced accumulation of free proline in a metal-tolerant and a nontolerant ecotype of *Silene vulgaris*. *Physiol. Plant.* 101: 477-482
- Sheen J (1990) Metabolic repression of transcription in higher plants. *Plant Cell* 2: 1027-1038.
- Sheen J, Zhou L and Jang JC (1999) Sugars as signaling molecules. *Curr. Opin. Plant Biol.* 2: 410-418.
- Shikanai T and Yamamoto H (2017) Contribution of cyclic and pseudo-cyclic electron transport to the formation of proton motive force in chloroplasts. *Mol. Plant* 10: 20-29.
- Yang SL, Lan SS and Gong M (2009) Hydrogen peroxide-induced proline and metabolic pathway of its accumulation in maize seedlings. *J. Plant Physiol.* 166(15): 1694-1699.

- Siaut M, Cuiné S, Cagnon C, Fessler B, Nguyen M, Carrier P, Beyly A, Beisson F, Triantaphylidès C, Li-Beisson Y and Peltier G (2011) Oil accumulation in the model green alga *Chlamydomonas reinhardtii*: characterization, variability between common laboratory strains and relationship with starch reserves. *BMC Biotechnol.* 11:7.
- Sievers F, Wilm A, Dineen D, Gibson TJ, Karplus K, Li W, Lopez R, McWilliam H, Remmert M, Söding J, Thompson JD and Higgins DG (2011) Fast, scalable generation of high-quality protein multiple sequence alignments using Clustal Omega. *Mol. Syst. Biol.* 7: 539-545.
- Signorelli S, Arellano JB, Melø TB, Borsani O and Monza J (2013) Proline does not quench singlet oxygen: evidence to reconsider its protective role in plants. *Plant Physiol. Biochem.* 64: 80-83.
- Silver DM, Silva LP, Issakidis-Bourguet E, Glaring MA, Schriemer DC and Moorhead GBG (2013). Insight into the redox regulation of the phosphoglucan phosphatase SEX4 involved in starch degradation. *FEBS J.* 280: 538-548.
- Simankova MV, Kotsyurbenko OR, Stackebrandt E, Kostrikina NA, Lysenko AM, Osipov GA and Nozhevnikova AN (2000) *Acetobacterium tundrae* sp. nov., a new psychrophilic acetogenic bacterium from tundra soil. *Arch. Microbiol.* 174(6): 440-447.
- Singh M, Kumar J, Singh S, Singh VP, Prasad SM (2015) Roles of osmoprotectants in improving salinity and drought tolerance in plants: a review. *Rev. Environ. Sci. Biotechnol.* 14: 407-426.
- Singh R, Parihar P, Singh S, Mishra RK, Singh VP and Prasad SM (2017) Reactive oxygen species signaling and stomatal movement: Current updates and future perspectives. *Redox Biol.* 11: 213-218.
- Sivak MN and Preiss J (1995) Progress in the genetic manipulation of crops aimed at changing starch structure and increasing starch accumulation. *J. Environ. Polym. Degr.* 3(3): 145-152.
- Sivitz AB, A Reinders and Ward JM (2008) Arabidopsis sucrose transporter AtSUC1 is important for pollen germination and sucrose-induced anthocyanin accumulation. *Plant Physiology* 147: 92–100.
- Skeffington AW, Graf A, Duxbury Z, Gruissem W and Smith AM (2014) Glucan, water dikinase exerts little control over starch degradation in Arabidopsis leaves at night. *Plant Physiol.* 165: 866-879.
- Skryhan K, Cuesta-Seijo JA, Nielsen MM, Marri L, Mellor SB, Glaring MA, Jensen PE, Palcic MM, Blennow A (2015). The role of cysteine residues in redox regulation and protein stability of *Arabidopsis thaliana* starch synthase 1. *PLoS One* 10: e0136997.
- Slewiniski TL and Braun DM (2010) Current perspectives on the regulation of whole-plant carbohydrate partitioning. *Plant Sci.* 178: 341-349.
- Slewiniski TL, Zhang C and Turgeon R (2013) Structural and functional heterogeneity in phloem loading and transport. *Front. Plant Sci.* 4: 244.
- Smirnoff N and Cumber QJ (1989) Hydroxyl radical scavenging activity of compatible solutes. *Phytochemistry* 28(4): 1057-1060.
- Smith IK, Kendall AC, Keys AJ, Turner JC and Lea PJ (1985) The regulation of the biosynthesis of glutathione in leaves of barley (*Hordeum vulgare* L.). *Plant Sci.* 41: 11-17.
- Smith SM, Fulton DC, Chia T, Thorneycroft D, Chapple A, Dunstan H, Hylton C, Zeeman SC and Smith AM (2004) Diurnal changes in the transcriptome encoding enzymes of starch metabolism provide evidence for both transcriptional and posttranscriptional regulation of starch metabolism in Arabidopsis leaves. *Plant Physiol.* 136(1): 2687-2699.
- Smith AM and Zeeman SC (2006) Quantification of starch in plant tissues. *Nat. Protoc.* 1: 1342-1345.
- Smith AM, Zeeman SC and Smith SM (2005) Starch degradation. *Annu. Rev. Plant Biol.* 56: 73–98.
- Smith AM and Stitt M (2007) Coordination of carbon supply and plant growth. *Plant Cell Environ.* 30: 1126-1149.
- Smith AM (2012) Starch in the Arabidopsis plant. *Starch* 64: 421-434.

- Søgaard M, Andersen JS, Roepstorff P and Svensson B (1993) Electrospray mass spectrometry characterization of post-translational modifications of barley α -amylase 1 produced in yeast. *Biotechnology (NY)* 11(10): 1162-1165.
- Solís-Guzmán MG, Argüello-Astorga G, López-Bucio J, Ruiz-Herrera LF, López-Meza JE, Sánchez-Calderón L, Carreón-Abud Y and Martínez-Trujillo M (2017) *Arabidopsis thaliana* sucrose phosphate synthase (sps) genes are expressed differentially in organs and tissues, and their transcription is regulated by osmotic stress. *Gene Expr. Patterns* 25-26:92-101
- Soyk S, Simková K, Zürcher E, Luginbühl L, Brand LH, Vaughan CK, Wanke D and Zeeman SC (2014) The enzyme-like domain of arabidopsis nuclear β -amylases is critical for dna sequence recognition and transcriptional activation. *Plant Cell* 26(4): 1746-1763.
- Sparla F, Pupillo P and Trost P (2002) The c-terminal extension of glyceraldehyde-3-phosphate dehydrogenase subunit b acts as an autoinhibitory domain regulated by thioredoxins and nicotinamide adenine dinucleotide. *J. Biol. Chem.* 277(47): 44946-44952.
- Sparla F, Costa A, Lo Schiavo F, Pupillo P and Trost P (2006) Redox regulation of a novel plastid-targeted β -amylase of *Arabidopsis*. *Plant Physiol.* 141(3): 840-850.
- Sparla F, Falini G, Botticella E, Pirone C, Talamè V, Bovina R, Salvi S, Tuberosa R, Sestili F, Trost P (2014) New starch phenotypes produced by TILLING in barley. *PLoS One* 9: e107779
- Staiger D and Green R (2011) RNA-based regulation in the plant circadian clock. *Trends Plant Sci.* 16(10): 517-523.
- Stitt M, Gerhardt R, Kürzel B, Heldt HW (1983) A role for fructose 2,6-bisphosphate in the regulation of sucrose synthesis in spinach leaves. *Plant Physiol.* 72(4): 1139-1141.
- Stitt M and Zeeman SC (2012) Starch turnover: pathways, regulation and role in growth. *Curr. Opin. Plant Biol.* 15: 282-292.
- Sulpice R, Flis A, Ivakov AA, Apelt F, Krohn N, Encke B, Abel C, Feil R, Lunn JE and Stitt M. (2014) *Arabidopsis* coordinates the diurnal regulation of carbon allocation and growth across a wide range of photoperiods. *Mol Plant.* 7(1): 137-155.
- Sun J, Zhang J, Larue CT and Huber SC (2011) Decrease in leaf sucrose synthesis leads to increased leaf starch turnover and decreased RuBP regeneration-limited photosynthesis but not Rubisco-limited photosynthesis in *Arabidopsis* null mutants of SPSA1. *Plant Cell Environ.* 34: 592-604.
- Svergun DI, Petoukhov MV and Koch MH (2001) Determination of domain structure of proteins from X-ray solution scattering. *Biophys. J.* 80: 2946-2953.
- Strand A, Zrenner R, Trevanion S, Stitt M, Gustafsson P and Gardeström P (2000) Decreased expression of two key enzymes in the sucrose biosynthesis pathway, cytosolic fructose-1,6- biphosphatase and sucrose phosphate synthase, has remarkably different consequences for photosynthetic carbon metabolism in transgenic *Arabidopsis thaliana*. *Plant J.* 23(6): 759-770.
- Streb S, Egli B, Eicke S and Zeeman SC (2009) The debate on the pathway of starch synthesis: a closer look at low-starch mutants lacking plastidial phosphoglucomutase supports the chloroplast-localized pathway. *Plant Physiol.* 151(4): 1769-1772.
- Szabados L and Savourè A (2010) Proline: a multifunctional amino acid. *Trends Plant Sci.* 15(2): 89-97.
- Székely G, Abrahám E, Csépló A, Rigó G, Zsigmond L, Csiszár J, Ayaydin F, Strizhov N, Jásik J, Schmelzer E, Koncz C and Szabados L (2008) Duplicated P5CS genes of *Arabidopsis* play distinct roles in stress regulation and developmental control of proline biosynthesis. *Plant J.* 53: 11-28.
- Tabita FR, Satagopan S, Hanson TE, Kreel NE and Scott SS (2008) Distinct form I, II, III, and IV Rubisco proteins from the three kingdoms of life provide clues about Rubisco evolution and structure/function relationships. *J. Exp. Bot.* 59: 1515-1524.

- Taiz L and Zeiger E (2010) *Plant Physiology*. 5th Edition, Sinauer Associates Inc., Sunderland.
- Takahashi T, Inoue-Kashino N, Ozawa S, Takahashi Y, Kashino Y and Satoh K (2009) Photosystem II Complex in Vivo Is a Monomer. *J. Biol. Chem.* 284(23): 15598-15606.
- Takeda H, Niikura M, Narumi A, Aoki H, Sasaki T, Shimada H (2017) Phosphorylation of rice sucrose synthase isoforms promotes the activity of sucrose degradation. *Plant Biotechnol.* 34: 107-113.
- Tamoi M, Miyazaki T, Fukamizo T and Shigeoka S (2005) The Calvin cycle in cyanobacteria is regulated by CP12 via the NAD(H)/NADP(H) ratio under light/dark conditions. *Plant J.* 42, 504–513.
- Tarrago L, Laugier E, Zaffagnini M, Marchand C, Le Maréchal P, Rouhier N, Lemaire SD and Rey P (2009) Regeneration mechanisms of arabidopsis thaliana methionine sulfoxide reductases b by glutaredoxins and thioredoxins. *J. Biol. Chem.* 284(28): 18963-18971.
- Taylor TC and Andersson I (1997) Structure of a product complex of spinach Ribulose-1,5- Bisphosphate Carboxylase/Oxygenase. *Biochemistry* 36: 4041- 4046.
- Tester RF, Karkalas J and Qi X (2004) Starch-Composition, Fine Structure and Architecture. *J. Cereal Sci.* 39: 151-165.
- Tetlow IJ, Morell MK and Emes MJ (2004) Recent developments in understanding the regulation of starch metabolism in higher plants. *J. Exp. Bot.* 55(406): 2131-2145.
- Thalmann M, Pazmino D, Seung D, Horrer D, Nigro A, Meier T, Kölling K, Pfeifhofer WH, Zeeman SC and Santelia D (2016) Regulation of leaf starch degradation by abscisic acid is important for osmotic stress tolerance in plants. *Plant Cell* 28: 1860-1878.
- Thalmann M and Santelia D (2017) Starch as a determinant of plant fitness under abiotic stress. *New Phytol.* 214: 943–951.
- Thieulin-Pardo G, Remy T, Lignon S, Lebrun R and Gontero B (2015) Phosphoribulokinase from *Chlamydomonas reinhardtii*: a Benson- Calvin cycle enzyme enslaved to its cysteine residues. *Mol. Biosyst.* 11, 1134–1145.
- Thu Hoai NT, Shim IS, Kobayashi K and Kenji U (2003) Accumulation of some nitrogen compounds in response to salt stress and their relationships with salt tolerance in rice (*Oryza sativa* L.) seedlings. *Plant Growth Regul.* 41: 159-164
- Tiessen A, Hendriks JH, Stitt M, Branscheid A, Gibon Y, Farré EM, Geigenberger P (2002) Starch synthesis in potato tubers is regulated by post-translational redox modification of ADP-glucose pyrophosphorylase: a novel regulatory mechanism linking starch synthesis to the sucrose supply. *Plant Cell* 14(9): 2191-2213.
- Torri C, Samorì C, Adamiano A, Fabbri D, Faraloni C and Torzillo G (2011) Preliminary investigation on the production of fuels and bio-char from *Chlamydomonas reinhardtii* biomass residue after bio-hydrogen production. *Bioresour. Technol.* 102: 8707–8713
- Troein C, Locke JC, Turner MS and Millar AJ (2009) Weather and seasons together demand complex biological clocks. *Curr. Biol.* 19: 1961–1964.
- Trost P, Fermani S, Marri L, Zaffagnini M, Falini G, Scagliarini S, Pupillo P and Sparla F (2006) Thioredoxin-dependent regulation of photosynthetic glyceraldehyde-3-phosphate dehydrogenase: autonomous vs. CP12-dependent mechanisms. *Photosynth. Res.* 89:263–275
- Trouverie J, Thevenot C, Rocher JP, Sotta B and Prioul JL (2003) The role of abscisic acid in the response of a specific vacuolar invertase to water stress in the adult maize leaf. *J. Exp. Bot.* 54(390): 2177-2186.
- Umbreen S, Lubega J, Cui B, Pan Q, Jiang J and Loake GJ (2018) Specificity in nitric oxide signalling. *J. Exp. Bot.* 69(14): 3439-3448.
- Upmeyer DJ and Koller HR (1973) Diurnal trends in net photosynthetic rate and carbohydrate levels of soybean leaves. *Plant Physiol.* 51(5): 871-874.

- Vagin A and Teplyakov A (2010) Molecular replacement with MOLREP. *Acta Cryst. D Biol. Cryst.* 66: 22–25.
- Valerio C, Costa A, Marri L, Issakidis-Bourguet E, Pupillo P, Trost P and Sparla F (2011) Thioredoxin-regulated β -amylase (BAM1) triggers diurnal starch degradation in guard cells, and in mesophyll cells under osmotic stress. *J. Exp. Bot.* 62: 545–555
- Vanacker H, Carver TLW and Foyer CH (2000) Early H₂O₂ accumulation in mesophyll cells leads to induction of glutathione during the hyper-sensitive response in the barley-powdery mildew interaction. *Plant Physiol.* 123: 1289–1300.
- Varkonyi-Gasic E and White DW(2002) The white clover enod40 gene family. Expression patterns of two types of genes indicate a role in vascular function. *Plant Physiol.* 129(3): 1107-1118.
- Veith T and Buchel C (2007) The monomeric photosystem I-complex of the diatom *Phaeodactylum tricornutum* binds specific fucoxanthin chlorophyll proteins (FCPs) as light-harvesting complexes. *Biochim. Biophys. Acta.* 1767(12):1428-1435.
- Veramendi J, Fernie AR, Leisse A, Willmitzer L and Trethewey RN (2002) Potato hexokinase 2 complements transgenic Arabidopsis plants deficient in hexokinase 1 but does not play a key role in tuber carbohydrate metabolism. *Plant Mol. Biol.* 49: 491–501.
- Villadsen D and Smith SM (2004) Identification of more than 200 glucose-responsive Arabidopsis genes none of which responds to 3-O-methylglucose or 6-deoxyglucose. *Plant Mol. Biol.* 55: 467-477.
- Villadsen D, Rung JH and Nielsen TH (2005) Osmotic stress changes carbohydrate partitioning and fructose-2,6-bisphosphate metabolism in barley leaves. *Funct. Plant Biol.* 32: 1033-1043.
- Vishwakarma K, Upadhyay N, Kumar N, Yadav G, Singh J, Mishra RK, Kumar V, Verma R, Upadhyay RG, Pandey M and Sharma S (2017) Abscisic acid signaling and abiotic stress tolerance in plants: a review on current knowledge and future prospects. *Front. Plant Sci.* 8: 161.
- Vogel C and Marcotte EM (2012) Insights into the regulation of protein abundance from proteomic and transcriptomic analyses. *Nat. Rev. Genet.* 13(4): 227-232.
- Voiniciuc C, Yang B, Schmidt MH, Günl M and Usadel B (2015) Starting to gel: how Arabidopsis seed coat epidermal cells produce specialized secondary cell walls. *Int. J. Mol. Sci.* 16: 3452–3473
- Volkert K, Debast S, Voll LM, Voll H, Schießl I, Hofmann J, Schneider S and Börnke F (2014) Loss of the two major leaf isoforms of sucrose-phosphate synthase in *Arabidopsis thaliana* limits sucrose synthesis and nocturnal starch degradation but does not alter carbon partitioning during photosynthesis. *J. Exp. Bot.* 65(18): 5217-5229.
- Volkov VV and Svergun DI (2003) Uniqueness of ab initio shape determination in small-angle scattering. *J. Appl. Crystallogr.* 36: 860–864.
- Wahl V, Ponnu J, Schlereth A, Arrivault S, Langenecker T, Franke A, Feil R, Lunn JE, Stitt M and Schmid M (2013) Regulation of Flowering by Trehalose-6-Phosphate Signaling in *Arabidopsis thaliana*. *Science* 339(6120): 704-707.
- Walker JE Saraste M, Runswick MJ and Gay NJ (1982) Distantly related sequences in the alpha- and beta-subunits of ATP synthase, myosin, kinases and other ATP-requiring enzymes and a common nucleotide binding fold. *EMBO J.* 1: 945–951.
- Wang Q, Monroe J, Sjolund RD (1995) Identification and characterization of a phloem specific β -amylase. *Plant Physiol.* 109: 743–750
- Wang F, Zeng B, Sun Z and Zhu C (2009) Relationship between proline and Hg 2⁺-induced oxidative stress in a tolerant rice mutant. *Arch. Environ. Contam. Toxicol.* 56: 723-731
- Wang L, Fujiwara S and Somers DE (2010) PRR5 regulates phosphorylation, nuclear import and subnuclear localization of TOC1 in the *Arabidopsis circadian* clock. *EMBO J.* 29(11): 1903-1915.

- Wang X, Chang L, Wang B, Wang D, Li P, Wang L, Yi X, Huang Q, Peng M and Guo A (2013) Comparative proteomics of *Thellungiella halophila* leaves from plants subjected to salinity reveals the importance of chloroplastic starch and soluble sugars in halophyte salt tolerance. *Mol. Cell. Proteomics* 12(8): 2174-1295.
- Wang Z, Wei P, Wu M, Xu Y, Li F, Luo Z, Zhang J, Chen A, Xie X, Cao P, Lin F and Yang J (2015) Analysis of the sucrose synthase gene family in tobacco: structure, phylogeny, and expression patterns. *Planta* 242(1): 153-166.
- Wani AA, Singh P, Shah MA, Schweiggert-Weisz U, Gul K and Wani IA (2012) Rice starch diversity: effects on structural, morphological, thermal, and physicochemical properties. *Compr. Rev. Food. Sci. Food Saf.* 11: 417-436
- Wattebled F, Dong Y, Dumez S, Delvallé D, Planchot V, Berbezy P, Vyas D, Colonna P, Chatterjee M, Ball S and D'Hulst C (2005) Mutants of *Arabidopsis* lacking a chloroplastic isoamylase accumulate phytyglycogen and an abnormal form of amylopectin. *Plant Physiol.* 138(1): 184-95.
- Weber A, Servaites JC, Geiger DR, Kofler H, Hille D, Gröner F, Hebbeker U and Flügge UI (2000) Identification, purification, and molecular cloning of a putative plastidic glucose translocator. *Plant Cell.* 12(5): 787-802.
- Wedel N and Soll J (1998) Evolutionary conserved light regulation of Calvin cycle activity by NADPH-mediated reversible phosphoribulokinase/CP12/glyceraldehyde-3-phosphate dehydrogenase complex dissociation. *Proc. Natl. Acad. Sci. USA* 95: 9699-9704.
- Weise SE, van Wijk KJ and Sharkey TD (2011) The role of transitory starch in C3, CAM, and C4 metabolism and opportunities for engineering leaf starch accumulation. *J. Exp. Bot.* 62(9): 3109-3118.
- Weise SE, Aung K, Jarou ZJ, Mehrshahi P, Li Z, Hardy AC, Carr DJ and Sharkey TD (2012) Engineering starch accumulation by manipulation of phosphate metabolism of starch. *Plant Biotechnol. J.* 10: 545-554
- Wenderoth I, Scheibe R and von Schaewen A (1997) Identification of the cysteine residues involved in redox modification of plant plastidic glucose-6-phosphate dehydrogenase. *J. Biol. Chem.* 272(43): 26985-26990.
- Wharton MJ (1955) The use of tetrazolium test for determining the viability of seeds of the genus *Brassica*. *Proc. Int. Seed. Test Assoc.* 20: 81-88
- White-Gloria C, Johnson JJ, Marritt K, Kataya A, Vahab A and Moorhead GB (2018) Protein kinases and phosphatases of the plastid and their potential role in starch metabolism. *Front. Plant Sci.* 9:1032.
- Wilhelm C and Selmar D (2011) Energy dissipation is an essential mechanism to sustain the viability of plants: The physiological limits of improved photosynthesis. *J. Plant Physiol.* 168(2): 79-87.
- Wingenter K, Schulz A, Wormit A, Wic S, Trentmann O, Hoermiller II, Heyer AG, Marten I, Hedrich R and Neuhaus HE (2010) Increased activity of the vacuolar monosaccharide transporter TMT1 alters cellular sugar partitioning, sugar signaling, and seed yield in *Arabidopsis*. *Plant Physiol.* 154: 665-677
- Wingler A, Delatte TL, O'Hara LE, Primavesi LF, Jhurrea D, Paul MJ and Schluepmann H (2012) Trehalose 6-phosphate is required for the onset of leaf senescence associated with high carbon availability. *Plant Physiol.* 158(3): 1241-1251.
- Winter H and Huber SC (2000) Regulation of sucrose metabolism in higher plants: localization and regulation of activity of key enzymes. *Crit. Rev. Biochem. Mol. Biol.* 35(4): 253-289.
- Winter D, Vinegar B, Nahal H, Ammar R, Wilson GV and Provart NJ (2007) An "Electronic Fluorescent Pictograph" browser for exploring and analyzing large-scale biological data sets. *PLoS One* 2(8):e718.
- Wolosiuk RA and Buchanan BB (1978) Activation of chloroplast NADP-linked glyceraldehyde-3-phosphate dehydrogenase by the ferredoxin/thioredoxin system. *Plant Physiol.* 61(4):669-71.
- Xiong Y, McCormack M, Li L, Hall Q, Xiang C and Sheen J (2013) Glucose-TOR signalling reprograms the transcriptome and activates meristems. *Nature.* 496(7444): 181-186.

- Xu SM, Liu LX, Woo KC and Wang DL (2007) Changes in photosynthesis, xanthophyll cycle, and sugar accumulation in two North Australia tropical species differing in leaf angles. *Photosynthetica* 45(3): 348-354.
- Yadav UP, Ivakov A, Feil R, Duan GY, Walther D, Giavalisco P, Piques M, Carillo P, Hubberten HM, Stitt M and Lunn JE (2014) The sucrose–trehalose 6-phosphate (Tre6P) nexus: specificity and mechanisms of sucrose signalling by Tre6P. *J. Exp. Bot.* 65(4): 1051-1068.
- Yakir E, Hilman D, Kron I, Hassidim M, Melamed-Book N and Green RM (2009) Posttranslational regulation of CIRCADIAN CLOCK ASSOCIATED1 in the circadian oscillator of Arabidopsis. *Plant Physiol.* 150(2): 844-857.
- Yang L, Fountain JC, Ji P, Ni X, Chen S, Lee RD, Kemerait RC and Guo B (2018) Deciphering drought-induced metabolic responses and regulation in developing maize kernels. *Plant Biotechnol. J.* 16: 1616-1628.
- Yano R, Nakamura M, Yoneyama T and Nishida I (2005) Starch-related α -glucan/water dikinase is involved in the cold-induced development of freezing tolerance in Arabidopsis. *Plant Physiol.* 138: 837-846.
- Yoshida Y, Kiyosue T, Katagiri T, Ueda H, Mizoguchi T, Yamaguchi-Shinozaki K, Wada K, Harada Y and Shinozaki K (1999) Correlation between the induction of a gene for Δ 1-pyrroline-5-carboxylate synthetase and the accumulation of proline in Arabidopsis thaliana under osmotic stress. *Plant J.* 7(5): 751-60.
- Yu TS, Kofler H, Häusler RE, Hille D, Flügge UI, Zeeman SC, Smith AM, Kossmann J, Lloyd J, Ritte G, Steup M, Lue WL, Chen J and Weber A (2001) The Arabidopsis sex1 mutant is defective in the R1 protein, a general regulator of starch degradation in plants, and not in the chloroplast hexose transporter. *Plant Cell* 13: 1907–1918.
- Yu LX and Setter TL (2003) Comparative transcriptional profiling of placenta and endosperm in developing maize kernels in response to water deficit. *Plant Physiol.* 131(2): 568-82.
- Yu TS, Zeeman SC, Thorneycroft D, Fulton DC, Dunstan H, Lue WL, Hegemann B, Tung SY, Umemoto T, Chapple A, Tsai DL, Wang SM, Smith AM, Chen J and Smith SM (2005) α -Amylase is not required for breakdown of transitory starch in Arabidopsis leaves. *J. Biol. Chem.* 280(11): 9773-9779.
- Yuanyuan M, Yali Z, Jiang L, Hongbo S (2009) Roles of plant soluble sugars and their responses to plant cold stress. *Afr. J. Biotechnol.* 8(10): 2004-2010.
- Zaffagnini M, Michelet L, Marchand C, Sparla F, Decottignies P, Le Maréchal P, Miginiac-Maslow M, Noctor G, Trost P and Lemaire SD (2007) The thioredoxin-independent isoform of chloroplastic glyceraldehyde-3-phosphate dehydrogenase is selectively regulated by glutathionylation. *FEBS J.* 274(1): 212-26.
- Zaffagnini M, Bedhomme M, Marchand CH, Morisse S, Trost P and Lemaire SD (2012) Redox regulation in photosynthetic organisms: focus on glutathionylation. *Antioxid. Redox Signal.* 16(6): 567-86.
- Zaffagnini M, Fermani S, Costa A, Lemaire SD and Trost P (2013) Plant cytoplasmic GAPDH: redox post-translational modifications and moonlighting properties. *Front. Plant Sci.* 4:450.
- Zaffagnini M, Michelet L, Sciabolini C, Di Giacinto N, Morisse S, Marchand CH, Trost P, Fermani S, Lemaire SD (2014) High resolution crystal structure and redox properties of chloroplastic triosephosphate isomerase from *Chlamydomonas reinhardtii*. *Mol. Plant* 7: 101-120.
- Zaffagnini M, Fermani S, Calvaresi M, Orrù R, Iommarini L, Sparla F, Falini G, Bottoni A and Trost P (2016) Tuning cysteine reactivity and sulfenic acid stability by protein microenvironment in glyceraldehyde-3-phosphate dehydrogenases of *Arabidopsis thaliana*. *Antioxid. Redox Signal.* 24(9): 502-17.
- Zanella M, Borghi GL, Pirone C, Thalmann M, Pazmino D, Costa A, Santelia D, Trost P, Sparla F (2016) β -amylase 1 (BAM1) degrades transitory starch to sustain proline biosynthesis during drought stress. *J. Exp. Bot.* 67: 1819–1826
- Zarzycki J, Brecht V, Müller M and Fuchs G (2009) Identifying the missing steps of the autotrophic 3-hydroxypropionate CO₂ fixation cycle in *Chloroflexus aurantiacus*. *Proc. Natl. Acad. Sci. USA* 106(50): 21317-21322.
- Zeller G, Henz SR, Widmer CK, Sachsenberg T, Rättsch G, Weigel D and Laubinger S (2009) Stress-induced changes in the *Arabidopsis thaliana* transcriptome analyzed using whole-genome tiling arrays. *Plant J.* 58(6): 1068-1082.

- Zeng Y, Wu Y, Avigne WT and Koch KE (1998) Differential regulation of sugar-sensitive sucrose synthases by hypoxia and anoxia indicate complementary transcriptional and postranscriptional responses. *Plant Physiol.* 116(4): 1573-1583.
- Zhang XQ, Lund AA, Sarath G, Cerny RL, Roberts DM and Chollet R (1999) Soybean nodule sucrose synthase (nodulin-100): further analysis of its phosphorylation using recombinant and authentic root-nodule enzymes. *Arch. Biochem. Biophys.* 371(1): 70-82.
- Zhang N and Portis AR Jr. (1999) Mechanism of light regulation of Rubisco: A specific role for the larger Rubisco activase isoform involving reductive activation by thioredoxin-f. *Proc. Natl. Acad. Sci. USA* 96: 9438-9443
- Zhang N, Schürmann P and Portis AR Jr. (2001) Characterization of the regulatory function of the 46-kDa isoform of Rubisco activase from Arabidopsis. *Photosynth. Res.* 68(1): 29-37.
- Zhang N, Kallis RP, Ewy RG and Portis AR Jr. (2002) Light modulation of Rubisco in Arabidopsis requires a capacity for redox regulation of the larger Rubisco activase isoform. *Proc. Natl. Acad. Sci. USA.* 99(5): 3330-3334.
- Y Zhang (2008) I-TASSER server for protein 3D structure prediction. *BMC Bioinformatics* 9: 40.
- Zhang Y, Primavesi LF, Jhurrea D, Andralojc PJ, Mitchell RA, Powers SJ, Schluepmann H, Delatte T, Wingler A and Paul MJ (2009) Inhibition of SNF1-related protein kinase1 activity and regulation of metabolic pathways by trehalose-6-phosphate. *Plant Physiol.* 149(4): 1860-1871.
- Zhang C, Han L, Slewinski TL, Sun J, Zhang J, Wang ZY and Turgeon R (2014) Symplastic phloem loading in poplar. *Plant Physiol.* 166(1): 306-13.
- Zhang Z, Deng Y, Song X and Miao M (2015) Trehalose-6-phosphate and SNF1-related protein kinase 1 are involved in the first-fruit inhibition of cucumber. *J. Plant Physiol.* 177: 110-120.
- Zhang J, Ye ZW, Singh S, Townsend DM and Tew KD (2018) An evolving understanding of the S-glutathionylation cycle in pathways of redox regulation. *Free Radic. Biol. Med.* 120: 204-216.
- Zhang C and Turgeon R (2018) Mechanisms of phloem loading. *Curr. Opin. Plant Biol.* 43:71–75.
- Zhou Y, Qu H, Dibley KE, Offler CE and Patrick JW (2007) A suite of sucrose transporters expressed in coats of developing legume seeds includes novel pH-independent facilitators. *Plant J.* 49(4): 750-764.
- Zeeman SC and ap Rees T (1999) Changes in carbohydrate metabolism and assimilate export in starch-excess mutants of Arabidopsis. *Plant Cell Environ.* 22: 1445-1453.
- Zeeman SC, Thorneycroft D, Schupp N, Chapple A, Weck M, Dunstan H, Haldimann P, Bechtold N, Smith AM and Smith SM (2004) Plastidial alpha-glucan phosphorylase is not required for starch degradation in Arabidopsis leaves but has a role in the tolerance of abiotic stress. *Plant Physiol.* 135(2): 849-858.
- Zeeman SC, Smith SM and Smith AM (2007) The diurnal metabolism of leaf starch. *Biochem. J.* 401: 13-28
- Zeeman SC, Kossmann J and Smith AM (2010) Starch: its metabolism, evolution, and biotechnological modification in plants. *Annu. Rev. Plant Biol.* 61: 209–234